Investigating the effect of the KSHV vIRF2 and vIRF4 proteins on the interferon response

By

LAURA NAMBIKAI HINDLE

A thesis submitted to
The University of Birmingham
for the degree of
DOCTOR OF PHILOSOPHY

The School of Cancer Sciences
College of Medical and Dental Sciences
The University of Birmingham
September 2013

Abstract

The type I IFN response forms part of the innate immune system, which is the first line of defence against invading viruses. Kaposi's sarcoma-associated herpesvirus, a gamma herpesvirus, encodes a number of genes that down regulate the type I IFN response. These include four viral interferon regulatory factors (vIRFs). vIRFs 1, 2 and 3 have been shown to inhibit type I IFN signalling previously, whereas vIRF4 was, until now, not thought to inhibit this pathway. The aim of this study was to determine the mechanism by which vIRF2 inhibits type I IFN signalling and to characterise the effects of the vIRF4 protein on this system. Cell lines were engineered to express inducible vIRF2 or vIRF4 proteins that both demonstrated significant inhibition of JAK-STAT signalling via ISRE-luc reporter assays. Electrophoretic mobility shift assays showed that vIRF2 and vIRF4 could significantly reduce ISGF3:ISRE complex formation. Stable isotope labelling of amino acids in cell culture coupled to LC-MS/MS was employed to facilitate the identification of the vIRF2 and vIRF4 interactomes. USP7 and CBP were identified as binding partners for both viral proteins and their contribution to inhibition of JAK-STAT signalling was explored.

Acknowledgements

Firstly, I would like to express my heartfelt thanks to my supervisor Prof. David Blackbourn for the continued guidance, support and motivation he has shown me throughout my PhD. I would also like to thank members of the Blackbourn group- both past and present, especially Rachel Wheat and Dr. Simon Chanas for their help and friendship within our lab. Additionally, I would like to thank the B-cell group, in particular Dr. Jianmin Zuo for answering questions and discussing techniques with me. I also thank Dr. Andrew Bell for sharing with me his expertise in qPCR. I have made some amazing friends and memories with the other PhD students at Birmingham; thanks to you guys for making my time in Birmingham a very happy one. For looking after me during my times away from Birmingham and for hosting some great parties I would like to say a big thankyou to John and Aileen.

I am grateful to the Medical Research council (MRC) and the University of Birmingham for funding my research and to the Society for General Microbiology (SGM) for funding the proteomics aspects of this project. I was fortunate to have spent some time at the University of Cambridge in the laboratory of Prof. Ian Goodfellow, working with Dr. Edward Emmott in order to learn the NTAP-pulldown approaches used in this thesis and I am grateful for their time and help. I also thank Dr Nicolas Locker (University of Surrey) for performing the polysome profiling experiment.

Importantly, I would like to thank my boyfriend and soon to be husband, Nicholas Morley, for the amazing support you have shown me throughout my PhD. I couldn’t have done this without you!

Finally, I want to say thanks to my brother Mark and my parents Paul and Rita for their love and guidance. I could not wish for a better family, and I dedicate this thesis to them.

Publications arising from this thesis

Mutocheluh, M., **Hindle, L.,** Areste, C., Chanas, S. A., Butler, L. M., Lowry, K., Shah, K., Evans, D. J. & Blackbourn, D. J. 2011. Kaposi's sarcoma-associated herpesvirus viral interferon regulatory factor-2 inhibits type 1 interferon signalling by targeting interferon-stimulated gene factor-3. *J Gen Virol,* 92, 2394-8.

Table of contents

List of Figures

List of tables

293 cells were plated on coverslips in 24-well plate and left to adhere overnight. They were then co-transfected with the pcDNA4/HisMax, pvIRF2-HisMax or pvIRF4-HisMax expression plasmids and the CBP-GFP plasmid. After 48 hours, cells were fixed in 4% paraformaldehyde and permeabilized with ice cold methanol

List of abbreviations

Abbreviation	Meaning
AIDS	Acquired immunodeficiency syndrome
BRG1	Brahma-related gene 1
CARD	Caspase recruitment domain
CBP	CREB binding protein
cGAMP	Cyclic GMP-AMP
cGAS	Cgamp synthase
CMV	Cytomegalovirus
CREB	cAMP response element-binding protein
DAI	DNA-dependent activator of IFN-regulatory factors
DAMP	Damage-associated molecular pattern
DBD	DNA binding domain
DCs	Dendritic cells
DC-SIGN	Dendritic Cell-Specific Intercellular adhesion molecule-3-Grabbing Non-integrin
DENV	Dengue virus
DEPC	Diethylpyrocarbonate
DLA	Dual luciferase assay
E	Early
EBV	Epstein barr virus
eIF2α	Eukaryotic initiation factor 2 α
EMCV	Encephalomyocarditis virus
EpHA2	Ephrin-A2
FAK	Focal adhesion kinase
GCN5	General control of amino acid synthesis 5
HAART	Highly active antiretroviral therapy
HAT	Histone acetyltransferases
HBV	Hepatitis B virus
HCV	Hepatitis C virus
HFF	Human foreskin fibroblast
HHV	Human herpesvirus
HIV	Human immunodeficiency virus
HRSV	Human respiratory syncytial virus
HS	Heparan sulphate
HVS	Herpesvirus Saimiri
IE	Immediate early
IFN	Interferon
IFNAR1/2	The interferon-α/β receptor 1/2
IPS-1	Interferon-beta promoter stimulator 1
IRAK	Interleukin-1 receptor-associated kinase
IRF	Interferon response element
ISGF3	Interferon stimulated gene factor 3
ISGs	Interferon stimulated gene

ISRE	Interferon stimulated response element
JAK	Janus activated kinase
KS	Kaposi’s sarcoma
KSHV	Kaposi’s sarcoma-associated herpesvirus
L	Late
LANA	Latency-associated nuclear antigen
LUR	Long unique region
MCD	Multicentric Castleman's disease
MDA5	Melanoma Differentiation-Associated protein 5
MDM2	Murine double minute 2
MM-1	Myc modulator 1
MOI	Multiplicity of infection
NTAP	N-terminal tandem affinity purification tag
OAS	Oligoadenylate synthetase
ORF	Open reading frame
PAMP	Pathogen-associated molecular pattern
PBS	Phosphate buffered saline
PEL	Primary effusion lymphoma
PKR	Protein kinase R
PMA	Phorbol myristate acetate
PRD	Positive regulatory domains
PRR	Pattern recognition receptor
RAUL	Rta-associated ubiquitin ligase
RBPJκ	Recombination signal sequence-binding protein Jκ
RFHV	Retroperitoneal fibromatosis herpes virus
RIF	Regulator of IFN function
RIG-I	Retinoic acid-inducible gene 1
RRV	Rhesus rhadinovirus
RTA	Replication Transcriptional Activator
SBD	Streptavidin binding domain
SILAC	Stable isotope labelling by amino acids in cell culture
STAT	Signal transducer and activators of transcription
STAT	Signal transducer and activator of transcription
STING	Stimulator of IFN genes
TAP	Tandem affinity purification
TBK-1	TANK-binding kinase 1
TBP	TATA-binding protein
TEV	Tobacco etch virus
TFIID	Transcription factor II D
TLR	Toll-like receptor
TR	Terminal repeats
TRAF	TNF receptor associated factor
TRI	Triplex component
USP7	Ubiquitin-specific-processing protease 7
v-Cyclin	Viral-cyclin
v-FLIP	Viral-Flice-inhibitory protein

vIL6	Viral-interleukin 6
vIRF	Viral interferon regulatory factor
VSV	Vesicular Stomatitis Virus

CHAPTER 1

INTRODUCTION

1.1. Overview of introduction

This thesis aims to identify if and how the Kaposi's sarcoma-associated herpesvirus (KSHV) encoded viral interferon regulator factor 2 (vIRF2) and vIRF4 proteins regulate the immune system. Specifically, the type I interferon (IFN) signalling pathways will be examined. This introduction covers the relevant background to these studies. Initially, information regarding KSHV will be detailed, followed by an overview of the type I IFN signalling system. Finally current knowledge of KSHV-encoded vIRFs will be described.

1.2. KSHV

The first part of this introduction provides an overview of KSHV, its discovery, related diseases and its lifecycle.

1.2.1. Classification

The *Herpesviridae* family belongs to the order *Herpesvirale*, of which there are three families. The *Malacoherpesviridae* family contains viruses which infect molluscs, the *Alloherpesviridae* family contains fish and amphibian viruses and the *Herpesviridae* family contains viruses which infect humans and animals. The *Herpesviridae* family is further divided into three subfamilies; *Alpha* (α), *Beta* (β) and *Gamma* (γ) *herpesvirinae* (reviewed in Davidson et al, (2009)). The two human γ-herpesviruses are Epstein–Barr virus (EBV or HHV 4) which is a member of the *Lymphocryptoviridae* and KSHV, a member of the *Rhadinoviridae*. Rhesus rhadinovirus (RRV) is closely related to KSHV (Alexander et al., 2000), and the

genomic organization between KSHV and RRV is essentially co-linear (Searles et al., 1999). As such, RRV has been used as an animal model for KSHV. See Figure 1.1 for a diagram of how KSHV fits into the *Herpesvirales* order.

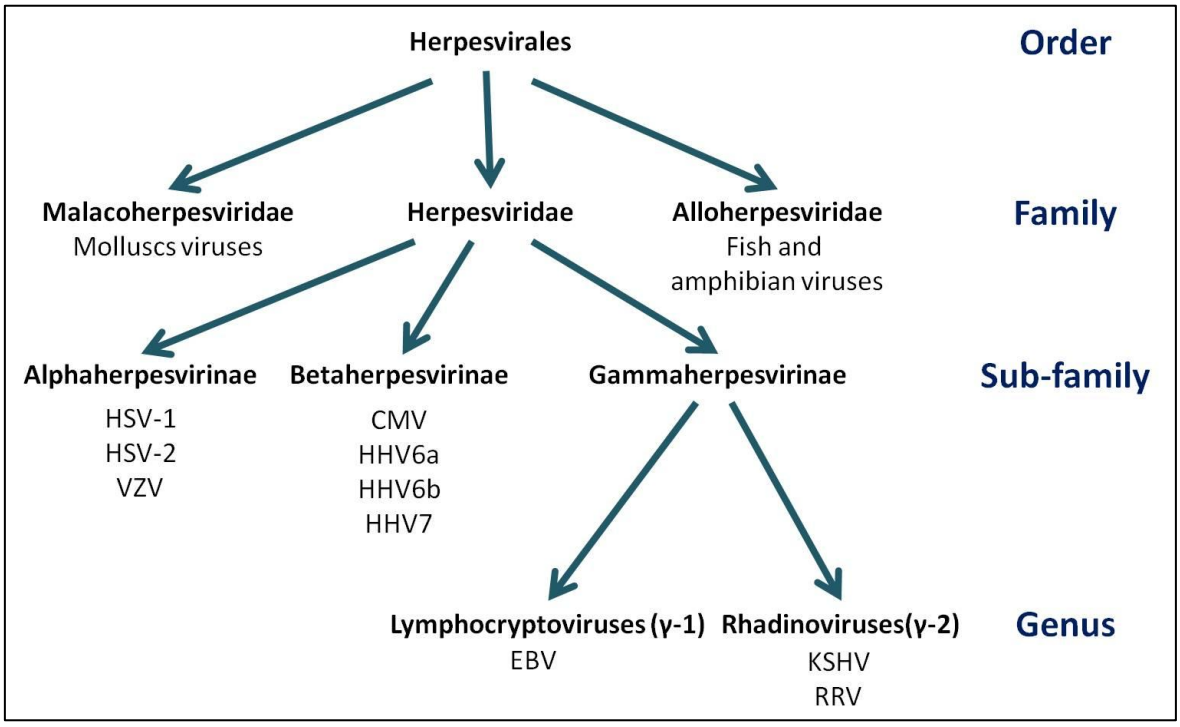

Figure 1.1: A brief overview of where KSHV fits into the Herpesvirale order.

The human herpesviruses are shown in their respective sub-families (Based on Davison et al (2009)). KSHV is a γ-2 herpesvirus. HSV1 = Herpes simplex virus 1. HSV-2 = Herpes simplex virus 2. VZV = Varicella zoster virus. CMV = Cytomegalovirus. HHV6 = Human herpesvirus. RRV = Rhesus Rhadinovirus (non-human virus). There are many more herpesviruses which are not shown, as they infect other non-human species.

1.2.2. Discovery

A virus was suspected to be the cause of Kaposi's sarcoma (KS), which led to research of KS tissues to identify the putative virus. In 1972, herpesvirus-like particles were identified in analyses of KS biopsies by electron microscopy (Giraldo et al., 1972). However, these were thought to be that of cytomegalovirus (CMV). It was not until 1994, that a new herpesvirus was identified from KS tissues. Yuan Chang and Patrick Moore used representational difference analysis to identify DNA sequences which were present in KS lesions but absent in control samples from the same patient. They identified sequences which were homologous, but distinct from γ-herpesvirus genes, and named this new virus KSHV (Chang et al., 1994). KSHV was the second human herpesvirus identified which showed oncogenic potential, with EBV being the first.

1.2.3. Diseases associated with KSHV

In 2009, KSHV was formally defined as the causative agent of KS and Primary Effusion Lymphoma (PEL), and was said to be associated with Multicentric Castleman's Disease (MCD) (Bouvard et al., 2009).

1.2.3.1. Kaposi's sarcoma

KS was originally described by Moriz Kaposi more than a century ago (Kaposi, 1872). Then, it was a rare pigmented growth most commonly found in elderly men in the mediteranian. However, during the AIDS epidemic of the 1980s there was an increase of KS in AIDS patients and this malignancy became known as an AIDS-defining illness. There are currently four forms of KS, each prevalent in

certain areas of the globe, occurring among different demographic groups. All forms of KS are associated with KSHV infection.

Classical KS was the form identified by Kaposi. It is typically seen in elderly Mediterranean patients, or those of Arabic or Jewish decent.

AIDS-associated KS, sometimes referred to as epidemic KS, was described during the 1980s and is very aggressive. The incidence of AIDS-KS has decreased in the western world due to highly active antiretroviral therapy (HAART) to treat Human immunodeficiency virus (HIV) infection (Franceschi et al., 2008), but in some developing countries, particularly those in sub-Saharan Africa, the incidence of KS continues to grow.

Endemic KS occurs in people living in Equatorial Africa. KSHV infection is much more common in Africa than in other parts of the world, so the risk of KS is higher. Endemic KS used to be the most common type of KS in Africa but as HIV infection increased AIDS-KS became more common.

Iatrogenic KS presents following organ transplantation, due to the administration of immunosuppressant drugs. However, the reactivation of the immune system through removal of immunosuppressant drugs or lowering the dose can cause KS to regress spontaneously (reviewed in Szajerka and Jablecki, (2007) and Restrepo and Ocaziones, (2011)).

1.2.3.2. Primary Effusion Lymphoma

PEL is an aggressive, non-Hodgkin's lymphoma that is usually fatal. It arises in immunocompromised individuals, and as such is often associated with HIV infection. The majority of cases arise in body cavities such as the pleural, pericardial, and peritoneal spaces. In most cases, the lymphoma cells are also infected with EBV, but EBV negative PELs have been described (reviewed in Verma and Robertson (2003)). The role of EBV in PEL remains unclear (Chen et al., 2007).

1.2.3.3. Multicentric Castleman's Disease

MCD is rare lymphoproliferative disorder characterized by non-cancerous growths in a microenvironment of excess interleukin 6 (IL-6). Lesions develop at multiple sites and are polyclonal. KSHV is found in almost all HIV positive cases and in about 40% of HIV negative cases (Soulier et al., 1995)

1.2.4. Structure of the KSHV virion

All herpesviruses share a similar structure, comprising four elements; the core, the capsid, the tegument and the envelope (Figure 1.2). The capsid, tegument and envelop proteins can be visualised by electron microscopy, and in the past this was used to define membership of the *Herpesviridae* family. Nowadays, genomic analyses are the means by which such assignments are made (reviewed in McGeoch et al, (2006)). The core contains a single linear double stranded DNA (dsDNA) genome which is surrounded, and protected by an icosahedral capsid. The KSHV capsid consists of 162 surface capsomeres, made from the major

capsid protein. The capsid is held together and stabilised with triplexes made from triplex-1 protein (TRI-1/ORF62) and triplex-2 protein (TRI-2/ORF26) (Wu et al., 2000). Surrounding the capsid is a protein-filled tegument. The tegument was previously considered amorphous, but it is now thought to be more organised due to interactions between the tegument proteins and also between tegument proteins and either envelop proteins or capsid proteins. The KSHV proteins found in the tegument are involved in many stages of the viral life cycle, such assembly and transportation of viral particles and immune evasion processes (reviewed in Sathish et al, (2012)). The outer layer of the virus particle is the envelope, comprised of numerous glycoproteins which are thought to mediate KSHV entry (see section 1.2.6).

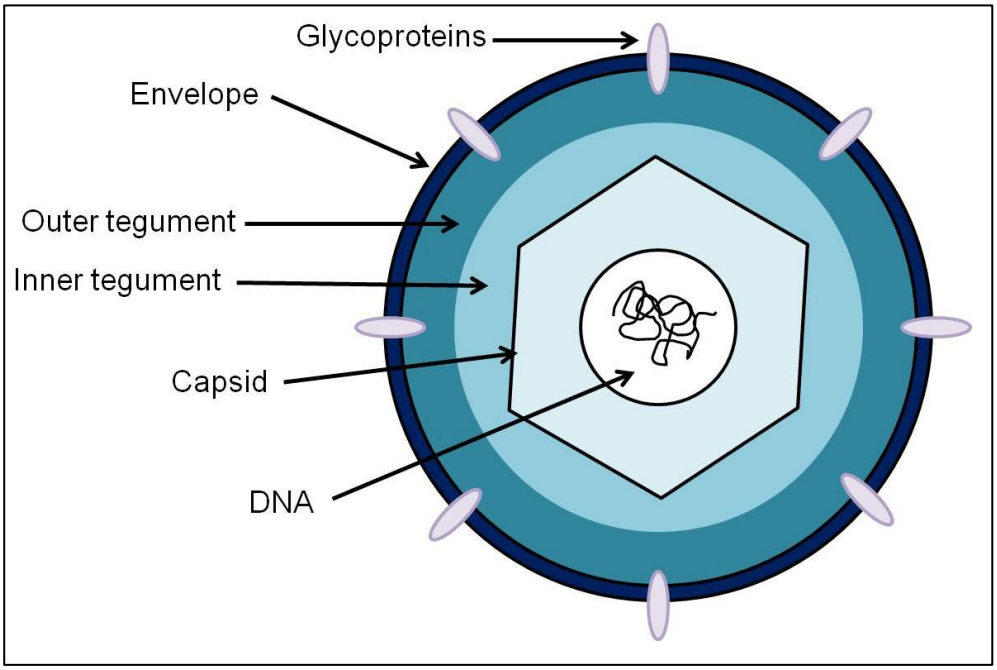

Figure 1.2: The structure of KSHV.
The simplified structure of a KSHV virion is illustrated. The Inner core is surrounded by the capsid. Surrounding the capsid are the inner and outer teguments and these are enclosed by the envelope.

1.2.5. The KSHV genome

The KSHV genome organisation is similar to that of other *gammaherpesviruses*, especially Herpesvirus saimiri (HVS), retroperitoneal fibromatosis associated herpesvirus (RFHV) and EBV, its closest human relative (Chang et al., 1994, Russo et al., 1996, Neipel et al., 1998, Rose et al., 2003). KSHV exhibits collinear homology between these viruses, and contains a long unique region (LUR) flanked by terminal repeat (TR) sequences (Russo et al., 1996). The size of the genome is between 165-170kb, and this variation is due to differences in the number of TR between KSHV isolates. The LUR is about 138-140.5kb (Wen 2009). The KSHV genome contains 86 genes of which at least 22 are potentially immunomodulatory (Rezaee et al., 2006). When KSHV was first sequenced, its closest homologue was HVS, with at least 66 of its open reading frames (ORFs) being homologous to HVS. These KSHV genes were named after the HVS genes and have the prefix ‘ORF’ (Russo et al., 1996). Genes unique to KSHV were named with the prefix ‘k’ (Figure 1.3.).

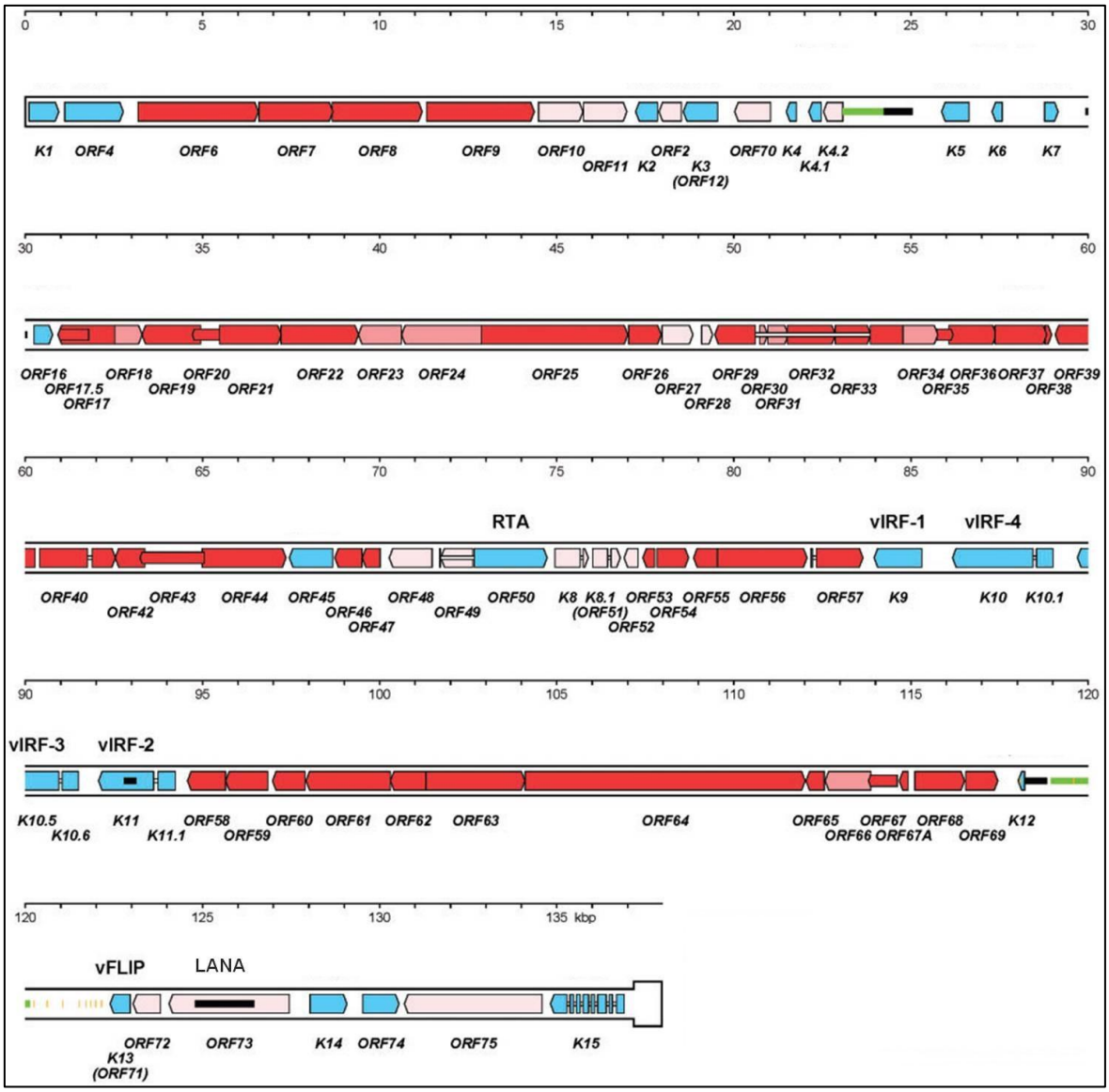

Figure 1.3: The genome arrangement of KSHV.

The genome consists of a unique region flanked at each end by terminal repeats. Coloured regions indicate protein coding regions. Red regions are genes inherited from α, β and γ *herpesvirinae*. Pink regions are genes inherited from β and γ *herpesvirinae*. Blue regions are immunomodulatory genes. Gene names are shown below while names of important proteins mentioned in this thesis are shown above. This figure is reproduced from (Rezaee et al., 2006)

1.2.6. KSHV entry

An overview of the proposed KSHV entry process is illustrated in Figure 1.4. KSHV encodes a number of glycoproteins which are conserved among herpesviruses (gB, gH, gL, gM and gN) along with unique glycoproteins (ORF4, gpK8.1A, gpK8.1b, K1, K14 and K15) (Russo et al., 1996, Neipel et al., 1998). These proteins enable KSHV to interact with a multitude of cellular receptors. KSHV entry is incompletely understood, but is likely a very complex process involving multiple host cell surface factors which vary in different cell types.

Like many herpesviruses, KSHV binds heparan sulphate (HS). It is thought that KSHV binds HS to increase the local concentration of virions on the surface of the cells, enhancing opportunities for KSHV to bind to other cellular receptors which lead to cell entry. Thus HS is classed as an attachment factor. KSHV binds HS predominantly through gB, gH, ORF4 and gpK8.1A. The importance of HS as an attachment factor can be see in the removal of this receptor, using heparinases, which decrease KSHV infectivity (Birkmann et al., 2001, Wang et al., 2001).

The binding of KSHV to dendritic cell-specific intercellular adhesion molecule grabbing non-integrin (DC-SIGN) has been shown in myeloid dendritic cells (DCs) and macrophages. Blocking DC-SIGN with anti-DC-SIGN antibodies inhibits KSHV binding and infection (Rappocciolo et al., 2006), but it is not known how KSHV interacts with this cellular protein.

Recently, it has been shown that the gH and gL glycoproteins of KSHV bind to the epinephrine-A2 (EpHA2) receptor. Han et al, (2012) showed that EpHA2 co-precipitated with gH-gL and KSHV virions, and overexpression of EpHA2 led to an increase in KSHV infection. Blocking EpHA2 with antibodies or siRNA against EpHA2 decreased infection and treatment of KSHV with soluble EpHA2 also decreased infection. The authors also found that binding of gH-gL to EpHA2 caused phosphorylation of this receptor and resulted in endocytosis (Hahn et al., 2012). Thus, EpHA2 is thought to bind to KSHV and mediate its entry via endocytosis.

The 12-transmembrane transporter protein xCT was identified as being important in KSHV entry. xCT is a light chain component of the CD98 glycoprotein complex. Ectopic expression of xCT rendered non-susceptible adherent target cells to become susceptible to KSHV infection (Kaleeba and Berger, 2006). However, the role of xCT in KSHV entry is unclear as Veettil et al, (2008) showed that xCT does not affect KSHV binding or entry. They used RT-PCR to measure viral DNA levels at different time points post KSHV infection. They found that incubation with anti-xCT antibodies did not decrease viral binding or entry, but rather decreased KSHV gene expression following entry. Therefore, binding of KSHV to xCT was proposed to activate signalling cascades leading to an increase in viral gene expression (Veettil et al., 2008).

KSHV has been found to associate with integrins which have roles in KSHV binding and entry. Akula et al, (2002) identified the cellular integrin α3β1 as a

potential entry receptor for KSHV. When cellular integrins were blocked with antibodies, or KSHV virions were incubated with soluble integrins, a decrease in infection of KSHV was observed. The gB glycoprotein was proposed to interact with α3β1, as anti-gB antibodies immunoprecipitated virus-α3β1complexes (Akula 2002). Integrin α5β3 is also proposed to be important for KSHV entry into cells. α5β3 was shown to bind to KSHV virions by confocal microscopy, and α5β3 function-blocking antibodies inhibited KSHV infection by 70 to 80% (Garrigues et al., 2008). Veettil et al, (2008) found that α3β1, α5β3 and α5β5 play roles in KSHV infection of adherent cells. Pre-incubation of soluble α3β1, α5β3 or α5β5 reduced KSHV infection, and incubation of these integrins in combination reduced infection further, suggesting that they act together. xCT was also found to associate with these integrins and the theory that KSHV causes the formation of a multi molecular complex containing α3β1, α5β3 and α5β5 and CD98/xCT was proposed (Veettil et al., 2008).

When KSHV binds to host cell receptors, it activates a range of signalling pathways, which are thought to mediate its uptake into cells. As mentioned previously, EphA2 phosphorylation, induced by KSHV binding can lead to endocytosis (Hahn et al., 2012). It has recently been shown that KSHV induces the interaction of integrins with EphA2 and the adapter protein c-Cbl. C-Cbl can then ubiquitinate EphA2, leading to endocytosis (Dutta et al., 2013). Integrin signalling is also thought to be important in KSHV uptake into the host cell. Ligand binding to integrins activates focal adhesion kinase (FAK), which is a key activator of cell signalling pathways. Using RT-PCR, to measure internalised viral DNA,

Krishnan et al, (2006) showed that a cell line lacking FAK resulted in a 70% reduction in the internalization of viral DNA compared to a control, indicating that FAK is involved in KSHV entry. Activation of FAK leads to induction of downstream Src and PI3-Kinases, which are thought to trigger the endocytosis of virions (reviewed in Chandran (2010) and Chakraborty et al, (2012).

Using electron microscopy KSHV virions in endocytic vesicles have been observed along with the fusion of the virus envelope with the vesicle following infection (Akula et al., 2003, Raghu et al., 2009). As mentioned above, KSHV binding to integrins and EphA2 activates signalling cascades which results in endocytosis. However, the precise mechanism of endocytosis seems to vary between cell types. For example, in human foreskin fibroblasts (HFF) cells, inhibition of clathrin-coated pits (using chlorpromazine) inhibited KSHV entry, whereas inhibition of endocytosis mediated by caveolae or dissociation of lipid rafts did not (Akula et al., 2003). This suggests that KSHV enters HFFs via clathrin-coated pits. However, chlorpromazine had no effect on KSHV entry in human dermal microvascular endothelial (HMVEC-d) cells or human umbilical vein endothelial (HUVEC) cells. In these cells, inhibitors of macropinocytosis and actin polymerization decreased virus entry instead (Raghu et al., 2009), suggesting macropinocytosis is the means by which KSHV enters HMVEC-d and HUVEC cells.

It is believed that KSHV reaches the nucleus using the microtubule network. Naranatt et al, (2005) found that KSHV capsids colocalised with microtubules and

the inactivation of Rho GTPases reduced the delivery of viral DNA to the nucleus. Conversely, nuclear delivery of viral DNA increased in cells expressing a constitutively active RhoA mutant (Naranatt et al., 2005). It was therefore proposed that KSHV induces Rho-GTPases to modulate microtubule stability which allows reorganization of microtubules occurs, enabling capsid transport to the nucleus (reviewed in Chandran (2010) and Chakraborty et al, (2012)).

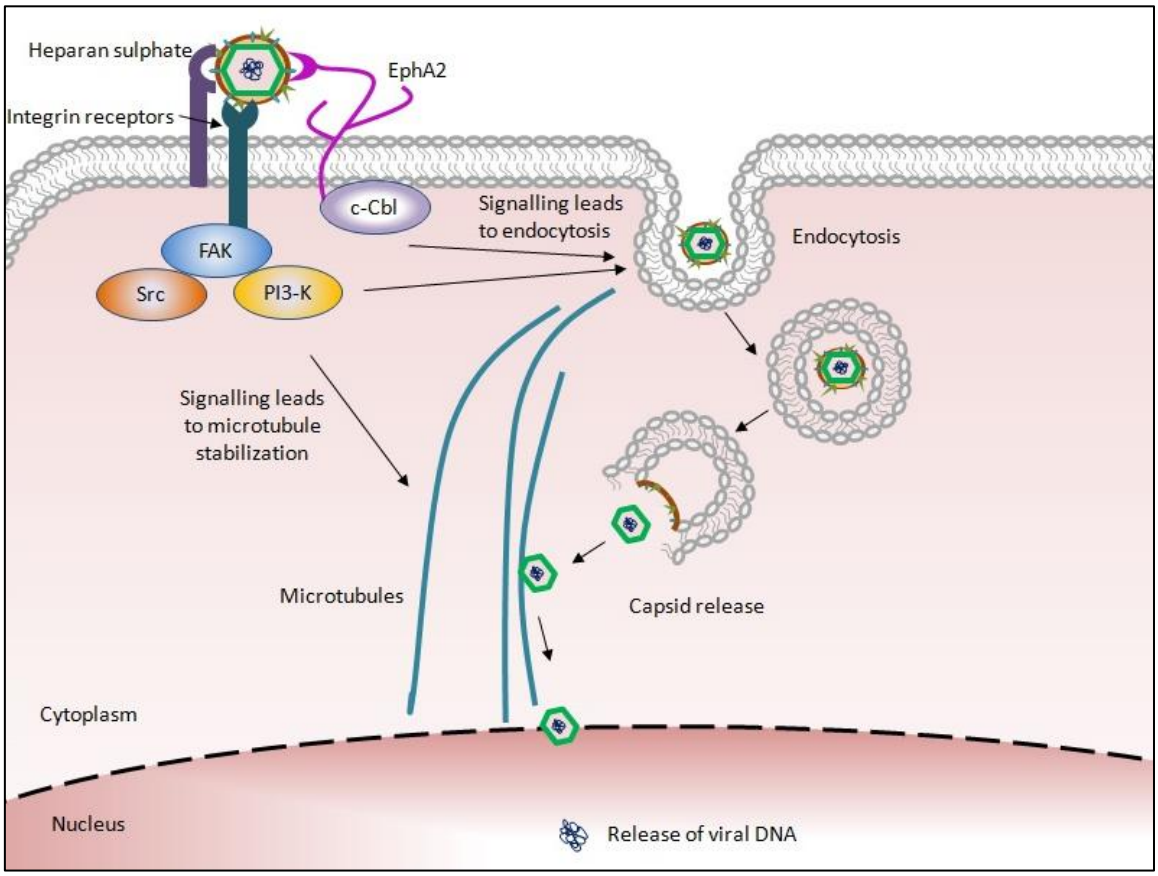

Figure 1.4: KSHV entry into host cells.

KSHV binds to HS, which enables interaction of the virus with other receptors. These include integrins α3β1, α5β3 and α5β5 and the EphA2 receptor. Integrins activate FAK and this leads to endocytosis. EphA2 can interact with the c-Cbl proteins which ubiquitinates EphA2 which also results in endocytosis. Following KSHV entry by endocytosis, the endocytic vesicle then releases the KSHV capsid, which moves to the nucleus along the microtubule network. At the nucleus, the KSHV DNA is released. Figure based on (Chandran, 2010).

1.2.7. KSHV lifecycle overview

Like other herpesviruses, upon entry into the nucleus, the KSHV genome can enter one of two phases, the latent or the lytic life cycles. In the latent state the virus genome is maintained as an episome and only a small sub-set of the KSHV genes are expressed which are essential to its survival in the host. No new virus particles are produced during this phase. The lytic phase involves replication of the genome and production of new virus particles.

1.2.8. Maintenance of latency

During latency, the KSHV genome is maintained in the nucleus of the host as a circular episome. Only a very small sub-set of genes are expressed but the genome is propagated between daughter cells. In KS, PEL and MCD, the Latency associated nuclear antigen (LANA), viral cyclin (v-cyclin), v–Flice-inhibitory protein (v-FLIP), Kaposins A, B, and C and microRNAs are expressed (Cai et al., 2005, Greene et al., 2007). In PEL and MCD, the vIRF3 and viral Interleukin 6 (vIL6) genes are also expressed. Recently ORF-K1 has also been assigned as a latency protein (Chandriani and Ganem, 2010). Following primary infection, latency is typically established (Bechtel et al., 2003). To maintain this latent state, some of the latent genes have functions which promote latency and inhibit transition to the lytic cycle. Their products are discusses in this context in the following paragraphs.

1.2.8.1. LANA

LANA is encoded by ORF73. LANA is highly expressed in KSHV-infected cells and its detection is hence used to determine cells which are KSHV positive (Gao

et al., 1996). LANA associates with the KSHV TRs and also with the host chromosome. These associations tether the KSHV DNA to chromosomes during mitosis and enable the episomes to segregate with daughter cells (Cotter and Robertson, 1999, Ballestas et al., 1999). The interaction of LANA with the TR of KSHV has also been shown to be sufficient for episomal DNA replication (Fejer et al., 2003). Therefore, during latent replication LANA functions to replicate the DNA, maintain the viral episomes and then segregate these into daughter cells, thus maintaining the infection of cells (reviewed in Ye et al, (2011), Greene et al, (2007)). Another important function of LANA is to maintain latency, and it achieves this by also downregulating the expression of the lytic switch protein, replication transcriptional activator (RTA). RTA regulates the switch to lytic replication (see section 1.2.9). LANA can downregulate the promoter activity of RTA, and thus inhibit its expression (Lan et al., 2004). LANA can also bind to the recombination signal sequence-binding protein Jκ (RBPJκ), which acts either as a repressor or activator of transcription, depending on the proteins it is bound to. The LANA-RBPJκ complex binds to the RBPJκ cognate DNA sequence within the RTA promoter and inhibits its transcription (Lan et al., 2005). LANA is therefore a key component in maintaining latent infection of host cells and inhibiting lytic reactivation.

1.2.8.2. v-Flip

v-FLIP is encoded by ORF71 (K13) and is involved in promoting latency though a number of mechanisms. Firstly, it prevents death receptor signalling, by inhibiting caspase activation, which therefore inhibits apoptosis and thus promotes cell

survival (Djerbi et al., 1999). It also promotes NFkB signalling, which was found to be important in decreasing lytic reactivation (Grossmann and Ganem, 2008). Finally, it inhibits the expression of RTA, which is a key promoter of lytic reactivation (Ye et al., 2008).

1.2.8.3. V-Cyclin

Viral cyclin, encoded by ORF72 is structurally similar to cellular cyclin D. v-cyclin can bind to and activate CDK6 kinase. The v-cyclin-CDK6 complex overcomes cell cycle arrest, induced by cdk-inhibitors, and causes cell cycle progression and cell transformation that may contribute to KS formation (Swanton et al., 1997). The v-cyclin-CDK6 kinase complex also phosphorylates nucleophosmin, stabilising the LANA-nucleophosmin interaction. Nucleophosmin (NPM) is a nuclear phosphoprotein and a histone chaperone which has been implicated in transcription control. The interaction between nucleophosmin and LANA enables the silencing of KSHV lytic genes (Sarek et al., 2010).

1.2.9. Lytic reactivation

Lytic cycle results in replication of the viral genome and assembly of new viral particles which are released from the cells. RTA, encoded by ORF50, is a lytic switch protein for KSHV viral reactivation from latency which is both necessary and sufficient to trigger this programme (Lukac et al., 1998, Sun et al., 1998). Activation of RTA expression is thought to involve epigenetic changes, as methylation of the RTA promoter is responsible for its repression. Additionally, the

association of regulators of acetylation, such as HDACs, are thought to have a role in RTA activation (reviewed in Greene et al, (2007)). RTA can bind some KSHV promoters directly and initiate their transcription, and these are known as RBPJκ-independent promoters. RTA can also induce transcription through the RBPJκ protein, which recruits additional co-activators of transcription (Guito and Lukac, 2012). RTA expression triggers the expression of KSHV genes in a temporal manner beginning with the immediate early (IE) genes, followed by early (E) genes and finally late (L) genes.

1.3. Viruses and cancer

In 2008, 16% of all cancers were attributable to infectious agents. In developing countries, this frequency rises to almost 23% (de Martel, 2012). The majority of these oncogenic agents are viruses. KSHV is one such virus out of a total of 7 currently known human oncogenic viruses (summarised in Table 1.1).

Table 1.1: The seven human oncogenic viruses and the major malignancies with which they are associated.

Virus	Malignant disease
Epstein–Barr virus	Burkitt's lymphoma; Nasopharyngeal carcinoma; Hodgkin lymphoma
Hepatitis B virus	Liver cancer
Human papillomavirus	Cervical cancer
Human T-cell leukaemia virus type 1	Adult T-cell leukaemia
Hepatitis C virus	Liver cancer
Kaposi's sarcoma-associated herpesvirus	Kaposi's sarcoma; Primary effusion lymphoma
Merkel cell polyomavirus*	Merkel cell carcinoma

*A causal association between Merkel cell polyomavirus and Merkel cell carcinoma has yet to be formally established.

1.4. The innate immune system

The aims of this thesis are to investigate how the KSHV-encoded vIRF2 and vIRF4 proteins regulate the innate immune system. The next part of this introduction will therefore outline the innate immune system. It will focus on how viral components are detected by cells, and in turn how the cell brings about an antiviral response. Examples of how viral proteins downregulate the innate immune system will also be provided.

1.4.1. Overview of innate immune signalling

The innate immune system is the first line of defence against invading organisms. The main role of this system is to detect pathogens and to bring about a response which removes them from the host cell and the host. The innate immune system detects microorganisms through proteins called pattern recognition receptors (PRRs). PRRs recognise either common features of pathogens known as pathogen-associated molecular patterns (PAMPs) or danger-associated molecular patterns (DAMPs) which are endogenous molecules released from dying cells. Different PRRs react with specific PAMPs and in the case of viruses, viral RNA or DNA can be detected by a variety of PRRs including toll like receptors (TLRs) and cytosolic receptors sensing RNA or DNA. These will be detailed in the following sections. After the detection of PAMPs, signalling cascades are evoked, which lead to the production of type I IFNs. There are three types of IFN; I, II, and III. In humans type I IFNs include IFNα and IFNβ (which are the focus of much of this thesis) as well as IFNω, IFNε and IFNκ. Type II IFN consists of IFNγ only (Pestka et al., 2004) and it is produced by T-cells and natural killer cells in order to activate

cells of the immune system. Type III IFNs consist of IFN-λ1, -λ 2, and -λ 3 (also called interleukin-29 [IL-29], IL-28A, and IL-28B, respectively) (Kotenko et al., 2003). Following production of type I IFNs, a second signalling cascade is triggered, which is referred to in this thesis as the JAK-STAT signalling pathway. This pathway leads to the production of proteins which have antiviral effects.

1.4.2. The IFN production pathway

The detection of viral components by a variety of mechanisms leads to the activation of signalling pathways. These result in the production of type I IFNs and pro-inflammatory cytokines. These pathways will be discussed in the following, and throughout this thesis these pathways will be collectively known as the IFN production pathway.

1.4.3. TLRs

TLRs are the best characterised PRRs, and they are evolutionarily conserved. TLRs were first identified in *Drosophila melanogaster* (Lemaitre et al., 1996) and there are currently 10 known human TLRs. They are located in different areas of the cell, to enable the recognition of different PAMPs (see Table 1.2). TLRs have three main domains, the extracellular domain, which is responsible for ligand binding, the transmembrane domain, and the cytoplasmic Toll-IL-1 receptor (TIR) domain which interacts with adapter proteins to activate signalling cascades. The myeloid differentiation factor 88 (MyD88) is a key protein recruited to activated TLRs and it is used by all but TLR3 in downstream signalling (reviewed in

Takeuchi and Akira, (2010)). Activation of such pathways results in the production of pro-inflammatory cytokines. TLRs 3, 7 and 9 are important sensors of viral PAMPs and their downstream signalling pathways also result in the production of type I IFNs. These TLRs are located in endosomes, and they detect viral nucleic acids. The specific signalling pathways are discussed in more detail below.

Table 1.2: PRRs: Location and ligands

Receptor	Location	Ligands detected
TLR1	Plasma membrane	Lipoproteins
TLR2	Plasma membrane	Lipoproteins
TLR3	Endosome	dsRNA
TLR4	Plasma membrane	LPS
TLR5	Plasma membrane	Flagellin
TLR6	Plasma membrane	Lipoproteins
TLR7	Endosome	ssRNA
TLR8	Endosome	ssRNA
TLR9	Endosome	Un-methylated CpG
TLR10	Endosome/Plasma membrane	Unknown
RIG-I	Cytosol	dsRNA
mda-5	Cytosol	dsRNA
STING	Cytosol	Activated by other sensors
DAI	Cytosol	dsDNA
RNA Pol III	Cytosol	dsDNA
IFI16	Cytosol/Nucleus	DsDNA
cGAS	Cytosol	dsDNA

1.4.3.1. TLR3 signalling

TLR3 senses dsRNA and signals via a MyD88-independent route (Alexopoulou et al., 2001). dsRNA is a key feature of infection by many viruses. Positive stranded RNA viruses, dsRNA viruses and DNA viruses have been shown to produce dsRNA following infection of cells (Weber et al., 2006) and hence, the immune system has evolved to detect these viral signatures. A synthetic form of dsRNA, polyinosinic-polycytidylic acid (poly(I:C)) is an efficient inducer of the IFN response

and is commonly used to study IFN induction (Fuld et al., 2006, Areste et al., 2009).

When dsRNA binds to TLR3, it activates a signalling cascade which results in the production of pro-inflammatory cytokines and type I IFNs. Activated TLR3 recruits the adaptor protein TIR-domain-containing adapter-inducing interferon-β (TRIF) via its TIR domain (Yamamoto et al., 2002). TRIF can then recruit both TNF receptor associated factor 3 (TRAF3) and TRAF6. These two proteins allow signalling to diverge into two pathways, one which activates IRF3, and the other which activates NFκB.

Recruitment of TRAF3 causes activation of TANK-binding kinase 1 (TBK-1) and IκB kinase. These activated kinases lead to phosphorylation and dimerization of Interferon regulatory factor 3 (IRF3) (Matsumoto and Seya, 2008) allowing it to translocate to the nucleus and activate the transcription of type I IFNs as part of the IFNβ enhanceosome (Honda et al., 2006).

TRIF can also associate with TRAF6 (Sato et al., 2003) and this association leads to phosphorylation and activation of the IκB kinase (IKK) complex which enables the translocation of NFκB into the nucleus. NFκB is normally found in the cytoplasm. It is retained here due to its interaction with the inhibitor molecule IκB. IκB is phosphorylated by activated IKK which leads to its ubiquitination and degradation, allowing NFκB nuclear translocation. Activated NFκB can induce the

production of pro-inflammatory cytokines and type I IFN genes (reviewed in Hayden and Ghosh (2004) and Takeuchi and Akira (2010)) (see Figure 1.5).

1.4.3.2. TLR7 signalling

TLR7 recognizes single stranded RNA (ssRNA) (Diebold et al., 2004) as well as small purine compounds (imidazoquinolines) (Hemmi et al., 2002). TLR7 signalling involves the MyD88 adapter protein. Activation of TLR7 recruits MyD88, which then recruits IL-1R-associated kinase (IRAK4). IRAK4 activates other IRAK family members, IRAK1 and IRAK2 which interact with TRAF6 (Takeuchi and Akira, 2010, Randall and Goodbourn, 2008). As described for TLR3 signalling, TRAF6 leads to the activation of NFkB and production of pro-inflammatory cytokines.

A complex consisting of MyD88, TRAF6, IRAK-1 and IRAK-4 binds directly to IRF7 which leads to the phosphorylation of IRF7 (Kawai et al., 2004). Phosphorylated IRF7 can then translocate to the nucleus where it activates the transcription of type I IFNs (see Figure 1.5) (Takeuchi and Akira, 2010, Randall and Goodbourn, 2008).

1.4.3.3. TLR9 signalling

TLR9 detects unmethylated DNA. This is in contrast to human DNA, which is heavily methylated, and thus the detection of unmethylated DNA by TLR9 enables distinction between self and pathogen (Randall and Goodbourn, 2008). Once activated, TLR9 signals as described for TLR7 (see Figure 1.5).

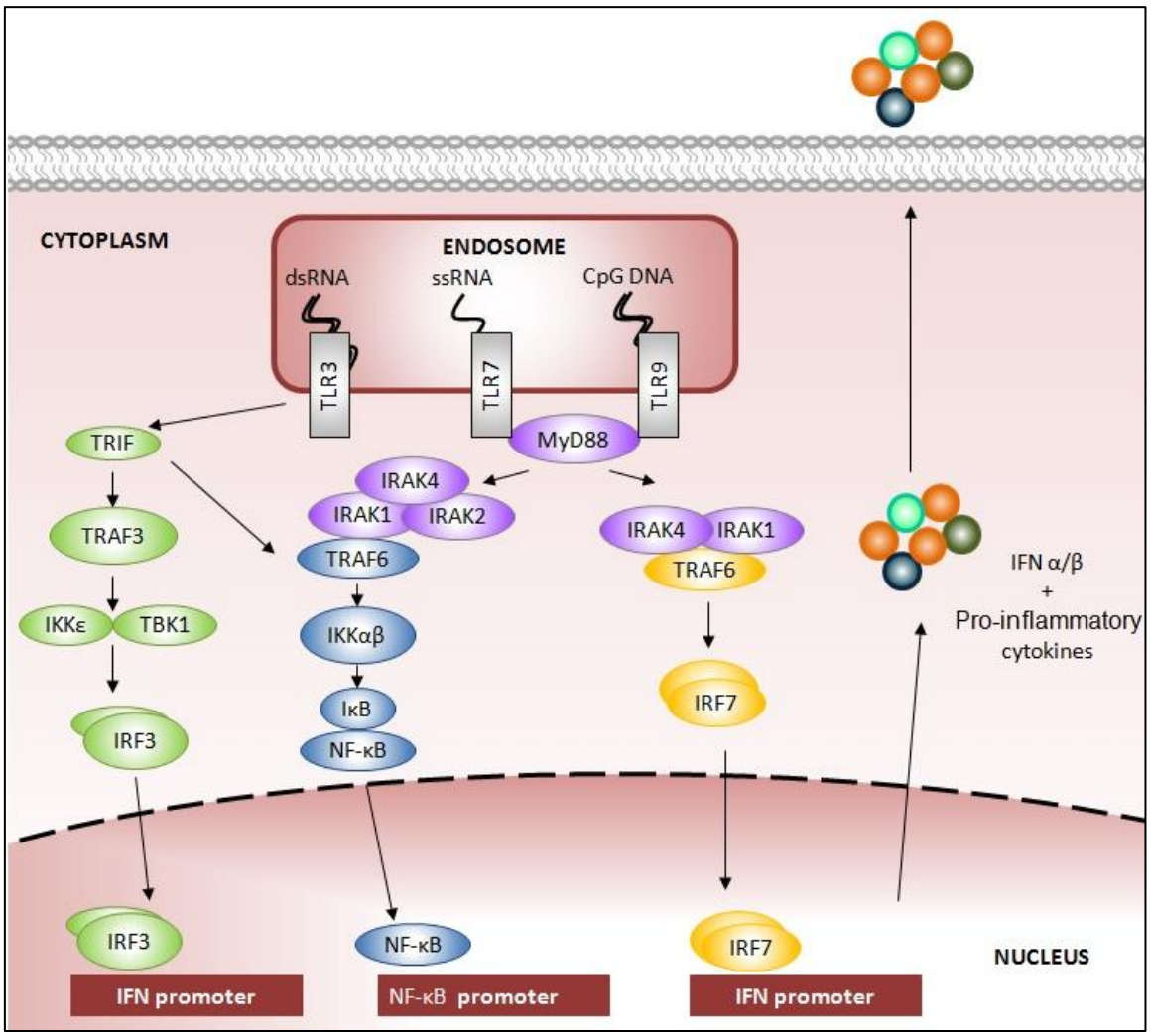

Figure 1.5: TLR signalling in response to viral nucleic acids.

TLRs 3, 7 and 9 are found in endosomes. Detection of ligands triggers signalling cascades. TLR3 recognises dsRNA and signals via a MyD88-independent pathway, inducing production of IFNs and pro-inflammatory cytokines. TLR7 recognises ssRNA and TLR9 recognises CpG-unmethylated DNA. Both TLR7 and TLR9 signal via MyD88-dependent pathways, inducing production of IFNs and pro-inflammatory cytokines.

1.4.4. Cytoplasmic RNA sensors

Two key cytoplasmic sensors of RNA are retinoic acid inducible gene I (RIG-I) and melanoma differentiation-associated gene 5 (MDA5). These receptors are members of the RIG-I-like receptor (RLR) family and recognize dsRNA. RIG-I was identified by Yoneyama et al, (2004) as a regulator for dsRNA-induced signalling. RIG-I has a caspase recruitment domain (CARD) which can induce IRF3 and NFκB signalling resulting in the production of type I IFNs (Yoneyama et al., 2004). MDA5 was identified by Andrejeva et al, (2004) when they found that the V proteins of paramyxoviruses bound to it and repressed IFNβ promoter activity (Andrejeva et al., 2004). Examination of MDA5 revealed that it contained a CARD and overexpression of this protein activated the IFNβ promoter in the presence of dsRNA (Andrejeva et al., 2004).

The CARDs of RIG-I and MDA5 trigger signalling cascades by recruiting a CARD-containing adaptor protein called IFN-β-promoter stimulator 1 (IPS-1) (also known as CARD adaptor inducing IFN-β (Cardif) or virus-induced signalling adaptor (VISA) or mitochondrial antiviral signalling protein (MAVS)) (Kawai et al., 2005, Seth et al., 2005, Xu et al., 2005, Gale and Foy, 2005), from now on referred to as IPS-1. This protein is found at mitochondrial membranes. The resulting signalling cascades are thought to proceed in a similar manner to TLR3 signalling through TRAF3 and TRAF6, and thus activate the production of type I IFNs and pro-inflammatory cytokines (Randall and Goodbourn, 2008). This pathway is illustrated in Figure 1.6.

1.4.5. DNA sensors

In recent years, many DNA sensors have been identified, and the following will outline some of these sensors. The stimulator of interferon genes (STING) is an important signalling protein which activates type I IFN genes in response to cytosolic DNA (Burdette and Vance, 2013). STING does not bind DNA directly, instead other DNA sensors have been identified which sense DNA, and then activate STING (see below and Figure 1.6). The C-terminal domain of STING provides a scaffold and recruits IRF3 in close proximity to TBK1, leading to TBK1-dependent phosphorylation of IRF3 (Tanaka and Chen, 2012) and thus activation of type I IFN genes.

Unterholzner et al, (2010) identified IFI16 as a DNA sensor which acts through STING. IFI16 binds dsDNA and recruits STING to induce signalling which causes production of type I IFNs (Unterholzner et al., 2010). IFI16 can be found cytoplasmically and in the nucleus, giving rise to the idea that DNA sensors could be found in the nucleus also.

Recently, Wu et al, (2013) identified that cyclic-GMP-AMP (cGAMP) could activate IFN production in response to cytosolic DNA. They found that cGAMP could bind to STING leading to activation of IRF3. Sun et al, (2013) then identified that cGAMP synthase (cGAS), which binds to DNA, could induce the synthesis of cGAMP from ATP and GTP. These results combined with those of Wu et al, (2013), indicate that cGAS is a cytosolic DNA sensor that binds to DNA and

synthesises the production of cGAMP. cGAMP then activates type I IFN genes via STING.

Ablasser et al., (2009) and Chiu et al, (2009) identified RNA polymerase III as a cytoplasmic DNA sensor. RNA polymerase III shown to use DNA as a template, to make 5'triphosphoate RNAs, which would then activate RIG-I and activate the production of type I IFNs as described in section 1.4.4. Ishikawa and Barber (2008) showed that RIG-I can associate with STING and thereby activate IFN promoter activation (Ablasser et al., 2009, Chiu et al., 2009). Hence the transcription of DNA to RNA by RNA polymerase III allows the utilisation of RIG-I and STING to activate type I IFN production.

Takaoka et al (2007) identified the DNA-dependent activator of IFN-regulatory factors (DAI) protein as a cytoplasmic sensor of DNA. It was found to bind to DNA and activate IRF3, leading to an increase in type I IFN genes in response to DNA stimulation. Increasing the significance of this observation, DeFilippis et al, (2010) showed that DAI is essential for activation of type I IFN genes following CMV infections. It remains to be seen if DAI functions through STING.

Figure 1.6 illustrates how the DNA sensors described above feed into signalling pathways which activate the production of type I IFNs.

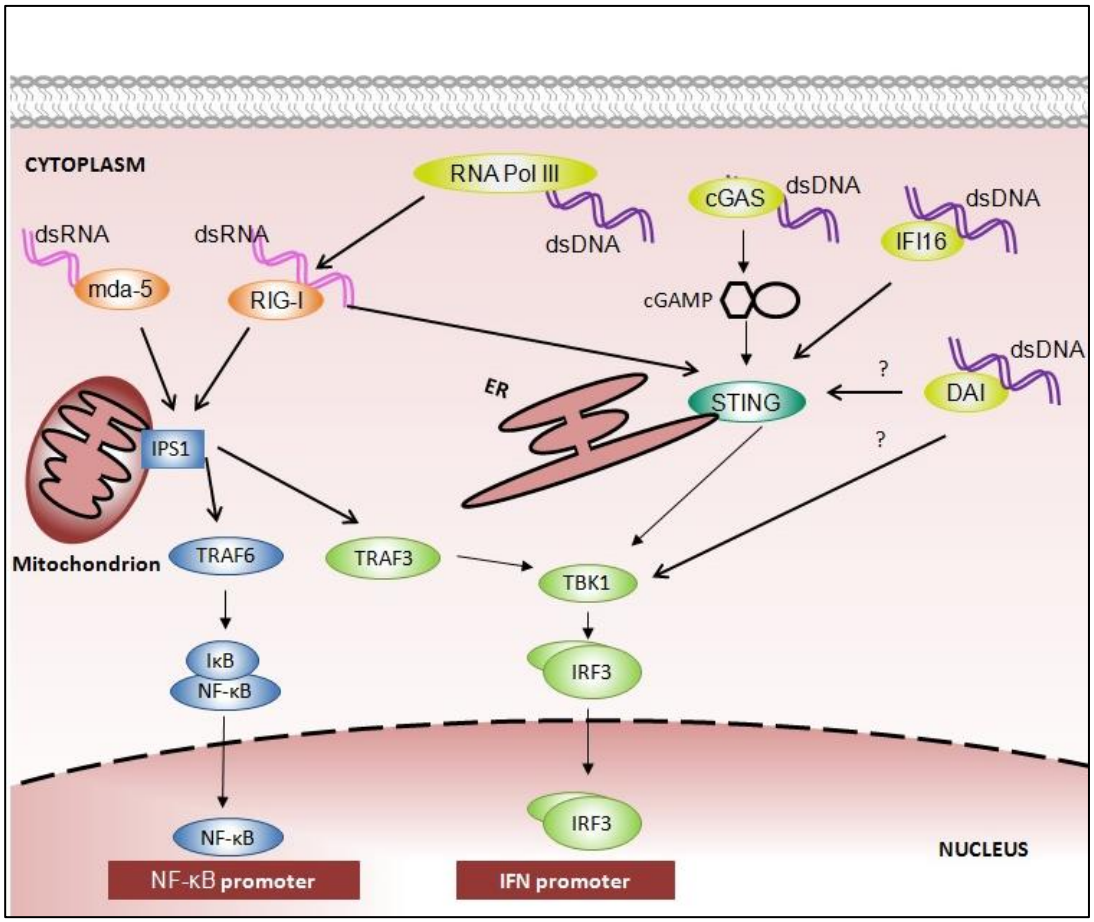

Figure 1.6: Cytoplasmic sensors of nucleic acids.

RNA is sensed by RIG-I and MDA5, which signal via IPS-1 to activated IRF3. DNA can be converted to RNA by RNA polymerase III, and this RNA can then activate RIG-I. DNA can also be sensed by IFI16, cGAS and DAI, and these sensors activate IRF3 via STING.

1.4.6. The IFNβ enhanceosome

The transactivation of the IFNβ promoter is understood in detail and involves the formation of the IFNβ enhanceosome. This process will be briefly outlined. The IFNβ promoter element contains four positive regulatory domains (PRD) I, II, III and IV, which are nucleosome-free. Transcription factors are able to bind these regions specifically. The IRF proteins bind to PRD I and III, NFκB binds to PRD II, and AP-1 (a heterodimer composed of activating transcription factor 2 (ATF2) and c-Jun) binds to PRD IV. Together these are known as the IFNβ enhanceosome. The IFNβ enhanceosome can recruit histone acetyltransferases (HATs) including the general control of amino acid synthesis 5 (GCN5) and CREB binding protein (CBP). The transcriptional start site for the IFNβ promoter is blocked by the presence of the nucleosome, but acetylation of histones within this nucleosome by GCN5 and CBP lead to its displacement. Transcription factor II D (TFIID) and RNA polymerase II can then be recruited to the start site of the IFNβ promoter, leading to transcription initiation (Panne, 2008, Honda et al., 2006)

1.4.7. Viral evasion of the IFN production pathways

Since the TLR and cytoplasmic nucleic acid sensing pathways allow the detection of viral components in order to bring about antiviral effects, it is not surprising that viruses have evolved to evade and augment these signalling systems. There are so many ways in which viruses can do this, and a few examples will be described briefly in the following. Figure 1.7 illustrates these mechanisms.

TRIF is a key component of the MyD88-independent signalling as it brings about the activation of IRF3 and NFκB. The hepatitis C virus (HCV) encoded NS3/4A protease cleaves the TRIF protein, inhibiting IRF3 and NFκB signalling (Li et al., 2005a).

IRF3 activates the transcription of type I IFNs, many of the signalling pathways described above result in the activation of IRF3, and thus it is an important protein. The KSHV-encoded vIRF2 protein targets IRF3, and this mechanism is discussed in section 1.5.2. Another example of a virus protein targeting IRF3 is the rotavirus NSP1 protein. NSP1 inhibits IFNβ promoter activation by binding to IRF3 and causing its degradation via the proteasome (Barro and Patton, 2005).

Cytoplasmic sensing of RNA is important in the detection of RNA viruses. As described in section 1.4.4, RIG-I is a cytoplasmic sensor of dsRNA which activates signalling via its CARD domain through the mitochondrion-located IPS-1 protein. Human Respiratory Syncytial Virus (HRSV) encodes the non-structural protein 2 (NS2), which can inhibit RIG-I mediated signalling. NS2 binds to the CARD domain of RIG-I and prevents the interaction with IPS-1 which turn represses the production of Type I IFNs (Ling et al., 2009). IPS-1 is a vital signalling component in RIG-I and MDA5 activated signalling following dsRNA detection. Hence, viruses also target this protein. One example is the HCV NS3/4A protein that cleaves IPS-1, resulting in its dislocation from the mitochondria. This dislocation blocks IFNβ induction (Li et al., 2005b).

The HCV encoded NS4B protein, identified as an inhibitor of the IFNβ promoter, functions by down-regulating DNA sensing pathways. Through immunoprecipitation studies, NS4B was shown to bind to STING, blocking its interaction with TBK-1, thus inhibiting downstream signalling pathways (Ding et al., 2013).

Finally, the IFNβ enhanceosome enables the transcription of IFNβ, and again is targeted by viral proteins. The KSHV-encoded LANA protein inhibits the production of IFNβ by disrupting the formation of the IFNβ enhanceosome. LANA can bind to the PRD I and III, and compete with IRF3 for these binding sites. In the presence of LANA, IRF3 binding to the IFNβ promoter was reduced (Cloutier and Flamand, 2010).

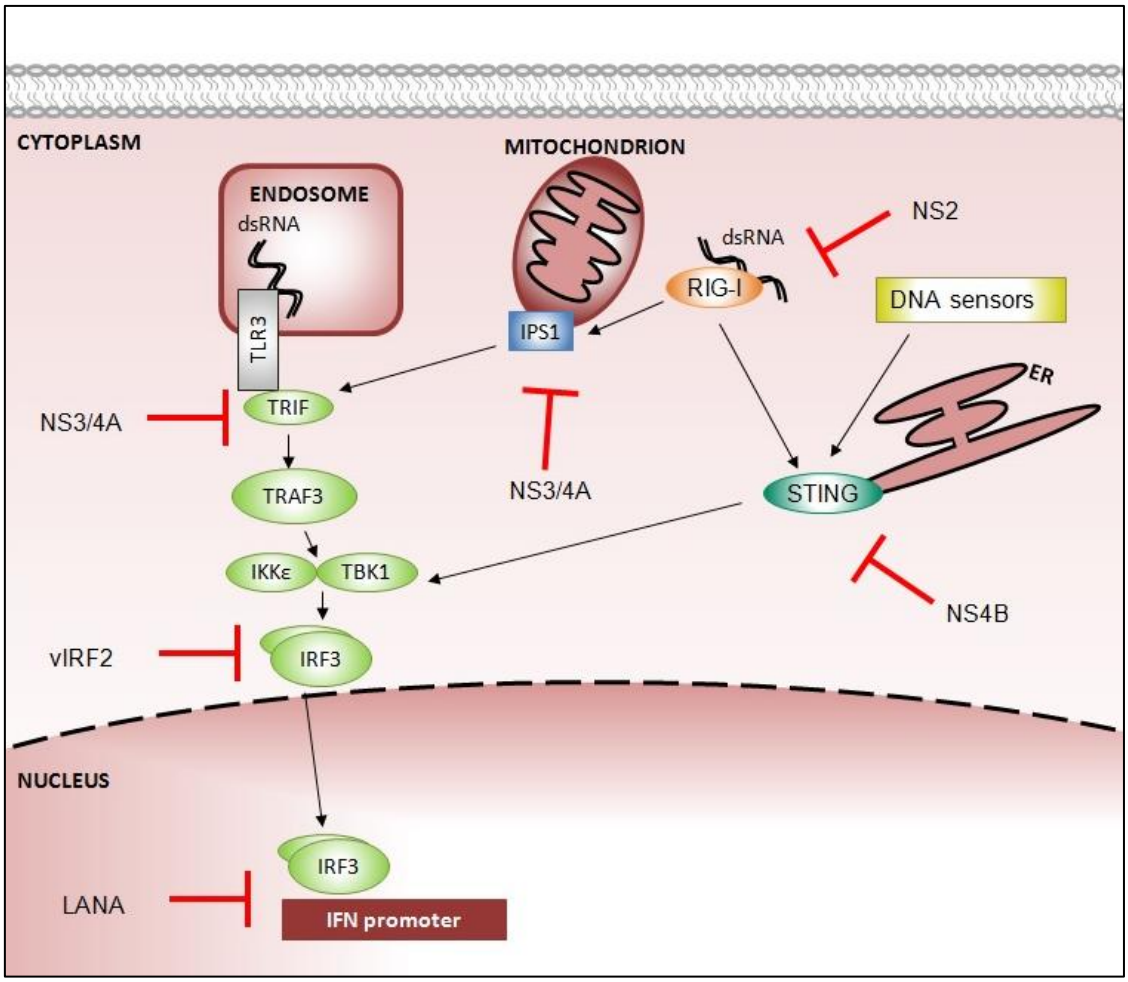

Figure 1.7: Viral inhibition of the IFN production pathway.

An Illustration of how viral proteins, mentioned in section 1.4.7, can target components of the IFN production pathway. This figure shows selected signalling components of the IFN production pathway. For more detailed signalling pathways see Figure 1.5 and Figure 1.6. The TLR3 activation pathway is shown as the NS3/4A protein, encoded by HCV targets TRIF, and KSHV-encoded vIRF2 cause IRF3 degradation. The RIG-I cytoplasmic sensor of RNA is inhibited by the HRSV encoded NS2 protein and IPS1 is cleaved by NS3/4A. The regulator of DNA sensors, STING is targeted by the HCV encoded NS4B protein. Finally, formation of the IFNβ enhanceosome is targeted by LANA.

1.4.8. JAK-STAT signalling

The pathways described in the previous sections above are collectively known throughout this thesis as the IFN production pathway. This signalling pathway results in the production of IFNα/β, which are secreted from cells. These cytokines bind to receptors on the surface of cells and activate the JAK-STAT signalling pathway. This signalling pathway results in activation of interferon stimulated response element (ISRE)-containing promoters, which are present in most IFN stimulated genes (ISGs). ISGs encode proteins which have antiviral effects. Thus, the antiviral effect of the type I IFNs are exerted by the induction of ISGs. This thesis examined the JAK-STAT signalling pathway, and therefore it will be described in detail in the following.

The JAK-STAT signalling pathway is activated by binding of IFNα/β to IFNα receptors 1 and 2 (IFNAR1 and IFNAR2) (Novick et al., 1994, Darnell et al., 1994). These receptors are transmembrane proteins which are located separately prior to IFN stimulation. The cytoplasmic tail of IFNAR1 is associated with tyrosine kinase 2 (Tyk2) and the IFNAR2 subunit is associated with the tyrosine kinase JAK1. Upon binding of IFNα/β, the receptors dimerize, which causes a conformational change (Darnell et al., 1994). Tyk2 phosphorylates tyrosine 466 on IFNAR1 (Colamonici et al., 1994) which serves as a docking site for Signal Transducer and Activator of Transcription (STAT) 2 via its Src Homology 2 (SH2) domain, which is subsequently phosphorylated (Yan et al., 1996). Phosphorylated STAT2 recruits STAT1, which then becomes phosphorylated by JAK1 (Leung et al., 1995, Randall and Goodbourn, 2008). STAT1 and STAT2 can now associate with IRF9 to form

the interferon-stimulated gene factor 3 (ISGF3) complex (Fu et al., 1990, Randall and Goodbourn, 2008). Phosphorylated STAT1-STAT2 dimers form a nuclear localisation sequence (NLS which causes the translocation of this complex into the nucleus. As well as phosphorylation, acetylation is important in the formation and function of ISGF3. Tang et al, (2007) showed that in response to type I IFN stimulation, CBP is recruited to the IFNAR2 and acetylates it. This creates a docking site for IRF9 which is then acetylated. Receptor bound STAT1 and STAT2 are also acetylated by CBP. The acetylation of IRF9 and STAT2 is critical for ISGF3 function (Randall and Goodbourn, 2008, Tang et al., 2007). Figure 1.8 illustrates this pathway.

In the nucleus the ISGF3 complex binds to ISRE sequences in the promoters of ISGs. The consensus ISRE sequence is AGTTTCNNTTTCNC/T (Darenell 1994), where 'N' is any nucleotide. IRF9 participates in binding to ISRE and the STAT1 and STAT2 proteins stabilise the association (Kessler et al., 1990). Both STAT1 and STAT2 associate with HATs CBP/p300 (Bhattacharya et al., 1996, Zhang et al., 1996) that are thought to be important in the transcription of ISGs following ISGF3 binding to ISREs. CBP/p300 have the ability to acetylate histones which makes DNA more accessible to transcriptional activators. The STAT2-CBP association occurs at the C-terminal domain of STAT2 (Bhattacharya et al., 1996), which is essential for transactivation of ISGs (Qureshi et al., 1996). Both the C- and N- terminal domains of STAT1 bind to CBP/p300 (Zhang et al., 1996). STAT2 also interacts with the general control non-depressible 5 (GCN5), another HAT transcriptional co-activator which promotes transcriptional activation. Interaction of

STAT2 with HATs results in localised acetylation of histones (Paulson et al., 2002). STAT2 also associates with the Brahma-related gene 1 (BRG1) protein, which is a key component of the ATP-dependent chromatin-remodelling complex. BRG1 can enhance the IFN-α-induced expression of certain ISGs (Huang et al., 2002). Further work in this area is necessary to identify how these HATs and associated factors contribute to ISGs transactivation.

1.4.9. Viral evasion of JAK-STAT signalling

Viruses target all stages of JAK-STAT signalling, from the IFNARs to the formation of the ISGF3 complex. Similar to section 1.4.7, some examples of viruses which evade the JAK-STAT signalling pathway will now be provided, focusing on the ISGF3 complex. Figure 1.8 illustrates these mechanisms.

STAT1 is part of the ISGF3 complex and is necessary for induction of ISGs. As such, STAT1 is a viral target. The C proteins of Sendai virus can interact with STAT1 to prevent JAK-STAT signalling. The larger C proteins cause proteasome-mediated degradation of STAT1 (Garcin et al., 2002). Additionally the P protein encoded by Nipah virus can sequester inactive STAT1 in the cytoplasm to prevent its nuclear translocation (Ciancanelli et al., 2009).

STAT2 is another member of the ISGF3 complex, and is again targeted by viruses. Dengue Virus (DENV) infection causes the degradation of STAT2, which enables it to limit type I IFN signalling transduction decreasing ISG expression

(Jones et al., 2005). The NS5 protein of DENV prevents the phosphorylation of STAT2 and consequently, IFNα mediated signalling (Mazzon et al., 2009). Similarly, the expression of HRSV NS1 and NS2 proteins cause the degradation of STAT2 (Lo et al., 2005).

IRF9, the third member of the ISGF3 complex is targeted by the E7 protein encoded by the human papillomavirus (HPV) 16. The E7 protein can inhibit the activation of ISGs following IFNα stimulation and is thought to do so by preventing the translocation of IRF9 into the nucleus (Barnard and McMillan, 1999).

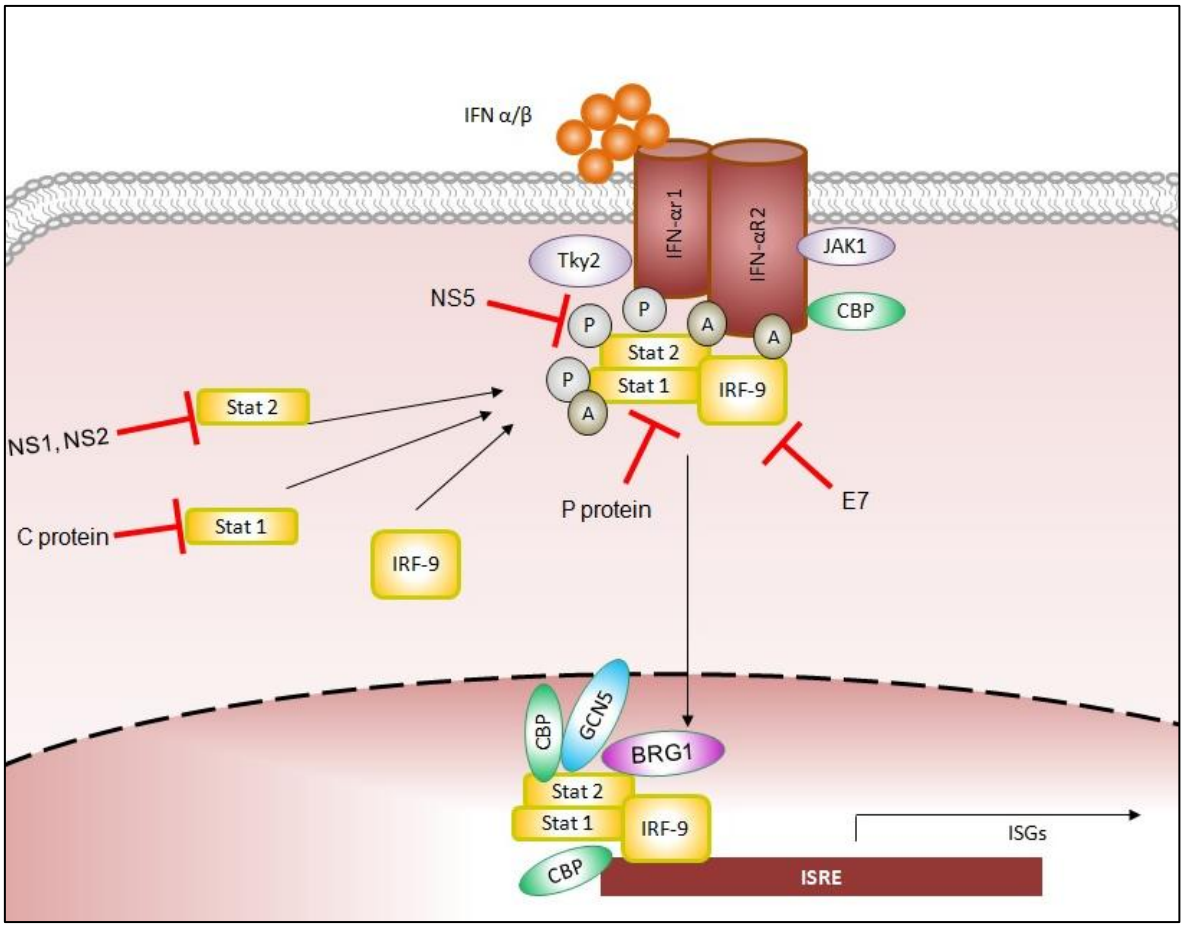

Figure 1.8: The JAK-STAT signalling pathway, and viral proteins which inhibit it.

Activation of the IFN receptors causes dimerization and activation of the JAK-STAT signalling pathway. STAT1, STAT2 and IRF9 are recruited to the IFN receptors, and are phosphorylated and acetylated. The resultant ISGF3 complex translocates to the nucleus and binds to the ISRE consensus sequences transactivating ISGs. Viral proteins which downregulate JAK-STAT signalling, by targeting components of this pathway, are indicated. The C proteins of Sendai virus lead to the degradation of STAT, while The P protein of Nipah virus inhibits STAT1 translocation. The NS1 and NS2 proteins encoded by HRSV cause STAT2 degradation and DENV NS5 protein inhibits STAT2 phosphorylation. Finally, the E7 protein encoded by HPV inhibits IRF9 translocation.

1.4.10. Activation of antiviral genes and their effects

The activation of the JAK-STAT signalling pathway up-regulates the expression of many genes which bring about an antiviral state. The following sections will detail some of these genes and the effects of the proteins they encode. Examples of viruses which target these proteins will also be included.

1.4.10.1. Protein kinase R

The dsRNA-dependent protein kinase (PKR) is up-regulated by type I IFNs. PKR is a serine threonine kinase which has many roles in the antiviral defence mechanism of the host. This protein normally exists in an inactive form as a monomer. PKR binds to dsRNA with its N-terminal dsRNA-binding motifs, and this leads to dimerization of two PKR monomers. These are then autophosphorylated, which leads to the formation of an active PKR dimer (Garcia et al., 2006). Eukaryotic initiation factor 2 (eIF2*α*) is phosphorylated by active PKR, which prevents the recycling of this factor leading to a halt in translation initiation within the cell (Randall and Goodbourn, 2008). This inhibitis the translation of viral (and cellular) mRNAs, and is thus an antiviral effect.

The vIRF2 protein downregulates the antiviral effect of IFN as it can rescue translation of vesicular stomatitis virus (VSV) mRNA translation (Burysek and Pitha, 2001). These same authors also showed that vIRF2 binds to PKR and can inhibit the phosphorylation of eIF2α, hence evading antiviral effects induced by IFN stimulated PKR. However, it must be noted that these studies were performed only on the first exon of vIRF2, and not the full length protein.

1.4.10.2. Mx

The Mx proteins, comprised of MxA and MxB in humans, are large GTPases and their expression is dependent on type I IFN stimulation. Mx is very important in controlling the infections of RNA viruses. For example, mice with Mx are less susceptible to influenza infection than those without (Haller et al., 1980). In mice, Mx inhibited viral RNA synthesis of Measles virus (Schneider-Schaulies et al., 1994). Mx can recognise nucleocapsid proteins in the cytoplasm and restrict their movement into the nucleus, which prevents the virus from replicating. Both the central interacting domain and the C-terminal domain of Mx proteins are required to recognise target viral structures (Kochs and Haller, 1999).

Hepatitis B virus (HBV) precore or core protein can interact with the MxA promoter to prevent MxA gene expression, highlighting a mechanism of viral evasion from ISGs (Fernandez et al., 2003).

1.4.10.3. ISG15

ISG15 is induced by IFNs. It functions in a similar manner to ubiquitin, as it can be joined covalently to many cellular proteins via its C-terminal LRLRGG motif which is referred to ISGylation. The mechanism of how it exerts its antiviral effects remains unknown, but ISGylation does not lead to degradation of the target protein, rather its activation or inactivation (Sadler and Williams, 2008). Many proteins which are ISGylated are involved in the IFN signalling, for example JAK1, STAT1, RIG-I, MxA, PKR and RNaseL (Zhao 2005). The importance of ISG15 is highlighted in IFNAR knockout mice, as they were protected against Sindbis virus-

induced lethality when ISG15 was expressed (Lenschow et al., 2005). ISGylation of IRF3 has also been shown to prevent proteolysis of IRF3 mediated by viruses, increasing production of type I IFNs (Lu et al., 2006).

1.4.10.4. 2’5’ Oligoadenylate synthetase and RNAse L

Oligoadenylate synthetase (OAS) and RNase L are induced by type I IFNs. They are involved in a pathway activated by dsRNA, which results in the degradation of viral and cellular RNAs, leading to a block in viral infections (Silverman, 2007). Like PKR, OAS is natively inactive and dsRNA stimulates its activation. Active OAS uses ATP to produce 2’5’-linked oligoadenylates, which bind to the endoribonuclease RNase L, and cause inactive RNase L monomers to form active dimers (Dong and Silverman, 1995). These dimers can cleave both viral and cellular mRNA, inhibiting viral replication and protein synthesis (Silverman, 2007). Furthermore, these cleaved mRNAs can then be detected by MDA5 and RIG-I leading to the production of type I IFNs (see section 1.4.4).

Murine Coronavirus NS2 protein can cleave 2’5’-oligoadenylate, preventing RNase L activation. This block on RNA degradation is thus a mechanism by which a virus evades the ISGs effects (Zhao et al., 2012).

1.5. KSHV-encoded vIRFs

An introduction to the KSHV-encoded vIRFs will now be provided, and will focus on their effects on IFN signalling.

The vIRF genes are found in a cluster within the KSHV genome between ORFs 57 and 58. They are encoded by ORFs K9 (vIRF1), K11/11.1 (vIRF2), K10.5/10.6 (vIRF3), and K10 (vIRF4) (see Figure 1.3) (Russo et al., 1996). These vIRFs have some homology to cellular IRFs, but they are predicted not to bind to DNA directly as they encode only 2 of the 5 tryptophan repeats found within the DNA-binding domain (DBD) of cellular IRFs (Cunningham et al., 2003).

1.5.1. vIRF1

The lytic vIRF1 protein can downregulate both the IFN production pathway and the JAK-STAT signalling pathway and is thus an important immunomodulatory protein. vIRF1 inhibits the activation of IFNα by binding to CBP/p300 (Burysek et al., 1999a). vIRF1 competes with IRF3 for binding to CBP, leading to a reduction of IRF3-CBP complexes (Lin et al., 2001). This complex is important in the formation of the IFNβ enhanceosome (see section 1.4.6). vIRF1 also inhibits the activation of ISRE-containing reporters (Gao et al., 1997, Li et al., 1998). This viral protein may also contribute to tumour formation as it inhibits the activation and stabilisation of the tumour suppressor, p53 (Baresova et al., 2013) . p53 responds to signals, such as DNA damage, or viral infections and can halt the cell cycle and lead to apoptosis. Attenuation of p53 function is a frequent event leading to development of human cancers (Vogelstein et al., 2000).

1.5.2. vIRF2

The lytic vIRF2 is the focus of much of this thesis. Studies performed by Burysek et al, (1999b) examined only the first exon encoded by ORF K11.1 which they believed to be the full length vIRF2. However, it was later shown that full length vIRF2 is encoded by ORFs K11.1 and K11. Nonetheless, Burysek et al, (1999b) identified that the ORF K11.1 encoded protein could downregulate activation of the IFNα promoter (Burysek et al., 1999b). Later, experiments examining the effects of full length vIRF2 upon the IFN production pathways found that it also inhibited the activation of the IFNβ promoter. vIRF2 forms a multi-protein complex with IRF3 and caspase-3 that leads to the turnover of IRF3, meaning that the IFNβ promoter cannot be effectively transactivated (Areste et al., 2009, Fuld et al., 2006). Additionally, vIRF2 also downregulates JAK-STAT signalling and one proposed mechanism for this inhibition is through decreasing levels of the ISGF3 components, STAT1 and IRF9 (Mutocheluh et al., 2011, Fuld et al., 2006). The mechanisms of such degradation are unknown.

As discussed in section 1.4.10.1, another activity of the 1st exon of vIRF2 is to bind to the IFN induced PKR kinase, and inhibit the subsequent phosphorylation of eIF-2α and thus down stream antiviral effects of the type I IFNs (Burysek and Pitha, 2001).

1.5.3. vIRF3

The spliced vIRF3 gene product is expressed in latently infected PEL and MCD cells, but not in KS lesions. vIRF3 interacts with IRF7 to prevent the cellular

protein from binding DNA, thereby inhibiting IFNα promoter activation (Joo et al., 2007). vIRF3 also associates with IRF5. IRF5 can be activated by DNA damage, as well as by TLR7 and TLR9 signalling resulting in the activation of pro-inflammatory cytokines (Takaoka et al., 2005). IRF5 can also activate type I IFN promoters (Barnes et al., 2001). vIRF3 represses the activation of ISRE and IFNβ promoter elements by inhibiting binding of IRF5 to them (Wies et al., 2009). Moreover, the IκB kinase (see section 1.4.3.1) is targeted by vIRF3 decreasing NFκB activation (Seo et al., 2004). Additionally, vIRF3 targets the activity of the ISG product, PKR. vIRF3 expression decreases the PKR-mediated inhibition of protein synthesis and was shown to decrease the phosphorylation of eIF-2alpha (Esteban et al., 2003).

vIRF3 is classed as an oncogene as it inhibits the activity of p53. This viral protein directly interacts with p53 resulting in inhibition of p53 transcriptional activation. (Rivas et al., 2001). vIRF3 also activates the transcription of the cellular oncogene, c-Myc. c-Myc activates the expression of many genes involved in cell growth, proliferation and survival. vIRF3 interacts with an inhibitor of c-myc activity called Myc modulator 1 (MM-1). This interaction prevents MM-1 from suppressing c-myc activity, and thus increases activity of the oncogene (Lubyova et al., 2007).

1.5.4. vIRF4

Limited studies to date suggest that the lytic vIRF4 protein has no effect on the IFN production pathway, as no reduction in IFNβ promoter activity was observed following activation with Sendai Virus in the presence of vIRF4 (Kanno et al.,

2006). The effect of vIRF4 on the JAK-STAT signalling pathway remains to be identified, and much of this thesis focuses on this area.

Like vIRF1 and vIRF3, vIRF4 can also affect the tumour suppressor p53. Lee et al, (2009) showed that vIRF4 can interact with murine double minute 2 (MDM2), leading to decreased levels of p53. MDM2 can ubiquitinate p53, which targets it for proteasome-mediated degradation. The stability of MDM2 is self regulated, through autoubiquitination. vIRF4 stabilizes MDM2 by inhibiting MDM2 autoubiquitination, hence increasing MDM2 levels and therefore decreasing p53 levels (Lee et al., 2009). This is therefore one mechanism by which KSHV can evade the antiviral effects p53.

vIRF4 also interacts with Ubiquitin-specific-processing protease 7 (USP7) also known as herpesvirus-associated ubiquitin-specific protease (HAUSP). USP7 is a deubiquitylating enzyme, which can deubiquitinate p53, for example, protecting it from MDM2-mediated degradation (Lee et al., 2011).

1.5.5. Other KSHV-encoded inhibitors of type I IFN signalling

As well as the vIRFs, KSHV encodes other proteins which downregulate type I IFN signalling. As described in section 1.4.7, LANA competes with IRF3 for binding to the IFNβ promoter and therefore prevents the expression of this cytokine (Cloutier and Flamand, 2010). The immediate early protein K-bZIP, encoded by ORFK8 inhibits IRF3 from binding to the to IFNβ promoter. K-bZIP binds directly to the PRD I and III regions of the IFNβ promoter which causes low levels of IFNβ

transcription. However, this binding also prevents IRF3 from binding to the IFNβ promoter and inhibits the formation of the enhanceosome (Lefort et al., 2007). ORF45 is a key tegument protein, and an immediate-early gene. It can inhibit virus-mediated activation of type I IFN genes by suppressing IRF7 phosphorylation, which in turn prevents IRF7 nuclear accumulation and the subsequent transcription of IFNα and IFNβ (Zhu et al., 2002).

RTA, the lytic switch protein can also inhibit the type I IFN response. It does so by increasing the association between RTA-Associated Ubiquitin Ligase (RAUL) and USP7. RAUL can cause the proteasome-mediated degradation of IRF3 and IRF7, and USP7 stabilises RAUL. RTA enhances this interaction, and thus increases IRF3 and IRF7 degradation, leading to an inhibition in the activation of type I IFN promoters (Yu and Hayward, 2010). The KSHV regulator of IFN function (RIF) protein can also inhibit ISRE-containing reporter plasmids. It decreases phosphorylation of STAT1, STAT2 and inhibits their nuclear translocation. RIF associates with STAT2, JAK1 and both subunits of the IFN receptor, but the mechanism of it action is presently unclear (Bisson et al., 2009).

1.6. Aims and objectives of this thesis

The aims and objective of this thesis are divided into aims relating to the function fo vIRF2 and to those relating to the function of vIRF4.

1.6.1. Aims and objectives concering vIRF2

The aim of this thesis is to investigate if and how the KSHV-encoded vIRF2 and vIRF4 proteins can downregulate type I IFN signalling. The vIRF2 protein has been shown to downregulate both the IFN production pathway and JAK-STAT signalling. The mechanisms of such inhibitions are not fully understood and therefore more detailed understanding of the biology of vIRF2 in IFN signalling will be sought.

The objectives of this thesis are to:

1) Confirm the effect of vIRF2 on the IFN production pathway
2) Confirm the effect of vIRF2 on the JAK-STAT signalling pathway
3) Determine if vIRF2 can inhibit binding of the ISGF3 complex to ISRE sequences
4) Identify whether vIRF2 reduces levels of the components of the JAK-STAT signalling pathway
5) Identify the cellular protein binding partners of vIRF2 and investigate their relevance in IFN signalling

1.6.2. Aims and objectives concering vIRF4

Through limited studies to date, vIRF4 is not thought to modulate the IFN production pathway. However, its effects on JAK-STAT signalling are unknown. Therefore vIRF4 will be investigated in the context of JAK-STAT signalling and where any inhibitory effect is identified, the molecular mechanism will be sought.

The objectives are to:

1) Assess the effect of vIRF4 on the IFN production pathway
2) Assess the effect of vIRF4 on the JAK-STAT signalling pathway
3) Elucidate the mechanism of vIRF4-mediated inhibition on either of these pathways by identifying the cellular partner proteins of vIRF4 and understand their possible roles in modulating IFN signalling.

CHAPTER 2

MATERIALS AND METHODS

2.1. Tissue culture methods

The following will outline the materials and methods used for tissue culture techniques. All such techniques were carried out in laminar flow hoods under sterile conditions. Table 2.1 provides a list of media and supplements used for tissue culture techniques.

Table 2.1 Tissue culture media and supplements

Item	Source
Dulbecco's Modified Eagle's Medium (DMEM)	Sigma (D6429)
MemAQ	Sigma (M0446)
RPMI	Sigma (R8758)
Foetal Calf Serum (FCS)	PAA (A15-101)
Foetal Calf Serum (FCS) –No Tetracycline	Clone tech (631107)
Penicillin/Streptomycin	Invitrogen (15070063)
Glutamine	Invitrogen (25030123)
Trypsin	Invitrogen (12605010)
Non essential amino acids (NEAA)	Sigma (M7145)
DMEM complete	DMEM supplemented with 10% FCS, 1%Glutamine, 1%Penicillin/ Streptomycin and 1% NEAA.
SILAC-DMEM	DMEM supplemented with 10% FCS-No Tetracycline, 1%Glutamine, 1%Penicillin/ Streptomycin and 1% NEAA.
Zeocin	Invitrogen (R250-01)
Blasticidin	Merck Millipore (203351)
Tetracycline	Sigma (T7660)
Freezing media	90% FCS, 10% Dimethyl sulfoxide (DMSO)
Fibronectin	Sigma (F0895)
Trypan blue	Sigma (T10282)
Recombinant IFN α2b	Stratech (11115-1)
Phorbol myristate acetate (PMA)	Sigma (P8139)

2.1.1. Cell lines

Table 2.2 summarises the cell lines used throughout this study, detailing the media required for their maintenance. All cells lines were grown and maintained at

37°C in a humidified environment supplied with 5% CO_2. Cells were grown on various treated plastic vessels. For passage of adherent cells, the existing medium was removed, cells were then washed with phosphate buffered saline (PBS) and trypsin was added (37°C, until cells detached). Culture medium was then added to quench the trypsin and the cells were pelleted by centrifugation (5 minutes, 300*g*). Pellets were resuspended in fresh media, plated at the required number and stored in the incubator. For suspension cells, cells were pelleted by centrifugation (5 minutes, 300*g*), washed in PBS and resuspended at the required concentration using fresh media.

Table 2.2 Cell lines used in this study

Cell line	Suspension/ Adherent	Source	Origin	Culture media
239	Adherent	Embryonic kidney	Human	DMEM complete
T-Rex-293	Adherent	Invitrogen (R710-07)	Human	DMEM complete with 5µg/mL Blasticidin
BCBL1	Suspension	PEL	Human	RPMI
L929	Adherent	Adipose tissue	Mouse	DMEM complete
EV-NTAP, vIRF2-NTAP, vIRF4-NTAP	Adherent	T-Rex-293 cells stably transfected	Human	DMEM complete with 5µg/mL Blasticidin and 200µg/ml Zeocin

2.1.1.1. T-Rex-293 cell line

The Tetracycline-Regulated Expression (T-REX) cell lines stably express the tetracycline (Tet) repressor, from the pcDNA™6/TR plasmid which carries the Blasticidin resistance gene. These cells were used to create stable, tetracycline inducible, cell lines expressing the vIRF2-NTAP, vIRF4-NTAP or NTAP proteins.

The plasmids of choice (pvIRF2-NTAP, pvIRF4-NTAP or pCDNA4TO-NTAP) were linearised and transfected into these cells. Selection of stable transfectants was performed using Zeocin™ and Blasticidin.

2.1.2. Cell counting

Cell suspensions were diluted in Trypan blue solution at a 1:1 ratio and 10µl of this mixture was transferred to each chamber of a heamocytometer. The cells were counted under a light microscope. Since dead cells take up trypan blue dye it is possible to distinguish between dead and live cells.

2.1.3. Cryopreservation of cell lines

To keep a permanent stock, cells were stored as frozen stocks in liquid nitrogen. Cells were pelleted through centrifugation (5 minutes, 300*g*), the supernatant was removed and the cell pellet was resuspended in 1ml of freezing medium (90%FBS, 10% DMSO), in general, 1 x10^6 cells/ml of freezing medium, and added to a sterile 1.5ml cryovial. These vials were placed in a cryopreservation box (Mr Frosty, Nalgene), containing isopropanol, which was placed in a -80^{o}C freezer, allowing the cells to cool by 1^{o}C per minute. This method prevents lysis of cells through the freezing of water molecules. Vials were transferred into liquid nitrogen for long term storage.

2.1.4. Recovery of cryopreserved cells

Stock culture cell lines stored in liquid nitrogen were thawed in a 37°C water bath and washed in 10ml of appropriate complete media. The cells were then centrifuged (5 minutes, 300*g*) and the resultant pellet was resuspended in appropriate complete media before seeding in the normal manner.

2.1.5. Generating stable HEK-293 cell lines using the T-Rex system from Invitrogen

T-Rex-293 cells which stably express the tetracycline repressor, were plated out in a 6 well plate (4 X 10^5 per well) and left to adhere over night in antibiotic free media. The cells were transfected, using Lipofectamine 2000 with either the EV-NTAP, vIRF2-NTAP or vIRF4-NTAP vector which had been linearised with PvuI. 24 hours post transfection, the medium was changed to DMEM complete with 5µg/ml Blasticidin. After 24 hours, the cells were trypsinised and plated out in a T-25, in selective medium (DMEM complete with 5µg/ml Blasticidin and 200µg/ml Zeocin). This selective medium was changed every 3-4 days until Zeocin resistant colonies were detected. These colonies were cultured until the T-25 was confluent.

2.1.5.1. USP7 inhibitor

The P22077 USP7 inhibitor was purchased from R&D (4485). It was made up to a 10mM solution with DMSO, aliquotted and stored at -20º. Prior to use, an aliquot was thawed and diluted in DMEM to the desired concentration and added to cells.

2.1.6. Transfection of cells

Cells were transfected using Lipofectamine 2000 (Invitrogen), according to the manufacturer's instructions. Lipofectamine 2000 is a lipid-based system of delivering DNA plasmids into cultured eukaryotic cells. The amount of Lipofectamine 2000 and DMEM used were dependent on the size of the cell culture plate containing cells to be transfected. The required amount of DNA was added to one volume of DMEM, while at the same time adding Lipofectamine to another one volume of DMEM. These solutions were incubated at room temperature for five minutes, combined and left to incubate for a further 20 minutes, before being added drop wise onto cells.

2.2. Dual luciferase reporter assay

The dual luciferase reporter assay (DLA) system (Promega) measures the activities of two distinct luciferase enzymes, firefly (*Photinus pyralis)* and *Renilla* (*Renilla reinformis),* expressed from the same sample. The firefly luciferase signal is expressed by the promoter of interest and relates to the activity of that promoter. The constitutively active *Renilla* luciferase signal serves as internal control, to which the experimental reporter gene (firefly signal) is normalised. Cells were transfected (using Lipofectamine 2000 as described in section 2.1.6) with reporter plasmids containing either the firefly luciferase gene (driven by the promoter of interest), or the constitutively active *Renilla* luciferase plasmid (pRLSV40). After a specific time (dependent on the experiment), the cell medium was removed and the cells were washed gently with PBS. Cells were lysed using Passive Lysis Buffer (Promega) for a minimum of 10 minutes. To obtain results, 20µl of each

sample was added to the wells of a 96-well microtitre plate (Nunc) in duplicate. Samples were assayed using a luminometer (Gene Flow) which was purged by repeat priming with 2 ml of sterile distilled water per auto-injector, followed by priming with 600 µl of Luciferase Assay Reagent II (LARII) and 600 µl of the Stop & Glo Reagent through separate injectors. The programme for assaying samples is shown in Table 2.3. Relative activity is calculated by normalising the firefly values to their *Renilla* counterparts. Reporter plasmids use in this thesis are shown in Table 2.4.

Table 2.3: The programme for reading DLAs

Reporter plasmid	Information	Purpose
LARII	50µl	Activate firefly luciferase
Measurement	10 seconds	Measure firefly luciferse
Stop & Glo	50µl	Quenches firefly luciferase and Measures *Renilla* luciferase
Measurement	10 seconds	Measure *Renilla* luciferse

Table 2.4: Reporter plasmids

Reporter plasmid	Information
p125-luc	Full length IFN-beta promoter driving expression of a firefly luciferase reporter gene
pISRE-luc	Luciferase reporter vector containing tandem repeats of the ISRE element driving expression of the firefly luciferase reproter gene

2.3. Immunoblotting

Solutions and buffers used for immune blotting are shown in Table 9.1.

2.3.1. Protein extraction- sonication

Cells were washed twice with ice-cold PBS, on ice. 50µl (per well of a 6 well plate) of ice-cold sonication buffer was then added to the cells and they were collected using a cell scraper and transferred to a microfuge tube and placed on ice. Cells were sonicated for 15 seconds and centrifuged (10 minutes, 16,000*g* 4˚C) to remove cell debris. The supernatant was then transferred to a new tube and stored at -80˚C until further use.

2.3.2. Protein extraction- non-ionic detergent lysis buffer

Cells were washed twice with ice-cold PBS, on ice. 50ul (per well of a 6 well plate) of ice-cold non-ionic lysis buffer (see Table 9.1) was then added to the cells, which were then collected using a cell scraper, transferred to a fresh tube and placed on ice. The samples were rotated in a cold room (30 minutes, 4°C) before being centrifuged (10 minutes, 16,000*g* 4˚C) to remove cell debris. The supernatant was then transferred to a new tube and stored at -80˚C until further use.

2.3.3. Determination of protein concentration

Protein concentrations were determined by Bradford assay (Bio-Rad). Briefly, 5µl of each sample was mixed with 45µl of dH_2O, and 10µl aliquots of this mixture were pipetted into the wells of a 96 well plate in triplicate. Bovine serum albumin (BSA) standards, of known concentrations were made up in dH_2O and 10µl aliquots were also pipetted into the wells of the plate in triplicate. Bradford reagent was diluted 1:4 with dH_2O and 200µl of this mixture was added to each well.

Absorbance readings, at 595nm, were determined using a microplate reader and sample concentrations were calculated using a standard curve generated from the absorbance of the standards.

2.3.4. Sodium Dodecyl Sulphate-polyacrylamide gel electrophoresis, (SDS-PAGE)

SDS-polyacrylamide gels were cast using the Mini-Protean 3 electrophoresis kit (BioRad, UK). The resolving part of the gel was prepared first based on the SDS percentage required (Table 9.2). Following addition of the ammonium persulphate (APS) & TEMED, the solution was poured into glass plate sandwiches and allowed to polymerise. The stacking gel was then prepared (Table 9.2), poured on top of the resolving gel, and combs were inserted. Once this gel had polymerised, the combs were removed and the wells were washed with sterile distilled water (SDW). Protein samples in 2X loading buffer mixtures were loaded into wells of the gels alongside a protein molecular weight marker. Gels were run at 100 V in 1 x running buffer for 1-2 hours.

2.3.5. Western blotting

Following electrophoresis the resolved protein samples, contained within the SDS-polyacrylamide gel, were transferred to a nitrocellulose membrane using the Mini-Protean 3 transblot apparatus (Biorad). The gel was first removed from the glass plates and sandwiched with an activated nitrocellulose between two layers of 3MM filter paper (Whatman). This sandwich was placed in the transblot apparatus and run at 90V for 1.5 hours with an ice block in the tank. Post transfer the non-specific

antibody binding sites on the blotted membrane were blocked with milk or BSA (depending on primary antibody) for a minimum of 1 hour. The membrane was probed overnight with the desired primary antibody (see Table 9.3) diluted in blocking buffer. Following primary antibody incubation, the membrane was washed (3 x 15 minutes) with TBS-T or PBS-T (depending on the primary antibody used). The membrane was then incubated for at least 1 hour with the desired secondary antibody (see Table 9.4) diluted in blocking buffer. The membrane was then washed (3 x 15 minutes) with TBS-T or PBS-T (depending on the antibody used). Immunoreactive bands were detected using Enhanced chemiluminescence (ECL) and visualised using autoradiography on hyperfilm and developed on a automatic X-ray film processor.

2.4. Co-Immunoprecipitation

Cells lysates from cells transfected with pvIRF2-HisMax or pvIRF4-HisMax vectors were prepared as in section 2.3.2. A sample of each lysate was removed to be kept as an 'input' lysate. 250µg of each sample was pre-cleared by incubation with protein G-Sepharose 4B fast flow (Sigma-Aldrich) on a rotating wheel (at least 1 hour, 4°C). Supernatants were collected by centrifugation (1 minute, 16,000*g*, 4°C) and were incubated with anti-Xpress or the mouse isotype control (see Table 2.5) on a rotating wheel (5 hours, 4°C). Protein G-Sepharose 4B fast flow was then added to these samples to allow immunoprecipitation and they were left to incubate further on the rotating wheel (overnight, 4°C). The beads were washed three times by centrifugation (1 min, 16,000*g*, 4°C) and careful removal of the supernatant followed by addition of ice cold PBS. Proteins were recovered by

boiling the samples in 50µl of 2 x loading sample buffer for 5 minutes. Samples were then centrifuged (1 minute, 16,000*g*, 4°C) and the supernatants were collected in a fresh tube. Immunoprecipitates were analysed by western blot.

Table 2.5: Antibodies used for immunoprecipitation

Antibody	Dilution	Supplier
Xpress	1µl per sample	Invitrogen (R910-25)
Mouse IgG1 Isotype control	Matched to that of primary antibody	R&D Systems (MAB002)

2.5. Identifying Protein Interaction Partners Using SILAC-based Proteomics

To identify protein binding partners of vIRF2 and vIRF4, stable isotope labelling of amino acids in cell culture (SILAC) was used in conjunction with mass spectrometry.

2.5.1. Labelling of Amino acids

The EV-NTAP, vIRF2-NTAP and vIRF4-NTAP stable cell lines were cultured in SILAC-DMEM (Invitrogen 41965-039) lacking arginine (R) and lysine (K), Differentially labelled versions of these amino acids, containing different levels of $^{12}C/^{13}C$ and $^{14}N/^{15}N$ or deuterium ^{2}H (see Table 2.6 and Table 2.7), were used to supplement the SILAC-DMEM in order to produce 'light' media, 'medium' media and 'heavy' media. Normal L-arginine and L-lysine were added to the 'light' media, L-arginine ^{13}C and L-lysine 4,4,5,5-D4 to the 'medium' media, and L-arginine $^{13}C/^{15}N$ and L-lysine $^{13}C/^{15}N$ to the 'heavy' media (see Table 2.7). Arginine and lysine were added to final concentrations of 84µg/ml and 146µg/ml respectively. Cells were maintained in the labelled SILAC-DMEM medias, supplemented with 10% dialysed FBS with a 10kDa cutoff (Dundee cell products), to ensure that no amino acids were added from the FBS, and 5% penicillin/streptomycin for at least 5 cell divisions to obtain complete labelling of cells. Trypsinisation was avoided to prevent addition of un-labelled amino acids and cell dissociation buffer (Invitrogen) was used instead. This method is based on that of Trinkle-Mulcahy et al, (2008).

Table 2.6: The amino acids used to label cells

R= Arginine, K = Lysine

Amino acids	Source
R0	Sigma (A8094)
K0	Sigma (L8862)
R6	Cambridge isotype labs (CLM-2265)
R10	Cambridge isotype labs (CNLM – 539)
K4	Cambridge isotype labs (DLM-2640)
K8	Cambridge isotype labs (CNLM-291)

Table 2.7: Radiolabelled amino acids

Composition	Arginine composition	Lysine Composition
R0K0 (Light)	(^{12}C6, ^{14}N4)	(^{12}C6, ^{14}N2)
R6K4 (Medium)	(^{13}C6, ^{14}N4)	D4 (Deuterium)
R10K8 (Heavy)	(^{13}C6, ^{15}N4)	(^{13}C6, ^{15}N2)

2.5.2. Preparation of SILAC labeled samples for immunoprecipitation

For each sample to be immunoprecipitated, one T-75 flask of labelled cells was used. The SILAC-labelled cells were prepared for immunoprecipitation by scraping the cells from the flask and pooling in a tube. Cells were pelleted (10 minutes, 16,000*g* 4˚C). The pellets were washed three times by addition of ice cold PBS and centrifuged (5 minutes, 16,000*g* 4˚C). To lyse the cells, 1ml of IP lysis buffer (see Table 9.1) was added to each sample which was then pipetted up and down 10 x and left on ice for 5 minutes. Samples were then syringed up and down 10 x with a blunt needle before incubation on ice for a further 5 minutes. After centrifuging (1 minute, 16,000*g* 4˚C), the supernatant was collected, and the protein concentration determined by Bradford assay (see section 2.3.3). The samples were then normalised with IP lysis buffer to the concentration of the lowest sample. 50µl of these samples were kept aside for subsequent analysis

(lysate sample), the remainder was submitted for purification by immunoprecipitation.

2.5.3. Immunoprecipitation of SILAC samples

To pull out the NTAP-tagged proteins, streptavin beads were used. First, the beads were washed in 300µl of ice cold PBS by centrifugation (5 minutes, 16,000*g* 4˚C) after which the supernatant was discarded. 5ml of IP lysis buffer was then added to the beads and this mix was centrifuged (5 minutes, 16,000*g* 4˚C) and again the supernatant was discarded. This process was repeated 3 times, and following the final wash, the beads were resuspended in 1ml of IP lysis buffer. 100µl of this mix was added to each normalised SILAC lysate sample and left overnight on a rotating wheel in a cold room. The following day, the samples were centrifuged (5 minutes, 16,000*g,* 4˚C) and before discarding the supernatant, 50µl was kept aside for subsequent analysis ('flow through sample'). The beads were washed three times with IP lysis buffer. On the final removal of supernatant, care was taken to ensure all the supernatant was removed. The beads and associated proteins were boiled in 50µl of 2x loading buffer at 95˚C for 5 minutes, followed by centrifugation (5 minutes, 16,000*g* 4˚C). The supernatant ('final eluate'), which contained the NTAP-tagged proteins and binding partners was collected. Equal volumes of the samples labelled with light, medium and heavy amino acids were pooled and sent for processing at the proteomics facility at the University of Bristol.

2.5.4. Preparation of samples for LC-MS/MS by the University of Bristol Proteomics Facility

The following information was provided directly from the by the Proteomics Facility at the University of Bristol (Dr Kate Heesom, k.heesom@bristol.ac.uk):

Each sample was run briefly on a one-dimensional SDS-PAGE (4-12% Bis-Tris Novex mini-gel, Invitrogen) and the whole sample was excised as a single band and subjected to tryptic digestion using a ProGest automated digestion unit (Digilab UK). The resulting peptides were fractionated using a Dionex Ultimate 3000 nanoHPLC system in line with an LTQ-Orbitrap Velos mass spectrometer (Thermo Scientific). Briefly, peptides in 1% (v/v) formic acid were injected onto an Acclaim PepMap C18 nano-trap column (Dionex). After washing with 0.5% (v/v) acetonitrile, 0.1% (v/v) formic acid peptides were resolved on a 250 mm × 75 μm Acclaim PepMap C18 reverse phase analytical column (Dionex) over a 150 min organic gradient, using 7 gradient segments (1-6% solvent B over 1min., 6-15% solvent B over 58min., 15-32% solvent B over 58min., 32-40% solvent B over 3min., 40-90% solvent B over 1min., held at 90% solvent B for 6min and then reduced to 1% solvent B over 1min.) The flow rate was 300 nl min^{-1}. Solvent A was 0.1% formic acid and Solvent B was aqueous 80% acetonitrile in 0.1% formic acid. Peptides were ionized by nano-electrospray ionization at 2.1 kV using a stainless steel emitter with an internal diameter of 30 μm (Thermo Scientific) and a capillary temperature of 250°C. Tandem mass spectra were acquired using an LTQ-Orbitrap Velos mass spectrometer controlled by Xcalibur 2.1 software (Thermo Scientific) and operated in data-dependent acquisition mode. The Orbitrap was set to analyse the survey scans at 60,000 resolution (at m/z 400) in the mass range m/z 300 to 2000 and the top six multiply charged ions in each duty

cycle selected for MS/MS in the LTQ linear ion trap. Charge state filtering, where unassigned precursor ions were not selected for fragmentation, and dynamic exclusion (repeat count, 1; repeat duration, 30s; exclusion list size, 500) were used. Fragmentation conditions in the LTQ were as follows: normalised collision energy, 40%; activation q, 0.25; activation time 10ms; and minimum ion selection intensity, 500 counts.

The raw data files were processed and quantified using Proteome Discoverer software v1.2 (Thermo Scientific) and searched against the UniProt/SwissProt Human database release version 57.3 (20326 entries) plus vIRF sequences using the SEQUEST (Ver. 28 Rev. 13) algorithm. Peptide precursor mass tolerance was set at 10ppm, and MS/MS tolerance was set at 0.8Da. Search criteria included carbamidomethylation of cysteine (+57.0214) as a fixed modification and oxidation of methionine (+15.9949) and appropriate SILAC labels ($^{2}H_4$-Lys, $^{13}C_6$-Arg for duplex and $^{13}C_6{}^{15}N_2$-Lys and $^{13}C_6{}^{15}N_4$-Arg for triplex) as variable modifications. Searches were performed with full tryptic digestion and a maximum of 1 missed cleavage was allowed. The reverse database search option was enabled and all peptide data was filtered to satisfy false discovery rate (FDR) of 5%. The Proteome Discoverer software generates a reverse “decoy” database from the same protein database and any peptides passing the initial filtering parameters that were derived from this decoy database are defined as false positive identifications. The minimum cross-correlation factor (Xcorr) filter was readjusted for each individual charge state separately to optimally meet the predetermined target FDR of 5% based on the number of random false positive matches from the reverse decoy database. Thus each data set has its own passing parameters.

Quantitation was done using a mass precision of 2ppm. After extracting each ion chromatogram the Proteome Discoverer software runs several filters to check for, among other things, interfering peaks and the presence of the expected isotope pattern. Peptides which did not pass these filters are not used in calculating the final ratio for each protein.

2.5.5. Silver staining

Silver staining was used to ensure the presence of protein bands before sending samples for mass spectrometric analysis. 10µl of the final eluted samples were run on a 10% Bis-Tris NuPage gel (Invitrogen) using MES buffer (Invitrogen) according to the manufacturer's instructions. Gels were then silver-stained using the Silverquest silver-staining kit (Invitrogen) and the manufacturers 'rapid' protocol.

2.6. Immunofluorescence assay

2.6.1. Plating, fixing and permeabilizing – Adherent cells

For adherent cells, cells were grown on glass 12-well multispot microscope glass slides (Hendley-Essex). PBS was used to wash the cells prior to fixing in 4% (w/v) paraformaldehyde (10 minutes). Ice cold methanol was then to permeabilize the cells (10 minutes) and then cells were blocked in blocking solution (1 hour, room temperature), which comprised of 20% heat inactivated normal goat serum (HINGS), diluted to 20% (v/v) in PBS.

2.6.2. Plating, fixing and permeabilizing – suspension cells

Suspension cells (that were BCBL1 cells only in this thesis) were grown in normal tissue culture dishes, and then spotted onto the microscope slides. The cells were left to dry for 2 minutes before being fixed in ice cold Methanol:Acetone 1:1 (5 minutes) then permeabilized in 0.5% Triton-X-100 (Triton-X-100 detergent, diluted to 0.5% (v/v) in PBS, 10 minutes). Cells were then blocked in blocking solution (1 hour, room temperature).

2.7. Immunofluorescence staining

Primary antibodies (see Table 2.8) were diluted in blocking solution and incubated on cells (overnight, 4˚C). The next day, the slides were washed three times in PBS before addition of the secondary antibody (see Table 9.4), also diluted in blocking solution, and incubated in the dark (1 hour, room temperature). Slides were again washed three times and incubated in Bisbenzamide (25µg/ml in PBS) (1minute, room temperature). After a final wash, the slides were mounted with prolong gold (Invitrogen) and protected with 20-70 mm glass coverslips (Menzel-Gläser).

2.7.1. Cell imaging

Cells were viewed using a LSM 510 META confocal laser scanning microscope (Carl Zeiss). Either a 40x or 63x oiled objective was used and each laser was set to an equal optical slice and a pinhole diameter of approximately 1 Airy unit.

Table 2.8: Primary antibodies used in immunofluorescence assay

Antibody	Dilution	Supplier
RTA (ORF50)	1:100	From our laboratory
Rabbit Isotype control	Matched to primary	Abcam ab37415
Anti-Xpress	1:200	Invitrogen (R910-25)

Table 2.9: Primary antibodies used in immunofluorescence assay

Antibody	Dilution	Supplier
Anti rabbit FITC Conjugate	1:50	Sigma: F1262
Anti-mouse 594	1:500	

2.8. DNA-binding ELISAs

TransAM Kits (Active motif) are DNA-binding ELISAs which allow transcription factor activation to be assayed from cell extracts. In this thesis, the TransAM IRF3 kit was used to measure the activation of IRF3 in the presence and absence of vIRF2. Whole cell lysate (containing the activated IRF3) was added to the wells of the kit, which contained oligonucleotides with the IRF3 binding sequence. The binding of these oligonucleotides to activated IRF3 could then be quantified using the anti-activated IRF3 antibody (included in the kit), which is specific for the bound, active form of the transcription factor. A HRP-conjugated secondary antibody was then used to binding to the primary antibody, and provide a means of quantification (using a spectrophotometer at 450nm). This experiment was performed according to the IRF3 TransAM protocol, and all solutions and buffer were provided in the kit.

2.9. Electrophoretic mobility shift assay (EMSA)

EMSA is a method used to examine DNA and protein interactions. A labelled probe, which contains the DNA sequence of interest, is mixed with a protein

sample, and loaded onto a non-denaturing polyacrylamide gel. Because complexes of DNA and protein move through the gel slower than unbound DNA a band shift is observed. The intensity of this DNA:protein band is a measure of the amount of protein bound. This intensity is measured by densitometry. Traditionally, the DNA probes have been labelled with radioactive isotopes. However, the methods throughout this thesis utilised the IRDye-700 flurophore.

2.9.1. Solutions, buffers and probes

The solutions used for EMSA are outlined in Table 2.10. The sequences of the probes used are shown in Table 2.11.

Table 2.10: Solutions used in EMSA

Solution	Composition
1% TBE Buffer	10.8g Tris, 4.5g orthoboric acid and 0.74g EDTA in 1 litre SDW, 10mls in 990mls of SDW.
0.5% TBE Buffer	Diluted from 1% TBE in SDW 0.5% and autoclaved
Odyssey EMSA Buffer Kit	LI-COR (829-07910)
STAT2 (C-20)	Santa Cruz (sc-476)

Table 2.11: Probes used in EMSA

Probe	Sequence
ISRE FWD-IRDye-700 end labelled	5′-GATCAGGAAATAGAAACTG-3′
ISRE REV- unlabelled	5′-CAGTTTCTATTTCCTGATC-3′
ISRE FWD- unlabelled	5′-GATCAGGAAATAGAAACTG-3′

2.9.2. Nuclear and cytosolic protein extractions

Cells of interest were seeded in tissue culture dishes and allowed to adhere. 24 hours later, the medium was removed, and replaced with serum-free medium so that only basal level transcription factor binding would be observed in untreated samples. 24 hours later, the cells were treated/stimulated, as appropriate for the specific assay. Cells were washed in ice-cold PBS and cell lysis and nuclear and cytosolic protein extraction was performed using the NE-PER nuclear and cytosolic extraction reagents according to the manufacturers instructions (Pierce Biotechnology, 78833). Briefly, CERI reagent (100µl), containing protease inhibitors, was added to the cells and the lysates were scraped, collected and transferred to 1.5ml tubes. Samples were vortexed (15 seconds) and incubated on ice (10 minutes). CERII (5.5µl) was then added to each sample, vortexed and incubated on ice (1 minute). Lysates were then centrifuged (5 minutes, 13000*g*, 4°C) and the supernatant, containing the cytoplasmic fraction, was removed and transferred to a clean 1.5ml tube. The nuclear pellet was resuspended in NERI (50µl), containing protease inhibitors, on ice and vortexed (15 seconds) every 10 minutes for 40 minutes. Samples were then centrifuged (10 minutes, 13000*g*, 4°C) and the supernatant containing the nuclear fraction was removed and transferred to 1.5ml tubes. Protein concentration was measured as described previously (section 2.3.3) and samples stored at –80°C until required.

2.9.3. Preparation and annealing of probes

The ISRE probe sequences were based on the ISRE consensus sequence (GAAANNGAAACT). The actual sequence used was that of the ISG54 response

element (Darnell et al., 1994). The single stranded EMSA probes were produced by MWG, and the sequences are shown in Table 2.11. Probes were created by annealing one end-labelled probe with a complementary non-labelled probe specific. Briefly, the oligonucleotides were diluted with DEPC treated water to 100pmole and 5µl of each of the complementary probes were mixed with 90µl of Restriction buffer B (Roche). This mixture was incubated (95°C for 10 minutes) in a heat block, which was then switched off to allow the samples to cool overnight in the dark and anneal. The annealed probes were then aliquoted (20µl), covered in foil (to protect from light) and stored at –20°C until further use. Labelled probed was produced by annealing the ISRE FWD-IRDye-700 end labelled probe with the ISRE REV- unlabelled. The 'cold competitor' probe was produced by annealing the ISRE FWD- unlabelled probes with the ISRE FWD- unlabelled.

2.9.4. DNA: Protein binding reactions

Nuclear lysates (5µg) were mixed with 1µl of 5′-IRDye-700-labelled EMSA probe, 2µl of 10x binding buffer (Odyssey EMSA Buffer Kit), 2µl 25mM DTT/2.5% Tween-20, 1µl poly(I:C), and made up to 20ul with DEPC treated water. Reagents were incubated (30 minutes, room temperature, in the dark). 2µl of gel loading buffer (Odyssey EMSA Buffer Kit) was then added to each sample and samples were resolved on 6% polyacrylamide-TBE gels (Invitrogen). The bands were visualized and quantified using an Odyssey infrared imaging system (LI-COR Biotechnology). For supershift experiments, the STAT2 antibody was used.

2.10. Cloning

The vIRF4 and vIRF2 genes were cloned into various vectors throughout this study. Expression plasmids into which vIRF2 or vIRF4 genes were cloned are described below and detailed in Table 2.12. Primers used for cloning procedures thought this thesis are shown in Table 2.14. For specific cloning procedures, see the results sections. Restriction enzymes were purchased from New England Biolabs, Promega or Roche and used according to the manufacturers instructions. DNA inserts, generated by PCR or through restriction digestion from an existing vector were separated by agarose gel electrophoresis and purified using a Qiagen gel extraction kit. Vector DNA was restriction digested and gel purified. Alternatively, pCR-Blunt was used to clone blunt-ended PCR fragments. A typical ligation reaction consisted of DNA insert (6µl), recipient vector (2µl), T4 DNA ligase buffer (1µl) and T4 DNA ligase (1µl). Ligation reactions were incubated overnight at 16˚C before being used to transform competent E. coli cells.

2.10.1.1. pCDNA4TO-NTAP

This vector (provided by Prof. Ian Goodfellow, University of Cambridge) consists of the N-terminal tandem affinity purification (NTAP)-tag cloned into the pCDNATO Invitrogen vector. The NTAP-tag encodes two copies of the IgG binding units of protein G from *Streptococcus* spp and a streptavidin binding peptide separated by a Tobacco Etch Virus (TEV) protease cleavage sequence. This vector was the backbone for some cloning procedures in this thesis, however, the pCDNA4TO-NTAP vector produces a protein in its own right which is referred to as the ‘NTAP’ protein throughout this thesis. Either the vIRF2 or the vIRF4 genes were cloned

into this vector to produce the pvIRF2-NTAP and pvIRF2-NTAP vectors respectively. The proteins produced from these vectors are referred to as vIRF2-NTAP and vIRF4-NTAP respectively.

2.10.1.2. pcDNA4/HisMax

The pcDNA4/HisMax vector (Invitrogen) was used as the backbone for the pvIRF2-His/Max and pvIRF4-His/Max vectors. These vectors encode an Xpress and a polyhistidine tag, contiguous to the vIRF2 and vIRF4 proteins enables their detection.

Table 2.12: The expression plasmids used throughout this thesis

Plasmid name	Source
pCDNA4TO-NTAP	Prof. Ian Good fellow (University of Cambridge)
pvIRF2-NTAP	vIRF2 cloned into pCDNA4TO-NTAP
pvIRF4-NTAP	vIRF4 cloned into pCDNA4TO-NTAP
pcDNA4/HisMax	Invitrogen
pvIRF2-His/Max	vIRF2 cloned into pcDNA4/HisMax
pvIRF4-His/Max	vIRF2 cloned into pcDNA4/HisMax
CBP-GFP	Provided by A.Turnell (University of Birmingham)

2.10.2. Transformation reactions

Frozen One Shot Chemically Competent E. coli (Invitrogen), or in the case of pCR-Blunt cloning, One Shot® TOP10 (Invitrogen) were thawed on ice. The plasmid or the product of a ligation reaction was added to the competent cells, mixed, and kept on ice for 30 minutes. The cells were subject to a heat shock (42°C, 45 seconds) and then transferred to 900µl of room temperature SOC media

(Invitrogen). This mixture was then incubated (1 hour, 37˚C). Bacteria were then plated on agar contained 100µg/ml ampicillin or 50µg/ml Kanomycin (dependent on the plasmids) to select transformed cells. The chemically competent cells and vectors used are shown in Table 2.13.

2.10.3. Small-scale preparation of plasmid DNA: Mini prep

A single bacterial colony from an agar plate was selected with a sterile loop and used to inoculate 3ml of LB medium containing 100µg/ml of ampicillin or 50µg/ml Kanomycin. The cells were cultured at 37˚C overnight in a shaking incubator (150rpm). The following day the cells were pelleted by centrifugation (5 minutes 16,000*g*) and DNA was extracted from the resultant pellet using a QIAprep spin miniprep kit (Qiagen) according to the manufacturer's instructions.

2.10.4. Large-scale preparation of plasmid DNA: Maxi Prep

For bulk preparation of DNA, a 3ml starter culture of LB media with antibiotics was inoculated with a single colony and grown overnight at 37˚C in a shaking incubator (150rpm). 250ml of L-broth (containing 100µg/ml of ampicillin) was inoculated with 1ml of the starter culture and grown overnight at 37°C in a shaking incubator (150rpm). The cells were centrifuged (15 minutes 5000*g*) and the resultant pellets were subject to a maxiprep kit (Qiagen) according to the manufacturer's instructions.

Table 2.13: Chemically Competent cells and cloning vectors used in this study

Product name	Source
One Shot® MAX Efficiency® DH5α	Invitrogen (12297-016)
One Shot® TOP10 Chemically Competent E. coli	Invitrogen (C4040-10)
pCR®-Blunt vector	Invitrogen
pCDNA4TO-NTAP	Prof. Ian Goodfellow (University of Cambridge)
pCDNA4-his\max	Invitrogen

Table 2.14: Primers used for cloning.

Primers were ordered from Invitrogen

Primer Name	Primer Sequence 5'-3'
vIRF4 Forward BCBL1 vIRF4 Reverse BCBL1	ATCGGTTTCTGTGTCGGACCATG GGACTACAAGATTACATCCGGTTTT
vIRF4 Forward Acc65I NTAP-PCR blunt vIRF4 Reverse XbaI NTAP-PCR blunt	GGTTTCGGGTACCACCATGCCTC CGGTTTTCTAGATCACATATATG
vIRF2 forward with BsIWI vIRF2 reverse with XbaI	ATCTTACGTACGATGCCTCGCTACA CCACTGTGCTGTCTAGATGCAGGCG
vIRF4 Forward HisMaxA-BamHI vIRF4 Reverse HisMaxA	GCTGGGGATCCGGATGCCT TATCTGCAGAATTCAGG

2.11. PCR and qRT-PCR

For both PCR and qRT-PCR assays, RNA, extracted from cells was used as a template for cDNA synthesis. This cDNA was then used in subsequent PCR or qRT-PCR reactions. Table 2.15 provides details of the reagents used for PCR and qRT-PCR techniques throughout this thesis.

Table 2.15: Reagents used for PCR and qRT-PCR techniques

Product name	Source
RNeasy mini kit	Qiagen
GoTaq DNA Polymerase	Promega (M3171)
Velocity DNA Polymerase	Bioline (BIO-21098)
RNase-Free DNase	Promega (M6101)
Random primers	Promega (C1181)
dNTP mix	Invitrogen (10297018)
Moloney Murine Leukemia Virus Reverse Transcriptase (M-MLV-RT)	Invitrogen (28025013)
RNAseOUT	Invitrogen (10777019)
DEPC treated water	Ambion (AM9906)
VIC labelled huGAPDH primer/probe set	Applied Biosystems (4310884E)
MicroAmp Optical 96 well PCR plates	Applied Biosystems (403012)

2.11.1. RNA extraction

RNA was extracted from cell pellets using the RNeasy mini kit (Qiagen), according to the kit instructions. The resultant RNA was quantified and DNase treated using RNase-Free DNase (promega), according to the manufacturer's instructions. The samples were then subject to cDNA synthesis, or stored at -80^{o}C for future experiments.

2.11.2. Complementary DNA (cDNA) synthesis

For each sample, cDNA synthesis was performed by mixing 500ng of the extracted RNA, with 50ng of random primers and 1ul of 10mM dNTP mix in a volume made up to 11µl with sterile distilled water. This was heated (5 minutes, 65°C) followed by a quick chill on ice. To each sample, 4ul of 5X First-Strand Buffer and 2µl of 0.1 M DTT (part of the M-MLV-RT kit, Invitrogen) was added along with 1 unit of RNAseOUT, to minimise degradation of the RNA. The contents were mixed and incubated (2 minutes, 37°C) followed by the addition of 200U of M-MLV RT. Samples were incubated (10 minutes, 25°C), and then further incubated (50 minutes, 37°C). Inactivation of the reaction was achieved through heating at 70°C for 15 minutes. 80µl of DEPC treated water was added to the resultant cDNA and it was stored at -80^{o}C until used as a template for amplification in PCR or qPCR experiments.

2.11.3. Polymerase chain reaction (PCR)

PCR reactions were carried out using GoTaq DNA Polymerase (promega), except when cloning, where velocity DNA polymerase (Bioline) was used. In sterile PCR tubes, the desired amount of template cDNA was mixed with 10µl of 5x GoTaq Reaction Buffer 1, 1µl of dNTPs (10mM), 1µl of forward primer (200ng/ul), 1µl of reverse primer (200ng/ul) and 0.5µl of GoTaq DNA Polymerase and made up to 50ul with DEPC treated water. The tubes were spun (5 seconds) in a microcentrifuge and PCRs were performed as indicated in

Table 2.16.

Table 2.16: PCR protocol

Step	Temperature	Time	Number of cycles
Initial Denaturation	95°C	2 minutes	1 cycle
Denaturation	95°C	1 minute	
Annealing	42–65°C	45 seconds	
Extension	72°C	1 minute/kb	25–35 cycles (from Denaturation to extension)
Final Extension	72°C	5 minutes	1 cycle
Soak	4°C	Indefinite	1 cycle

Table 2.17: The sequences of primer and probes used to detect vIRF2 and vIRF4 cDNA

Gene	Sequence
vIRF2	Forward:5'- GCATCGCGAAGAAGAATAGG -3'
	Reverse: 5'- TGGTAAAATGGGGCAAGGTA-3'
vIRF4	Forward:5'- GGGATGGTGGCCTCAGGGCG -3'
	Reverse: 5'- CTAGCACATTGGCCGCTTTG-3'

2.11.4. Agarose gel electrophoresis

Agarose (Sigma) was dissolved in a solution of 1 x Tris/Boric EDTA (TBE) using a microwave, resulting in a final concentration of 0.8-2.0% (w/v) depending on the size of fragments to be separated. Ethidium bromide was added to a final concentration of 0.5µg/ml prior to pouring into a Mini Sub Gel GT Electrophoresis Tank (BioRad). DNA samples were mixed with loading buffer (at a ratio of 5:1) and loaded on the gel. The gel was run at 50-80V (dependent on gel percentage), for a time sufficient to separate desired bands, in 1 x TBE. DNA bands were visualised with a UV light box.

Table 2.18: Solutions for Agarose gel

Solution	Composition/Source
Agarose	Sigma
1 x Tris/Boric EDTA (TBE)	45mM Tris HCl, 45mM orthoboric acid and 1mM EDTA, pH 8.0
Loading buffer	25mg Bromophenol Blue, 1.5g Ficoll 400, 10ml sterile distilled water

2.11.5. Real time quantitative PCR (qPCR)

qPCR was performed on cDNA generated as described in section 2.11.2. Primer/probe sets for vIRF2 and vIRF4 genes were designed to span intron-exon boundaries to ensure mRNA specific amplification (Table 2.19). Primers were ordered from Invitrogen, while FAM labelled probes were ordered from Alta Bioscience. As an internal control for each reaction, a VIC labelled human GAPDH primer/probe set was used, to which data was normalised. Reactions were set up using the values shown in Table 2.20. A master mix was generated based on the number of samples to be analysed and 20µl of this was pipetted into the wells of a 96 well PCR plate. 5µl of cDNA template was then added separately, for each sample in the 96well plate. Negative controls (no template and samples synthesised in the absence of reverse transcriptase) were also included for each experiment. Samples were analysed on an Applied Biosystems 7500 Sequence Detection System using the following conditions 95°C for 10 minutes, followed by

40 cycles of 95°C for 15 seconds and 60°C for 60 seconds

Table 2.19: The sequences of primer and probes used to quantify levels of mRNA by qPCR

Gene	Sequence/Source
vIRF2	Forward:5'- TCAGCTGCGGAGGATGTTG -3'
	Reverse: 5'- CCATGATGACAAACACAGAGAAAAG -3'
	FAM-labelled Probe:5'- CGGCCTCCCTCTGGGCTTTTTTTC -3'
vIRF4	Forward:5'- GCCCCTGCCTCCTCGTA -3'
	Reverse: 5'- TGTCCCCCCCAATGCA -3'
	FAM-labelled Probe:5'- CTTTGTTCTCTAGTGTCACTGCGTCGCG -3'
GAPDH	Applied Biosystems (4310884E), VIC-labelled

Table 2.20: qPCR reaction mix. The volumes used for 1 sample are given.

Component	Volume
TaqMan Universal Mastermix x2 Applied Biosystems (4324018)	12.5ul
Forward primer	2.5ul
Reverse primer	2.5ul
FAM-labelled probe	1ul
VIC-labelled GAPDH primers/probe Applied Biosystems (4310884E)	0.5ul
DEPEC treated water	1ul
cDNA template (added to plate)	5ul

2.12. Polysome profiling experiments

The following methods were performed by Dr Nicolas Locker (University of Surrey). The following details how he performed the experiments.

2.12.1. Sucrose Density Gradient Centrifugation

Sucrose density gradient centrifugation enables the separation of small ribosomes through centrifuging cell lysates in a sucrose gradient at high centrifugal force. Components come to rest when their density is equivalent to that of the surrounding sucrose, allowing cellular components to be analysed according to density. 10X TMN buffer was diluted 1 in 10 to produce 1X TMN buffer. 1X TMN buffer was then used to produce sucrose solutions at 10%, 18%, 26%, 34%, 42%, 50% and 60% sucrose in 20ml 1X TMN. To each of these, 1mg/ml cyclohexamide was added. Sucrose solutions were layered in ultracentrifuge tubes (Beckman Coulter Inc., Brea, CA, USA) at a volume of 1.6ml for each concentration by deposition and subsequent freezing of each layer at -80ºC, with the most dense layer (60% sucrose) at the bottom and the least dense (10%) at the top. Gradients were frozen at -20ºC overnight and thawed the morning before ultracentrifugation to allow layers to equilibrate. Upon thawing, 500µl of cytoplasmic cell lysates were added to the top of the thawed gradients and ultracentrifuged (150,000*g*, 2 hours, 4ºC).

2.12.2. Polysome Profiling

Polysome profiling is the spectrophotometric analysis of lysates ultracentrifuged through a sucrose gradient at 254nm, an absorbance wavelength of RNA. Peaks

at higher densities are indicative of polysomes, which are strands of mRNA being translated by multiple ribosomes. Peaks at lower densities are indicative of rRNA in singular 40S and 60S subunits, as well as free RNAs. Previously ultracentrifuged lysates were run through a density gradient fractionator (Teledyne ISCO, Lincoln, NE, USA), using 70% sucrose with 0.1% bromophenol blue as a dense chase solution (dispensed using a syringe pump (kd Scientific Inc.,Holliston, MA, USA)) to displace the gradient upwards. Absorbance was measured using PeakTrak software (Teledyne ISCO).

Table 2.21: Solutions used for polysome profiling experiments

Solution	Composition
10X TMN buffer	3M NaCl, 150mM MgCl2, 150mM Tris-HCl at pH 7.5, 10mg.ml-1 heparin
Cyclohexamide	Sigma-Aldrich

2.13. EMCV plaque assay

Plaque assays were used to quantify titres of Encephalomyocarditis virus (EMCV), which had been grown in rIFNα pre-treated EV-NTAP, vIRF2-NTAP or vIRF4-NTAP cell lines.

Table 2.22: Solutions used for the plaque assay

Solution	Composition
Plaque assay medium	DMEM containing 1% penicillin-streptomycin
Overlay medium	Overlay medium (10% v/v Minimum Essential Medium (MEM) with 10X Earl's salt, 1% v/v L-glutamine, 2% v/v foetal calf serum heat inactivated, 1% v/v penicillin/streptomycin)
Crystal violet	0.5g crystal violet, 20ml ethanol, 0.9gNaCl, 100ml 40% formaldehyde, 880ml dH_20

2.13.1. Infection of cells with EMCV

The EV-NTAP, vIRF2-NTAP or vIRF4-NTAP cell lines were plated into 6-well plates at a density of 5 x 10^5 cells per well and left overnight to adhere in a culture medium of DMEM complete with 5µg/mL Blasticidin and 200µg/ml zeocin. After 24 hours, the medium was replaced with DMEM complete, supplemented again with with 5µg/ml Blasticidin and 200µg/ml Zeocin but also with 0.125µg/ml Tetracycline, to induce the expression of the desired proteins. 24 hours later, rIFNα (final concentration of 300U /ml), or medium without rIFNα was added to the cells. After a further 24 hours, culture medium was carefully removed and the cells were infected with the EMCV virus at a multiplicity of infection (MOI) of 0.1 in 500µl of culture medium (1 hour at 37^{o}C). The medium was removed from the cells, which were then washed twice with sterile PBS, and left in fresh culture medium

with or without rIFNα (300U/ml). 24 hours later the supernatant was harvested in order to quantify EMCV by plaque assay.

2.13.2. Plaque assay

To determine the titre of the EMCV virus in the supernatants from EMCV infected EV-NTAP, vIRF2-NTAP or vIRF4-NTAP cell lines, plaque assays were performed using L929 cells. L929 cells were plated in 12-well plates in DMEM complete medium and grown until a monolayer of cells formed. The supernatants from EMCV infected EV-NTAP, vIRF2-NTAP or vIRF4-NTAP cells were diluted from 10^{-1} to 10^{-7} in plaque assay medium (Table 2.22). 250 µl of each of each of these dilutions was then used to infect the L929 cells by carefully pipetting the volume onto the cells and incubating (30 minutes, 37^{o}C). Overlay medium (Table 2.22) was mixed with molten 2% agar, to give a final agar concentration of 0.6%. 1ml of this mixture was then added to each well of infected L929 cells. The plates were left at room temperature for about 30 minutes until the overlay medium had set and then the L929 cells were incubated at 37^{o}C for between 72-96 hours, so that plaques could form.

2.13.3. Counting plaques

To visualise the plaques, 1ml of crystal violet was added to each well and the plates were incubated (10 minutes, room temperature) with gentle agitation. To remove the overlay gel the plates were carefully washed in tap water. The Plaques were easily observed at the bottom of each well. To calculate the titre of virus in

plaque forming units per ml (PFU/ml), the number of plaques per well was multiplied by 4 (to account for the 250ul of virus dilution used to infect each well, giving the titre per ml). This value was then multiplied by the dilution factor of the virus sample used to infect that particular well.

CHAPTER 3

THE KSHV PROTEINS, vIRF2 AND vIRF4, DOWNREGULATE IFN SIGNALLING

3.1. Introduction to chapter 3

The aim of this thesis is to understand how a cancer-causing virus regulates the type I interferon system. My studies centre on the function of the KSHV-encoded vIRF2 and vIRF4 proteins. In this chapter, the effects of vIRF2 and vIRF4 on the type I IFN signalling are examined.

Type I IFN signalling is a key mechanism through which host cells activate an initial antiviral response to invading viruses. The outcome is reduced virus replication and dissemination throughout the host, limiting possible disease development. An initial signalling pathway, the IFN production pathway, is invoked when virus-associated features are detected by the cell, leading to production of type I IFNs. This pathway leads to the nuclear translocation of NFκB and IRF3 from the cytoplasm and the formation of the IFNβ enhanceosome, consisting of NFκB, IRF3 and ATF-2/c-Jun. The IFNβ enhanceosome, together with the recruited CBP/p300 co-activator proteins, activates the transcription of the IFNβ gene, which leads to the production of this cytokine (see sections 1.4.2 and 1.4.6). Type I IFNs are released from the cell and then activate JAK-STAT.

Type I IFNs bind to their cognate receptors and induce another signalling pathway, the JAK-STAT pathway, in both an autocrine and paracrine fashion. This response is orchestrated by a heterotrimeric complex the ISGF3, formed from IRF9 and activated STAT1 and STAT2. ISGF3 transactivates ISGs, by binding to

the ISREs in the promoters of these genes (see section 1.4.8). The activation of these genes collectively brings about an antiviral response (see section 1.4.10).

Both the IFN production pathway and the JAK-STAT signalling pathway are heavily targeted by proteins encoded by a wide array of viruses (see sections 1.4.7 and 1.4.9). KSHV is unique among human viruses in that it encodes a family of four vIRFs which share some homology to cellular IRFs (Cunningham et al., 2003). As discussed in chapter 1, vIRF1, vIRF2 and vIRF3 have been shown to modulate type I IFN signalling.

vIRF1 downregulates the activation of the IFNβ promoter (Burysek et al., 1999a). It is thought to act though its association with CBP/p300, by inhibiting the transactivation of CBP and the histone acetyltransferase activity of p300 (Lin et al., 2001). CBP and p300 are components of the CBP/p300-IRF3 complex, which is vital for the activation of the IFNβ promoter. vIRF1 is also able to downregulate IFNβ induced JAK-STAT signalling (Gao et al., 1997).

vIRF2 has been shown, by our group, to downregulate the activation of the IFNβ promoter by accelerating the turnover of IRF3 (a key player in IFNβ promoter activation) in a mechanism involving caspase-3 (Areste et al., 2009, Fuld et al., 2006). vIRF2 is also able inhibit ISRE-containing promoter activation, following IFN activation. It does this by targeting pSTAT1, a component of the ISGF3 complex, but the precise mechanism for this is unknown (Fuld et al., 2006, Mutocheluh et al., 2011).

vIRF3 is able to interact with either the DNA binding domain or the central association domain of IRF7, leading to a suppression in IFNα production (Joo et al., 2007). It can also target IRF5 leading to an inhibition of type I IFN, and ISRE promoter activation (Takaoka et al., 2005, Wies et al., 2009).

There is only one published study that has investigated vIRF4 function with respect to IFN signalling in which the authors concluded that this KSHV protein does not inhibit the activation of the IFNβ promoter in response to Sendai Virus infection (Kanno et al., 2006). The effect of vIRF4 on IFN stimulated ISRE-containing promoter activation has not been published. Since vIRF4 shares homology with cellular IRFs, and since the other three vIRFs can downregulate type I IFN signalling, the hypothesis that vIRF4 can modulate type I IFN signalling was investigated further.

The aims of this chapter are to:

1) Confirm that vIRF2 can inhibit both activation of the IFNβ promoter and activation of ISRE-containing promoters
2) Reasses the effect of vIRF4 on IFN gene activation by examining activation of the IFNβ promoter
3) Investigate the effect of vIRF4 on JAK-STAT signalling and therefore ISRE-containing promoter activation

This chapter details how the vIRF4 gene was obtained from BCBL1, a cell line naturally infected with KSHV, and subsequently cloned into the pCDNA4TO-NTAP vector, resulting in the pvIRF4-NTAP expression vector.

This expression vector was used in reporter studies to investigate the effect of vIRF4 on the IFN production pathway (through examining activation of the IFNβ promoter) and the JAK-STAT signalling pathway (through examining activation of an ISRE-containing promoter). Since previous work in our laboratory has shown that vIRF2 downregulates the IFN production pathway (Fuld et al., 2006, Areste et al., 2009) -and the IFN signalling pathway (Fuld et al., 2006, Mutocheluh et al., 2011), vIRF2 was used as a positive control throughout experiments.

To study in detail the effects of vIRF2 on IFN signalling, the effect of vIRF2 on the IFN production pathway was further investigated through DNA-binding ELISAs, which measured the activation of IRF3. The aim was to identify if vIRF2 could decrease IRF3 activity. Finally, the effects of truncated vIRF2 proteins on the IFN production and the IFN signalling pathways were also examined through reporter assays. These experiments revealed which regions of the vIRF2 protein could downregulate IFN signalling.

3.2. Cloning of vIRF4 cDNA, obtained from BCBL1 cells, and cloning itinto the pCR-Blunt vector

In order to perform *in vitro* functional studies with vIRF4, the vIRF4 gene was obtained from BCBL1 cells and cloned into the pCR-Blunt cloning vector. This vector was subsequently used to clone vIRF4 into other expression vectors (described in later chapters).

Firstly, vIRF4 mDNA was obtained from lytically infected BCBL1 cells, in order to amplify the spliced vIRF4 gene (Figure 3.1). BCBL1 is a PEL cell line that is latently infected with KSHV but is EBV negative (Renne et al., 1996). To induce expression of the lytic vIRF4 gene, KSHV was re-activated into lytic cycle by PMA treatment for 48 hours before harvesting the cells. In order to verify that lytic replication had been induced, a portion of the harvested cells were set aside to measure expression of the KSHV lytic switch protein, RTA, through western blot analysis (Figure 3.2 A). RNA was extracted from the remaining cell pellet and subject to RT-PCR using primers specific for vIRF4 (Table 2.14, 'vIRF4 Forward BCBL1' and 'vIRF4 Reverse BCBL1'). Following gel electrophoresis, a PCR product corresponding to the expected size of the spliced vIRF4 gene (2736bp) was observed (Figure 3.2B). The vIRF4 band was excised, purified and ligated with pCR-Blunt. This ligation reaction was then transformed into One Shot TOP10 Chemically Competent *E. coli* (Invitrogen). The identity of the pCR-Blunt-vIRF4 construct was confirmed by restriction digestion with EcoRI (Figure 3.2C) and sequencing.

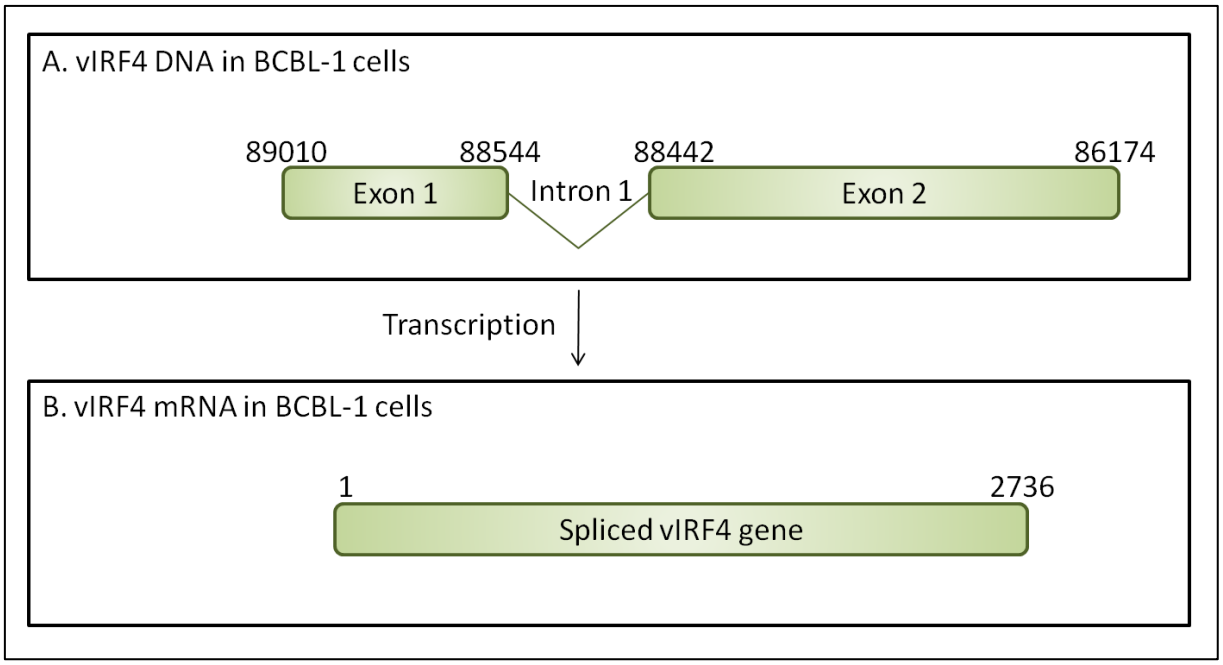

Figure 3.1: Illustration of genomic vIRF4 and vIRF4 mRNA

(A) An illustration of the genomic vIRF4 from accession number NC_009333. The numbers refer to the position within the KSHV genome. (B) The spliced vIRF4 mRNA obtained from BCBL1 cells and cloned into the pCR-Blunt vector. The numbers refer to base pairs along the vIRF4 spliced gene.

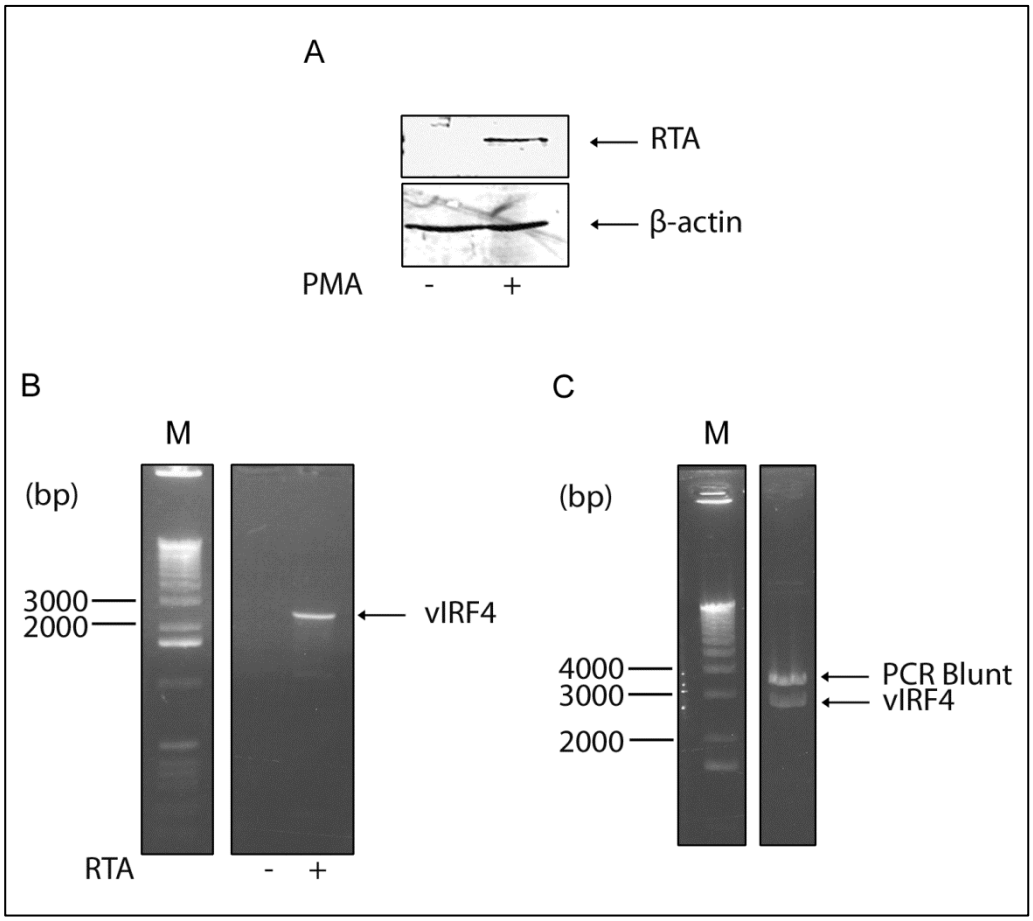

Figure 3.2: Cloning the vIRF4 gene into the pCR-Blunt cloning vector.

(A) Detection of the KSHV lytic switch protein, RTA. Lysate (20µg), from BCBL1 cells which were incubated with (+) or without (-) PMA (20ng/ml for 48 hours), was analysed by western blot to detect RTA. Primary antibodies: anti-ORF50 (detecting RTA) and anti-β-actin. Secondary antibodies: anti-rabbit IRDye800LT-conjugated secondary antibody and anti-mouse IRDye680LT-conjugated secondary antibody. The bands were visualised using the 'Odyssey' imaging system (LI-COR). (B) Amplification of the vIRF4 spliced gene from PMA-treated BCBL1 cells. RNA, extracted from PMA-treated BCBL1 cells was subject to reverse transcription. The resultant cDNA was amplified with vIRF4 primers (Table 2.14, vIRF4 Forward BCBL1' and 'vIRF4 Reverse BCBL1'). The PCR product was separated by agarose gel electrophoresis. The lanes shown were from the same gel, but were not contiguous, hence the gap. (C) Confirmation that pCR-Blunt-vIRF4 contains a fragment of the same size as that expected for vIRF4 (2736bp). pCR-Blunt, transformed with the PCR product from Figure 3.2B was digested with EcoRI and visualised following agarose gel electrophoresis. The labelled bands correspond in size to pCR-Blunt and the vIRF4 gene. The lanes shown were from the same gel, but were not contiguous, hence the gap M, marker.

3.3. Cloning the vIRF4 gene into the pCDNA4TO-NTAP vector

In order to express the vIRF4 protein in eukaryotic cells, the vIRF4 gene was cloned into the pCDNA4TO-NTAP expression vector. This vector contains a tandem affinity purification (TAP) tag which facilitates the tandem purification of proteins containing this tag, along with their binding partners. NTAP-vIRF4 could therefore aid investigations into vIRF4 binding partners as well as enabling vIRF4 functional studies to be performed. An overview of the cloning scheme is illustrated in Figure 3.3. To enable the cloning of vIRF4 into the pCDNA4TO-NTAP vector, specific PCR primers (Table 2.14 'vIRF4 Forward Acc65I NTAP-PCR blunt' and 'vIRF4 Reverse XbaI NTAP-PCR blunt') containing appropriate restriction sites (XbaI and Acc65I) were used to amplify the vIRF4 gene from the pCR-Blunt-vIRF4 template (Figure 3.3B). The fragment produced was ligated into pCR-Blunt (Figure 3.3C). The resultant pCR-Blunt-vIRF4 (XbaI and Acc65I) (Figure 3.3D) was confirmed by restriction digestion (Figure 3.4). The vIRF4 gene was excised, via enzymatic digestion from pCR-Blunt-vIRF4 (XbaI and Acc65I) with XbaI and Acc65I (Figure 3.3E). This fragment was ligated into the pCDNA4TO-NTAP vector which had been digested with XbaI and BsiWI (Figure 3.3F). Acc65I cleaves to leave ends compatible with BsiWI. The resultant vIRF4-NTAP construct (Figure 3.3G) was confirmed by sequencing.

3.4. Transient expression of vIRF4 in 293 cells

To ensure the vIRF4-NTAP expression vector expressed the vIRF4-NTAP protein in 293 cells a transfection titration was performed. 293 cells were transfected with increasing amounts of NTAP-vIRF4 plasmid from 0-1000ng. Following 16 hours

incubation the cells were harvested. The NTAP-tag contains protein G that will bind any immunoglobulin. In this experiment, the primary β-actin and secondary antibody bound to both β-actin, and the NTAP-tag. However, because the bands were separated by SDS gel electrophoresis, they were distinguished based on their size. Western blot analysis showed, as expected, that as the amount of vIRF4-NTAP plasmid transfected increases, the expression level of vIRF4-NTAP also increases (Figure 3.5). This experiment confirmed that the vector could be used to sucessfully express vIRF4 in 293 cells.

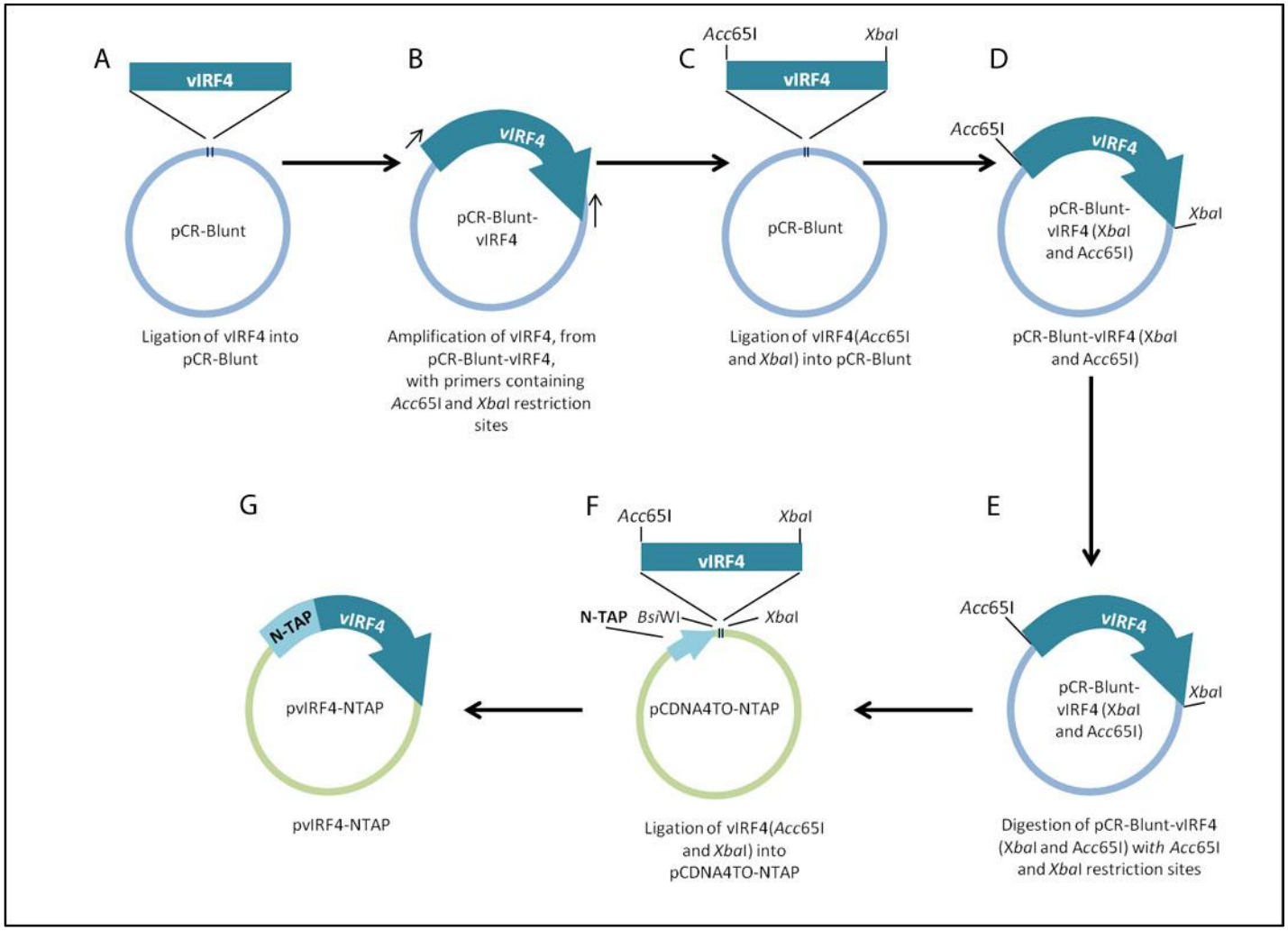

Figure 3.3: Cloning the vIRF4 gene into the pCDNATO-NTAP vector.

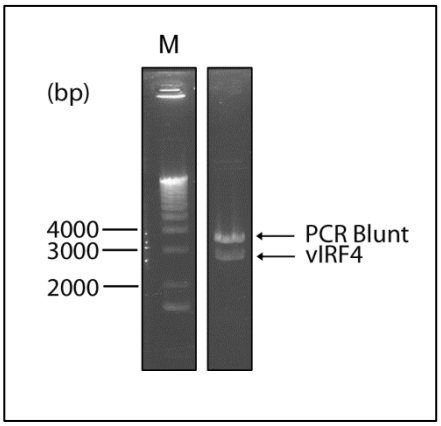

Figure 3.4: Electrophoretic analysis confirming that pCR-Blunt-vIRF4(XbaI and Acc65I) contains a fragment equal in size to that of vIRF4 with XbaI and Acc65I restriction sites.

The pCR-Blunt-vIRF4 vector was digested with EcoRI and analysed by gel electrophoresis. Bands were observed at around 2700-2800kb and around 3500kb corresponding to vIRF4 with XbaI and Acc65I and pCR-Blunt. M, marker.

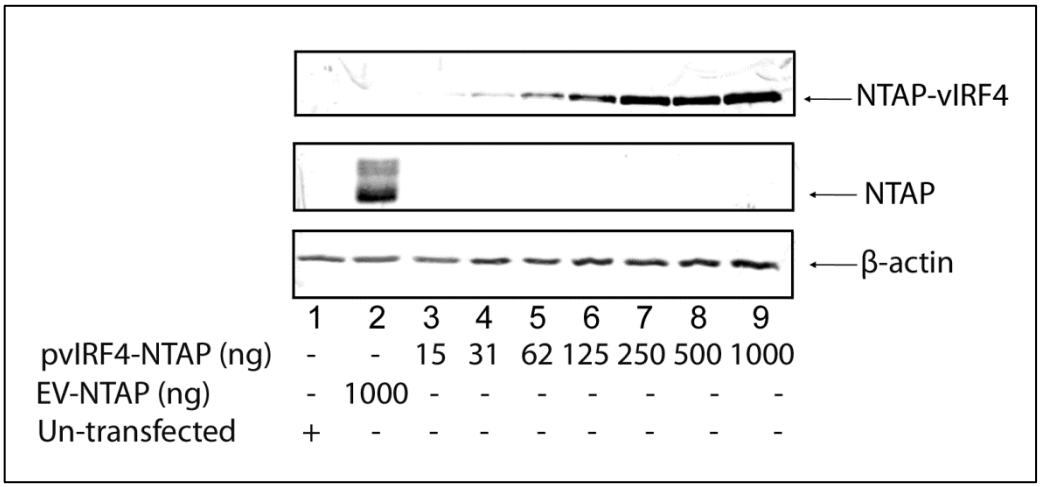

Figure 3.5: vIRF4 expressed in 293 cells transfected with the vIRF4-NTAP vector.

293 cells were transfected with the vIRF4-NTAP vector (0-1000ng, as indicated in figure), and harvested 16 hours later. The lysate (20µg) was analysed by western blot to detect the NTAP-tag. Primary antibody: anti-β-actin. Secondary antibody: anti-mouse IRDye 680LT-conjugated secondary antibody. The NTAP tagged vIRF4 (vIRF4-NTAP) and the TAP tag produced from EV-NTAP transfected cells are indicated (NTAP). β-actin is also indicated. The anti-mouse IRDye 680LT-conjugated secondary antibody was sufficient to detect the NTAP-tag as it contains protein G. As a control for the specificity of these NTAP-containing bands, un-transfected cell lysate was also analysed (Lane 1). The bands were visualised using the 'Odyssey' imaging system (LI-COR).

3.5. Optimisation of dual luciferase reporter assays to measure IFNβ and ISRE promoter activities

The dual luciferase assay (DLA) reporter system (see section 2.2) enabled examination into the effect of vIRF2 and vIRF4 on the IFN production and JAK-STAT signalling pathways. The activity of the IFN production pathway was measured using a p125-luc reporter plasmid (see Table 2.4), containing the IFNβ promoter. The JAK-STAT pathway was measured with the pISRE-luc reporter plasmid (see Table 2.4), containing an ISRE promoter. DLAs make dual measurements of both firefly (*Photinus pyralis*) and *Renilla* (*Renilla reniformis*) luciferase activities from the same sample. The firefly luciferase measurement, expressed from the promoter to be studied (IFNβ or ISRE element), relates to the activity of the promoter of interest. The constitutively expressed *Renilla* luciferase signal normalises changes in luminescence due to factors other than the transcriptional control being studied, for example transfection efficiency between samples. In order to assay the role of vIRF2 and vIRF4 in modulating IFNβ and ISRE promoters, DLA conditions were optimised.

DLAs were performed using poly(I:C) to activate the IFNβ promoter in order to assess its activity. poly(I:C) is a synthetic dsRNA which interacts with TLR3 and triggers activation of the IFN signalling pathway. The active form of IRF3 translocates into the nucleus and activates the IFNβ promoter. Hence, transfection of poly(I:C) leads to the activation the IFNβ promoter. Previous work in our group has determined the optimal concentrations and duration of poly(I:C) treatment on cells (Areste et al., 2009, Fuld et al., 2006).

rIFNα was used to activate the ISRE-containing promoter in order to assess its activity. IFN binds to receptors (IFNAR1 and IFNAR2) on the cell surface, which results in activation of the JAK-STAT signalling pathway. This pathway drives the activation of the ISRE promoter. To determine the conditions for optimum activation of the ISRE reporter plasmid, an interferon titration and a time course were performed separately on 293 cells. Normalised luciferase activity, and hence ISRE-containing promoter activity, peaked after 16 hours of rIFNα treatment (Figure 3.6A, row 5) and with 300IU/ml (Figure 3.6B, row 6).

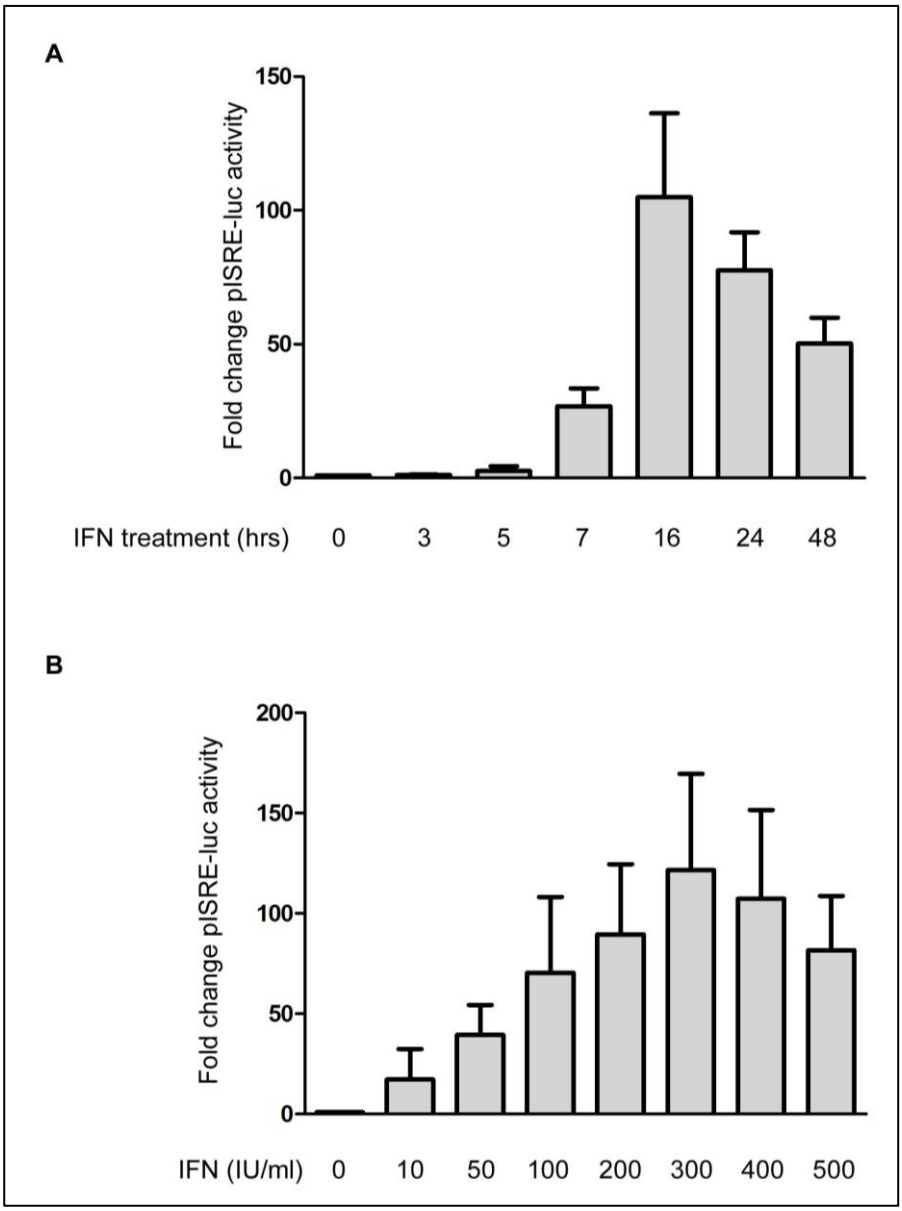

Figure 3.6: ISRE-*luc* expression peaked 16 hours post rIFNα treatment and following treatment with 300 IU/ml rIFNα.

(A) 293 cells were co-transfected with pISRE-luc (250ng) and the constitutively expressing *Renilla* luciferase plasmid (pRLSV40-luc, 1ng). Following 5 hours incubation, the cells were treated with rIFNα (300IU/ml) for different durations of time (shown in figure), before being harvested and subject to DLA. pRLSV40-luc was added as an internal control to which firefly luciferase levels were normalised. The data has been normalised to give fold increase compared to the un-stimulated samples (no rIFNα). Each time point represents the mean ± SEM of three independent experiments, which were each assayed in duplicate. For results from individual experiments see Figure 9.1. (B) The experiment was performed as described in A, except that the cells were treated with different amount of rIFNα (shown in figure) for 16 hours and then harvested for DLA. Again, luciferase levels were normalised to *Renilla* levels, and the data have been normalised to give fold increase compares to the un-stimulated (no rIFNα) samples. Each point

represents the mean ± SEM of three independent experiments which were assayed in duplicate. For results from individual experiments see Figure 9.2.

3.6. Investigating the effect of vIRF2 upon early and late IFN signalling

As discussed in chapter 1, the KSHV vIRF2 protein has been shown to inhibit both the IFN production pathway and the JAK-STAT signalling pathway. This thesis aims to further examine the molecular mechanism by which vIRF2 causes these effects. Since vIRF2 has been previously shown to inhibit both the IFN production and JAK-STAT signalling pathways, it was also used as a positive control for experiments with vIRF4. Section 3.5 described the optimum conditions for assaying IFNβ and ISRE activity in DLAs. To confirm the inhibitory effect of vIRF2 on both the IFNβ promoter and an ISRE-containing promoter IFNβ and ISRE activities were measured in the context of vIRF2 expression.

3.6.1. Inhibition of poly(I:C)-driven activation of the IFNβ promoter by vIRF2 protein expression

To confirm the effect of vIRF2 on the transactivation of the IFNβ promoter, a reporter plasmid containing this promoter (p125-luc) was co-transfected into 293 cells with either the constitutively expressing vIRF2 plasmid (vIRF2-His/Max), or the corresponding empty vector (pcDNA4His/Max). 24 hours later poly(I:C) was transfected into the cells to activate IRF3. As expected firefly luciferase expression and therefore the IFNβ promoter transactivation was significantly inhibited (up to 75%) in the vIRF2 transfected cells compared to cells transfected with the empty vector control (Figure 3.7, compare rows 3 and 4).

3.6.2. Inhibition of rIFNα-driven expression of pISRE-luc by vIRF2 protein expression

To confirm the effect of vIRF2 on IFN signalling, reporter gene studies were conducted with the pISRE-luc vector. 293 cells were co-transfected with pISRE-luc and either the vIRF2 expression vector (vIRF2-His/Max) or corresponding empty vector (pcDNA4His/Max), in the presence or absence of rIFNα (300IU/ml). Under these conditions, ISRE-containing promoter transactivation was significantly inhibited by up to 88% in the vIRF2 transfected cells compared to the empty vector control as measured by firefly luciferase expression (Figure 3.8, compare rows 3 and 4).

3.6.3. vIRF2 inhibits IRF3 activity

Section 3.6.1 showed that vIRF2 inhibited poly(I:C) driven activation of the IFNβ promoter. Recent data from our group has shown that vIRF2 mediates IRF3 degradation by a mechanism involving caspase-3 (Areste et al., 2009). To confirm the effect of vIRF2 on the early IFN pathway and to investigate if vIRF2 can reduce IRF3 activity, IRF3 activity was quantified in the presence and absence of vIRF2 by IRF3 binding assays. An IRF3 TransAM kit (Active Motif) was used to quantify levels of active IRF3 in cells transfected with the vIRF2-expression plasmid, compared to those transfected with the corresponding EV (see section 2.8 for method). The results show that vIRF2 decreased IRF3 activation significantly (up to 65%) when compared to the EV transfected cells (Figure 3.9, compare rows 2 and 3).

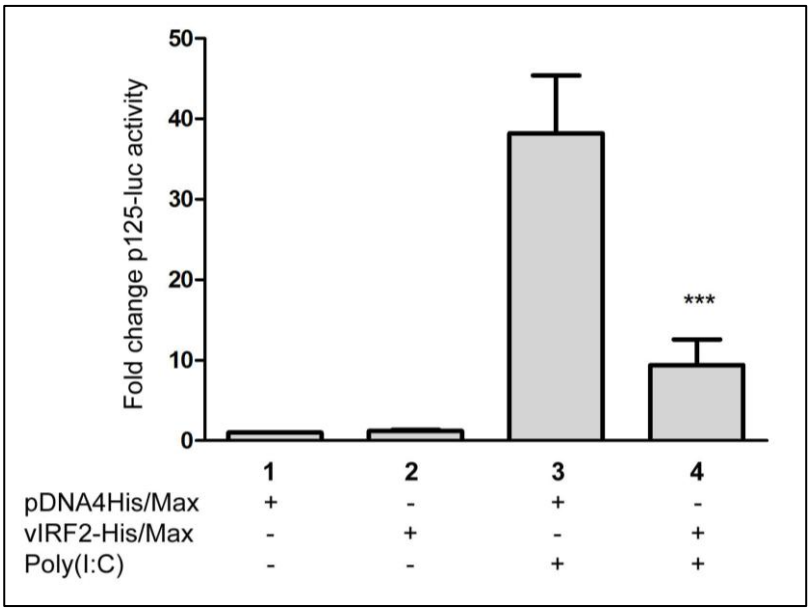

Figure 3.7: vIRF2 inhibits the poly(I:C) activated IFNβ promoter.

293 cells were transfected with p125-luc (containing the full length IFNβ promoter; 250ng) and 500ng of either the vIRF2-His/Max expression plasmid or the empty vector pcDNA4His/Max plasmid. 24 hours post-transfection, the cells were transfected with poly(I:C) (10µg/ml). After 20 hours the cells were harvested and subject to DLA. For all results, the pRLSV40 plasmid (1ng) constitutively expressing *Renilla* luciferase was added as an internal control to which firefly luciferase levels were normalised. The data were normalised to give fold increase compared to cells transfected with empty vector minus poly(I:C) stimulation (row 1). The data represent the mean and the SEM of three independent experiments that were each assayed in duplicate. *** = $p<0.001$ ANOVA followed by a Dunnett post hoc test compared to empty vector plus poly(I:C) (row 2). For results from individual experiments see Figure 9.3 (Appendix I)

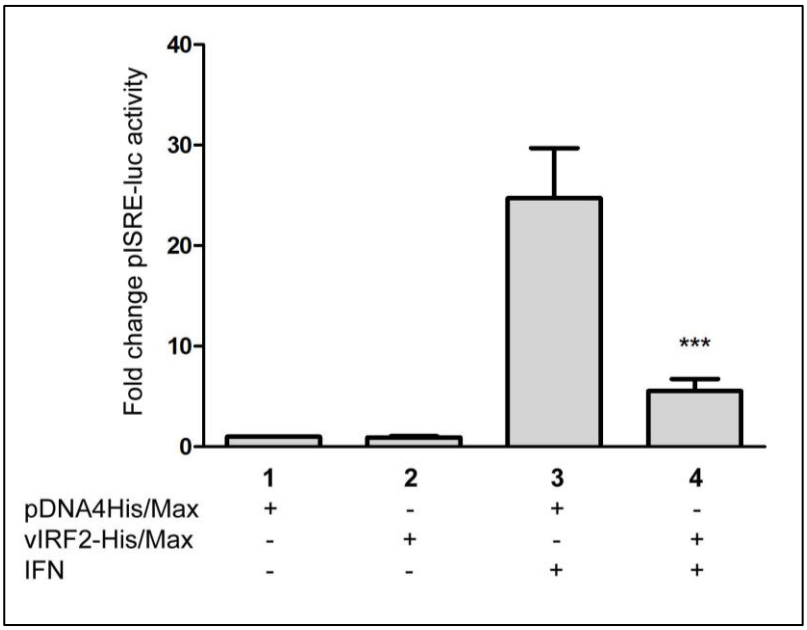

Figure 3.8: vIRF2 inhibits the rIFNα activated ISRE-containing promoter.

293 cells were transfected with pISRE-luc (250ng) and 500ng of either the vIRF2-His/Max expression plasmid or the empty vector pcDNA4His/Max plasmid. 5 h post-transfection, the cells were treated with rIFNα (300 IU/ml) and harvested 16 h later. For all results, the pRLSV40 plasmid (1ng) constitutively expressing *Renilla* luciferase was transfected as an internal control to which firefly luciferase levels were normalised. The data were normalised to give fold increase compared to transfections with empty vector minus rIFNα stimulation (row 1). The data represent the mean and the SEM of three independent experiments which were each assayed in duplicate. *** = $p<0.001$ ANOVA followed by a Dunnett post hoc test compared to empty vector plus rIFNα (row 2). For results from individual experiments see Figure 9.4 (Appendix I).

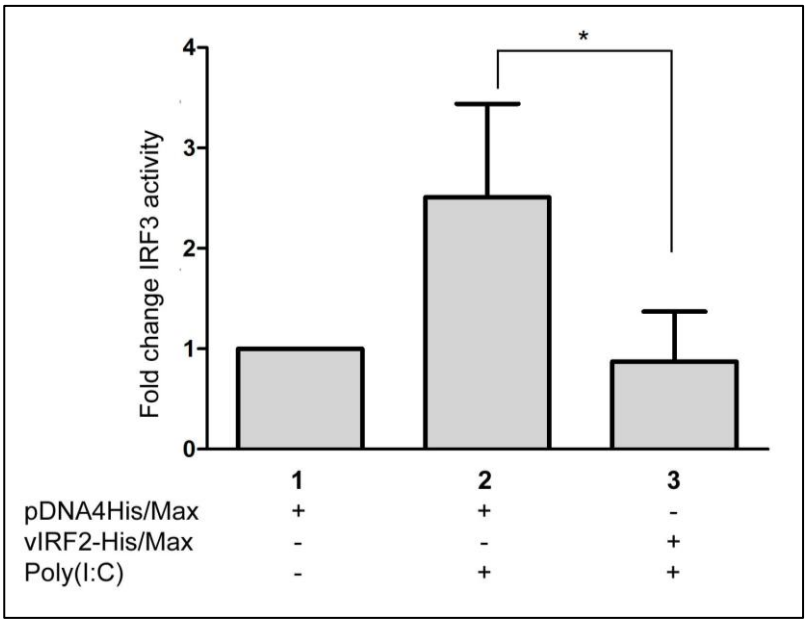

Figure 3.9: vIRF2 decreases the activity of IRF3.

IRF3 transcription factor activation was measured by TransAM assay. 293 cells were transfected with 500ng of either the vIRF2-His/Max expression plasmid or the empty vector pcDNA4His/Max plasmid. 24 hours post-transfection, the cells were transfected with poly(I:C) (10µg/ml). 20 hours later, the cells were lysed. 5µg of each sample was used in duplicate in the TransAM assay. The data were normalised to give fold increase compared to transfections with empty vector minus poly(I:C) stimulation (row 1). The data represent the mean and the SEM of three independent experiments which were each assayed in duplicate. * = $p<0.05$ ANOVA followed by a Dunnett post hoc test compared to empty vector plus poly(I:C) (row 2). For results from individual experiments see Figure 9.5.

3.7. Investigating the effect of vIRF4 upon early and late IFN signalling

To investigate any possible inhibitory effects vIRF4 might have on IFNβ promoter activation and ISRE-containing promoter activation, the activities of these promoters were measured in the context of vIRF4 expression.

3.7.1. vIRF4 does not inhibit poly(I:C)-driven activation of the IFNβ promoter in 293 cells.

To examine the effect of vIRF4 on the transactivation of the full-length IFNβ promoter, and hence early IFN signalling, the IFNβ promoter reporter plasmid (p125-luc) was co-transfected with increasing amounts of the constitutively expressing vIRF4 plasmid (vIRF4-NTAP). The empty parental plasmid backbone, pCDNA4TO-NTAP, was added as a “stuffer” plasmid to equalize the amount of DNA in each transfection to 1000ng. After 24 hours, poly(I:C) was transfected to activate IRF3 and therefore the p125-luc reporter promoter. The results show that even with up to 1000ng of vIRF4-NTAP transfected into the cells, p125-luc activity, and therefore IFNβ promoter activity did not decrease (Figure 3.10, rows 7-14). Since vIRF2 inhibits poly(I:C)-driven activation of the IFNβ promoter (section 3.6.1), it provided a positive control (Figure 3.10, compared rows 3 with 4).

3.7.2. vIRF4 inhibits rIFNα-driven expression of pISRE-luc in 293 cells.

To examine the effect of vIRF4 on JAK-STAT signalling, reporter gene studies were performed with the pISRE-luc vector. 293 cells were co-transfected with pISRE-luc and increasing amounts of the constitutively expressing vIRF4 plasmid (vIRF4-NTAP). The empty parental plasmid backbone, pCDNA4TO-NTAP, was

added as a “stuffer” plasmid to equalize the amount of DNA in each transfection to 1000ng. 5 hours post transfection the cells were treated with rIFNα (300IU/ml), to activate the IFN-sensitive reporter promoter. Under these conditions, *luciferase* expression and therefore ISRE transactivation was inhibited in a manner that depended upon the amount of vIRF4-NTAP expression vector (Figure 3.11, rows 7-14). ISRE transactivation was reduced by 51% in the presence of 1000ng of vIRF4-NTAP (Figure 3.11, row 14). Since vIRF2 can inhibit rIFNα driven activation of the ISRE-containing promoter, the pvIRF2-His/Max or corresponding empty vector pcDNA4His/Max plasmid were transfected into 293 cells in parallel experiments and compared to show ISRE inhibition (Figure 3.11, compare rows 3 and 4).

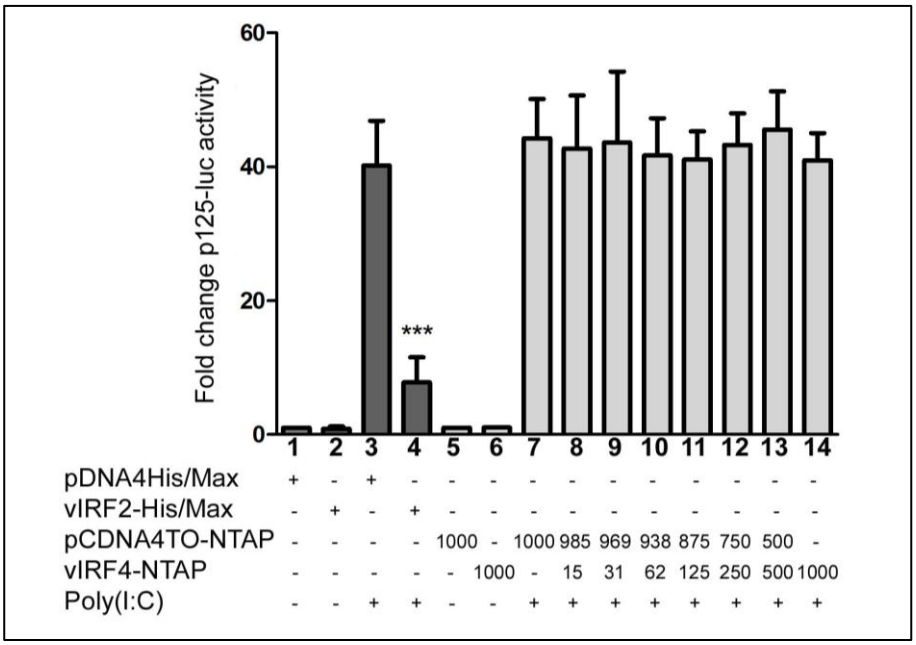

Figure 3.10: vIRF4 does not inhibit poly(I:C)-driven activation of the IFNβ promoter.

Rows 5-14: 293 cells were transfected with p125-luc (250ng) and increasing amounts of the vIRF4-NTAP expression vector (rows 6 and 8-14). 24 hours post-transfection, the cells were transfected with poly(I:C) (10µg/ml) and harvested 20 hours later. The empty parental plasmid backbone, pCDNA4TO-NTAP was added as required to equilibrate all transfectants to 1000ng of DNA. The pRLSV40 plasmid (1ng), was added as an internal control to which firefly luciferase levels were normalised. The results are shown as fold increase compared to the empty vector (pCDNA4TO-NTAP) transfections which were un-stimulated (row 5). The data represent the mean ± the SEM of the three independent experiments which were each assayed in duplicate. *** = $p<0.001$ ANOVA followed by a Dunnett post hoc test compared to empty vector (pCDNA4TO-NTAP) plus poly(I:C) (row 7). As a positive control for the assay, vIRF2 was used to show inhibition of 125-luc activity (rows 1-4, dark grey). To achieve this, the vIRF2-His/Max plasmid (1000ng) or pcDNA4His/Max plasmid (1000ng), were transfected into 293 cells with the p125-luc (250ng) pRLSV40 (1ng) plasmids. These results were normalised again using the pRLSV40 plasmid. These dark grey results are shown as fold increase compared to the empty vector (pcDNA4His/Max) transfections which were un-stimulated with poly(I:C) (row 1). The data represent the mean ± the SEM of the three independent experiments which were each assayed in duplicate. *** = $p<0.001$ ANOVA followed by a Dunnett post hoc test compared to empty vector (pcDNA4His/Max) plus poly(I:C) (row 3). For results from individual experiments see Figure 9.6 (Appendix I).

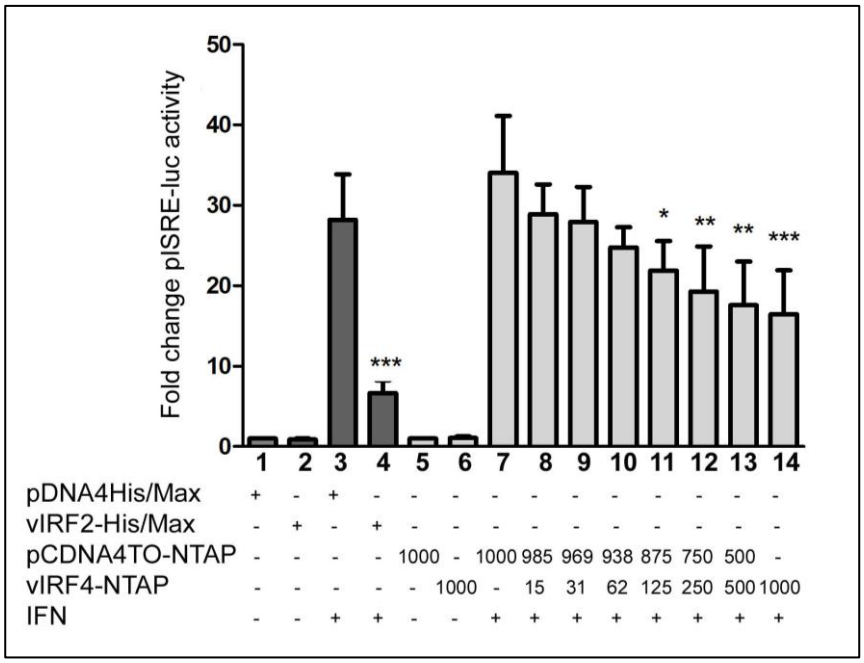

Figure 3.11: vIRF4 inhibits rIFNα-driven expression of pISRE-luc.

293 cells were transfected with pISRE-luc (250ng) and increasing amounts of the vIRF4-NTAP expression vector (rows 6 and 8-14). 5 hours post transfection, the cells were treated with rIFNα (300IU/ml) and harvested 16 hours later. The empty parental plasmid backbone, pCDNA4TO-NTAP was added as required to equilibrate all transfectants to 1000ng of DNA. The pRLSV40 plasmid (1ng), was added as an internal control to which firefly luciferase levels were normalised. The results are shown as fold increase compared to the empty vector (pCDNA4TO-NTAP) transfections which were un-stimulated with rIFNα (row 5).The data represent the mean ± the SEM of the three independent experiments which were each assayed in duplicate. *** = $p<0.001$ ANOVA followed by a Dunnett post hoc test compared to empty vector (pCDNA4TO-NTAP) plus rIFNα (row 7). As a positive control for the assay, vIRF2 was used to show inhibition of ISRE-luc activity (rows 1-4, dark grey). To achieve this, the vIRF2-His/Max plasmid (1000ng) or pcDNA4His/Max plasmid (1000ng), were transfected into 293 cells with the pISRE-luc (250ng) pRLSV40 (1ng) plasmids. These results were normalised again using the pRLSV40 plasmid. The dark grey results are shown as fold increase compared to the empty vector (pcDNA4His/Max) transfections which were un-stimulated (row 1). The data represent the mean ± the SEM of the three independent experiments which were each assayed in duplicate. *** = $p<0.001$ ANOVA followed by a Dunnett post hoc test compared to empty vector (pcDNA4His/Max) plus rIFNα (row 3). For results from individual experiments see Figure 9.7.

3.8. Examining the effect of vIRF2 truncated mutants on IFNβ-promoter and ISRE-containing promoter activity

To identify the region of vIRF2 responsible for the inhibition of the on IFNβ-promoter and ISRE-containing promoter, vIRF2 truncated mutants were used in DLAs. To produce these mutants, different regions of the vIRF2 gene were cloned into the pcDNA4His/Max expression vector (cloning performed by Christina Areste) (Figure 3.12A). The expression of each mutant in 293 cells was confirmed by western blot analysis (Figure 3.12B).

3.8.1. The effect of vIRF2 truncated mutants on the IFNβ-promoter

To examine the effect of vIRF2 mutants on the transactivation of the full-length IFNβ promoter, DLAs were performed, similar to section 3.6.1, with the full length IFNβ promoter reporter plasmid and with the different truncated forms of vIRF2, F1-F8, (Figure 3.13, rows 5-12). 24 hours later poly(I:C) was transfected into the cells to activate IRF3. The activities in these samples were compared to transfections containing the empty vector control and to those containing the full length vIRF2 expression plasmid (Figure 3.13, rows 3 and 4). The mutants that were able to significantly ($p<0.001$) inhibit the activity of the IFNβ promoter, compared to the empty vector, were F2 (by 42%) F3 (by 58%) F4 (by 40%) and F8 ($p<0.01$) (by 34%) compared to the empty vector (Figure 3.13, rows 6, 7, 8 and 12). Mutant F2 spans from amino acid residues 1-320, while F3 spans from amino acid residues 1-518 and mutant F4 spans from amino acid residues 118-680. The region in common between these three mutants is from amino acid residues 118-320. This is the region which the F8 mutant spans.

3.8.2. The effect of vIRF2 truncated mutants on the ISRE-containing promoter

To examine the effect of the vIRF2 mutants on the transactivation of the ISRE-containing promoter, DLAs were performed, similar to section 3.6.2 with the ISRE-containing promoter reporter plasmid. This plasmid was co-transfected with the different vIRF2 mutants, F1-F8, (Figure 3.14, rows 5-12). After 5 hours incubation, rIFNα was added to the cells to activate JAK-STAT signalling. The luciferase activities of these samples were compared to transfections containing the empty vector control and to those containing the full length vIRF2 expression plasmid (Figure 3.14, rows 3 and 4). The full length vIRF2 protein inhibited ISRE activity by 70% (Figure 3.14, row 4), but of the mutants, only F3 and F4 were able to significantly ($p<0.001$) inhibit the activity of the ISRE-containing promoter when compared to the empty vector (Figure 3.14, rows 7 and 8). Mutant F3 inhibited ISRE activity by 52%, whereas mutant F4 inhibited by 64%. The region in common between these two mutants is from amino acid residues 118-518.

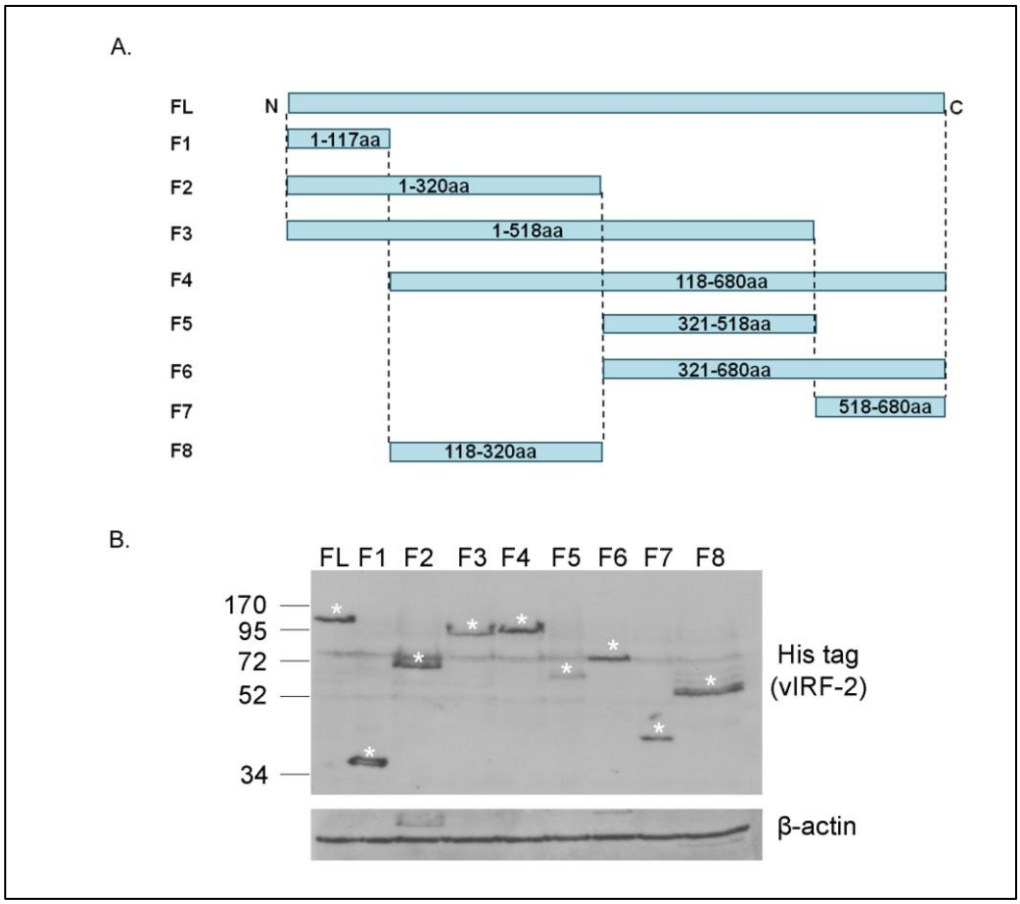

Figure 3.12: vIRF2 truncated mutants and their expression in 293 cells.

(**A**) Diagram of the vIRF2 truncated mutants F1-F8. FL=Full length protein. **(B)** Western blot showing the expression of the vIRF2 truncated mutants in 293 cells. 293 cells were transfected with 1000ng of the full length vIRF2-His/Max, or one of the truncated mutants pcDNA4/F1 - pcDNA4/F8 and harvested 16 hours later. The lysates (20µg) were analysed by western blot to detect the His-tag. Primary antibody: anti-His. Secondary antibody: anti-mouse HRP-conjugated secondary antibody. The position of each His-tagged protein is indicated tagged by *. β-actin, the loading control, is also indicated.

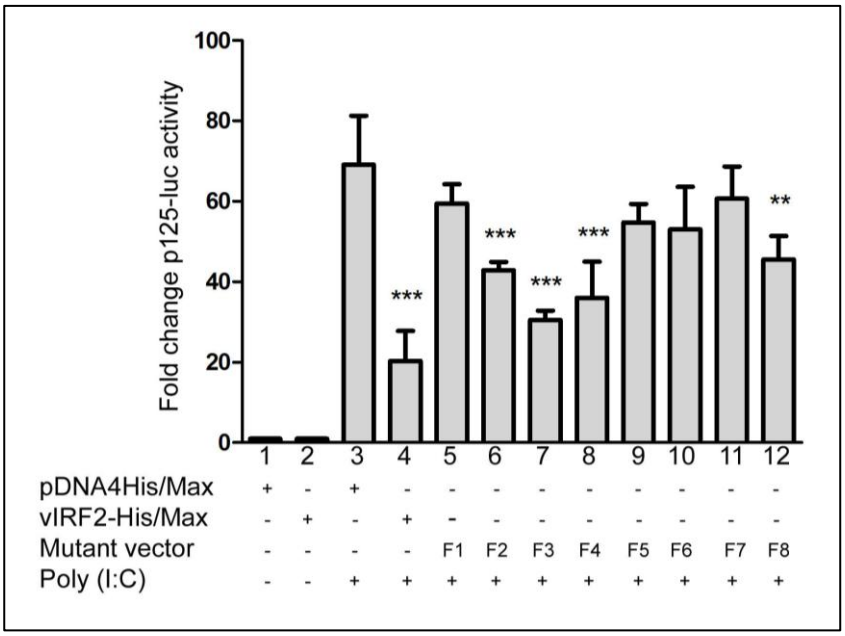

Figure 3.13: The effect of the vIRF2 truncated mutants on poly(I:C)-driven activation of the IFNβ promoter.

To examine the effect of the vIRF2 truncated mutants on the transactivation of the full-length IFNβ promoter, the full length IFNβ promoter firefly reporter plasmid was co-transfected with either the constitutively expressing vIRF2 plasmid (pcDNA4/vIRF2), or one of the truncated mutants pcDNA4/F1 - pcDNA4/F8 or the corresponding empty vector (pcDNA4His/Max). 24 hours later poly(I:C) was transfected to activate IRF3. For all results, the pRLSV40 plasmid (1ng) constitutively expressing *Renilla* luciferase was transfected as an internal control to which firefly luciferase levels were normalised. The results are shown as fold increase compared to the empty vector (pcDNA4His/Max) transfections which were un-stimulated (row 1). The data represent the mean ± the SEM of the three independent experiments which were each assayed in duplicate. ** = $p<0.01$, *** = $p<0.001$ ANOVA followed by a Dunnett post hoc test compared to empty vector (pcDNA4His/Max) plus poly(I:C (row 3)). For results from individual experiments see Figure 9.8.

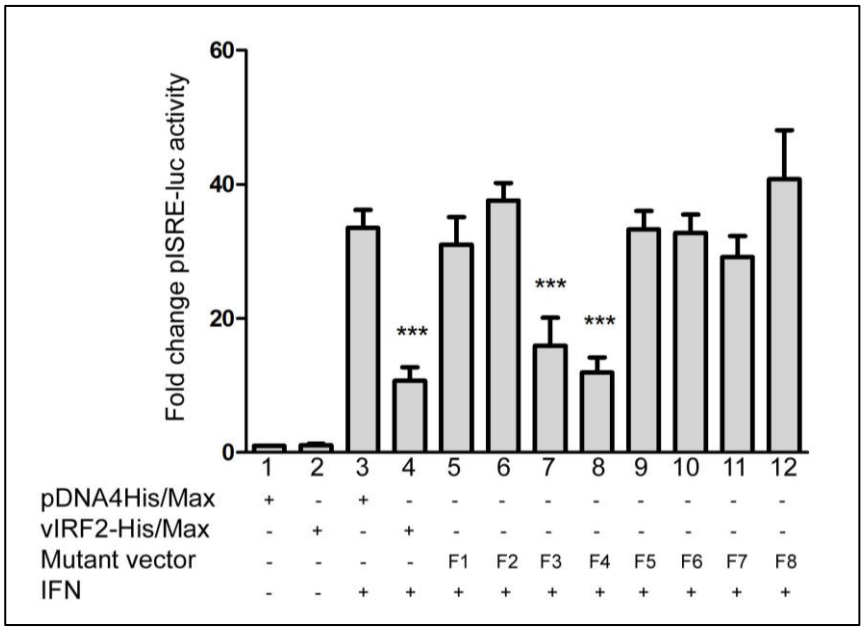

Figure 3.14 The effect of the vIRF2 truncated mutants on IFNα activation of an ISRE-containing promoter.

To examine the effect of the vIRF2 truncated mutants on the transactivation of an ISRE containing promoter, 293 cells were co-transfected with pISRE-luc (250ng) and 1000ng of either the constitutively expressing vIRF2 plasmid (vIRF2-His/Max), or one of the truncated mutants pcDNA4/F1 - pcDNA4/F8 or the corresponding empty vector (pcDNA4His/Max). 5 h post-transfection, the cells were treated with rIFNα (300IU/ml) and harvested 16 h later. For all results, the pRLSV40 plasmid (1ng) constitutively expressing *Renilla* luciferase was transfected as an internal control to which firefly luciferase levels were normalised. The results are shown as fold increase compared to the empty vector (pcDNA4His/Max) transfections minus rIFNα (row 1). The data represent the mean ± the SEM of the three independent experiments which were each assayed in duplicate. *** = $p<0.001$ ANOVA followed by a Dunnett post hoc test compared to empty vector (pcDNA4His/Max) plus poly(I:C) (row 3). For results from individual experiments see (Figure 9.9).

3.9. Discussion of Chapter 3

The experiments in this chapter confirmed the ability of vIRF2 to inhibit activation of both the IFNβ promoter (Figure 3.7) and the ISRE-containing promoter (Figure 3.8). Because of the inhibitory effect of vIRF2 on both the IFN production pathway, and the JAK-STAT pathway, it was used as a positive control throughout the experiments concerning vIRF4. Previous experiments performed in our laboratory revealed that vIRF2 is able to accelerate the caspase-3-dependent process of IRF3 turnover (Areste et al., 2009), suggesting a mechanism for inhibition of IFNβ promoter inactivation. However, vIRF2 is also able to repress IFNβ activity in the absence of caspase-3 (Areste et al., 2009). These observations reveal that vIRF2 can inhibit IFNβ promoter activity by more than one mechanism. To deduce whether or not vIRF2 could inhibit IRF3 activity, as well as the degradation of IRF3 as shown in Areste el at, (2009), IRF3 DNA binding assays were performed (Figure 3.9). These results showed that vIRF2 suppressed IRF3 activity, providing a further mechanism by which vIRF2 inhibits IFNβ promoter activity.

The mechanism behind the vIRF2 mediated inhibition of the JAK-STAT signalling pathway has not been fully identified. Mutochelu et al, (2011) showed that vIRF2 decreases levels of pSTAT1 in 293 cells. However, the mechanism underlying this activity is unknown. This area will be explored in further detail in the following chapters.

There is very little in the literature concerning the effects of vIRF4 on IFN signalling. Kanno et al, (2006) reported that vIRF4 is unable to repress the IFNβ

promoter when activated by Sendai virus, suggesting that vIRF4 cannot suppress the IFN production pathway. The results in this chapter support this conclusion; Figure 3.10 shows that vIRF4 is unable to inhibit the poly(I:C) driven activation of the IFNβ promoter. However, this chapter also investigated the effect of vIRF4 on the later part of type I IFN signalling, the JAK-STAT signalling pathway. Figure 3.11 demonstrates that vIRF4 can inhibit the rIFNα activated ISRE promoter by up to 51%. The involvement of vIRF4 in this later stage of the type I IFN response has not been reported in the literature previously, and hence this is a novel result.

The inhibition of ISRE activity by vIRF4 was 51% compared to the 76% inhibition by vIRF2 (Figure 3.11). However, comparing the inhibition by these proteins in these experiments is not meaningful, as differences in the extent of inhibition could simply be due to differences in their relative expression levels.

When examining the effect of the vIRF2 truncated mutants on the IFNβ promoter activity, mutants F2, F3, F4 and F8 significantly inhibited ISRE activity compared to the EV control (Figure 3.13). However, even though equal amounts of each plasmid was transfected into 293 cells, the protein expression of these mutants was not equal (Figure 3.12B), mutants F3 and F5 don't express as well as the rest of the mutants. Therefore, the inhibition by the F3 mutant on the IFNβ promoter may be greater than observed in Figure 3.13. In a similar manner, the lack of IFNβ promoter inhibition by F5 could be due to the low protein expression of this mutant. Nonetheless, the region in common between the mutants F2, F3 and F4 is the amino acid residues 118-320; the region which the F8 mutant spans. These

results indicate that the region of vIRF2 responsible for the inhibition of IFNβ promoter activity is encompassed by the F8 mutant. Further experiments could narrow down the region responsible through construction of more mutants containing regions within the amino acids 118-320.

When examining the effect of the vIRF2 truncated mutants on ISRE activity, it was found that only mutants F3 and F4 significantly inhibited ISRE activity compared to the EV control (Figure 3.14), and the extent of their inhibition (52% and 64% respectively) was comparable to that of the full-length vIRF2 (70%). Again, due to unequal protein expression of the mutants (Figure 3.12B) the inhibition of ISRE activity by the F3 may be greater than observed of in Figure 3.14 and the lack of ISRE promoter inhibition by F5 could be due to the low protein expression of this mutant. The region in common between the F3 and F4 mutants is amino acids 118-518. This result therefore suggests that amino acid residues 118-518 are necessary for ISRE inhibition by vIRF2. To test this theory, an additional vIRF2 mutant could be produced, comprising of amino acids 118-518.

Interestingly, the vIRF2 truncated mutant F1 is unable to inhibit either IFNβ promoter activity or ISRE-containing promoter activity. This mutant comprises the N-terminal region of vIRF2, which shares some homology to the DBD of the IRF family of transcription factors (Cunningham et al., 2003). This observation suggests that the mechanism of action of vIRF2 is not dependent on direct binding to DNA.

In summary, this chapter confirms the inhibition of both IFNβ promoter activity and ISRE-containing promoter activity by vIRF2 and demonstrates that vIRF2 can reduce IRF3 activity. The region of vIRF2 responsible for the inhibition of IFNβ promoter activity appears to be between amino acids 118-320, whereas the region responsible for inhibition of the ISRE-containing promoter seems to be a larger area between amino acids 118-518. Importantly, this chapter shows that like vIRFs 1-3, vIRF4 also negatively regulates the type I IFN response, but doesn't target the early IFN production pathway, rather it targets JAK-STAT signalling. In the next chapters, the mechanisms behind the inhibition of the ISRE-containing promoter by vIRF2 and vIRF4 will be explored.

CHAPTER 4

DERIVATION AND FUNCTIONAL ANALYSES OF STABLE CELL LINES EXPRESSING vIRF2 AND vIRF4

4.1. Introduction to chapter 4

Chapter 3 described how the vIRF4 gene was cloned into the pCDNATO-NTAP vector in order to perform *in vitro* functional studies. These functional studies revealed that, like vIRF2, vIRF4 is also able to inhibit rIFNα stimulated transactivation of an ISRE-containing promoter. These experiments were performed via transient transfection using the pvIRF4-NTAP vector with the pCDNA4TO-NTAP parental vector as a control. Throughout these studies, the effect of vIRF2, expressed from pvIRF2-His/Max, provided a positive control. In order to examine the mechanism by which vIRF2 and vIRF4 exert their inhibitory effect on the ISRE-containing promoter, it is necessary to have stable cell lines which express the vIRF2 or vIRF4 proteins. The advantage of stable cell lines compared with transiently transfected cells is that all the cells in a population will express the vIRF2 or vIRF4 protein, instead of only those which are transfected. This means that any effects of the vIRF2 or vIRF4 proteins are not masked by cells which don't express these proteins.

This chapter describes the production and characterisation of cell lines, which were engineered to contain antibiotic selectable plasmids that could be induced to express either the vIRF2-NTAP or vIRF4-NTAP proteins, or the NTAP protein. The NTAP protein is a tag expressed from the pCDNA4TO-NTAP vector, which is expressed contiguous to the vIRF2 or vIRF4 proteins in their respective cell lines. Throughout this thesis, these cell lines will be collectively referred to as 'stable cell lines'.

The aims of this chapter are to:

1) Clone the vIRF2 gene into the pCDNA4TO-NTAP expression vector and ensure that this vector expresses vIRF2-NTAP in 293 cells.
2) Create three stable cell lines expressing the NTAP-protein, the vIRF2-NTAP protein or the vIRF4-NTAP protein.
3) Confirm that these cell lines express the vIRF2 and vIRF4 proteins, and show that they behave as previously observed in chapter 3.
4) Determine whether the levels of the vIRF2 and vIRF4 mRNA in the stable cell lines are comparable to those in a naturally infected KSHV cell line.

It was decided that vIRF2 should be cloned into pCDNA4TO-NTAP, to form the resultant pvIRF2-NTAP vector, for a number of reasons. Firstly, the vIRF4 gene had been previously cloned into this vector and was shown to express well (chapter 3). The empty vector control, pCDNA4TO-NTAP, would be the same control for both pvIRF2-NTAP and pvIRF4-NTAP meaning vIRF2 and vIRF4 could be compared better. Secondly, previous studies on vIRF2 have found that its constitutive expression is detrimental to cells (Fuld & Blackbourn, un-published data). Because of this negative effect, any cell line engineered to express vIRF2 would ideally be inducible for the expression of this viral protein, so that its expression can be controlled. The pCDNA4TO-NTAP vector can be used to create stable cell lines which are tetracycline inducible, by transfecting the vector into a cell line which expresses the tetracycline repressor (Yao et al., 1998). Finally, the pCDNA4TO-NTAP vector encodes an N-terminal-TAP-tag which would be

expressed contiguously with the vIRF2 or vIRF4 proteins. This tag will enable the purification of the vIRF2 or vIRF4 proteins along with any protein binding partners. The identity of such partners may lead to understanding of how vIRF2 or vIRF4 exert their inhibition on the JAK-STAT signalling pathway.

The expression of vIRF2-NTAP from the pvIRF2-NTAP vector was demonstrated in 293 cells by western blotting, and the inhibitory effect of vIRF2 on both the IFN production and JAK-STAT signalling pathways was shown to be consistent with initial studies using the vIRF2-His/Max vector (section 3.6).

Stable cell lines containing the pCDNA4TO-NTAP, pvIRF2-NTAP, or pvIRF4-NTAP were produced. These cell lines were analysed to ensure that they expressed the NTAP, vIRF2-NTAP or vIRF4-NTAP proteins following tetracycline stimulation. The vIRF2-NTAP and vIRF4-NTAP cell lines were evaluated for their ability to inhibit IFN signalling, compared to the EV-NTAP control. These cell lines were further analysed to identify the sub cellular location of vIRF2-NTAP and vIRF4-NTAP, and to compare the levels of vIRF2 and vIRF4 mRNA with that of those in BCBL1 cells.

4.2. Cloning the vIRF2 gene into the pCDNATO-NTAP vector

Chapter 3 described how the vIRF4 gene was cloned into the pCDNATO-NTAP vector in order to perform *in vitro* functional studies. As explained in the introduction to this chapter, it was also necessary to clone the vIRF2 gene into the pCDNATO-NTAP vector. An overview of the cloning scheme is illustrated in Figure 4.1. The vIRF2 gene had been cloned into the pCR-Blunt sub-cloning vector in the past (performed by members of the Blackbourn lab). Therefore, the vIRF2 gene was amplified from pCR-Blunt-vIRF2, using specific primers containing BsiWI and XbaI restriction sites (see Table 2.14 'vIRF2 forward with BsiWI' and 'vIRF2 reverse with XbaI'). The PCR product was separated through gel electrophoresis, excised, purified, and ligated into pCR-Blunt. The resultant pCR-Blunt-vIRF2 (BsiWI and XbaI) was then digested with XbaI and BsiWI, separated through gel electrophoresis, excised, purified, and ligated and ligated into the purified NTAP vector which had been digested with XbaI and BsiWI. The resultant pvIRF2-NTAP construct was confirmed by sequencing (data not shown).

4.3. Transient expression of vIRF2 in 293 cells

To ensure the pvIRF2-NTAP expression vector expressed the vIRF2-NTAP protein in 293 cells a transfection titration was performed. 293 cells were transfected with varying amounts of vIRF2 from 0-1000ng and 16 hours later the cells were harvested. Western blot analysis showed, as expected, that as the amount of pvIRF2-NTAP transfected increased, the expression levels of vIRF2-NTAP also increased up to 500ng. The amount of vIRF2-NTAP is the same in the 1000ng sample compared to the 500ng indicating that the optimum expression of

vIRF2 results from between 500ng-1000ng of transfected pvIRF2-NTAP plasmid (Figure 4.2).

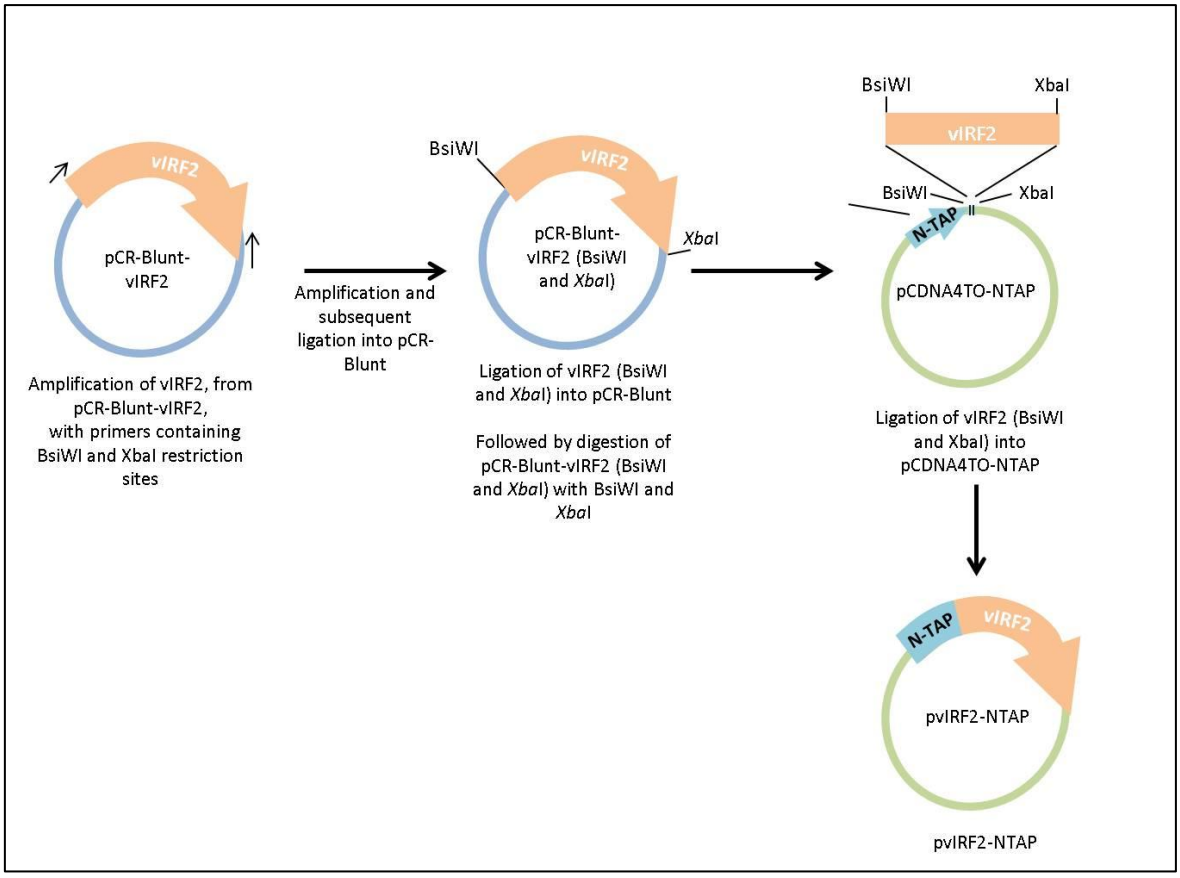

Figure 4.1: Cloning the vIRF2 gene into the pCDNATO-NTAP vector.

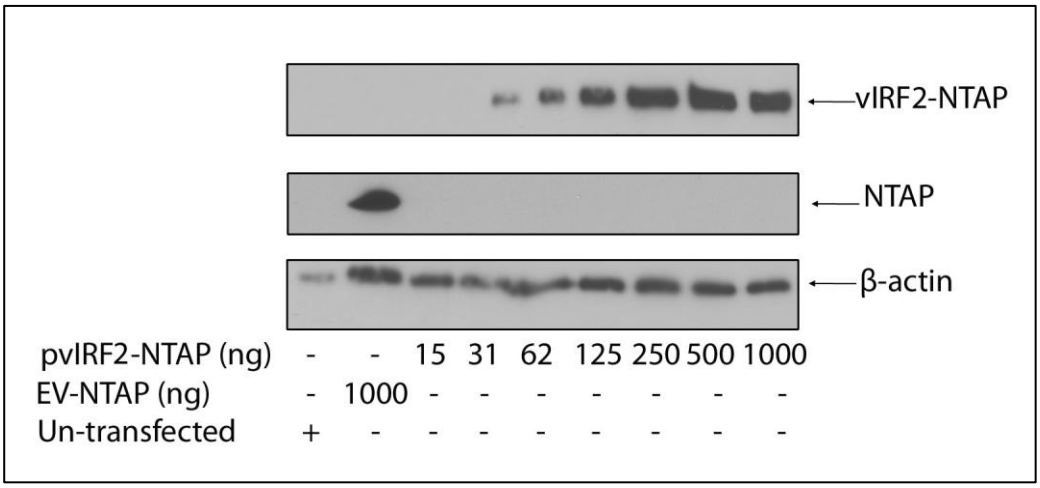

Figure 4.2: vIRF2 expression in 293 cells transiently transfected with the pvIRF2-NTAP vector.

293 cells were transfected with the pvIRF2-NTAP vector (0-1000ng), and harvested 16 hours later. The lysate (20µg) was analysed by western blot to detect the NTAP-tag. Primary antibody: anti-β-actin. Secondary antibody: anti-mouse HRP-conjugated secondary antibody. The NTAP tagged vIRF2 (vIRF2-NTAP) and the TAP tag produced from EV-NTAP transfected cells are indicated (NTAP). β-actin is also indicated. The use of the anti-mouse HRP-conjugated secondary antibody was sufficient to detect the NTAP-tag as this tag contains protein G binding domains. As a control for the specificity of these bands, un-transfected cell Lysate was also loaded. This experiment was repeated completely and the resultant blot is shown in Figure 9.10

4.4. Confirmation that vIRF2, expressed from the pvIRF2-NTAP vector, inhibits poly(I:C)-driven activation of the IFNβ promoter in 293 cells

To confirm that the vIRF2 protein, expressed from the pvIRF2-NTAP vector, can inhibit transactivation of the full-length IFNβ promoter, a reporter plasmid containing the full length IFNβ promoter was co-transfected with increasing amounts of the pvIRF2-NTAP vector. 24 hours later poly(I:C) was transfected to activate IRF3. As expected firefly luciferase expression and therefore the IFNβ promoter transactivation was significantly inhibited in the vIRF2 transfected cells compared to the empty vector control (Figure 4.3, compare columns 3 with 4, 5 and 6). IFNβ transactivation was inhibited by up to 70% in the presence of 1000ng of pvIRF2-NTAP (Figure 4.3, compare columns 3 and 6).

4.5. Confirmation that vIRF2, expressed from the pvIRF2-NTAP vector, inhibits rIFNα-driven expression of pISRE-luc in 293 cells

To confirm that the vIRF2 protein, expressed from the pvIRF2-NTAP vector, can inhibit the transactivation of the ISRE promoter, reporter gene studies were performed with the pISRE-luc vector. 293 cells were transiently co-transfected with pISRE-luc and increasing amounts of the constitutively expressing vIRF2 plasmid (pvIRF2-NTAP). 5 hours post transfection the cells were treated with rIFNα, to activate the JAK-STAT signalling pathway. Under these conditions, firefly luciferase expression and therefore the ISRE-containing promoter transactivation was significantly inhibited in the vIRF2 transfected cells compared to the empty vector control (Figure 4.4 compare column 3 with 4, 5 and 6). ISRE transactivation was inhibited by up to 70% in the presence of 1000ng of pvIRF2-NTAP (Figure 4.4, compare columns 3 and 6).

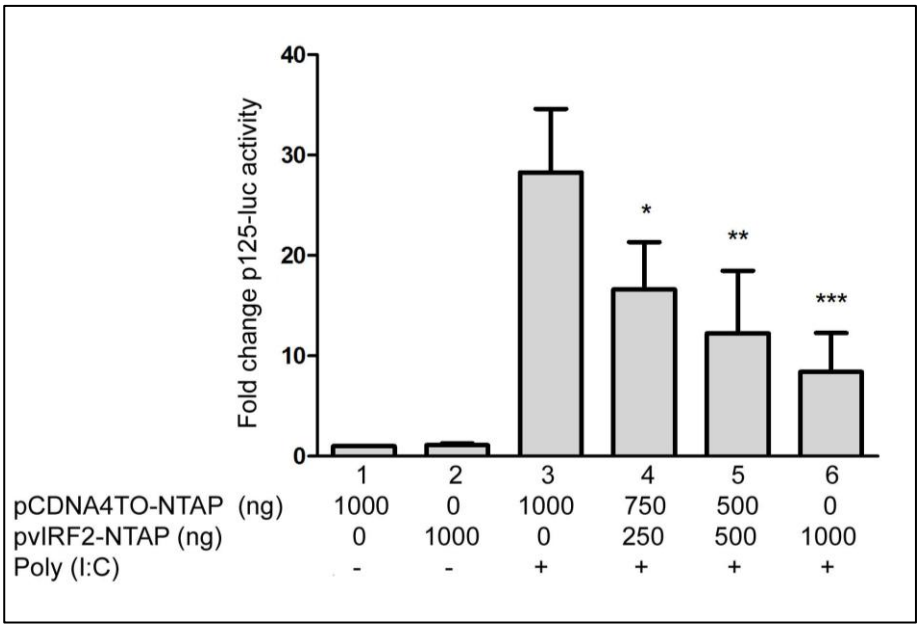

Figure 4.3: vIRF2, expressed from the pvIRF2-NTAP vector, inhibits poly(I:C)-driven activation of the IFNβ promoter.

293 cells were transfected with p125-luc (250ng) and increasing amounts of the pvIRF2-NTAP expression vector (indicated in figure, 0-1000ng). 24 hours post-transfection, the cells were transfected with poly(I:C) (10µg/ml) and harvested 20 hours later. The empty parental plasmid backbone, pCDNA4TO-NTAP was added as required to equilibrate all transfectants to 1000ng of DNA. The pRLSV40 plasmid (1ng), was added as an internal control to which firefly luciferase levels were normalised. The results are shown as fold increase compared to the empty vector (pCDNA4TO-NTAP) transfections which were un-stimulated (lane 2). The data represent the mean ± the SEM of three independent experiments which were each assayed in duplicate. * = $p<0.5$, * = $p<0.01$, *** = $p<0.001$ ANOVA followed by a Dunnett post hoc test compared to empty vector (pCDNA4TO-NTAP) plus poly(I:C) (lane 3). For results from individual experiments see Figure 9.11 (Appendix I).

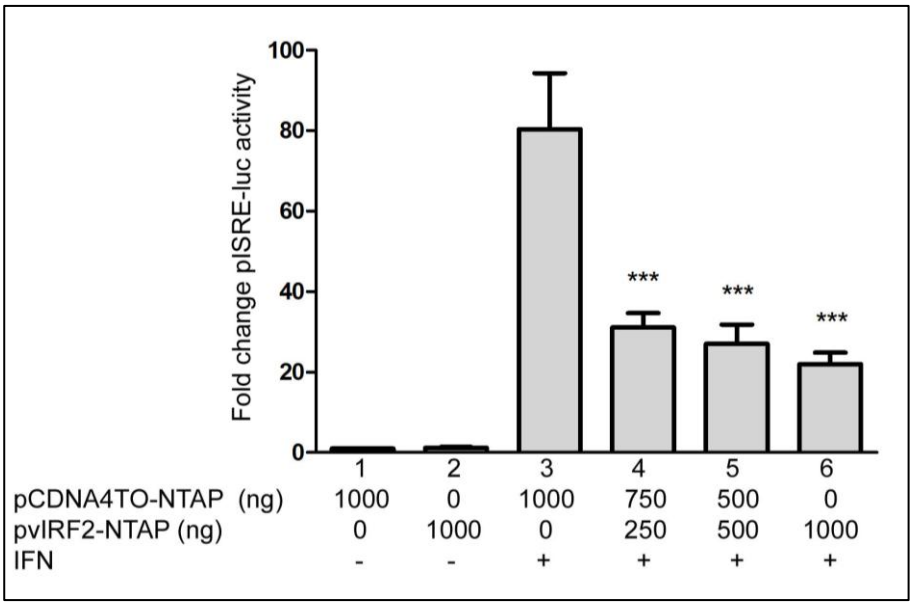

Figure 4.4: vIRF2, expressed from the pvIRF2-NTAP vector, inhibits rIFNα-driven expression of pISRE-luc.

293 cells were transfected with pISRE-luc (250ng) and increasing amounts of the pvIRF2-NTAP expression vector (indicated in figure, 0-1000ng). 5 hours post transfection, the cells were treated with rIFNα (300 U/ml), or left untreated and harvested 16 hours later. The empty parental plasmid backbone, pCDNA4TO-NTAP was added as required to equilibrate all transfectants to 1000ng of DNA. The pRLSV40 plasmid (1ng), was added as an internal control to which firefly luciferase levels were normalised. The results are shown as fold increase compared to the empty vector (pCDNA4TO-NTAP) transfections which were un-stimulated (lane2). The data represent the mean ± the SEM of three independent experiments which were each assayed in duplicate. *** = $p<0.001$ ANOVA followed by a Dunnett post hoc test compared to empty vector (pCDNA4TO-NTAP) plus rIFNα (lane 3). For results from individual experiments see Figure 9.12 (Appendix I).

4.6. Production of stable cell lines that express either vIRF2-NTAP, vIRF4-NTAP or the NTAP-tag

To facilitate experiments which aim to study the mechanism of the vIRF2 and vIRF4 proteins, stable cell lines, which express the NTAP-tag only, the vIRF2-NTAP or the vIRF4-NTAP proteins were produced. T-REX cell lines (see section 2.1.5), which express the tetracycline repressor under the selection of Blasticidin, were transfected with either the pCDNA4TO-NTAP, pvIRF2-NTAP or pvIRF4-NTAP vectors which had been linearised with PvuI. This enzyme cuts each plasmid once outside the inserted gene (vIRF2 of vIRF4). Cells were treated with Blasticidin and Zeocin to select for transfected cells, and colonies were established. For details see section 2.1.5. The resultant cell lines (called EV-NTAP, vIRF2-NTAP and vIRF4-NTAP) were cultured in 5µg/mL Blasticidin and 200µg/ml Zeocin.

4.7. Optimising vIRF2 &-4 expression with tetracycline

The EV-NTAP, vIRF2-NTAP and vIRF4-NTAP cell lines can be induced by tetracycline to express the NTAP, vIRF2-NTAP and vIRF4-NTAP proteins respectively. To confirm that these cell lines express the specific proteins, and to characterise the amount of tetracycline and time course of induction required to induce expression of the TAP-tagged proteins, optimisation experiments were performed.

4.7.1. Optimising the amount of tetracycline necessary to induce vIRF2 & 4 protein expression

To identify a suitable amount of tetracycline to induce the EV-NTAP, vIRF2-NTAP and vIRF4-NTAP cell lines to express their respective proteins, a tetracycline titration was performed. The cell lines were stimulated with tetracycline (ranging between 0–2µg/ml) and samples were obtained for western blot analysis 24 hours later. Figure 4.5 shows the results. The indicated bands correspond in size to that of each of the specific proteins (vIRF2 140kDa, vIRF4 130kDa) with the NTAP tag attached. In the three cell lines, 0.125µg/ml of tetracycline was sufficient to induce the expression of the respective proteins to their peak amount for this experiment (Figure 4.5 A, B and C, lanes 2); as a result 0.125µg/ml of tetracycline was used in all further experiments.

4.7.2. Optimising the tetracycline treatment time to induce vIRF2 & 4 protein expression

The time course of tetracycline stimulation of the vIRF2-NTAP, vIRF4-NTAP and NTAP proteins from their corresponding cell lines was investigated in order to aid in the design of further experiments. Cell lines were stimulated with tetracycline (0.125µg/ml) and samples were obtained for western blot analysis at specific time points post tetracycline stimulation (0, 8, 24, 48 and 72 hours). For the EV-NTAP and vIRF2-NTAP cell lines, 8 hours of tetracycline induction was sufficient to induce the expression of the NTAP and vIRF2-NTAP proteins respectively (Figure 4.6 A and B, lane 2). Expression of these proteins was maintained until at least 72 hours after treatment. This protein is present in similar quantities up to 72 hours post tetracycline stimulation. In the case of the vIRF4-NTAP cell line, weak

expression of the vIRF4-NTAP protein is observed after 8 hours of tetracycline induction (Figure 4.6C, lane 2), but after 24 hours of tetracycline, the level of protein increases (Figure 4.6 lane 3). Overall vIRF4-NTAP is expressed weaker than the vIRF2-NTAP and NTAP proteins. Based on these results, it was concluded that, in order to get optimum protein expression, further experiments using these cell lines should ideally be performed between 24-72 hours post tetracycline stimulation.

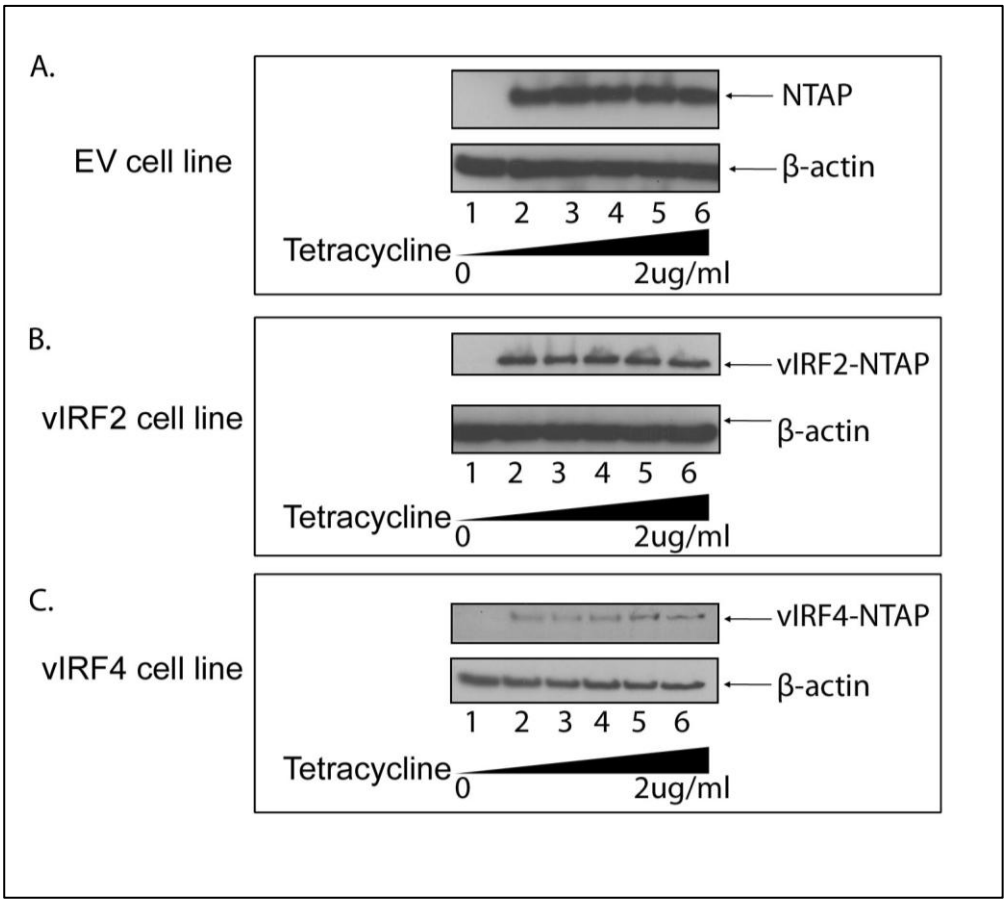

Figure 4.5: 0.125µg/ml of tetracycline is sufficient to induce expression of the NTAP-tagged proteins.

EV-NTAP, vIRF2-NTAP and vIRF4-NTAP cell lines were treated with tetracycline at different concentrations from 0-2µg/ml (lane 1=0µg/ml, 2=0.125µg/ml, 3=0.25µg/ml, 4=0.5µg/ml, 5=1µg/ml and lane 6=2µg/ml). Cells were harvested 24 hours later. The lysates (20µg per sample) were analysed by western blot to detect the NTAP-tag and β-actin. Primary antibody: anti-β-actin. Secondary antibody: anti-mouse HRP-conjugated secondary antibody (for β-actin detection). The use of the anti-mouse HRP-conjugated secondary antibody was sufficient to detect the NTAP-tag in all the cell lines as this tag contains protein G. The NTAP, and vIRF4-NTAP proteins produced from the EV-NTAP, vIRF2-NTAP and vIRF4-NTAP cell lines respectively are indicated. Probing for β-actin confirmed equal loading.

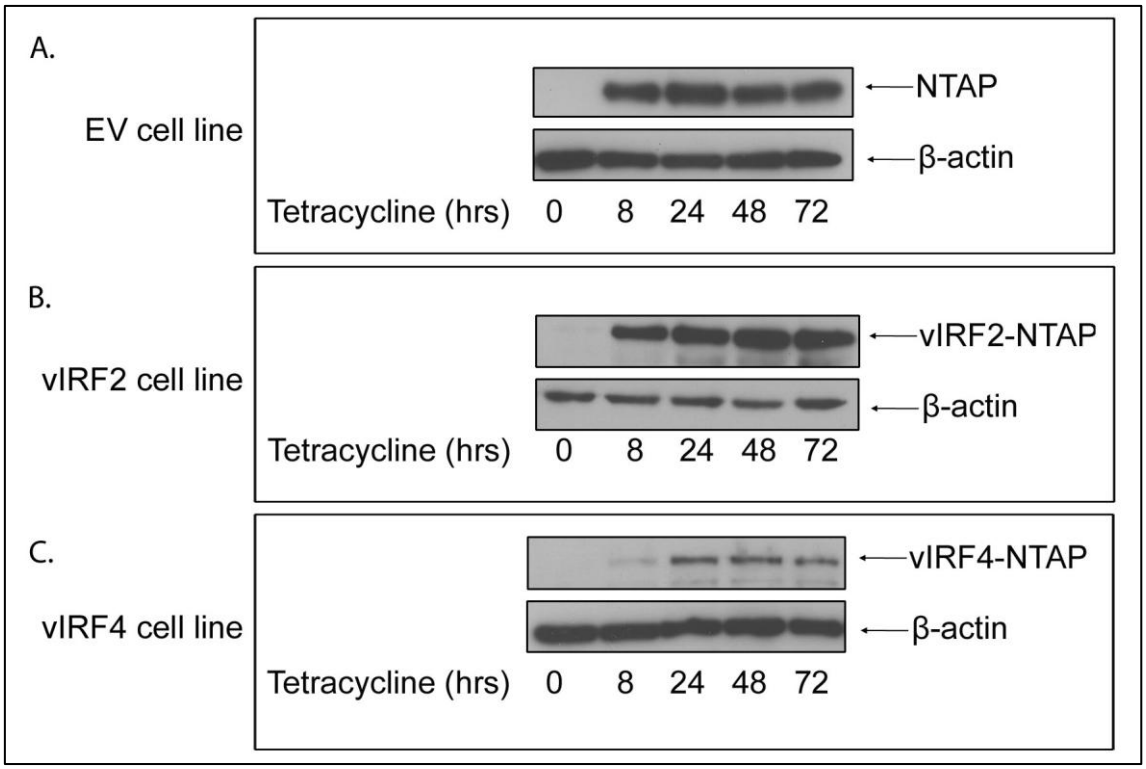

Figure 4.6: 24 hours of tetracycline treatment is necessary for expression of the NTAP-tagged proteins.

EV-NTAP, vIRF2-NTAP and vIRF4-NTAP cell lines were treated with tetracycline (0.125µg/ml), and harvested between 0-72 hours later. The lysates (20µg per sample) were analysed by western blot to detect the NTAP-tag and β-actin. Primary antibody: anti-β-actin. Secondary antibody: anti-mouse HRP-conjugated secondary antibody (for β-actin detection). The use of the anti-mouse HRP-conjugated secondary antibody was sufficient to detect the NTAP-tag in all the cell lines as this tag contains protein G. The NTAP, vIRF2-NTAP and vIRF4-NTAP proteins produced from the EV-NTAP, vIRF2-NTAP and vIRF4-NTAP cell lines respectively are indicated. Probing for β-actin confirmed equal loading. This experiment was repeated completely and the resultant blots are shown in Figure 9.13 (Appendix).

4.8. Confirming the presence of vIRF2 and vIRF4 gene expression in the cell lines

Section 4.7 described the concentration and duration tetracycline treatment to induce expression of the vIRF2-NTAP, vIRF4-NTAP and NTAP proteins. Western blot analyses demonstrated the presence of bands corresponding to the predicted sizes of the NTAP, vIRF2-NTAP and the vIRF4-NTAP proteins (30, 140 and 130kDa respectively). However to fully and more conclusively demonstrate that the cell lines do express the specific proteins, PCR analysis was used to demonstrate the presence of vIRF2 and vIRF4 mRNA.

4.8.1. Confirming the presence of vIRF2 and vIRF4 mRNA in the vIRF2-NTAP and vIRF4-NTAP expressing stable cell lines respectively

The EV-NTAP, vIRF2-NTAP and vIRF4-NTAP cell lines were stimulated with tetracycline for 24 hours and harvested. RNA was extracted from each sample, which was then DNAse treated and cDNA was created from these templates. PCR was performed on the cDNA samples using primers specific for either vIRF2 or vIRF4 (Table 2.17). These specific primers were designed to span the exon boundaries of the vIRF2 or vIRF4 genes. Primers which span the exon boundary do not provide any advantage when dealing with the stable cell lines (as they are stably transfected with expression plasmids that do not contain the intron of the vIRF2 of vIRF4 genes), however it may provide an advantage in further experiments examining the vIRF2 and vIRF4 mRNA in the context of KSHV infection.

As expected, the vIRF2-NTAP cell line contained mRNA which was amplified with the vIRF2 specific primers (Figure 4.7A, lane 3). No positive signals were observed for either the EV-NTAP of vIRF4-NTAP cell lines (lanes 1 and 5) indicating that these cell lines do not express the vIRF2 protein and there were no positive signals in the –RT samples and the no template control (lanes 2, 4, 6 and 7) demonstrating no contamination.

Similarly, the vIRF4-NTAP cell line contained mRNA which was amplified with the vIRF4 specific primers (Figure 4.7A, lane 5). Again, no positive signals were observed for either the EV-NTAP of vIRF2-NTAP cell lines (lanes 1 and 3) and there were no signals for the –RT or no template control samples (lanes 2, 4, 6 and 7). These results provide further confirmation that the vIRF2-NTAP and the vIRF4-NTAP cell lines express the vIRF2 and vIRF4 proteins respectively.

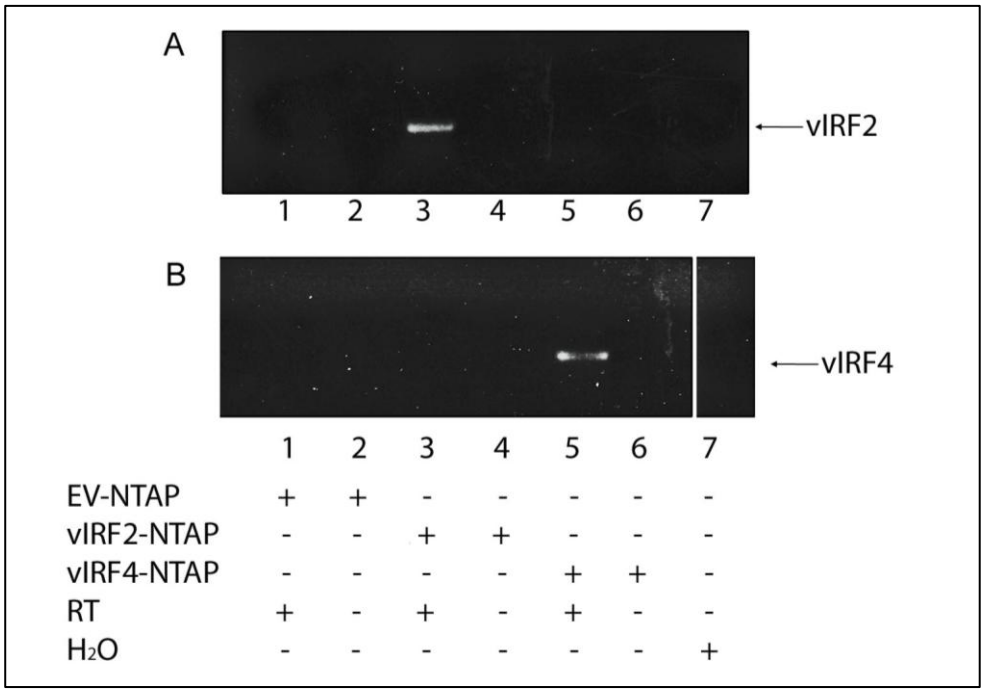

Figure 4.7: The vIRF2-NTAP and vIRF4-NTAP cell lines contain vIRF2 or vIRF4 mRNA respectively.

EV-NTAP, vIRF2-NTAP and vIRF4-NTAP cell lines were treated with tetracycline (0.125µg/ml) for 24 hours and harvested. RNA was extracted and the samples were DNAse treated. Reverse transcription was performed followed by PCR using (A) vIRF2 primers and (B) vIRF4 primers (Table 2.17). –RT=samples not treated with reverse transcriptase, H_2O=no template control. The gap between lanes 6 and 7 in B, is because the samples were not loaded contiguously. However, lane 7 is from the same gel as the other samples.

4.9. Investigating the function of vIRF2 and vIRF4 expressed in the vIRF2-NTAP and vIRF4-NTAP cell lines.

In order to confirm that the vIRF2-NTAP and vIRF4-NTAP proteins, expressed in the stable cell lines, were functioning in the same way, with respect to IFN signalling, as previously described in transient transfection experiments, DLAs were performed.

4.9.1. vIRF2 inhibits IFNβ promoter activation, while vIRF4 has no effect on IFNβ promoter activation

Section (3.7.1) showed that transient transfection of the vIRF2-His/Max plasmid into 293 cells resulted in inhibition of the polyI:C driven transactivation of the IFNβ promoter. However, transient transfection of the vIRF4-NTAP plasmid into 293 cells did not affect the IFNβ promoter (Figure 3.10).

To confirm that these effects are recapitulated in the stable cell lines, a DLA was performed using the IFNβ promoter reporter plasmid. The EV-NTAP, vIRF2-NTAP and vIRF4-NTAP cell lines were treated with tetracycline to induce protein expression, then transfected with the full length IFNβ promoter. 24 hours later poly(I:C) was transfected to activate IRF3. Cells were harvested and assayed by DLA 20 hours later. As expected, firefly luciferase expression and therefore the IFNβ promoter transactivation was significantly ($p=0.01$) inhibited (by 72%) in the vIRF2 expressing cell lines compared to EV-NTAP cell lines (Figure 4.8, compare columns 4 and 5). The vIRF4 expressing cell line showed no inhibition of IFNβ promoter transactivation when compared to the EV-NTAP cell line (Figure 4.8,

compare columns 4 and 6). These results confirm and support the results obtained through transient transfection experiments in chapter 3.

4.9.2. The vIRF2 and vIRF4 expressing cell lines inhibit ISRE-containing promoter activation

To confirm that vIRF2 and vIRF4 proteins, expressed from the stable cell lines, inhibit the rIFNα induced transactivation of an ISRE-containing promoter, as observed in section 3.7.2, ISRE-reporter assays were performed. The vIRF2-NTAP, vIRF4-NTAP and the EV-NTAP control cell lines were stimulated with tetracycline to induce the expression of the specific proteins and the ISRE-containing promoter was co-transfected with the constitutively expressing *Renilla* pRLSV40 plasmid. 5 hours later the cells were treated with rIFNα to activate the JAK-STAT signalling cascade. As expected firefly luciferase expression and therefore the ISRE-containing promoter transactivation was significantly inhibited ($p=0.001$) in both the vIRF2 and the vIRF4 expressing cell lines compared to the EV-NTAP cell lines. In the case of vIRF2, the level of inhibition was 80% (Figure 4.9, compare columns 4 and 5) and for vIRF4 it was 64% (Figure 4.9, compare columns 4 and 6). These results confirm and support the results obtained through transient transfection experiments in chapter 3.

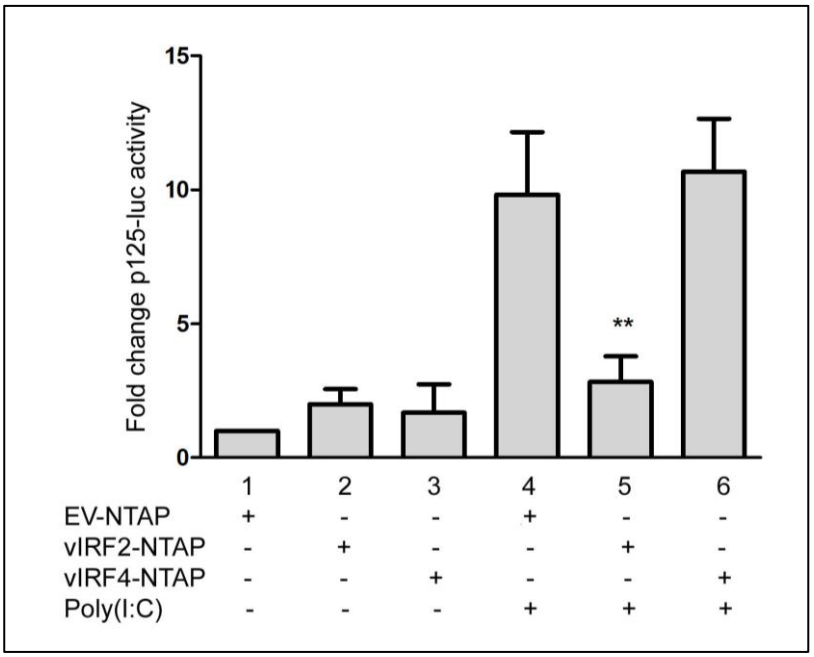

Figure 4.8: vIRF2 inhibits IFNβ promoter activation, while vIRF4 has no effect on IFNβ promoter activation.

The EV-NTAP, vIRF2-NTAP and vIRF4-NTAP cell lines were treated with tetracycline (0.125µg/ml)). 24 hours later, the cells were transfected with p125-luc (250ng) and the pRLSV40 plasmid (1ng). 24 hours post-transfection, the cells were transfected with poly(I:C) (10µg/ml) and harvested 20 hours later. The pRLSV40 plasmid (1ng), was added as an internal control to which firefly luciferase levels were normalised. The results are shown as fold increase compared to the EV-NTAP cell which was un-stimulated (column 1). The data represent the mean ± the SEM of the three independent experiments which were each assayed in duplicate. ** = $p<0.01$ ANOVA followed by a Dunnett post hoc test compared to EV-NTAP plus poly(I:C) (column 4). For results from individual experiments see Figure 9.14 (Appendix I).

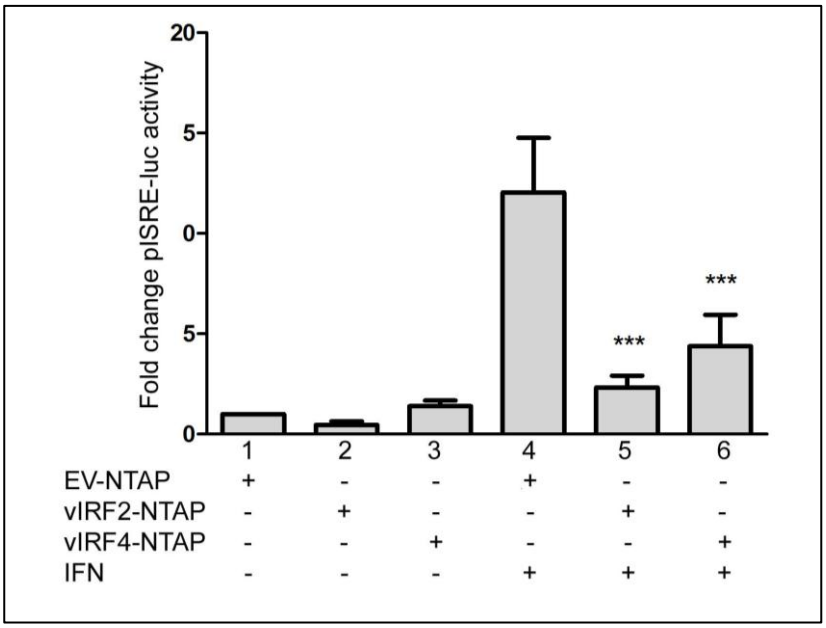

Figure 4.9: vIRF2 and vIRF4 inhibit ISRE-containing promoter activation. The EV-NTAP, vIRF2-NTAP and vIRF4-NTAP cell lines were treated with tetracycline (0.125µg/ml) for 24 hours and then transfected with pISRE-luc (250ng) and the pRLSV40 plasmid (1ng). 5 hours post transfection, the cells were treated with rIFNα (300 U/ml) and harvested 16 hours later. The pRLSV40 plasmid was added as an internal control to which firefly luciferase levels were normalised. The results are shown as fold increase compared to the EV-NTAP cell which was un-stimulated (column 1). The data represent the mean ± the SEM of the three independent experiments which were each assayed in duplicate. *** = $p<0.001$ ANOVA followed by a Dunnett post hoc test compared to EV-NTAP plus rIFNα (column 4). For results from individual experiments see Figure 9.15(Appendix I).

4.10. Comparing the levels of vIRF2 or vIRF4 in stable cell lines and a PEL cell line

The experiments performed in following sections utilize the EV-NTAP, vIRF2-NTAP and vIRF4-NTAP stable cell lines. Ectopically expressing these proteins in this way can aid understanding of the mechanisms of action of vIRF2 and vIRF4. However, since the cell lines ectopically express the viral proteins, it is important to compare the levels of vIRF2 and vIRF4 in the stable cells with those of naturally infected cells, such as PEL cells, providing biological relevance to natural KSHV infection.

Whilst methods such as western blotting and flow cytometry would be preferable to quantify vIRF2 or vIRF4 protein levels, there are no functional antibodies which can detect native vIRF2 and vIRF4. These antibodies would be necessary for the detection of wild type vIRF2 and vIRF4 in PEL cells, since these proteins do not have a tag. Instead, qPCR was employed to compare vIRF2 and vIRF4 mRNA levels in engineered and naturally infected cells.

4.10.1. Optimisation of qPCR assay to detect vIRF2 and vIRF4 mRNA

Primers and probes were designed against both vIRF2 and vIRF4 (See Table 2.19), the probes for each gene spanned an exon boundary in order to distinguish between message and genomic DNA. To validate the qPCR assay for the vIRF2 gene, experiments were performed which confirmed the specificity and optimised the primer and probe concentrations. For the vIRF2 qPCR assay, the pvIRF2-NTAP plasmid was used as a template for the assay, and added at varying

amounts from 10^2 - 10^6 copies. It was found that the assays for vIRF2 worked best with primer concentrations of 3µM, and probe concentrations of 5µM (Figure 9.16A). The same approach was taken for vIRF4, using the pvIRF4-NTAP as a template. For this assay the optimum primer concentrations were again 3µM but the probe concentration was increased to 10µM (Figure 9.16B). As expected, no amplification was observed when water was substituted for DNA, furthermore, vIRF2 primer/probe sets, did not amplify vIRF4 plasmid samples and vice versa, indicating specificity of the assays (data not shown).

4.10.2. Optimum time of vIRF2 and vIRF4 gene expression following BCBL1 reactivation

To find the peak vIRF2 and vIRF4 gene expression in BCBL1 cells, a KSHV reactivation time course experiment was performed. BCBL1 cells were treated with PMA, and collected at intervals from 0 hours – 144 hours later. At each time point samples were collected for analysis by immunofluorescence and qPCR. Immunofluorescence assays, staining for RTA (the lytic switch protein), were performed in order to investigate the percentage of cells which were reactivated. RTA expression peaked between 72 hours and 96 hours post PMA treatment. At 72 hours 56% of stained for RTA while at 96 hours this value was 60% of cells (Figure 4.10). From the qPCR data, it was found that vIRF2 expression peaked in BCBL1 cells following 72 hours of PMA treatment (Figure 4.11A, column 5), while expression of vIRF4 peaked a further 24 hours later at 96 hours post PMA treatment (Figure 4.11B, column 6).

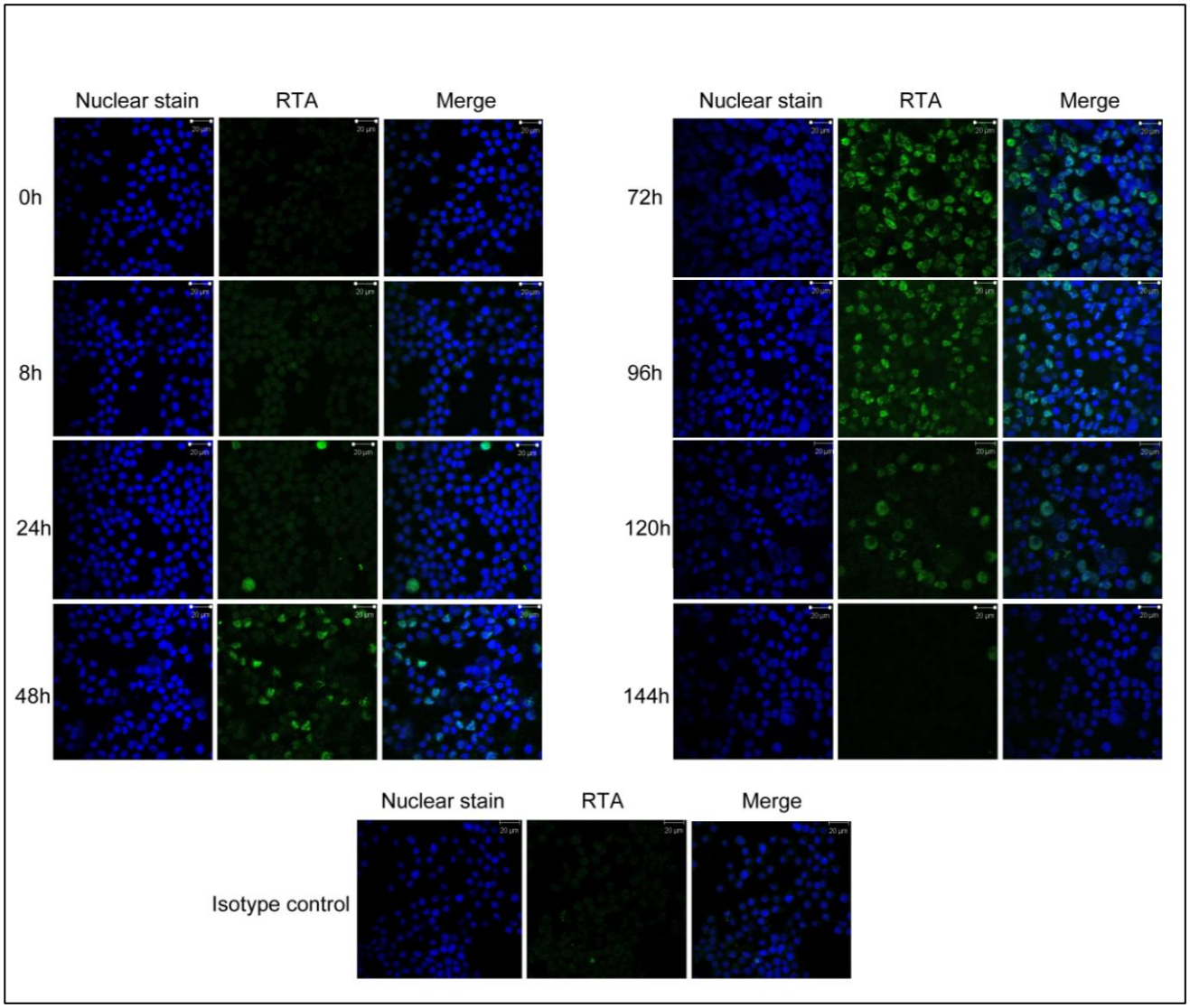

Figure 4.10: Time course of RTA expression in BCBL1 cells following reactivation.

PMA-treated (20ng/ml, for times shown in figure) BCBL1 cells were spotted onto slides, and fixed and permeabilized with methanol. The cells were stained for RTA (primary antibody: RTA (ORF50) see Table 2.8, secondary antibody: Anti-rabbit FITC Conjugate

Table **2.9**) and the nucleus (Bisbenzamide) and mounted using prolong gold. Results were visualised using confocal microscopy. The isotype control was stained with Rabbit IgG (see Table 2.8). To calculate the percentage of RTA positive cells, cells were counted manually. This experiment was repeated completely and the resultant images are shown in Figure 9.17.

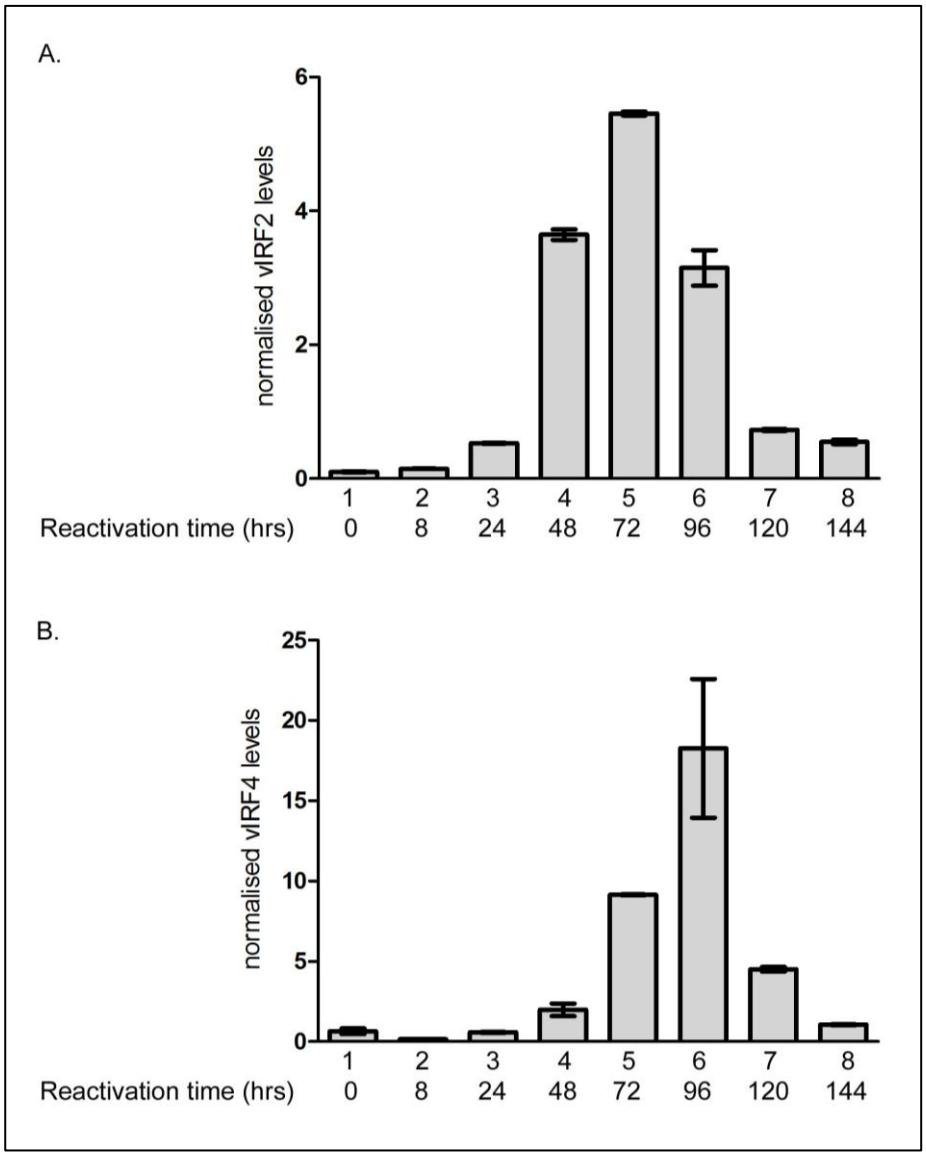

Figure 4.11: Optimum expression of vIRF2 and vIRF4 mRNA in BCBL1 cells, following lytic reactivation of KSHV.

(A) RNA extracted from PMA-treated (20ng/ml, for times shown in figure) BCBL1 cells was subject to reverse transcription. The resultant cDNA was used in qPCR assays with vIRF2 primers (3µM) and probe (5µM) (see Table 2.19). Data were normalized to cellular GAPDH levels, which were determined in the same qPCR reaction using the VIC-labelled reference GAPDH assay primer and probe set (see Table 2.19). Results were expressed relative to 0 hours (column 1). The data represent the mean from one representative experiment which was assayed in duplicate; the range between duplicate values is indicated. A negative control lacking reverse transcriptase was included for each sample as well as a no template control, and these were both negligible (data not shown). (B) Performed as in A, but with vIRF4 primers (see Table 2.20) 10µM and the FAM-labelled probe (see Table 2.19, vIRF4) used at 5µM. These experiments were repeated completely and the resultant graphs are shown in Figure 9.18 (Appendix).

4.10.3. Levels of vIRF2 and vIRF4 mRNA in the stable cells lines, compared to the levels in BCBL1 cells

The results obtained in 4.10.2, showed that vIRF2 mRNA levels peaked in BCBL1 cells which had been treated with PMA for 72 hours, whereas the vIRF4 mRNA levels peaked after 96 hours of reactivation. To compare the levels of vIRF2 or vIRF4 mRNA in the stable cell lines with those in the BCBL1 cells, RNA was obtained from BCBL1 cells which were treated with PMA for 0, 72 and 96 hours. RNA was also obtained from the EV-NTAP, vIRF2-NTAP and vIRF4-NTAP stable cell lines which had been treated with tetracycline for 24 hours. 24 hours of tetracycline treatment was chosen because this resulted in peak expression of the vIRF2 and vIRF4 proteins (see section 4.7.2). Following reverse transcription, the samples were analysed by qPCR using the vIRF2 or the vIRF4 primers at their optimised concentrations (see section 4.10.1).

The level of vIRF2 mRNA in the vIRF2-NTAP cell line was 3.8 fold (experiment 1), 3.5 fold (experiment 2) and 2.4 fold (experiment 3) greater than that in BCBL1 cells (Figure 4.12 compare columns 2 and 5 in all three experiments).

Likewise vIRF4 mRNA in the vIRF4-NTAP cell line was 2.9 fold (experiment 1), 6.4 fold (experiment 2) and 2.9 fold (experiment 3) greater than that in BCBL1 cells (Figure 4.13, compare columns 3 and 6 in all three experiments).

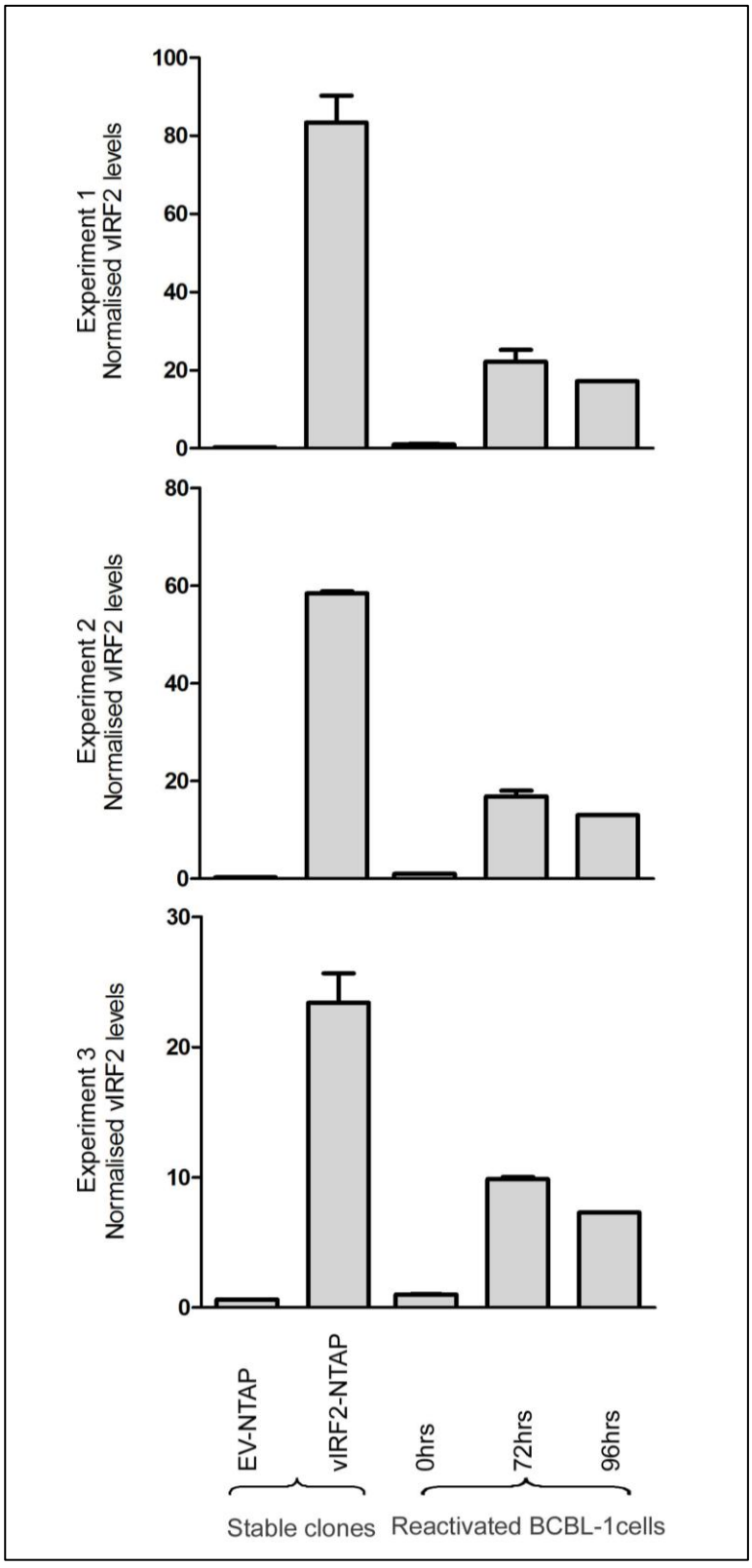

Figure 4.12: Comparing vIRF2 mRNA levels in stable cells and BCBL1 cells.

RNA was extracted from the EV-NTAP, vIRF2-NTAP and vIRF4-NTAP stable cell lines, which had been treated with tetracycline (0.125µg/ml). RNA was also extracted from PMA-treated (20ng/ml, for times shown in figure) BCBL1 cells.

Following reverse transcription, samples were analysed by qPCR using vIRF2 specific primers (3µM) and probe (5µM) (see Table 2.19). Data were normalized to cellular GAPDH levels, which were determined in the same qPCR reaction using the VIC-labelled reference GAPDH assay primer and probe set (see Table 2.19) and expressed relative to BCBL1 0 hours (column 4). The data shows the results of three independent experiments which were each assayed in duplicate; the range between duplicate values is indicated.

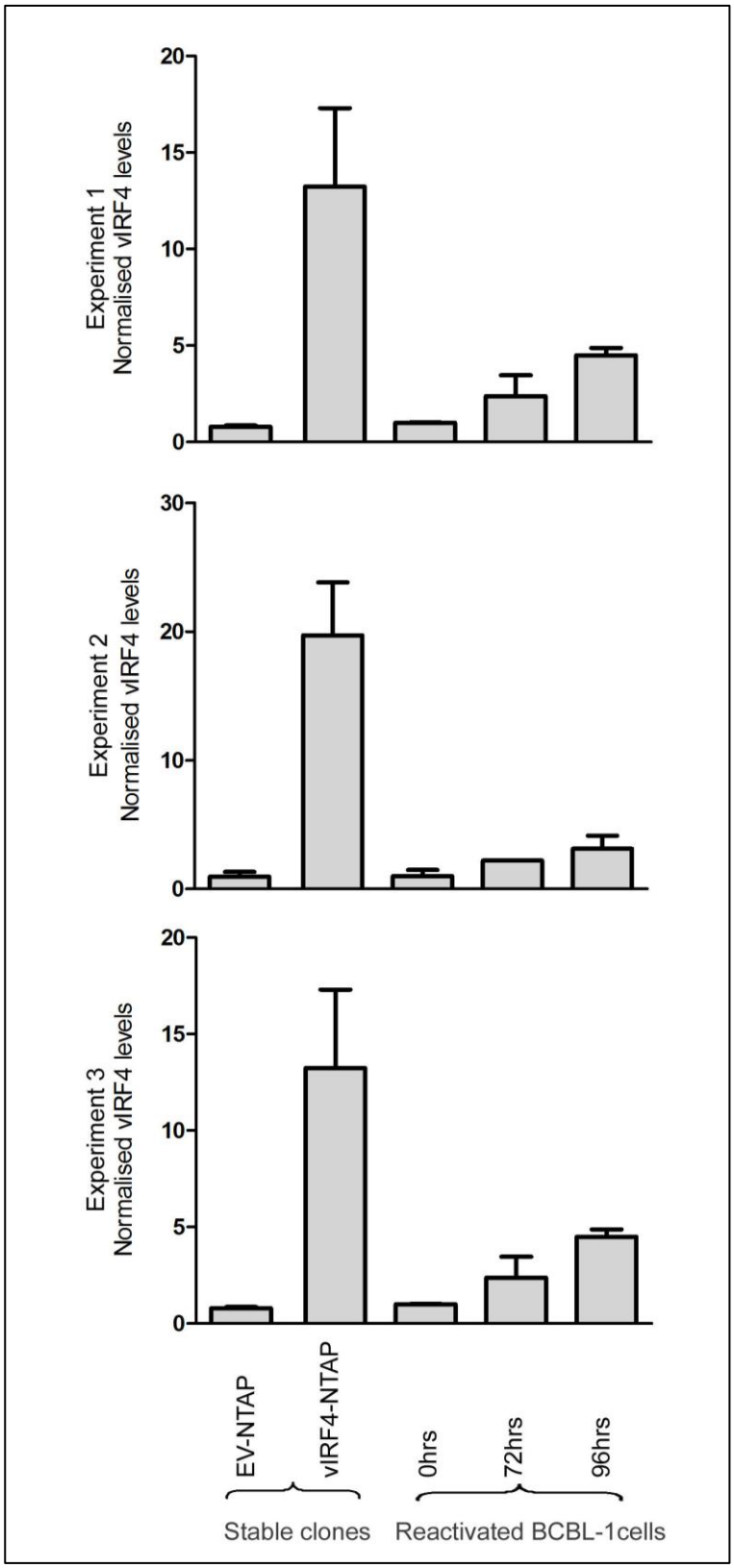

Figure 4.13: Comparing vIRF4 mRNA levels in stable cells and BCBL1 cells.

Performed as in Figure 4.12, expect vIRF4 specific primers were used at 3µM and the probe was used at 10µM (see Table 2.19).

4.11. The location of the vIRF2 and vIRF4 proteins

Previous studies have examined the cellular location of the vIRF2 and vIRF4 proteins in various cell types. In our own laboratory, vIRF2 has been shown to reside predominantly in the cytoplasm (Areste et al., 2009). vIRF4 has been found predominantly in the nucleus, but sometimes in the cytoplasm (Kanno et al., 2006, Xi et al., 2012).

To examine the subcellular location of the vIRF2 and vIRF4 proteins in the vIRF2-NTAP and vIRF4-NTAP cell lines, immunofluorescence assays were performed. The stable cell lines were seeded onto coverslips and induced to express the specific proteins. Cells were then fixed, permeabilized, stained and mounted. The staining patterns were visualised by confocal microscopy. Consistent with our previous work, vIRF2 was localised in the cytoplasm, while vIRF4 was found in both the nucleus and cytoplasm (Figure 4.14). Because the cell lines express the vIRF2 or vIRF4 proteins attached to the NTAP-tag, which is formed in part by two modules of protein G, any antibody will bind to the NTAP-tag. It was therefore important to ensure appropriate controls confirmed that staining was specific to the vIRF2 or vIRF4 proteins. The T-Rex parental cell line from which the vIRF2-NTAP and vIRF4-NTAP cell lines were created were used as a negative control (Figure 4.14, labelled parental cell line). The EV-NTAP cell line was used to show the location of the NTAP-tag only, which was found throughout the cell (Figure 4.14).

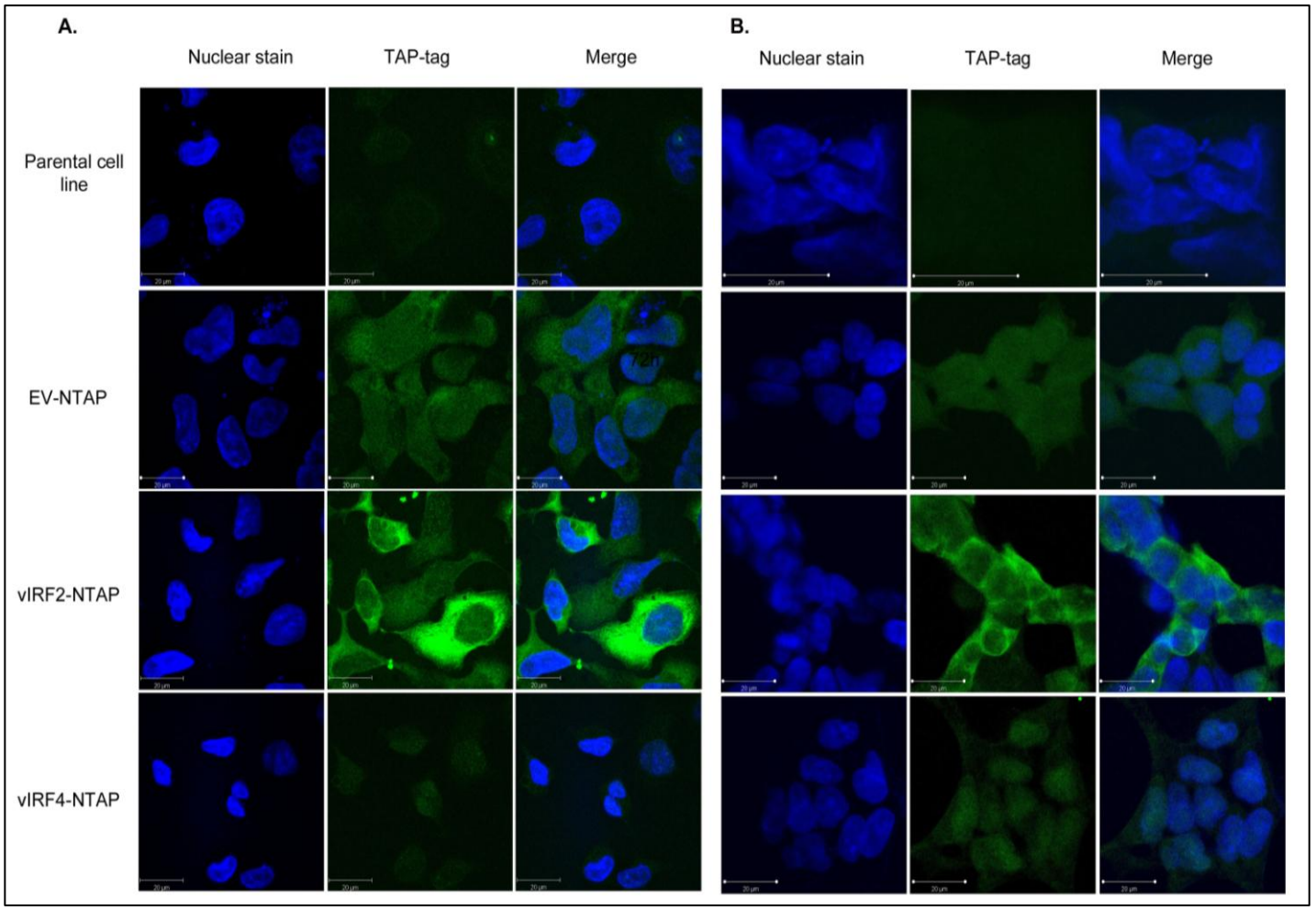

Figure 4.14: Immunofluorescence staining of the vIRF2 and vIRF4 proteins.

The EV-NTAP, vIRF2-NTAP of vIRF4-NTAP cell lines were plated on coverslips at the bottom of a 24 well plate. Following tetracycline treatment (0.125µg/ml, 24 hours), cells were fixed in 4% paraformaldehyde and permeabilized with ice cold methanol (10 minutes). Staining was achieved using secondary antibody only (Anti-rabbit FITC, see Table **2.9**) which detected the NTAP-tagged protein. Nuclear staining was achieved with Bisbenzamide. Results were visualised by confocal microscopy. T-Rex cells were treated in the same manner, to provide a negative control for the staining (labelled parental cell line). A. Experiment 1. B. Experiment 2.

4.12. Discussion

This chapter discusses the generation and characterisation of stable cell lines expressing the NTAP, vIRF2-NTAP and vIRF4-NTAP proteins. An aim of this work was to establish stable cell lines, which would aid future experiments designed to identify the mechanism of how vIRF2 and vIRF4 inhibit JAK-STAT signalling.

Following the cloning of the vIRF2 gene into the pCDNATO-NTAP vector, three stable cell lines were created using the pCDNATO-NTAP, pvIRF2-NTAP and pvIRF4-NTAP vectors. These stable cell lines can be induced, through tetracycline treatment, to express the NTAP, vIRF2-NTAP and vIRF4-NTAP proteins respectively. Experiments were therefore performed to identify the optimum amount, and time frame of tetracycline treatment. Figure 4.5 and Figure 4.6 show that optimum expression of the NTAP, vIRF2-NTAP and vIRF4-NTAP proteins was achieved following 0.125µg/ml of tetracycline for 24-72 hours. This information was necessary for future experiments (in later chapters), and as a result, future assays were performed within the 24-72 hours post 0.125µg/ml of tetracycline treatment, ensuring optimum protein expression.

Additionally PCR and qPCR analysis of cDNA from the EV-NTAP, vIRF2-NTAP and vIRF4-NTAP cell lines showed the presence of vIRF2 mRNA in the vIRF2-NTAP cell line, and vIRF4 mRNA in the vIRF4-NATP cell line (Figure 4.7, Figure 4.12 and Figure 4.13). The western blots, showing presence of the vIRF2 or vIRF4 proteins, and the PCR experiments showing presence of vIRF2 and vIRF4 mRNA

in the specific stable cell lines show the these stable cell lines are expressing the required proteins in an inducible manner.

Since the cell lines were shown to express the desired KSHV proteins, they were then characterised by examining the effect of the vIRF2 and vIRF4 proteins on IFN signalling. The vIRF2 and vIRF4 proteins were confirmed to function as described for transiently transfected cells in chapter 3. vIRF2 inhibited both the IFNβ promoter and ISRE-containing promoter activity (Figure 4.8 and Figure 4.9). vIRF4 was unable to inhibit IFNβ promoter activity (Figure 4.8) but significantly inhibited ISRE-containing promoter activation (Figure 4.9). These results provide further evidence for the inhibitory activity of the vIRF2 protein on IFN signalling, and confirm that the vIRF4 protein inhibits the JAK-STAT signalling pathway. Because these cell lines are functioning as previously observed, they will be used in further experiments which aim to understand the molecular mechanisms behind the action of vIRF2 and vIRF4.

The stable cell lines, created in this chapter, overexpress the vIRF2 or vIRF4 proteins. It is useful to know the protein levels of vIRF2 or vIRF4 relative to those of KSHV infected cell lines. The BCBL1 cell line is infected with KSHV, but not with EBV. KSHV within these cells is predominantly latent, but can be induced to the lytic state through treatment with the phorbol ester PMA (Renne et al., 1996). Comparison of the vIRF2 and vIRF4 protein levels in the stable cell lines and the BCBL1 cell lines was not possible because there are no available antibodies which recognise the wild type vIRF2 or vIRF4 proteins. The levels of vIRF2 and

vIRF4 mRNA were therefore examined. Optimum expression of vIRF2 and vIRF4 mRNA was determined in BCBL1 cells treated with PMA, to reactivated KSHV lytic replication, for varying times. It was necessary to reactivate the KSHV, because both vIRF2 and vIRF4 are lytic genes (Cunningham et al., 2003), therefore optimum levels of their mRNA would be detected in lytic replicating KSHV. It was found that vIRF2 mRNA expression peaked 72 hours post PMA treatment, whereas vIRF4 mRNA expression peaks after 96 hours (Figure 4.11). These results confirm, as reported in the literature, that vIRF2 and vIRF4 mRNAs display lytic kinetics (Cunningham et al., 2003). Using this information, the levels of vIRF2 or vIRF4 mRNA were compared between BCBL1 cells, at 72 and 96 hours post PMA treatment, and the stable cell lines. Levels of vIRF2 mRNA range from 2.4 fold – 3.8 fold greater in the stable cell lines compared to BCBL1 cells (Figure 4.12). vIRF4 mRNA levels ranged from 2.9 fold – 6.4 fold greater in the stable cell lines compared to BCBL1 cells (Figure 4.13). Whilst this result shows that vIRF2 and vIRF4 are overexpressed in the stable cell lines, it doesn't account for the fact that not all the BCBL1 cells contained lytic KSHV. Figure 4.10 shows BCBL1 cells which are stained for RTA, the KSHV lytic switch protein, at different time points post PMA treatment. Even at 72 hours and 96 hours post PMA treatment (time points containing the greatest percentage of cells with RTA) only 56% and 60% of cells respectively showed positive RTA staining, indicating not every cell contained reactivated KSHV. Because just over half of the cells contained reactivated KSHV, half the cells would therefore not be expressing vIRF2 or vIRF4 at their optimum amounts. An argument could be made that the levels of vIRF2 and vIRF4 mRNA, detected in the PMA treated BCBL1 cells, would be higher if 100% of the cells

contained reactivated KSHV. The values for the vIRF2 and vIRF4 mRNA levels in PMA treated BCBL1 cells could therefore be increased based on the percentage of cells which were actually reactivated. This would decrease the difference in vIRF2 or vIRF4 levels between the BCBL1 cells and the stable cell lines. However, due to time constraints, RTA staining was not performed in parallel to the qPCR experiments shown in Figure 4.12 and Figure 4.13, meaning an exact RTA positive cell percentage could not be determined on a per-experiment basis. Nonetheless, based on the RTA staining observations in Figure 4.10 and the replicate experiment Figure 9.17, it is clear that reactivation of every cell is not likely. Therefore it can be assumed that the calculated fold difference in viral mRNA levels, between BCBL1 cells and the stable cell lines, is larger than in reality. It should also be noted that the expression patterns observed in BCBL1 cells will not be the same as the patterns in other KSHV infected tissues, as these could be either higher or lower.

Finally, the location of the vIRF2 and vIRF4 proteins within the engineered cells was examined by immunofluorescence microscopy. vIRF2 was located in the cytoplasm, consistent with previous observations in our laboratory (Areste et al., 2009) and vIRF4 is found both in the cytoplasm and the nucleus, as reported by Kanno et al, (2006).

In summary, the work described in this chapter has detailed how stable cell lines which express either the EV-NTAP, vIRF2-NTAP or vIRF4-NTAP proteins were created. The vIRF2 or vIRF4 proteins expressed from these cell lines functioned

as previously described (Chapter 3) with respect to IFN signalling. These cell lines can therefore be used in subsequent experiments aiming to understand the mechanisms behind the inhibition of JAK-STAT signalling.

CHAPTER 5

THE BIOLOGICAL SIGNIFICANCE AND INVESTIGATION OF THE MECHANISMS BY WHICH vIRF2 AND vIRF4 ATTENUATE JAK-STAT SIGNALLING

5.1. Introduction

Chapter 3 and 4 have shown through luciferase reporter assays that both vIRF2 and vIRF4 inhibit rIFNα stimulated ISRE promoter activation, and thus inhibit the JAK-STAT signalling pathway. Chapter 4 described the production and characterisation of stable cell lines which can be induced to express the EV-NTAP, vIRF2-NTAP or the vIRF4-NTAP proteins. The present chapter describes the use of these cell lines to examine the mechanisms of the vIRF2 and vIRF4 proteins in the context of IFN signalling.

The aims of this chapter are to:

1) Examine the anti-IFN effect of vIRF2 and vIRF4 in a biological context by assessing their ability to rescue the titre of the IFN-sensitive virus EMCV
2) Identify if vIRF2 and vIRF4 can reduce binding of the ISGF3 complex to the ISRE sequence via EMSA studies
3) Determine whether vIRF2 or vIRF4 affect levels of individual ISGF3 components through western blot analysis.

To examine the biological significance of the vIRF2 or vIRF4 mediated inhibition of JAK-STAT signalling the hypothesis that vIRF2 and vIRF4 could rescue EMCV titre due to their anti-IFN effects was tested. The stable cell lines were infected with EMCV in the presence or absence of rIFNα, and EMCV titres were determined. This experiment provided *in vitro* results on the potential physiological significance of vIRF2 and vIRF4 in KSHV biology.

Having established that vIRF2 and vIRF4 inhibit ISRE promoter activation, the mechanism by which these proteins interfere with JAK-STAT signalling was sought. To identify where these proteins are interfering, the pathway must be examined in more detail.

Since ISRE activation is inhibited by vIRF2 and vIRF4, it follows that these proteins may inhibit the binding of the ISGF3 complex to ISRE promoter sequences. Therefore, EMSA studies were performed to determine the abundance of functional amounts of ISGF3 within the stable cell lines. EMSA studies are used to measure protein–DNA interactions. They can be used to verify that a protein mixture can bind to a specific DNA sequence, and determine the amount of binding taking place. A probe, consisting of the ISRE consensus sequence, was assayed with the nuclear lysates of rIFNα-stimulated EV-NTAP, vIRF2-NTAP and vIRF4-NTAP stable cell lines. The resultant bands, corresponding to the ISGF3-ISRE protein-DNA complexes, were measured and compared amongst all samples.

The three components of the ISGF3 complex, pSTAT1, pSTAT2 and IRF9, are essential in the JAK-STAT signalling pathway. Reduction in the levels of one of these components would decrease ISRE promoter activity. Many viruses encode proteins which target the levels of ISGF3 components (discussed in section 1.4.9). Therefore the levels of these proteins were compared among the stable cell lines, to identify if any were reduced in vIRF2 or vIRF4 expressing cell lines compared with the EV control cell line.

5.2. Examining the effect of vIRF2 and vIRF4 on EMCV titres following rIFNα treatment

Since vIRF2 and vIRF4 inhibit ISRE promoter activation (chapters 3 and 4), the hypothesis that these viral proteins can rescue the IFN sensitive EMCV from the antiviral pathway was tested. These experiments therefore examined the physiological potential of vIRF2 and vIRF4 activities against the type I IFN antiviral pathway.

5.2.1. EMCV

EMCV belongs to the *Picornaviridae* family, a diverse group of viruses that cause disease in both humans and animals. EMCV is a positive-strand RNA virus which is associated with sporadic cases and outbreaks of myocarditis and encephalitis in a wide range of vertebrates, but particularly in domestic pigs (Billinis et al., 1999).

5.2.2. Using EMCV to examine the biological effect of proteins which inhibit JAK-STAT signalling

The treatment of cells with rIFNα prior to EMCV infection results in reduced viral yield (Morrison and Racaniello, 2009, Whitaker-Dowling and Youngner, 1986, Munoz and Carrasco, 1981) and EMCV can therefore be classed as an IFN sensitive virus. Since EMCV is IFN sensitive, EMCV titre can provide a biological read out of the effectiveness of a protein that is believed to inhibit JAK-STAT signalling. If a protein inhibits JAK-STAT signalling, it will downregulate the antiviral IFN response to a certain degree, and therefore increase the EMCV titre. This premise has been used in other studies, for example, Morrison and

Racaniello, (2009) showed that the enteroviral 2A proteinase rescues the replication of EMCV in rIFNα pre-treated cells, using plaque assays to determine the virus titre.

5.2.3. vIRF2, but not vIRF4 is able to rescue EMCV titre from the effects of IFN

To test the hypothesis that, due to their inhibitory effect on JAK-STAT signalling, vIRF2 and vIRF4 can rescue EMCV titre following rIFNα treatment, plaque assays were performed. Monolayers of EV-NTAP, vIRF2-NTAP or vIRF4-NTAP cells were pre-treated with rIFNα and infected with EMCV at a MOI of 0.1 (see section 2.13.1 for details). The cell supernatant was harvested 24 hours later for quantification of the viral titre by plaque assay (see section 2.13.2 for plaque assay details and section 2.13.3 for how the plaques were counted).

Samples which were not treated with rIFNα resulted in similar EMCV titres. EV-NTAP cells gave an average EMCV titre of $5.9x10^7$ PFU/ml, the vIRF2-NTAP cells produced $3.2x10^7$ PFU/ml and the vIRF4-NTAP cells produced $2.5x10^7$ PFU/ml (Figure 5.1A, columns 1, 3 and 5 respectively). As expected, pre-treatment with rIFNα decreased the yield of EMCV in the EV-NTAP cells by two orders of magnitude, to $3.1x10^5$ PFU/ml (Figure 5.1A, compare columns 1 and 2). In contrast, the EMCV titre from the rIFNα treated vIRF2-NTAP cells ($2.9x10^7$ PFU/ml) was not decreased compared to the cells untreated with rIFNα (Figure 5.1A, compare columns 3 with 4). However in the case of vIRF4-NTAP cells treated with rIFNα the EMCV titre fell to $3.8x10^5$ PFU/ml, which is a drop of about

two orders of magnitude compared to the untreated vIRF4-NTAP cells (Figure 5.1A, compare columns 5 and 6). This value is comparable with that of rIFNα treated EV-NTAP cells. Pictures of a plaque assay from one representative experiment are shown in Figure 5.1B. The number of plaques in the EV-NTAP and vIRF4-NTAP samples can be seen to reduce in the presence of rIFNα, whereas for the vIRF2-NTAP samples, the number of plaques are similar in the –rIFNα and +rIFNα samples.

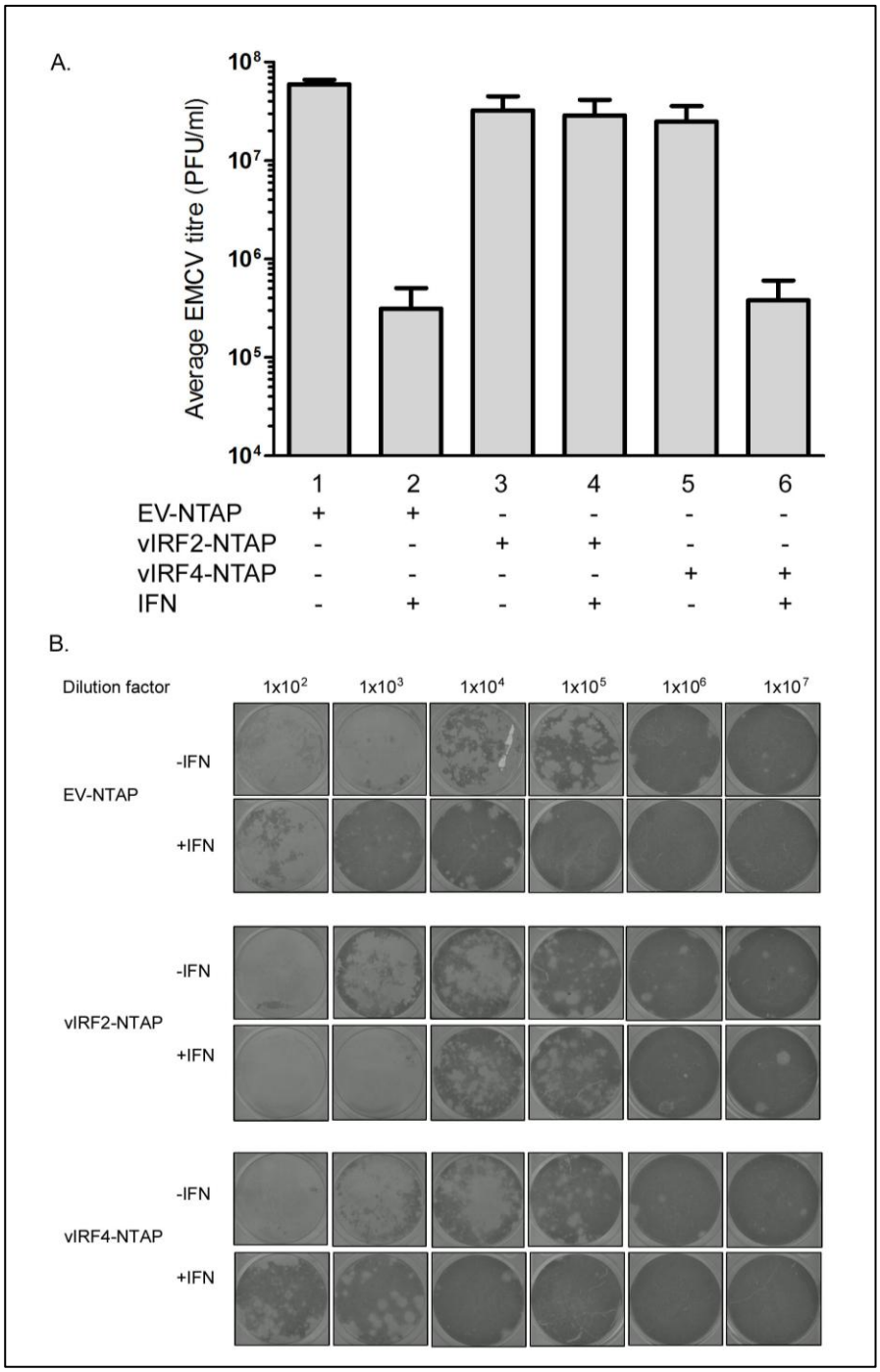

Figure 5.1 vIRF2, but not vIRF4 is able to rescue EMCV titre from the effects of rIFNα.

Monolayers of the EV-NTAP, vIRF2-NTAP or vIRF4-NTAP cell lines were pre-treated with tetracycline (0.125μg/ml) for 24 hours and then either rIFNα (300 IU/ml) or no rIFNα for 24 hours. The cells were then infected with EMCV (MOI = 0.1) and 24 hours later the culture medium was collected. EMCV titres were determined by plaque assays on L929 cells. (A) The mean EMCV titres +/- SEM from three independent experiments are shown. For results from individual experiments see Figure 9.20. (B) The results of one representative plaque assay.

5.3. The vIRF2 and vIRF4 expressing cell lines reduce the binding of ISGF3 components to an ISRE promoter sequence

Since both vIRF2 and vIRF4 have been shown to inhibit JAK-STAT signalling in chapters 3 and 4, their effect on this pathway was investigated further. JAK-STAT signalling results in the formation of the ISGF3 complex, which translocates into the nucleus and binds to ISRE sequences, causing activation of ISGs. Since vIRF2 and vIRF4 inhibit this pathway, it was hypothesised that they may reduce levels of functional ISGF3 available to bind ISRE sequences. To test this hypothesis, the binding of ISGF3 to an ISRE sequence was measured by EMSA. Nuclear extracts (see section 2.9.2) from EV-NTAP, vIRF2-NTAP and vIRF4-NTAP cell lines were subject to EMSA experiments. EMSA was performed as detailed in section 2.9.4 using an IRDye-700-labelled ISRE probe (see section 2.9.3 for details on how the probe was made). The results show that as expected the band corresponding to the ISGF3-ISRE complex increased through stimulation with rIFNα (Figure 5.2A, lane 1 compared with lane 2). In the vIRF2 and vIRF4 expressing cell lines, bands corresponding to the ISGF3-ISRE complex were reduced when compared to the EV-NTAP cell lines in the presence of rIFNα (Figure 5.2A, compare lane 2 with lanes 4 and 6), indicating that vIRF2 and vIRF4 reduced ISGF3-ISRE complex formation.

To ensure that the bands identified were actually the ISFG3 complex, two controls were run alongside the EMSA assay. Firstly, a ‘cold’ competitor probe (see Table 2.11) was incubated (in excess) with nuclear lysate, from the EV-NTAP cells stimulated with rIFNα, along with the other components of the EMSA binding

reaction (see section 2.9.4). This probe is an unlabelled identical probe to the IRDye-700-labelled ISRE probe. The results for this control show that the ISGF3 EMSA band density was reduced, indicating that the cold probe was competing for the binding to the ISGF3 complex with the IRdye-700-labelled probe. This result demonstrates that the EMSA shift (indicated ISGF3 on Figure 5.2A) was a result of a protein complex binding to the ISRE sequence. The second control was a 'supershift' experiment. The STAT2 antibody was incubated with the nuclear lysate, from the EV-NTAP cells stimulated with rIFNα, along with the other components of the EMSA binding reaction (see section 2.9.4) and run alongside the EMSA gel. The results show that the ISGF3 band has 'shifted' higher than the other bands in the experiment, due to the increase in molecular weight from the STAT2 antibody (Figure 5.2A, compare lane 2 with lane 8). This result shows that the STAT2 protein is part of the protein:DNA complex, and this control confirms the presence of ISGF3 as part of this band.

The densitometry of the ISGF3-ISRE bands from Figure 5.2A were quantified using the Odyssey infrared imaging system and the results are shown in Figure 5.2B. From this graph, is clear that in the presence of vIRF2 or vIRF4, the intensity of the ISGF3-ISRE bands are reduced compared to the EV control in rIFNα stimulated conditions (Figure 5.2B, compare column 2 with columns 4 and 6). Figure 5.2C shows the zoomed bands from Figure 5.2A, lanes 1-6.

A portion of the extracted nuclear lysate was used in a western blot to detect TATA-binding protein (TBP), a nuclear protein (Figure 5.2D) which confirmed equal loading of nuclear lysates in the EMSA assay.

Taken together the results of Figure 5.2 demonstrate reduced binding of ISGF3 to the ISRE probe in both the vIRF2-NTAP and the vIRF4-NTAP cell lines when compared to the EV-NTAP cell lines. This experiment was repeated three times, and the densitometry results were collected together. The inhibition in ISGF3-ISRE complex binding was found to be a significantly decrease in rIFNα treated vIRF2-NTAP cells and vIRF4-NTAP cells compared to EV-NTAPS cells ($p<0.01$) (Figure 5.3 compare column 2 with columns 4 and 6).

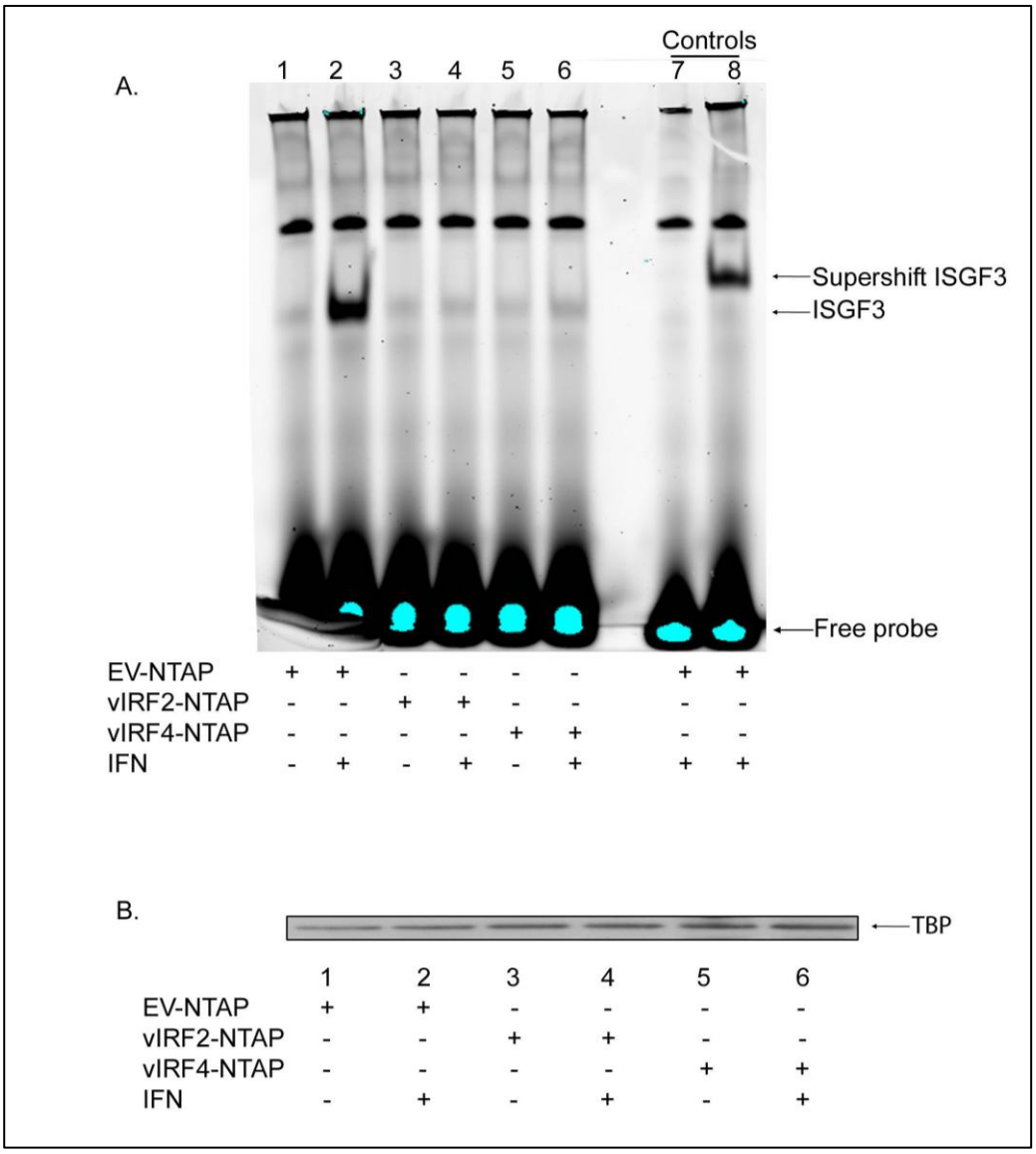

Figure 5.2: vIRF2 and vIRF4 inhibit binding of ISGF3 to an ISRE probe.

The EV-NTAP, vIRF2-NTAP and vIRF4-NTAP cell lines were treated with tetracycline (0.125µg/ml) for 24 h and treated or not with 300IU/ml rIFNα, as indicated, for 6 h. Nuclear extracts were then prepared by using a NE-PER nuclear extraction kit (Pierce Biotechnology). EMSAs were performed by incubating 5µg of each nuclear lysate sample with an ISRE probe for 30 minutes in a binding reaction (see Table 2.11) containing a 5′-IRDye-700-label. After binding, the reaction mixtures were resolved on 6% polyacrylamide-TBE gels (Invitrogen) and the bands were visualized by using an Odyssey infrared imaging system (LI-COR Biotechnology) (see section 2.9.4 for further details of method). (A) One representative EMSA experiment, demonstrating reduced nuclear binding in the rIFNα treated vIRF2-NTAP and vIRF4-NTAP samples (lanes 4 and 6 respectively). To ensure the bands were specific for ISGF3, a 'cold competitor' probe was added (3µl) to the rIFNα treated EV-NTAP sample and analysed in parallel (lane 7), which showed a reduction in band intensity compared to the

rIFNα treated EV-NTAP sample containing labelled probe only (compare lane 7 and lane 2). As an additional control, the STAT2 antibody (see 2.9.1 was added to the rIFNα treated EV-NTAP sample and analysed in parallel (lane 8) as a 'supershift' control. This resulted in the ISGF3 band migrating slower due to antibody increasing the size of the complex. (B) Western blot analysis of TBP with was performed in parallel on the nuclear extracts shown used in A, to confirm equal sample loading for the EMSA. This experiment was repeated twice more, and the EMSA results obtained, along with the band intensities and the TBP blots are shown in Figure 9.19.

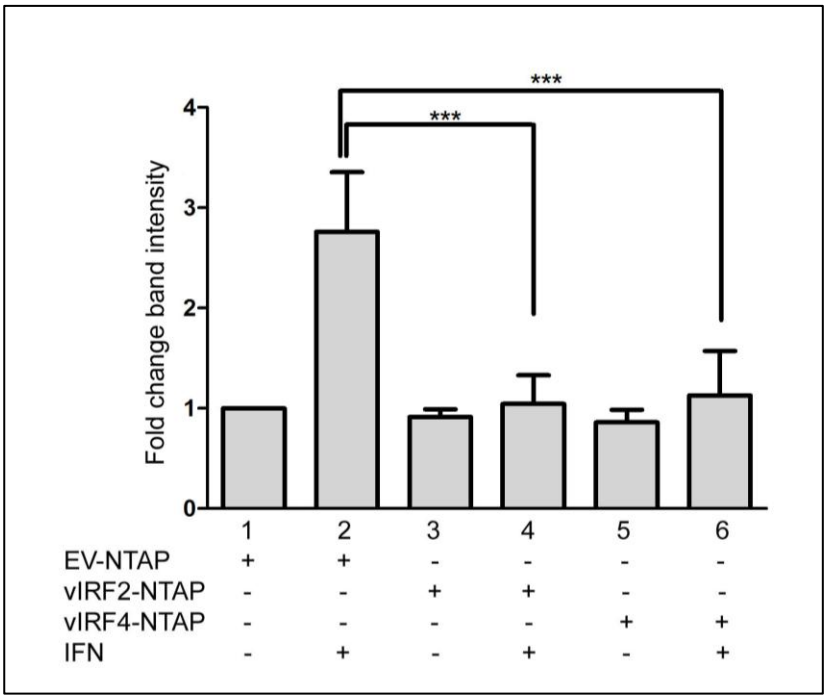

Figure 5.3: The vIRF2-NTAP and vIRF4-NTAP proteins reduce binding of ISGF3 to the ISRE sequence.

The band intensities from 3 independent EMSA assays performed as in Figure 5.2 are shown as fold increase compared to the EV-NTAP cell which was un-stimulated (column 1). The data represent the mean ± the SEM. *** = $p<0.01$ ANOVA followed by a Dunnett post hoc test compared to EV-NTAP plus rIFNα (lane 2). For results from individual experiments see Figure 9.19 .

5.4. Examining components of the JAK-STAT signalling pathway by western blotting

To investigate if the mechanism of the ISRE-containing promoter inhibition by vIRF2 and vIRF4 is due to modulation of ISGF3 components, the relative levels of these components were measured via western blotting.

The induced stable cell lines were treated with rIFNα to activate the JAK-STAT signalling pathway. Lysates were analysed for the presence of the NTAP, vIRF2-NTAP and vIRF4-NTAP proteins (Figure 5.4 rows 4 and 5) and the relative levels of IRF9, STAT1 and pSTAT1 were visualised. The levels of IRF9 and STAT1 were constant among all samples in both the presence and absence of rIFNα treatment (Figure 5.4 rows 1 and 2, look at all lanes). This lack of change indicates that neither vIRF2 nor vIRF4 decrease the levels of IRF9 or STAT1. As expected, pSTAT1 was only detected in rIFNα treated samples, as phosphorylation arises following rIFNα stimulation. In the rIFNα treated vIRF2-NTAP sample, the level of pSTAT1 was reduced compared to the rIFNα treated EV-NTAP sample (Figure 5.4, row 3, compare lanes 2 and 4). This reduction can be seen in all three experiments (Figure 9.21), and confirms that the presence of vIRF2 results in a decrease of pSTAT1 levels. The levels of pSTAT1 are unchanged in rIFNα stimulated vIRF4-NTAP samples compared to EV-NTAP samples, indicating that vIRF4 does not affect levels of pSTAT1 to any detectable extent (Figure 5.4, row 3, compare lanes 2 and 6).

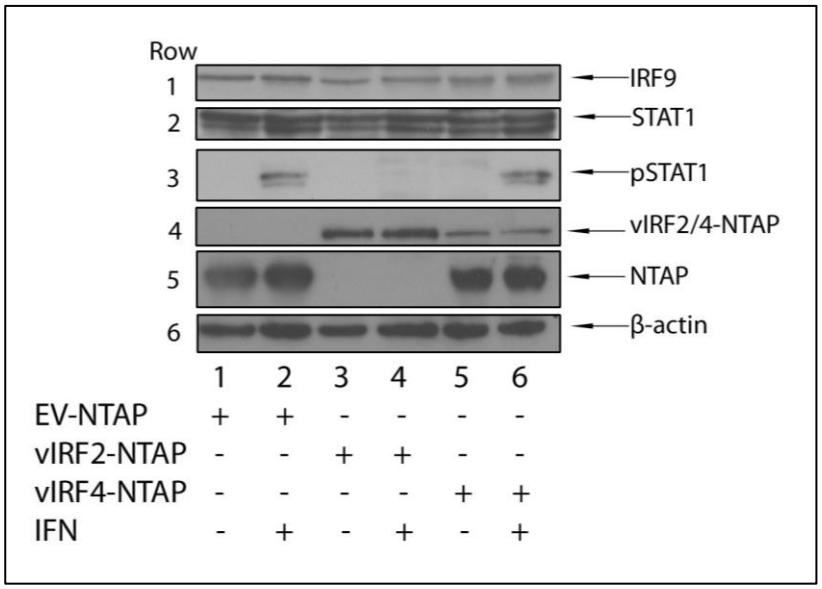

Figure 5.4: pSTAT1 is reduced in the vIRF2-NTAP cell line compared to the EV-NTAP cell line.

EV-NTAP, vIRF2-NTAP or vIRF4-NTAP cell lines were pre-treated with tetracycline (0.125μg/ml) for 24 hours and then stimulated with rIFNα (300IU/ml), or left un-stimulated, before being harvested 16 hours later. Lysates (40μg) were analysed by western blot to detect components of the JAK-STAT signalling pathway (IRF9, STAT1 and pSTAT1). For primary antibody concentrations and conditions see Table 9.3 . Probing for β-actin indicated equal loading and the NTAP, vIRF2-NTAP and vIRF4-NTAP proteins were detected using anti-mouse HRP-conjugated secondary antibody. The presence of bands in vIRF4-NTAP samples corresponding in size to that of the NTAP protein is most likely due to degradation of the vIRF4-NTAP protein (row 6 lanes 5 and 6). This experiment was repeated twice and the resultant blots are shown in Figure 9.21

5.5. Examining STAT2 and pSTAT2 levels in the vIRF2 and vIRF4 expressing cell lines

The previous section detailed how the levels of ISGF3 components were compared among the stable cell lines. However, the levels of STAT2 and pSTAT2 were not analysed in this way. The vIRF2-NTAP and the vIRF4-NTAP proteins exhibit degradation, resulting in bands which appear on the western blot. One of the vIRF4-NTAP degradation products results in a band which runs at the same size as STAT2 and pSTAT2, meaning that the level of pSTAT2 cannot be distinguished from the degradation products. To illustrate this problem, the lysates from the stable cell lines were separated on an SDS-PAGE gel, transferred and probed with anti-rabbit secondary-HRP antibody only. This analysis resulted in bands which correspond to the vIRF2-NTAP or vIRF4-NTAP proteins, along with their degradation products (Figure 5.5A), as they contain the NTAP tag which is comprised of protein G domains. Bands were observed in the vIRF4-NTAP lysates at a similar size to that of pSTAT2 (Figure 5.5A, lanes 7 and 8, marked with *). To confirm that these bands would obscure the visualisation of pSTAT2 bands, the same membrane was then probed for pSTAT2. The resultant blot shows clear pSTAT2 bands in the 293 cells, EV-NTAP and vIRF2-NTAP lysates from cells stimulated with rIFNα (Figure 5.5A lanes 10, 12 and 14). However, in the case of the vIRF4-NTAP lysates, the pSTAT2 bands cannot be distinguished from the degradation products (Figure 5.5B lanes 15 and 16). Therefore, levels of STAT2 and pSTAT2 in vIRF4-NTAP cells cannot be measured in this manner

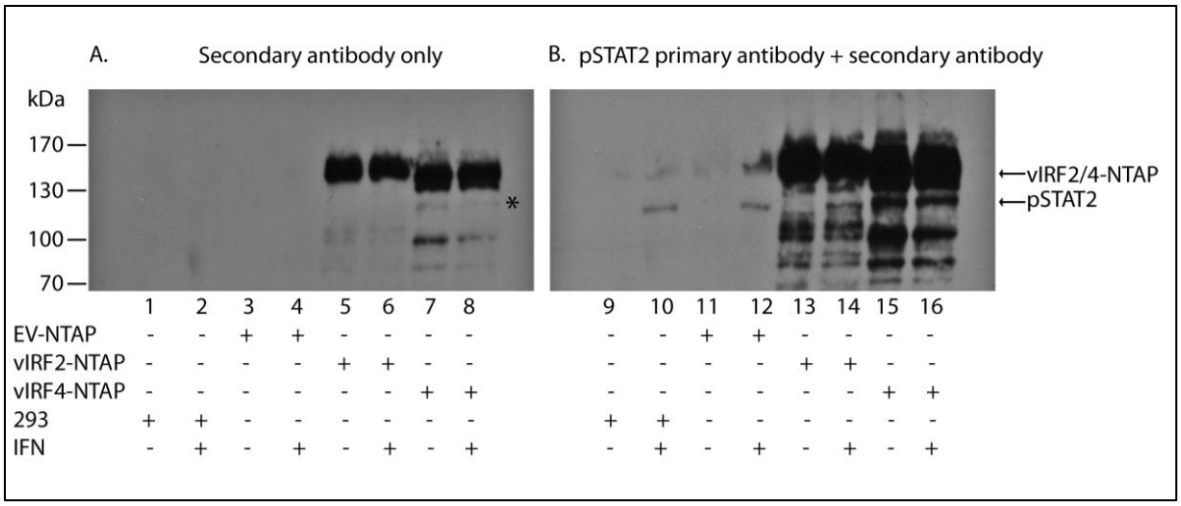

Figure 5.5: The degradation products from vIRF4-NTAP lysates obscure the pSTAT2 bands.

EV-NTAP, vIRF2-NTAP or vIRF4-NTAP cell lines were treated as in Figure 5.4. 293 cells were also stimulated with rIFNα (300IU/ml), or left un-stimulated. Cells were harvested 16 hours later. Lysates (40µg) were analysed by western blotting. (A) Probing with anti-rabbit HRP-conjugated secondary antibody only. The 140kDa and 130kDa bands in lanes 5-8 correspond to the vIRF2-NTAP or vIRF4-NTAP proteins respectively. Smaller bands in these lanes are degradation products of these proteins. The asterisk to the right of the degradation bands in the vIRF4-NTAP sample indicates the position of degradation products from vIRF4-NTAP which mask the pSTAT2 bands seen in B. The absence of the NTAP protein in the EV-NTAP samples is due to this protein being too small to be visualised on this percentage gel (7% acrylamide). (B) The same membrane as in A was probed with a pSTAT2 antibody, followed by incubation with the anti-rabbit HRP-conjugated secondary antibody only and development. The bands in lanes 10, 12 and 14 are of pSTAT2. The bands in lanes 15 and 16 cannot be distinguished from pSTAT2 or degradation products of vIRF4. 293 cells were used in this experiment to provide a negative control for degradation products, as these cells do not contain any NTAP protein.

5.5.1. Examining the levels of STAT2 and pSTAT2 in vIRF2-NTAP cells

Since the detection of pSTAT2 in the vIRF2-NTAP cell lysates was possible, it was investigated in comparison to EV-NTAP cell lysates. In the same way as described in section 5.4, EV-NTAP and vIRF2-NTAP lysates were analysed by western blot, this time for STAT2 and pSTAT2. The presence of vIRF2 did not result in a change in levels of STAT2 or pSTAT2 (Figure 5.6, row 1 and 2, compare lanes 2 and 4).

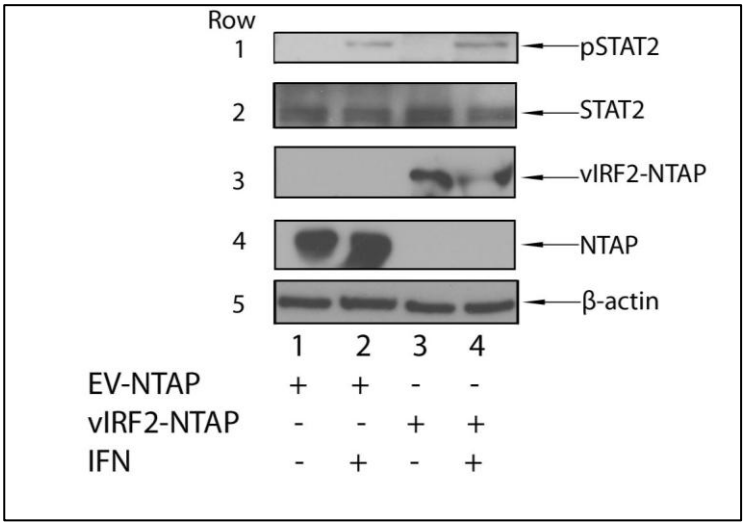

Figure 5.6: vIRF2 does not affect levels of STAT2 and pSTAT2.

EV-NTAP or vIRF2-NTAP cell lysates were produced as in Figure 5.4. Lysates (40µg) were analysed by western blot to detect STAT2 and pSTAT2. For primary antibody concentrations and conditions see Table 9.3. Probing for β-actin indicated equal loading, and the NTAP and vIRF2-NTAP proteins were detected using anti-mouse HRP-conjugated secondary antibody. This experiment was repeated once more and the resultant blot is shown in Figure 9.22

5.5.2. Examining the levels of STAT2 and pSTAT2 in vIRF4-NTAP cells

The NTAP tag contains two protein G domains, and these can be bound by any antibody. As shown in Figure 5.5, one of the vIRF4-NTAP degradation products is the same size as STAT2 and pSTAT2 which means their detection is obscured by this degradation product. It was therefore necessary to find a different way to measure levels of STAT2 and its phosphorylated derivative.

The NTAP-tag is comprised of two protein G domains and a streptavidin binding domain (SBD) separated by a tobacco etch virus cleavage site (TEV) (Figure 5.7). Since obscuring of the STAT2 and pSTAT2 proteins during western blot analysis is due to the presence of the protein G, its removal was necessary. Lysates from 293 cells, EV-NTAP or vIRF4-NTAP cells were incubated with TEV protease, in order to cleave the protein G domains from the EV-NTAP and vIRF4-NTAP (resulting in EV-SBD and vIRF4-SBP proteins), and their degradation products. These resultant proteins will not be detected non-specifically through incubation with any antibody, as they do not contain the protein G domains. The digested lysates were analysed by western blot to detect the STAT2 and pSTAT2 proteins. It was found that there is no change in levels of either STAT2 (Figure 5.8 row 2, compare lanes 4 and 5 with lanes 6 and 7) or pSTAT2 (Figure 5.8 row 1, compare lane 5 lane 7) between the EV-NTAP and vIRF4-NTAP samples, indicating that vIRF4 does not decrease levels of STAT2 or pSTAT2.

The vIRF4-NTAP samples which were untreated with the TEV protease showed bands at 130kDa. The lack of bands at the size of the full length vIRF4-NTAP in

the TEV protease treated vIRF4-NTAP samples, when probed with anti-STAT2 or anti-pSTAT2 antibodies confirms that the NTAP protein has been digested from these lysates (Figure 5.8 rows 1 and 2, compare lanes 6 and 7 with lanes 8 and 9). To confirm that vIRF4-SBP was present in the digested vIRF4-NTAP samples an antibody against SBP was used and this detected EV-SBP, vIRF4-SBP (Figure 5.8 rows 3 and 4, lanes 4-7) and also vIRF4-NTAP (Figure 5.8 rows 3 and 4, lanes 8 and 9). The vIRF4-SBP was shown to be about 15kDa smaller than the vIRF4-NTAP, a difference that corresponds to the size of the protein G domains (Figure 5.8 row 3, compare lanes 6 and 7 with lanes 8 and 9). Analysis of the 293 cell lysates confirmed that any bands were due to STAT2 or pSTAT2 and not from degradation products. One sample of 293 cell lysates, treated with rIFNα, was not digested with the TEV protease in order to show that digestion has no effect on either STAT2 or pSTAT2 levels (Figure 5.8 rows 1 and 2, lane 1).

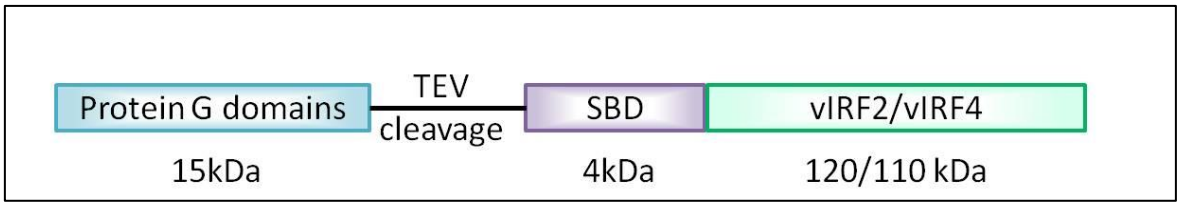

Figure 5.7: The NTAP tag.

The NTAP tag is comprised of two protein G domains and a streptavidin binding domain (SBD) separated by a Tobacco etch virus (TEV) cleavage site. The vIRF2 or vIRF4 proteins are contiguous with the SBD. The approximate molecular sizes of the domains are shown, but the figure is not dawn to scale.

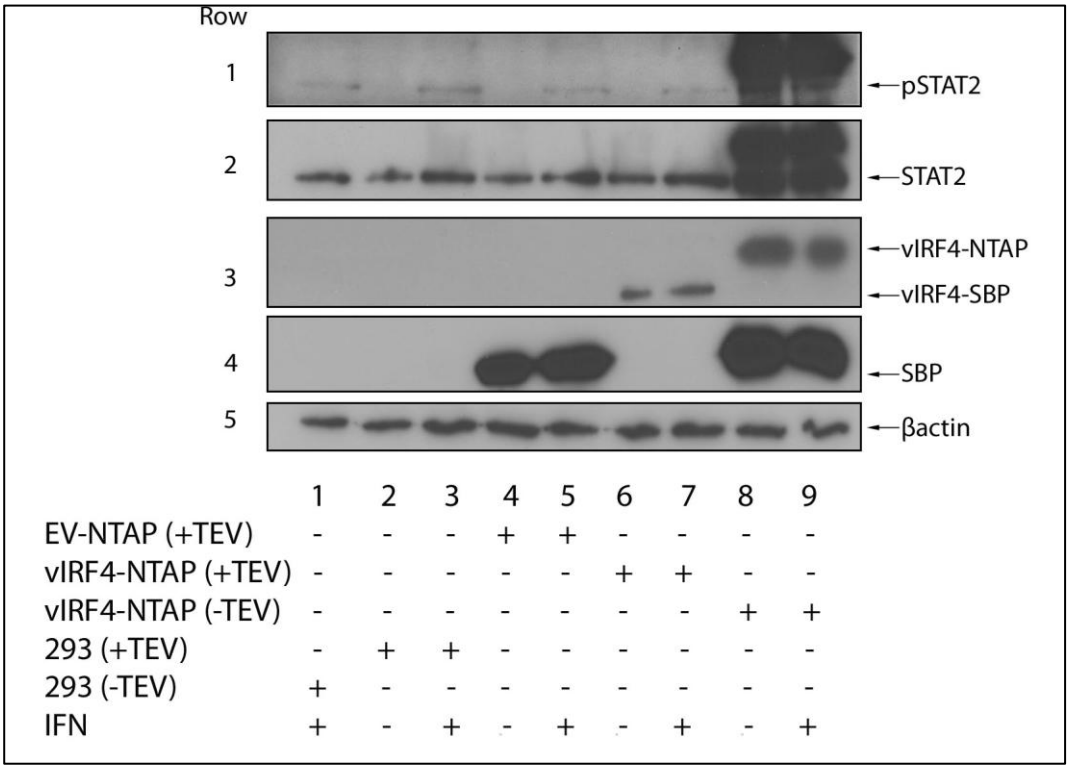

Figure 5.8: vIRF4 does not affect levels of STAT2 and pSTAT2.

293, EV-NTAP or vIRF4-NTAP cell lysates were produced as in Figure 5.4. Lysates were digested with AcTEV Protease (TEV protease) overnight on a rotating wheel at 4˚C. The digested lysates (40µg) were analysed by western blot to detect STAT2 and pSTAT2 as described in Figure 5.7. Probing for β-actin indicated equal loading and the vIRF4-NTAP protein was detected using anti-mouse HRP-conjugated secondary antibody. The vIRF4-SBP and SBP proteins resulting from TEV protease vIRF4-NTAP and EV-NTAP samples respectively were detected using an ant-streptavidin binding protein antibody. This experiment was repeated and the result is shown in Figure 9.23.

5.6. Discussion

Both vIRF2 and vIRF4 have been shown to negatively regulate the JAK-STAT signalling pathway (chapters 3 and 4), but the mechanisms behind their action are currently unknown. The aim of the work in this chapter was to assess the extent and the mechanisms of these viral proteins upon the antiviral response.

To provide a biological readout of the extent of the vIRF2 and vIRF4 anti-IFN effect, the rescue of the IFN sensitive EMCV titre was assessed. vIRF2 rescued EMCV titre following rIFNα treatment, whereas vIRF4 was unable to do so (Figure 5.1). This effect of vIRF2 is consistent with previously published findings from our laboratory (Mutocheluh et al., 2011). Since the vIRF2 mediated blockade on the JAK-STAT signalling pathway is strong enough to rescue EMCV from the effect of rIFNα, it could be hypothesised that vIRF2 may play a role in allowing more efficient infection by KSHV during primary infection or lytic reactivation. The lytic vIRF2 protein could suppress the IFN response resulting in increased infection. This hypothesis could be tested by infecting the stable cell lines with KSHV, and quantifying levels of the virus. The stable cell lines could be infected with rKSHV which constitutively expressed the GFP protein. The presence of GFP means that the levels of this virus could be quantified using flow cytometry. If the presence of vIRF2 increased the levels of KSHV it would provide evidence that vIRF2 is playing a role in increasing KSHV infection.

Contrastingly, vIRF4 was unable to rescue EMCV titre from IFN. There are some possibilities why this was the case. Firstly, vIRF2 can downregulate IFNβ promoter

activation (Fuld et al., 2006, Areste et al., 2009), whereas vIRF4 cannot. Since vIRF2 inhibits IFNβ promoter activation, and therefore IFN production, the vIRF2-NTAP cells would theoretically produce less endogenous IFN in response to EMCV infection than cells lacking vIRF2. However, in the vIRF4-NTAP cells the infection with EMCV would result in endogenous IFN production, in addition to the exogenous recombinant rIFNα added to the culture as part of the experiment. IFN can also positively regulate the production of more IFN by activating the IFN production pathway (Sato et al., 1998), so in vIRF2 expressing cells, this positive regulation would be inhibited, while in vIRF4 expressing cells this would not be inhibited. Overall, this additional endogenous IFN would increase the IFN concentration in the local cell environment. The increased IFN around the infected cells may activate the antiviral response to a level which vIRF4 could not inhibit, thus confounding the effect of vIRF4.

Secondly, the experiment used 300IU/ml of rIFNα which may have been an excessive amount of IFN to use for this readout. At lower IFN concentrations vIRF4 may rescue EMCV titre.

Thirdly, vIRF2 can interact with and inhibit PKR kinase activity reducing the inhibition of viral mRNA translation (Burysek and Pitha, 2001). PKR can detect dsRNA and lead to an inhibition of viral mRNA translation (see section 1.4.10.1). The EMCV titre in vIRF2 expressing cells may be increased as viral mRNA translation is not inhibited. Since vIRF4 has not been shown to interact with PKR, it is unlikely to prevent the activation of this kinase, and thus, mRNA translation is

halted, leading to reduced EMCV titre. Overall, the contrasting results observed between the effect of vIRF2 and vIRF4 on EMCV titre may reflect mechanistic differences in their mode of action.

The EMSA experiments aimed to examine the binding of ISGF3 to the ISRE sequence in the stable cell lines. It was found that in both vIRF2-NTAP and vIRF4-NTAP cells the binding of ISGF3 to the ISRE consensus sequence was significantly inhibited when compared to the EV-NTAP cell line (Figure 5.3). Since ISGF3 drives expression of ISGs, these results confirm the luciferase reporter studies (chapter 3 and 4) that vIRF2 and vIRF4 downregulate JAK-STAT signalling and repressing the host cell anti-viral response.

There are numerous steps in the JAK-STAT pathway, and thus numerous steps for viral proteins to target, in order to inhibit the antiviral response. A common way for viruses to attenuate JAK-STAT signalling is to reduce the levels of the components of the ISGF3 complex. For example, the Dengue virus NS5 protein binds to STAT2 and targets it for degradation, inhibiting JAK-STAT signalling (Ashour et al., 2009). Alternatively, the V Protein encoded by Simian Virus 5 inhibits interferon signalling by targeting STAT1 for proteasome-mediated degradation (Didcock et al., 1999).

To investigate if either vIRF2 or vIRF4 cause reduced levels of the ISGF3 components or their precursors, the levels of STAT1, pSTAT1, STAT2, pSTAT2

and IRF9 were compared in the stable cell lines. pSTAT1 levels reduced in the vIRF2-NTAP cell lines compared to the EV-NTAP cell lines (Figure 5.4). This result confirms the previous studies from our laboratory (Mutocheluh et al., 2011). Further experiments would aim to identify how pSTAT1 levels are reduced by vIRF2. Interestingly, the levels of STAT1 are not decreased in the vIRF2 expressing cells, suggesting that the reduction of pSTAT1 levels is not due to degradation of STAT1 or a reduction in STAT1 transcription. To confirm this theory, the stable cell lines could be treated with the proteasome inhibitor, MG132, and STAT1 and pSTAT1 levels re-assessed. If levels of pSTAT1 are not reduced in the vIRF2-NTAP cell lines, it indicates that proteasomal degradation is involved and vice versa. qPCR could be used to compare levels of STAT1 mRNA amongst the stable cell lines to rule out any effects from differences in transcription of STAT1.

Kumthip et al, (2012) found that the HCV NS5A protein decreases levels of pSTAT1, without affecting levels of STAT1. NS5A was shown to bind to STAT1 and it was proposed that this binding was responsible for the reduction of pSTAT1 and inhibition of the JAK-STAT signalling pathway (Kumthip et al., 2012). It can be hypothesised that, like NS5A, vIRF2 can also bind to STAT1, leading to a decrease in levels of pSTAT1. To determine if vIRF2 could bind to STAT1 and to identify any other vIRF2 binding partners, pull down experiments were analysed by mass spectrometry (see results chapter 6).

In the vIRF4-NTAP cells, none of the components of the ISGF3 complex were found to be reduced compared to the EV-NTAP cells. This result reveals that vIRF4 does not downregulate ISRE promoter activity by decreasing levels of the ISGF3 components. Because levels of ISGF3 components are not reduced in vIRF4-NTAP cells, vIRF4 is unlikely to be targeting protein levels of components upstream of the ISGF3 in the JAK-STAT signalling pathway. For example if levels of the IFNAR1 were reduced, it would be expected to reduce ISGF3 components.

Since vIRF4 is not down regulating ISRE promoter activity by reducing levels of the ISGF3 components, the mechanism behind its action remains to be found. The translocation of ISGF3 components from the cytoplasm to the nucleus is a vital step in activation of the ISRE promoter. The P protein encoded by Rabies virus attenuates JAK-STAT signalling by inhibiting the translocation of STAT1 into the nucleus (Vidy et al., 2005). Immunofluorescence staining of the ISGF3 components in vIRF4 expressing cells could determine whether vIRF4 is causing the sequestration of these signalling components in the cytoplasm, and restricting their translocation to the nucleus.

Collectively, the western blot analysis on ISGF3 components implies that vIRF2 and vIRF4 exert their anti-IFN effect in different manners. It is not surprising that vIRF2 and vIRF4 have different mechanisms to achieve the same overall result. KSHV encodes many proteins which inhibit IFN signalling, which points to the importance of innate immune evasion by the virus. KSHV would not have so many proteins which all work in the same way as they would be unnecessary and

selective pressure would result in loss of these genes over time. Additionally, if these proteins employed the same mechanism to achieve inhibition of IFN signalling, the host would only require one mechanism to overcome the effects of the viral proteins. Therefore, it makes sense that vIRF2 and vIRF4 have different mechanisms to inhibit IFN signalling. These proteins may also act at slightly different stages of the viral life cycle, or act in different cell types. Another possibility for the difference of results seen by western blot is simply that vIRF2 and vIRF4 may be expressed ectopically at different levels, making one mechanism more obvious, by western blotting, than the other.

Overall, this chapter has shown that ectopic expression of vIRF2, but not vIRF4, can rescue the IFN sensitive EMCV virus. EMSA experiments revealed that both vIRF2 and vIRF4 inhibit binding of the ISGF3 to the ISRE promoter. Finally, western blot analysis revealed that vIRF2 decreases the levels of pSTAT1 whereas vIRF4 has no effect on levels of the ISGF3 components.

CHAPTER 6

CELLULAR INTERACTIONS OF THE KSHV vIRF2 AND vIRF4 PROTEINS FOLLOWING rIFNα TREATMENT

6.1. Introduction

One of the aims of chapter 5 was to determine whether vIRF2 or vIRF4 exert their interferon inhibitory activities by down regulating levels of the ISGF3 components. It was found that vIRF2 caused a selective decrease in pSTAT1 levels, but did not affect levels of STAT1. This decrease in pSTAT1 is expected to lead to inhibition of JAK-STAT signalling, and is proposed to be one way in which vIRF2 inhibits the host antiviral effect. vIRF4 was not found to downregulate any of the ISGF3 components.

This chapter aims to build on these results by gaining further knowledge of how vIRF2 is decreasing levels of pSTAT1 and to identify how vIRF4 may be exerting its anti-IFN effect. Instead of testing each possible mechanism of inhibition separately, which is both time consuming and costly, it was decided that protein binding partners of both vIRF2 and vIRF4 should be identified, based on the hypothesis that this would reveal biologically significant interactions in terms of IFN signalling. This approach was therefore expected to narrow down the possible mechanism of action of vIRF4, and lead to understanding of how vIRF2 is decreasing pSTAT1.

The aims of this chapter are to:

1) Perform pull down experiments on lysates from the stable cell lines in order to purify NTAP-tagged KSHV proteins and their cellular binding partners
2) Identify these cellular protein binding partners of vIRF2 and vIRF4 by mass spectrometry

3) Select some of these binding partners for examination in more detail in the Chapter 7.

Some interaction partners of the KSHV vIRF2 or vIRF4 proteins have already been identified by other groups. For example, interactions have been found between vIRF2 and CBP (Burysek et al., 1999b) and vIRF2 and PKR (Burysek and Pitha, 2001). In the case of vIRF4, interactions have been confirmed between USP7 (Lee et al., 2011) and MDM2 (Lee et al., 2009) amongst others.

Since the work in this thesis focuses on the negative regulation of ISRE-containing promoter transactivation by the vIRF2 and vIRF4 proteins, the cellular interactions of these proteins following rIFNα treatment was examined. The aim was to determine any binding partners which contribute to the observed downregulation of JAK-STAT signalling.

As described previously, both the vIRF2 and the vIRF4 genes were cloned separately into an NTAP expression vector. This vector expresses an NTAP-tag, which allows for tandem affinity purification of the contiguous vIRF2 or vIRF4 proteins along with any binding partners. Tandem affinity purification (TAP) can be performed using a variety of vectors, with a variety of tags. The TAP-tag portion of the NTAP vector used in this study consisted of two IgG binding units of protein G from *Streptococcus* sp, linked to the SBP by a TEV cleavage site (Figure 5.7). The two-step purification therefore required the use of IgG agarose beads, which bind

to the protein G domains, followed by elution through TEV protease cleavage, and then a second purification step using Streptavadin beads to bind SBP and eluting with biotin. Following purification, the identity of any binding partners can be determined through mass spectrometry analysis. The advantage of tandem purification over single purification is that the final eluate often contains far fewer contaminants, and thus the results are more specific. However, the tandem step process can result in a lower yield of final product which is a disadvantage as the mass spectrometry analysis may not pick up weak or low abundance binding partners. Through preliminary experiments, it became clear that the yield of final proteins generated through the tandem affinity purification was very low. To rectify this, the method was changed to a single purification protocol by removing the IgG incubation and TEV protease cleavage steps in the protocol, and using the streptavidin beads only. This method resulted in a much higher yield of protein following initial experiments, and was thus used in the large scale protein purification. Because single purifications may result in more contaminants, SILAC was used in combination with the pull down to help to differentiate between specific and non-specific binding proteins.

6.2. TAP resulted in very little purified protein, therefore a single purification step was used instead

TAP is a two-step protocol that enables the affinity purification of proteins and their binding partners. The identity of these binding partners is determined by mass spectrometry. One major advantage of tandem purification compared to single affinity purification procedures is that the level of non-specific contaminants is greatly reduced.

Prior to full scale protein purification, a scaled down version of the TAP protocol (see Burckstummer et al (2006), for this method) was performed in order to confirm that the procedure worked. Briefly, lysates from the stable cell lines were incubated with IgG-coated beads, so that the protein G domains of the NTAP tagged proteins bound to the beads. Following washing, the tagged proteins are eluted using TEV protease, which cleaves the NTAP tag, leaving the Protein G domains bound to the beads and releasing the protein of interest attached to the SBP. The second purification step involves incubation with Streptavidin beads, followed by washing and elution with biotin.

Unfortunately, despite numerous attempts, either no or very little protein could be detected in the final eluate (data not shown). To increase the yield of final protein with binding partners, the first purification step with IgG beads was not performed and only the streptavadin bead step was implemented (see materials and method section 2.5.3 for details). However, because this procedure was a single purification process, the chance of non-specific proteins being identified was

increased considerably. One way to overcome this problem would be to use a higher salt concentration to wash the streptavidin beads, which would result in more stringent interactions. This solution has the disadvantage of also erroneously removing low abundance and/or low affinity binding partners, which may be important in the function of vIRF2 and vIRF4. Therefore, it was decided that proteins would be purified from differentially labelled samples, in order to quantify and compare levels of purified proteins in the vIRF2-NTAP and vIRF4-NTAP sample with the EV-NTAP control. By quantifying the protein partners, anything which increase in binding compared to the EV-NTAP samples could be thought of a possible interaction partners, whereas proteins which bound the same amount could be classed as background. The labelling of samples was achieved using isotope labelling of amino acids, more commonly known as SILAC.

6.3. Combining SILAC, mass spectrometry and pull down experiments

The stable cell lines were labelled by SILAC, followed by purification on streptavidin beads. The purified samples were then analysed by mass spectrometry to identify binding partners and to detect differences in protein abundance.

6.3.1. Labelling of the stable cell lines

In this thesis, the three cell lines to be analysed (EV-NTAP, vIRF2-NTAP and vIRF4-NTAP) were cultured in identical media except one contained ‘light’ amino acids, one contained ‘medium’ amino acids and the other contained ’heavy’ amino

acids. For details of how cells were labelled, see sections 2.5.1 and 2.5.2. These amino acids were incorporated into all newly synthesized proteins, so that after at least 5 passages all un-labelled amino acids were expected to have been replaced by the labelled amino acids.

6.3.2. Pull down of the NTAP-tagged proteins and their binding partners under SILAC conditions

The pull down strategy employed to purify the NTAP tagged proteins and binding partners is shown in Figure 6.1 and described in detail in sections 2.5.2 and 2.5.3. This experiment was performed three times. For experiments 1 and 3, the EV-NTAP cell lines were labelled with the light media, the vIRF2-NTAP cells were labelled with medium media and the vIRF4-NTAP cells were labelled with heavy media. For experiment 2, the vIRF2-NTAP cells were instead labelled with heavy media and the vIRF4-NTAP cells with the medium media. This switch in labelling media was to insure any proteins identified were not due to the differences in the labelling media.

Throughout this purification procedure, samples were collected as indicated in Figure 6.1A, B and C. These samples were later analysed by western blot (Figure 6.2A). Enrichment of all three proteins (NTAP, vIRF2-NTAP and vIRF4-NTAP) is evident (Figure 6.2A, lanes 7-9, compared with the other lanes). There was detection of NTAP and vIRF2-NTAP in the flow through samples (Figure 6.2A, lanes 4 and 5), indicating that not all of these bound to the streptavidin beads.

To show the presence of the NTAP-tagged proteins in the final eluates of all three separate experiments, a portion of these samples were analysed by western blot (Figure 6.2B). The presence of the NTAP, vIRF2-NTAP and vIRF4-NTAP proteins is clear in all three experiments. To ensure that proteins, other than the NTAP-tagged proteins, were present in the final eluate samples, these samples were run on a SDS gel and proteins were visualised by silver staining. Hence the samples could be analysed by mass spectrometry.

6.3.3. Mass spectrometric analysis of the eluted samples

Equal volumes of the R0K0 and R6K4 and R10K8-labelled samples (corresponding to the eluates from the NTAP, vIRF2-NTAP and vIRF4-NTAP samples) were mixed together, resulting in three final samples (corresponding to the three separate experiments). The combined samples were submitted to the Proteomics Facility at the University of Bristol for analysis. Details of how samples were analysed are found in 2.5.4

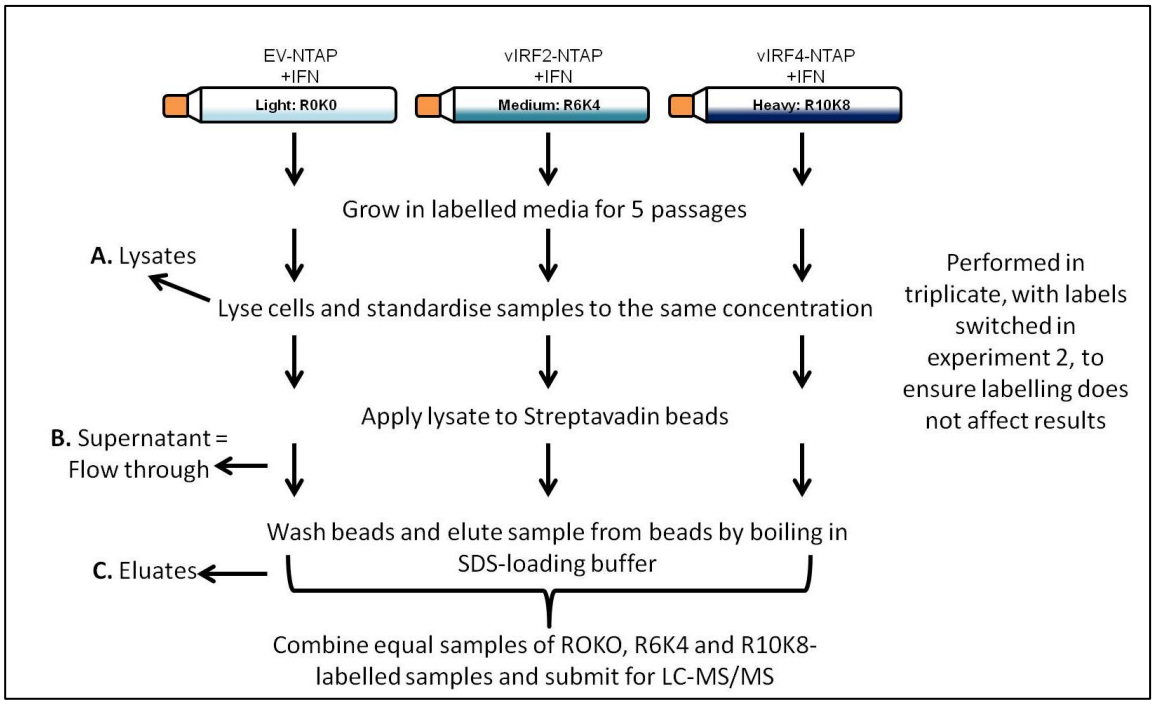

Figure 6.1: Strategy for identifying cellular interaction partners of vIRF2 and vIRF4.

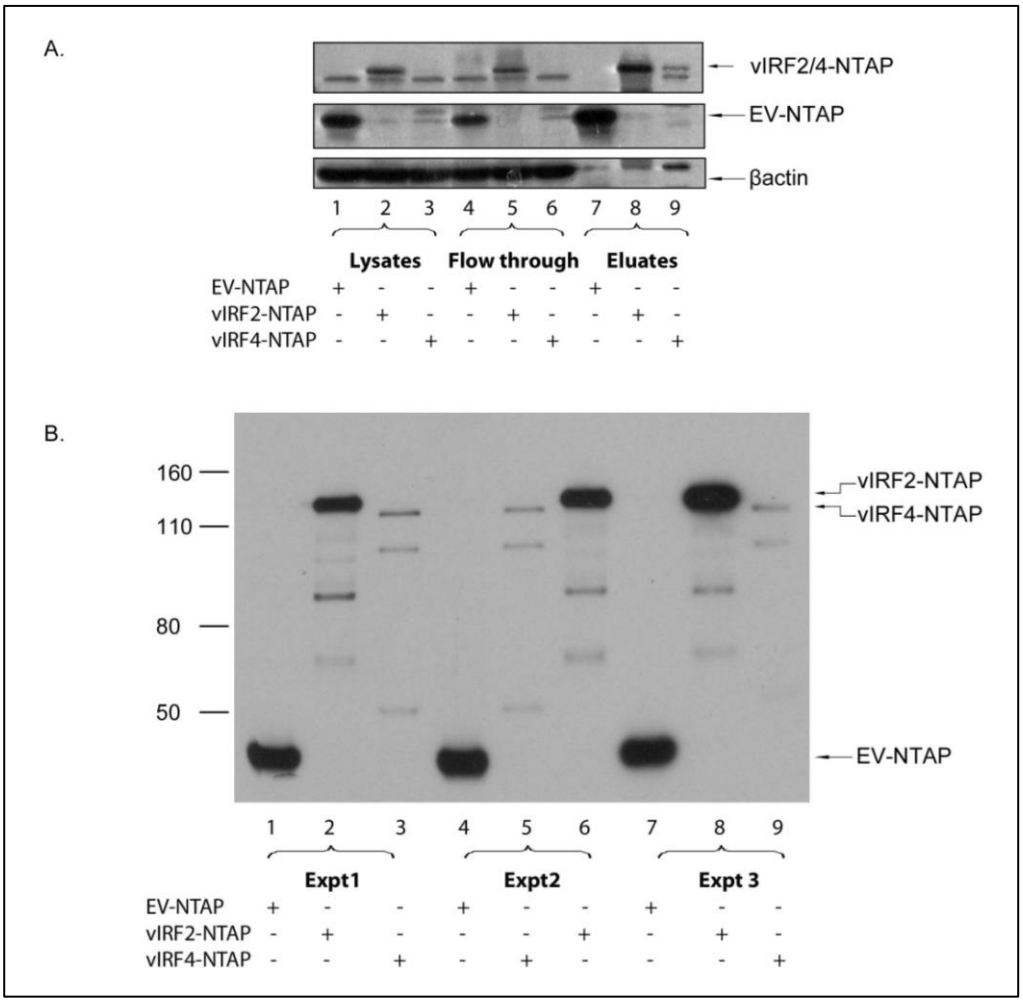

Figure 6.2: A. Samples collected at various stages of the pull down process. B. Final eluates from all three pull down experiments show the presence of the NTAP, vIRF2-NTAP and vIRF4-NTAP proteins.

A. Samples were put aside as described in sections 0 and 2.5.3. The lysate samples were collected following lysis of the cells (Figure 6.1A). The flow-through samples contained proteins which had not bound to the streptavidin beads (Figure 6.1B). The eluate samples were the final purified proteins (Figure 6.1C). 20µg of each sample was loaded on an SDS-PAGE gel and analysed by western blot to detect the NTAP tagged proteins and β-actin.'white*'s' represent the proteins of interest (NTAP, vIRF2-NTAP, vIRF4-NTAP) Primary antibody: anti-β-actin. Secondary antibody: anti-mouse HRP-conjugated secondary antibody (for β-actin detection). The use of the anti-mouse HRP-conjugated secondary antibody was sufficient to detect the NTAP-tag in all the cell lines as this tag contains protein G. Probing for β-actin confirmed equal loading between the lysate and flow through samples. This blot shows the result of one pull down experiment. This was repeated twice and the resultant blots can be seen in Figure 9.24 B.Final eluate samples from all 3 experiments were collected. 10ul of each sample was analysed by western blot to detect the NTAP, vIRF2-NTAP and vIRF4-NTAP proteins. The use of the anti-rabbit HRP-conjugated secondary antibody was sufficient to detect the NTAP-tag in all the samples as this tag contains protein G.

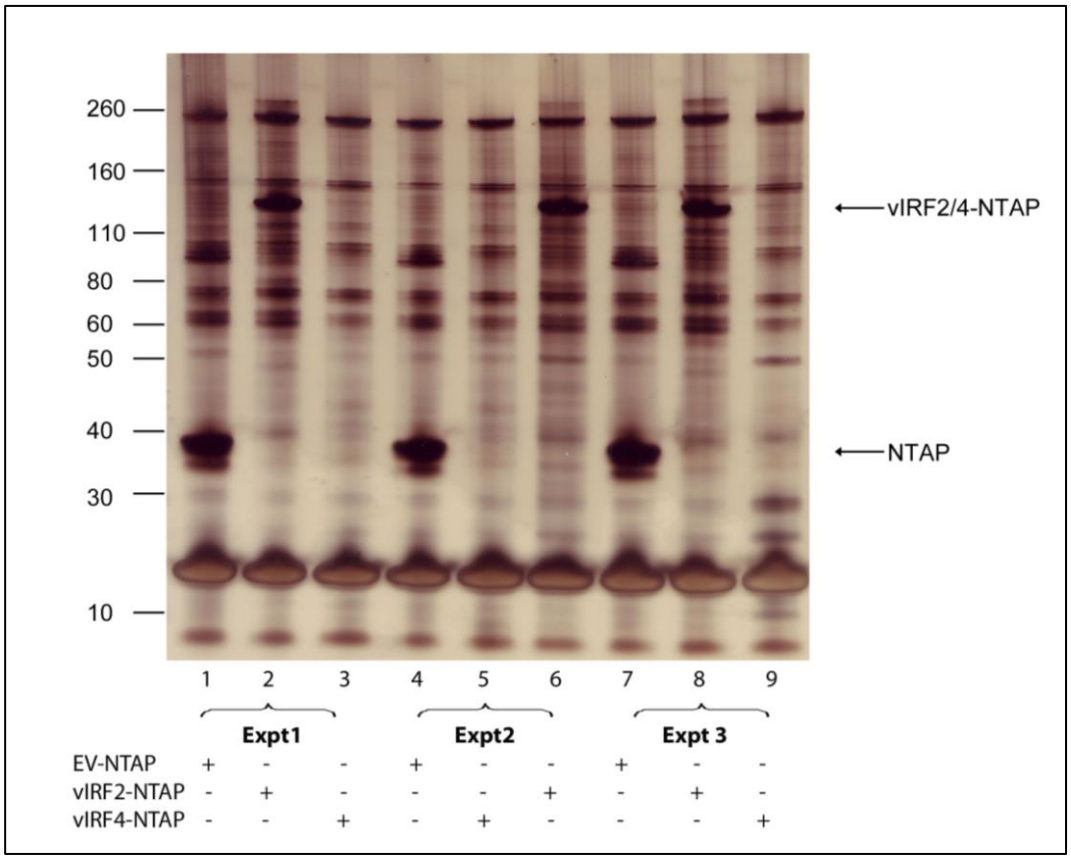

Figure 6.3: Silver-stained SDS-PAGE gel showing the pull downs from three separate experiments.

The final samples as shown in Figure 6.2 were run on a a precast NuPage (Invitrogen) 10% Bis-Tris gel. Silver staining was carried out as described in section 2.5.5.

6.4. Results of Mass Spectrometry:

Since the cells used to make the stable cell lines were 293 derived (a human cell line), proteins were identified by comparison to human sequences. In total 963 proteins were quantified in three experiments by SILAC LC-MS/MS (experiment 1 = 290 proteins, experiment 2 = 352 proteins, experiment 3 = 321 proteins). The results were 'cleaned', by removing any peptide sequences which appeared only once per experiment, as these proteins cannot be classed as 'real' results. 291 proteins were brought forward from the three experiments following this procedure (experiment 1 = 86 proteins, experiment 2 = 108 proteins, experiment 3 = 97 proteins). Of the 291 proteins 153 were unique. The Venn diagram (Figure 6.4) presents these results graphically.

6.4.1. Distinguishing between significant and non-significant results

One problem with SILAC mass spectrometry is deciding which identified proteins to class as significant and which to discard. Since mass spectrometry is so sensitive many identified proteins are in fact contaminants. Deciding on a cuttoff point for specific proteins and contaminants is therefore a key step in identifying real interactions. Two ways to separate significant and non-significant interactions will be discussed in this thesis.

1) Less stringent: This method is commonly used in the literature (Boulon et al., 2010), and is based on the principle that a protein showing a 1.5 fold increase in its abundance in the pull down compared to the control is a specific interaction.

2) Very stringent: This method ensures only the top 5% of hits are classed as specific interactions.

The less stringent approach uses the ratios of the proteins of interest compared to the control. The mass spectrometry results were presented as SILAC ratios for each identified protein. For example, each identified protein was given a medium/light ratio (which would be vIRF2/EV in experiments 1 and 2, and vIRF4/EV in experiment 2) and a heavy/light ratio (which would be vIRF4/EV in experiments 1 and 2, and vIRF2/EV in experiment 2). A higher ratio for a binding protein means that it is more likely to have bound specifically to the protein of interest. This approach means that proteins with low ratios, which are more likely to be background contamination or proteins which bound non-specifically to the beads, can be distinguished from proteins with higher ratios, which represent more significant interactions. A ratio of 1.5-fold is a commonly used cutoff when Orbitrap instruments are used (Boulon et al., 2010). When using arbitrary cutoff values, it is clear that a high threshold yields more 'real' results. However, some genuine interactions may also be lost. Conversely, using a low threshold, will include more contaminants, but may include some low abundance/low affinity interactions (Boulon et al., 2010).

As a conservative cutoff, a 2-fold ratio was used in this thesis to identify cellular proteins likely to be binding to vIRF2 or vIRF4 specifically. Usually, the average SILAC ratio for each identified binding protein would be calculated from the values from each experiment. However, in these results, experiment 2 yielded much

higher SILAC ratios than the other two, and averaging results from all three experiments would mean that peptides from experiment 2 could become un-significant. While these interactions may indeed be false, a search of the literature has shown some of these interactions to be real (the case of vIRF4 binding to USP7 is one example). Therefore, the number of peptides with a SILAC ratio over 2-fold in any experiment was determined. In the case of vIRF2/EV, 56/153 (37%) proteins had a ratio of greater than or equal to 2 (Table 6.1). In the case of vIRF4/EV, 23/153 (15%) proteins had a ratio of greater than or equal to 2 (Table 6.2).

The very stringent approach identifies the top 5% of proteins which bind to the vIRF2 or vIRF4 proteins, compared to the EV-NTAP control. To identify this category of interacting cellular proteins, firstly the SILAC ratios were converted to log2, so that the data were normally distributed. The average log2 ratios and standard deviation of the log2 ratios were determined for all for medium/heavy and light/heavy ratios. The log2 ratio for each protein was then converted into a Z-score so that protein ratios could be normalized to the mean and standard deviation of each experiment. The formula to calculate the z score was:

$$\text{Z score} = \frac{\text{log2 ratio (of peptide)} - \text{mean log2 ratio of all ratios for that experiment}}{\text{SD of all log2ratios for that experiment}}$$

A Z-score of ≥1.95, giving the top 5% of hits for each experiment, was then used to identify the significant peptide hits. Table 6.3 and Table 6.4 show the results for this approach.

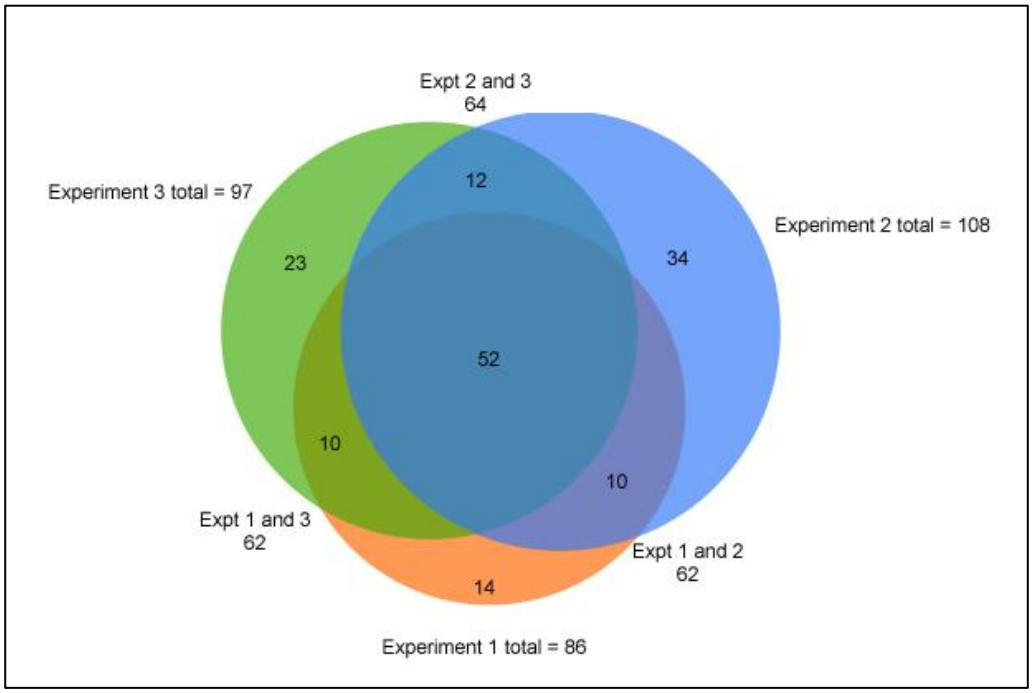

Figure 6.4: Triplicate experiments showing the extent of overlap of proteins identified in each of the 3 independent experiments.

Venn diagram of all proteins identified by SILAC.

Table 6.1: Potential vIRF2 binding partners based on a less stringent approach.

Proteins which showed an ≥ 2-fold change in abundance compared to the control were included in this table. * indicates proteins also identified in the very stringent approach.

Protein name	Accession number	Number of expts over ratio of 2	Number of expts below ratio of 2
CREB-binding protein*	Q92793	2	0
HAT p300*	Q09472	2	0
Ras GTPase-activating-like protein*	P46940	3	0
Ubiquitin carboxyl-terminal hydrolase*	F5H8E5	2	1
Protein Njmu-R1*	Q9HAS0	1	0
Nucleoside diphosphate kinase A*	P15531	2	0
Nucleoside diphosphate kinase*	Q32Q12	3	0
Protein RCC2	Q9P258	3	0
Trim3*	E7EUK0	1	1
40S ribosomal protein S6	P62753	1	0
60S acidic ribosomal protein P2	P05387	1	0
Ribosomal protein L18	E7EW92	1	0
6-phosphofructokinase type C	Q01813	2	1
Guanine nucleotide-binding protein subunit beta-2-like 1	P63244	1	0
60S acidic ribosomal protein P2	Q02878	1	0
60S acidic ribosomal protein P2	P05387	1	0
Ribosomal protein L15	E7EQV9	1	0
40S ribosomal protein S8	P62241	1	0
DHX9	F5GXA5	1	0
RPL4	E7EWF1	1	0
RPLP0 protein	Q3B7A4	1	0
Ribosomal protein L5	Q5T7N0	1	0
60S ribosomal protein L7a	P62424	1	0
60S ribosomal protein L12	P30050	1	0
RPSA	C9J9K3	1	0
RPS2	E9PQD7	1	0
PABPC1	E7EQV3	1	0
40S ribosomal protein S23	P62266	1	0
Ribosomal protein L28	C9JB50	1	0
60S ribosomal protein L19	P84098	1	0
LIM domain and actin-binding protein	Q9UHB6	1	0

40S ribosomal protein S3	P23396	1	0
RPL27A	E9PJD9	1	0
60S ribosomal protein L13	P26373	1	1
40S ribosomal protein S5	P46782	1	1
HNRNPU	B3KX72	1	2
Ribosomal protein S9	B5MCT8	1	0
Myosin light polypeptide 6	P60660	1	0
40S ribosomal protein S18	P62269	1	2
Actin, cytoplasmic 1	P60709	1	2
Heterogeneous nuclear ribonucleoprotein K	Q5T6W5	1	1
40S ribosomal protein S19	P39019	1	1
40S ribosomal protein S14	P62263	1	2
60S ribosomal protein L23a	P62750	1	0
60S ribosomal protein L11	P62913	1	2
60S ribosomal protein L38	P63173	1	1
40S ribosomal protein S13	P62277	1	2
Polypyrimidine tract-binding protein 1	P26599	1	0
1PL24	C9JXB8	1	2
DDX3X	B4E3E8	1	2
HMMR	E3W978	1	1
THO complex subunit 4	Q86V81	1	0
Splicing factor SFPQ	P23246	1	0
Histone H2B type 1	O60814	1	0
TFAM	A8MRB2	1	0

Table 6.2: Potential vIRF4 binding partners based on a less stringent approach.

Proteins which showed an ≥ 2-fold change in abundance compared to the control were included in this table * indicates proteins also identified in the very stringent approach.

Protein name	Accession number	Number of expts over ratio of 2	Number of expts below ratio of 2
CREB-binding protein*	Q92793	1	0
Ubiquitin carboxyl-terminal hydrolase*	F5H8E5	1	2
Heat shock protein HSP 90-ALPHA*	P07900	1	2
RCC2	Q9P258	1	2
40S ribosomal protein S6	P62753	1	0

Vimentin	P08670	1	2
60S acidic ribosomal protein P2	B3KX72	1	2
40S ribosomal protein S20*	P60866	1	2
40S ribosomal protein S3	P23396	1	1
40S ribosomal protein S18	P46782	1	2
40S ribosomal protein S17	P62269	1	0
Splicing factor, proline- and glutamine-rich	P23246	1	0
Splicing factor SFPQ	P0CW22	1	0
LIMA1	B4DN52	1	0
40S ribosomal protein S19	P39019	1	2
Myosin-9	P35579	1	0
40S ribosomal protein S14	P62263	1	2
40S ribosomal protein S11	P62280	1	0
RPL35	F2Z388	1	1
40S ribosomal protein S10	P46783	1	2
40S ribosomal protein S7	P62081	1	2
40S ribosomal protein S13	P62277	1	2
Actin, cytoplasmic 1	P60709	1	2

Table 6.3: Potential vIRF2 binding partners based on a very stringent approach

Protein name	Accession number	Number of expts in top 5%	Number of expts below top 5%
CREB-binding protein	Q92793	2	0
HAT p300	Q09472	2	0
Ras GTPase-activating-like protein	P46940	2	1
Ubiquitin carboxyl-terminal hydrolase	F5H8E5	2	0
Protein Njmu-R1	P15531	1	0
Nucleoside diphosphate kinase A	Q32Q12	1	0
Nucleoside diphosphate kinase	Q32Q12	1	0
Trim3	E7EUK0	1	1

Table 6.4: Potential vIRF4 binding partners based on a very stringent approach

Protein name	Accession number	Number of expts in top 5%	Number of expts below top 5%
CREB-binding protein	Q92793	1	0
Ubiquitin carboxyl-terminal hydrolase	F5H8E5	1	0
Heat shock protein HSP 90-ALPHA	P07900	1	2
40S ribosomal protein S20	P60866	1	0
RBPJ	B4DY22	1	0

6.5. Selecting proteins to analyse further:

The results in Table 6.1-Table 6.4 show possible binding partners for vIRF2 and vIRF4. To verify that these proteins are real interactors and not contaminants of the method, further experiments needed to be performed. Due to time constraints, it was not feasible to examine all possible binding partners, and therefore selected proteins were identified for further study. They were 1) CREB-binding protein (Q92793), 2) HAT p300 (Q09472), 3) Ubiquitin carboxyl-terminal hydrolase (F5H8E5) 4) 40S ribosomal protein S3 (P23396), 5) 40S ribosomal protein S6 (P62753). All these proteins were predicted to bind to both vIRF2 and vIRF4 in the less stringent approach and some of them were identified in the very stringent approach. The rationale for these selections is outlined in the discussion to this chapter.

6.6. Discussion

This chapter has described how pull down experiments were performed on lysates from the stable cell lines and how proteins were identified from these samples. The results from the mass spectrometry have been analysed in two ways to provide either less or very stringent predictions of the vIRF2 or vIRF4 interactome. As described in this chapter, identification of protein binding partners by mass spectrometry is very sensitive. This is very useful, as it may identify low abundance or weak interactions between proteins. However, it also means that contaminants may be misinterpreted as real interactions. Therefore to confirm if the predicted interactions are real, further experiments must be performed such as immunofluorescence experiments to examine co-localisation of proteins and immunoprecipitation. Based on the results in this chapter, five proteins have been chosen to confirm whether their interactions with vIRF2 and vIRF4 are genuine, thus justifying their examination in more detail in the context of IFN signalling. These 5 proteins are discussed in the following paragraphs.

6.6.1. CBP and p300

CBP was identified by Chrivia et al 1993 to bind to cAMP response element-binding protein (CREB) while p300 was found to associate with the adenovirus E1A protein (Eckner et al., 1994). These two proteins share a high degree of sequence homology (Figure 7.12). Both the CBP and p300 co-activator proteins are involved in binding to transcription factors and RNA polymerase II to stabilize the transcription complex and transcribe genes. They also exhibit HAT activity, which is involved in gene transcription (see section 7.9.3 for further details). As

well as being able to acetylate histones, these proteins can also acetylate other proteins (reviewed in Kalkhoven, (2004)).

Previous studies have found that vIRF2 can bind to the CBP/p300 protein (Burysek et al., 1999b). However no reports have identified CBP as an interacting partner for vIRF4. The results from this chapter found CBP as a possible binding partner for both vIRF2 and vIRF4 in both the less stringent (Table 6.1 and Table 6.2 respectively) and very stringent approaches (Table 6.3 and Table 6.4 respectively). p300 was identified as a potential binding protein for vIRF2 in both the less stringent (Table 6.1) and very stringent (Table 6.3) approaches. However it was not predicted to be a binding partner for vIRF4 in any approach to examine to data. The other KSHV-encoded vIRF proteins (vIRF1 and vIRF3), have also been shown to bind CBP/P300. vIRF1 inhibits IFN signalling by blocking the cellular IRF3 recruitment of the CBP/p300 coactivator (Lin et al., 2001). vIRF3 directly interacts with cellular IRF3, IRF7, and the transcriptional coactivator CBP/p300 (Lubyova et al., 2004).

Therefore, because CBP has been shown to associate with vIRF1, vIRF2 and vIRF3 and because vIRF4 has been predicted to bind CBP based on the results of this chapter, the interactions between CBP and either vIRF2 or vIRF4 were selected for further study. The yield of vIRF4 obtained from the pull down, prior to mass spectrometric analysis was low, and thus, possible interactions between vIRF4 and p300 may not have been present. Since CBP and p300 are very similar

proteins, it was decided that, even though vIRF4 was not predicted to bind to p300, immunoprecipitation should be used to confirm this prediction.

6.6.2. Ubiquitin carboxyl-terminal hydrolase

USP7, also known HAUSP is a de-ubiquitylating enzyme, which cleaves ubiquitin from specific proteins. USP7 was first identified by its interaction with the herpes simplex virus type I immediate early protein, ICP0 (Everett et al., 1997, Meredith et al., 1994). The EBV encoded EBNA1 protein is also a target of USP7 (Holowaty et al., 2003).

Lee et al, (2011) have shown that vIRF4 can bind to USP7. This interaction is believed to be important in the MDM2 and p53 signalling cascade, as expression of USP7 regulates levels of MDM2 and p53 and expression of vIRF4 decreases levels of p53 (see introduction section 1.5.4). There have been no reports of any interaction between vIRF2 and USP7.

Yu and Hayward, (2010) have shown that USP7 may be involved in inhibiting type I IFN production. USP7 stabilises the RTA-Associated Ubiquitin Ligase (RAUL) protein, which is a negative regulator of the IFN production pathway. This stabilisation leads to increased IRF7 and IRF3 degradation, in turn suppressing type I IFN production. They also showed that the KSHV lytic switch protein, RTA, enhanced this mechanism to inhibit the antiviral response.

In the present study, it was hypothesised that vIRF2 or vIRF4 may be using the de-ubiquitination activity of USP7 to inhibit the JAK-STAT signalling pathway in some manner. Hence, it was decided that the binding of vIRF2 and vIRF4 to USP7 should be confirmed by other methods, and if proven correct, studies should investigate USP7 in the context of IFN signalling.

6.6.3. Ribosomal proteins

23/56 of the proteins identified as binding to vIRF2, and 12/23 of the proteins identified as binding to vIRF4 were ribosomal proteins, based on the less stringent approach (Table 6.1 and Table 6.2 respectively). One hypothesis to explain the number of these putatively interacting ribosomal proteins is that it reflected their abundance in cells, i.e. ribosomal proteins may be so abundant that they can contaminate even SILAC based assays. To investigate if their abundance could be leading to contamination of SILAC, the data in Table 6.1 and Table 6.2 was compared with the 'PaxDb: Protein Abundance Across Organisms' (see http://pax-db.org/#!species/9606). This database ranks proteins based on their abundance in different species. At the time of analysis, the 8 most abundant proteins in human cells were APOA2, RBP4, APOC2, TTR, ALB, APOA1, ORM1 and TMSB4X in order of abundance. None of these proteins were found to be possible interaction partners with vIRF2 or vIRF4. CBP, which was found to bind to vIRF2 and vIRF4 in both the less and more stringent approaches ranked 17371 out of 19860 proteins. Therefore, there is no correlation between the abundance of a protein in a cell and its association with the vIRF2 and vIRF4 proteins. Hence, these ribosomal proteins were considered for further investigation

The ribosomal proteins which were common between vIRF2 and vIRF4 were 40S ribosomal protein S6, 60S acidic ribosomal protein P2, 40S ribosomal protein S3, 40S ribosomal protein S18, 40S ribosomal protein S19, 40S ribosomal protein S14, 40S ribosomal protein S13 (Table 6.1 and Table 6.2). It could be hypothesised that at least some of these ribosomal proteins are necessary for directing the expression of IFN-responsive genes. The idea that the ribosomal proteins provide regulatory transcript-specific translational control is not unprecedented. Kondrashov et al, (2011) have shown that the RPL38 ribosomal protein is involved in transcript-specific translational control, and suggest a role for ribosomal proteins in control of gene expression. Perhaps one of the ribosomal proteins identified in this chapter may select for translation of interferon-inducible proteins. Due to time constraints, not all ribosomal proteins could be examined individually, so it was necessary to pick two, to study in further detail. They were the 40S ribosomal protein S3 and the 40S ribosomal protein S6. These proteins are discussed briefly below including the justification for their choice in further studies.

6.6.3.1. 40S ribosomal protein S3

Ribosomal protein S3 (RPS3) is a component of the 40S ribosomal small subunit. This protein was investigated further because it was found to bind to heat shock protein 90 (HSP90). This interaction prevented the ubiquitination and degradation of RPS3, thereby retaining the integrity of the ribosome (Kim et al., 2006). The mass spectrometry results in this chapter found that vIRF4 also associated with HSP90 (Table 6.2 and Table 6.4). Therefore, the hypothesis that vIRF4 interacts

with RPS3 and HSP90 in order to regulate the stability of RPS3 and control translation was proposed.

6.6.3.2. 40S ribosomal protein S6

Ribosomal protein S6 (RPS6) is a component of the 40S ribosomal subunit. Interestingly, there is evidence suggesting that this protein is involved in regulating translation of ISGs. As well as the JAK-STAT signalling pathway, several other pathways are also activated by type I IFNs. These pathways have roles in transcription and translation of ISGs (reviewed in Platanias et al 2005). The PI3-kinase pathway is activated by type I IFNs, and results in activation of the target of rapamycin (mTOR)/ S6 kinase (S6K) pathway, causing phosphorylation of RPS6, which can then induce protein synthesis (Lekmine et al 2003, Kaur et al 2008, Kaur et al 2012). Due to the link with ISG translation, RPS6 was chosen as the second ribosomal protein to investigate further.

6.6.4. ISGF3 components

No ISGF3 components were identified as being binding partners of vIRF2 or vIRF4. This finding may represent a real lack of binding, or the interactions may not have been strong enough to be detected by the methods used here.

6.6.5. Summary

This chapter has described how immunoprecipitation experiments were performed on SILAC labelled stable cell lines. The immunoprecipitates were analysed by

mass spectrometry, and the interactomes of vIRF2 and vIRF4 were identified by both less stringent and very stringent analyses. Based on these results, five proteins were chosen for further study in the context of IFN signalling. The next chapter will confirm the interactions of these proteins with the vIRF2 and vIRF4 proteins and examine their association in the context of type I IFN signalling.

CHAPTER 7

CONFIRMING CELLULAR INTERACTIONS OF THE KSHV vIRF2 AND vIRF4 PROTEINS AND INVESTIGATING THE SIGNIFICANCE OF SUCH INTERACTIONS IN IFN SIGNALLING

7.1. Introduction

Chapter 6 identified a number of possible binding partners for vIRF2 and vIRF4. It was decided that the binding of five of these proteins could be significant interactions in the context of IFN signalling (see chapter 6 discussions) and should be validated. If confirmed, these interactions could then be analysed more specifically relating them to IFN signalling.

The aims of this chapter are to:

1) Identify if either the vIRF2 or vIRF4 proteins can interact with RPS3, RPS6, USP7, p300 or CBP.

2) Examine whether validated interactions are associated with the vIRF2- or vIRF4-mediated down-regulation of JAK-STAT signalling.

To verify the interaction partners of vIRF2 or vIRF4, identified by SILAC-MS, co-immunoprecipitation studies were performed on cells which were transfected to express either vIRF2 or vIRF4 transiently. Instead of using the pCDNA4TO-NTAP, pvIRF2-NTAP and pvIRF4-NTAP vectors to transfect cells, alternative expression vectors were used, so that the NTAP-tag, expressed from pCDNA4TO-NTAP-based vectors, would not interfere with the identification of specific proteins in the immunoprecipitates. vIRF2 was already cloned and expressed from the pvIRF2-His/Max vector (Areste et al., 2009). Therefore vIRF4 was cloned into the pcDNA4His/Max backbone, to produce the pvIRF4-His/Max expression vector. Both vIRF2-His/Max and pvIRF4-His/Max express the viral proteins with

contiguous Xpress and Histidine (His) epitope tags, and can therefore be immunoprecipitated/identified through use of the anti-Xpress or anti-His antibodies. This approach would express the vIRF2 and vIRF4 proteins with Xpress and His tags, meaning that they are different forms of the viral proteins to those expressed from the pvIRF2-NTAP and pvIRF4-NTAP vectors used in the mass spectrometry studies. Therefore this provides additional validation in the accurate identification of cellular partners.

7.2. Cloning vIRF4 into the pcDNA4/HisMax vector

vIRF2 had been previously cloned into the pcDNA4/HisMax vector, to produce vIRF2-His/Max, and chapters 3 and 4 have shown that the vIRF2 protein expressed from this plasmid functions the same as the vIRF2-NTAP protein in ISRE-luciferase assays. The vIRF2-His/Max vector has been used many times in experiments in our laboratory (Areste et al., 2009, Fuld et al., 2006) and is known to work well in both immunoprecipitation and immunofluorescence experiments. Therefore, it was decided that the vIRF4 gene should also be cloned in to the pcDNA4/HisMax vector.

An overview of the cloning scheme is illustrated in Figure 7.1. The pCR-Blunt-vIRF4 vector (described in section 3.3) was used as the amplification template for the vIRF4 gene. Specific PCR primers (Table 2.14 ‘vIRF4 Forward HisMaxA-BamHI’ and ‘vIRF4 Reverse HisMaxA’) containing the appropriate restriction site (BamHI) amplified the vIRF4 gene from the pCR-Blunt-vIRF4 template (Figure 7.1A) and the product was ligated into pCR-Blunt (Figure 7.1B). The resultant pCR-Blunt-vIRF4(BamHI) (Figure 7.1C) was confirmed by restriction digestion. The vIRF4 gene was excised, via enzymatic digestion from pCR-Blunt-vIRF4(BamHI) with BamHI first, and then digested with EcoRI (this restriction site is found in the pCR-Blunt vector) (Figure 7.1D). The resultant fragment was ligated into the pcDNA4/HisMax vector which had been digested with BamHI and EcoRI (Figure 7.1E). The resultant pvIRF4-HisMax construct was confirmed by sequencing. The expression of vIRF4 from this plasmid, transiently transfected into 293 cells, was confirmed by western blot (data not shown), and vIRF4 was

shown to inhibit rIFNα stimulated ISRE-containing promoter activation, through DLAs (data not shown).

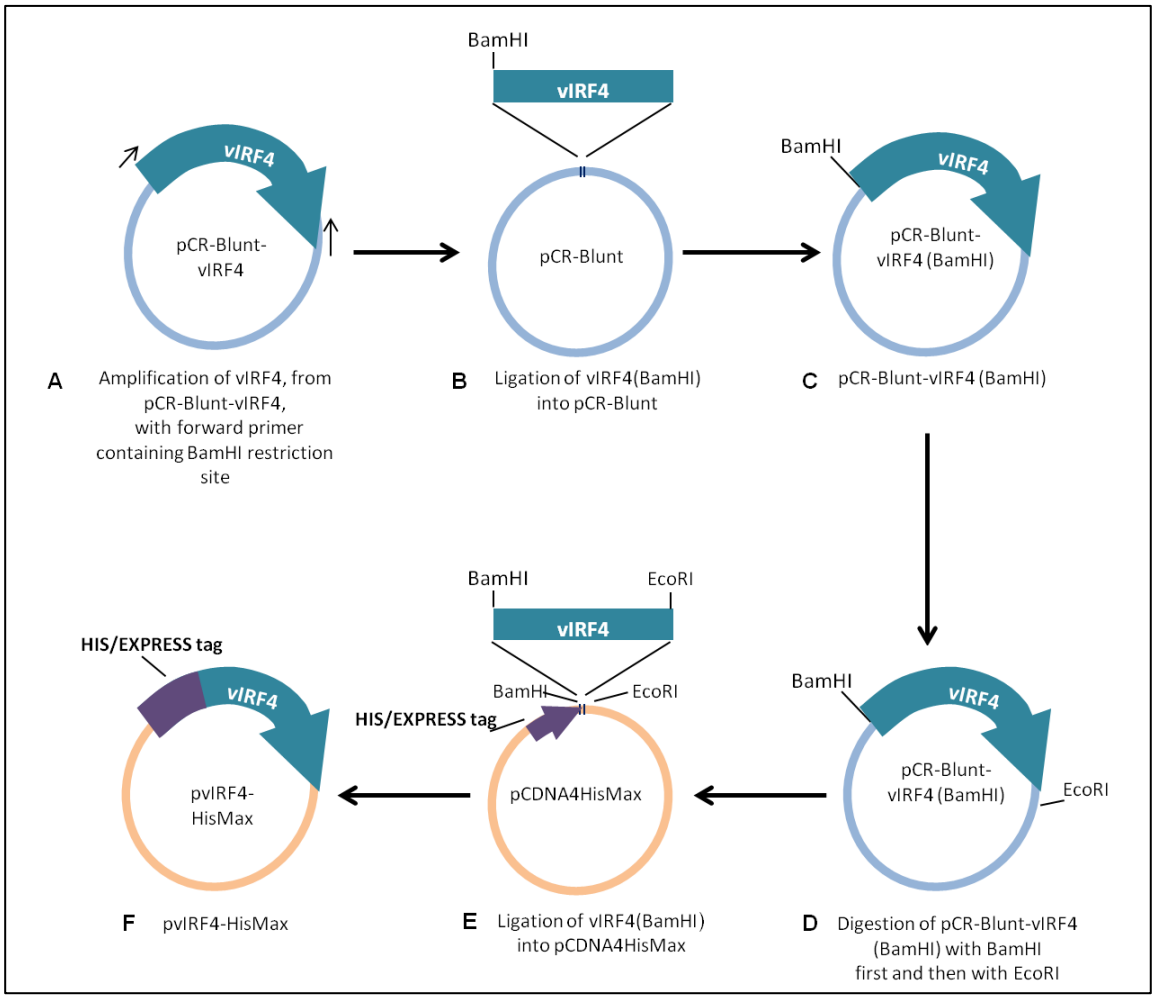

Figure 7.1: Cloning the vIRF4 gene into the pcDNA4/HisMax vector.

(A) vIRF4 was amplified from pCR-Blunt-vIRF4 with primers (see Table 2.14) and cloned into pCR-Blunt (B), to produce pCR-blunt-vIRF4(BamHI) (C) The vIRF4 fragment was then excised from the pCR-Blunt-vIRF4(BamHI) vector using BamHI and EcoRI (D) and this was ligated into pcDNA4/HisMax (E) to produce pcvIRF4-HisMax (F).

7.2.1. Ribosomal proteins

41% of proteins identified as binding to vIRF2 and 52% for vIRF4 were ribosomal proteins (Table 6.1 and Table 6.2 respectively). It was therefore decided that ribosomal interactions with the vIRF2 or vIRF4 proteins should be confirmed. Sections 6.6.3.1 and 6.6.3.2 explain why interactions with two of the ribosomal proteins (RPS3 and RPS6) were selected to be investigated first.

7.2.1.1. RPS3 immunoprecipitation

293 cells transfected with the pcDNA4/HisMax, pvIRF2-HisMax or pvIRF4-HisMax vectors, were lysed and immunoprecipitation was performed using the anti-Xpress antibody. This antibody binds to the Xpress-epitope tag, encoded by pvIRF2-HisMax and pvIRF4-HisMax vectors. To determine if RPS3 was binding to vIRF2 or vIRF4 the immunoprecipitate was analysed by western blot using the anti-RPS3 antibody. Figure 7.2A shows that RPS3 was detected in the input lysates (Figure 7.2A input row) and the positive control (Figure 7.2A lane 9) but RPS3 was not detected in the output immunoprecipitates from vIRF2 or vIRF4 transfected cells (Figure 7.2A lane 3-6, in the RPS3 output row). Therefore, RPS3 did not immunoprecipitate with vIRF2 or vIRF4.

7.2.1.2. RPS6 immunoprecipitation

Immunoprecipitation was performed as in section 7.2.1.1 however, the immunoprecipitates were analysed by western blot using the anti-RPS6 antibody. Figure 7.2B shows the results of this experiment. As for RPS3, RPS6 did not associate with either vIRF2 or vIRF4 as there are no RPS6 positive bands in the

immunoprecipitate samples containing either vIRF2 or vIRF4 (Figure 7.2B lane 3-6, in the RPS6 output row).

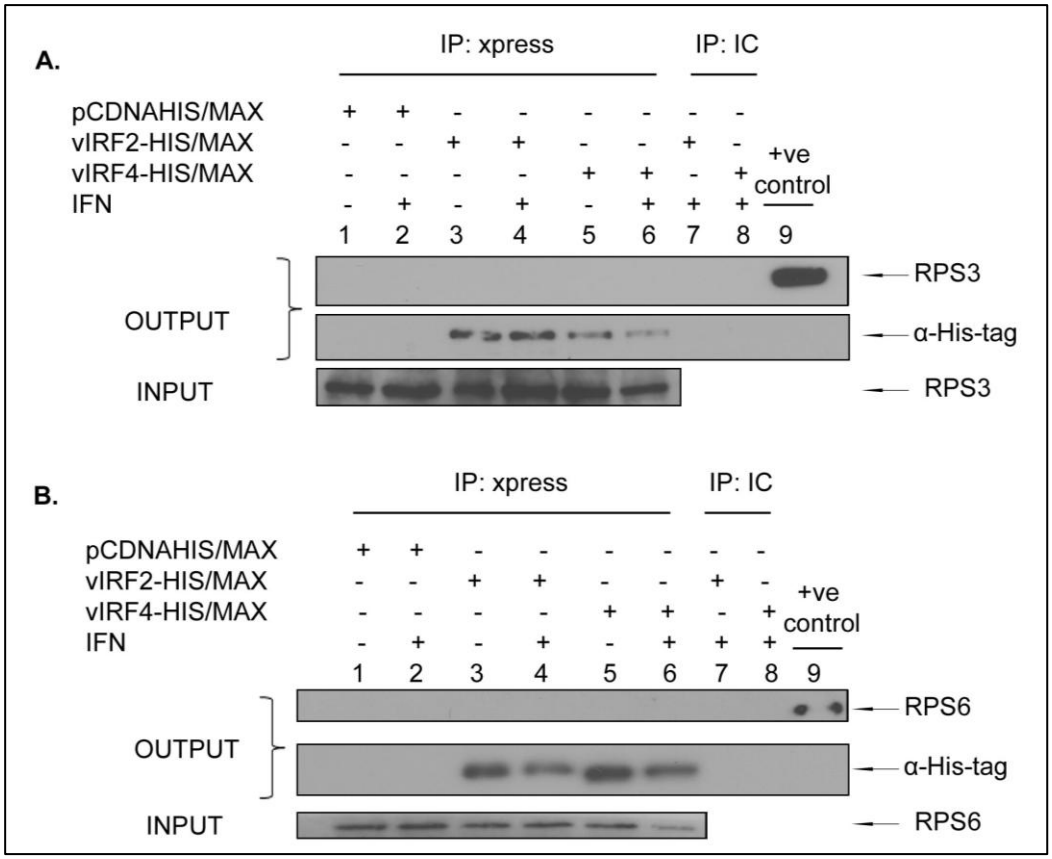

Figure 7.2: vIRF2 and vIRF4 do not associate with either RPS3 or RPS6.

Co-immunoprecipitation studies were performed with lysates of 293 cells that had been transiently transfected with the pcDNA4/HisMax, pvIRF2-HisMax or pvIRF4-HisMax expression plasmids (1000ng) and treated with or without rIFNα (300IU/ml). vIRF2 or vIRF4 were immunoprecipitate with anti-Xpress monoclonal antibody (IP: xpress) or the mouse IgG isotype control (IP:IC) (see section 2.4 for details). The isotype control antibody controlled for non specific binding to regions of the antibody. Immunoprecipitates were analysed by western blotting. The anti-His antibody detected the vIRF2 and vIRF4 proteins expressed from the pvIRF2-HisMax or pvIRF4-HisMax vectors respectively. The anti-RPS3 (A) or anti-RPS6 (B) antibodies were used to detect the respective ribosomal proteins. As a positive control for these proteins, 293 cell lysates were run in parallel (+ve control). The inputs to the immunoprecipitation were analysed by western blot using the RPS3 (A) or RPS6 (B) antibodies to show that RPS3 or RPS6 were present. These experiments were repeated, and the results are shown in Figure 9.25

7.2.1.3. Polysome profiling

The results described in sections 7.2.1.1 and 7.2.1.2 show that based on immunoprecipitation experiments, in contrast to the SILAC-MS experiments, RPS3 and RPS6 were not found to associate with vIRF2 or vIRF4. However, many ribosomal proteins were identified as potential binding partners in chapter 6. The RPS3 and RPS6 proteins were chosen because of reasons outlined in sections 6.6.3.1 and 6.6.3.2. One feature of using immunoprecipitation and SILAC mass spectrometry to characterize the interactome of protein, is that as well as direct interactions, this approach enables the identification of entire complexes which may be interacting with the target protein. Because so many ribosomal proteins were identified in chapter 6, it was unlikely that vIRF2 or vIRF4 were binding directly with all of these. One explanation for identifying so many ribosomal proteins is that the viral proteins were interacting with a specific ribosomal protein(s) which recruited the rest of the complex. Therefore, polysome profiling experiments were performed to investigate if vIRF2 or vIRF4 interact with any ribosomal proteins at all.

These polysome profiling experiments were designed to investigate whether either vIRF2 or vIRF4 can associate with ribosomal subunits, either actively translating (polysomes) or not (monosomes), and were performed by Dr. Nicolas Locker. Monosome and polysome fractions can be resolved by layering cytoplasmic extracts, from the stable cell lines, onto sucrose gradients and performing analytical sedimentation. The polysomes are multiple translation-competent 80S ribosome complexes translating a single mRNA (Masek et al., 2011). As these

form heavier complexes, they are found in the more dense fractions (fractions 6-10). Conversely, single ribosomal subunits that are not translation-competent are found in the less dense fractions (fractions 2/3 for the 40S subunit, fractions 4/5 for the 60S subunit and 80S complexes) (Masek et al., 2011).

Cytoplasmic extracts from the stable cell lines treated with rIFNα were separated on a sucrose gradient allowing the separation of the heavy actively translating mRNAs which contain the polysomes, from the light monosomal mRNAs that are inactive. If either vIRF2 or vIRF4 associate with ribosomes, they should also be eluted in these fractions. Each fraction was analysed by western blot for the presence of vIRF2-NTAP or vIRF4-NTAP and also for the ribosomal protein L5 as a positive control. The results show that EV-NTAP, vIRF2-NTAP and vIRF4-NTAP were found mainly in fractions 1-2 (Figure 7.3 A, B and C, lanes 1 and 2), which suggests that vIRF2 and vIRF4 are not associating with ribosomes. In the case of vIRF2, there are small amounts found in fractions 3, 4 and perhaps 5 (Figure 7.3B, lanes 3-5), however, in the EV control samples, trace amounts of the NTAP protein are also found in fractions 3 and 4 (Figure 7.3A, lanes 3-5). These data suggest that the presence of these NTAP proteins is simply due to bleed through due to their high levels of expression in the cell lines. The results confirm the immunoprecipitation studies that neither vIRF2 nor vIRF4 associate with ribosomes.

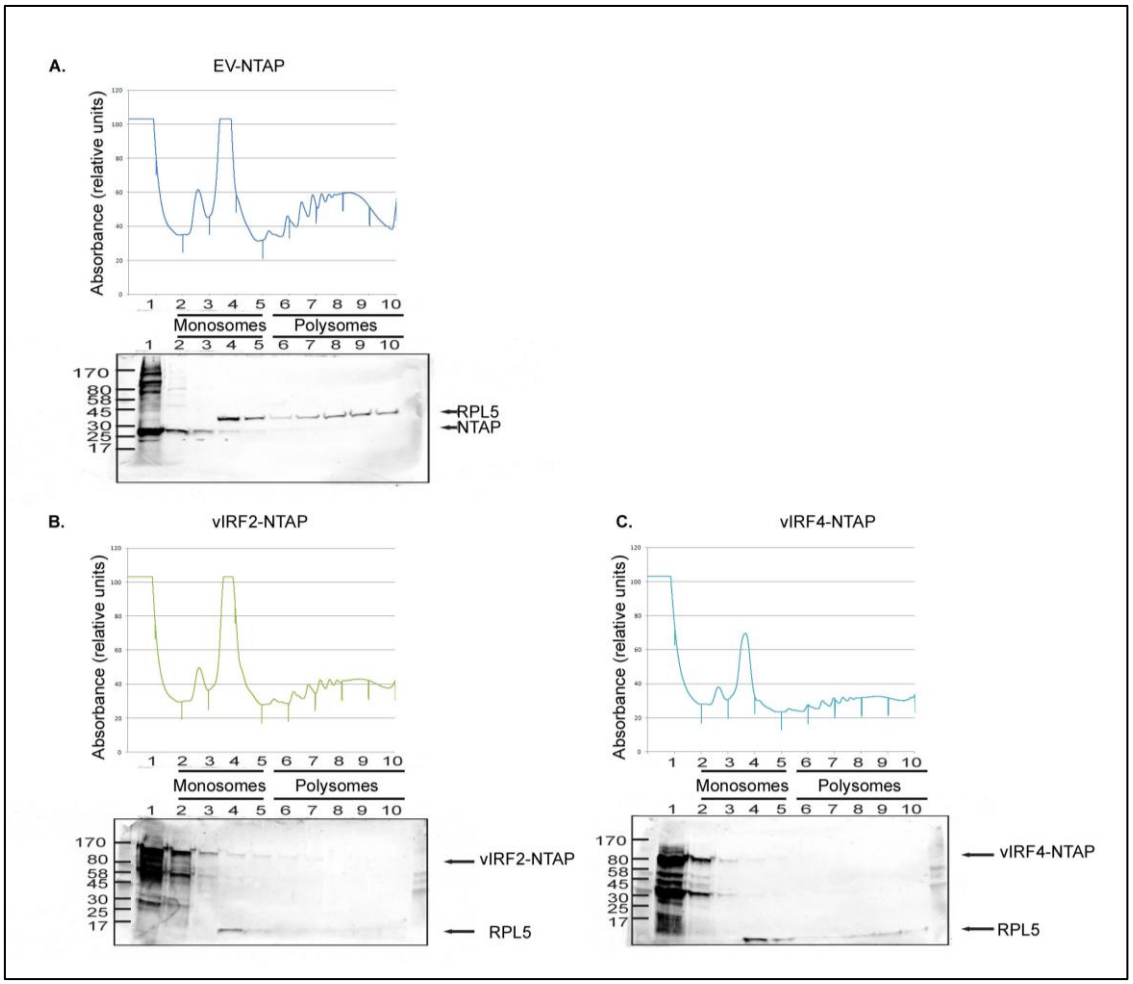

Figure 7.3: The polysome profiles of the stable cell lines suggest there is no interaction between either vIRF2 or vIRF4 and ribosomes.

The EV-NTAP, vIRF2-NTAP and vIRF4-NTAP cell lines were treated with tetracycline (0.125µg/ml) for 24 h and then with 300IU/ml rIFNα for a further 24 hours. Cytoplasmic extracts were collected and polysome profiling was performed (as described in methods section 2.12). The results show the polysome trace for each cell line (upper panel of each figure). The fractions collected were analysed by western blot for the NTAP-tagged proteins (using anti-mouse HRP secondary antibody) and for the L5 ribosomal protein (lower panel of each figure). These data were provided by Dr Nicolas Locker (University of Surrey).

7.3. USP7 immunoprecipitation

USP7 was predicted as a binding partner for both vIRF2 and vIRF4 in chapter 6. Other groups have shown that vIRF4 can associate with USP7 (Lee et al 2011). There has been no published link between vIRF2 and USP7. Immunoprecipitation experiments were performed to validate the interactions of either vIRF2 or vIRF4 with USP7. Immunoprecipitation was performed as in section 7.2.1.1, with the immunoprecipitates being analysed by western blot with the anti-USP7 antibody. Figure 7.4 shows the result of this experiment. USP7 was detected in the immunoprecipitates from pvIRF2-HisMax and pvIRF4-HisMax transfected cells, both with and without rIFNα treatment (Figure 7.4, lanes 3-6, see USP7 output row). These results confirm the SILAC data that vIRF2 and vIRF4 interact with USP7.

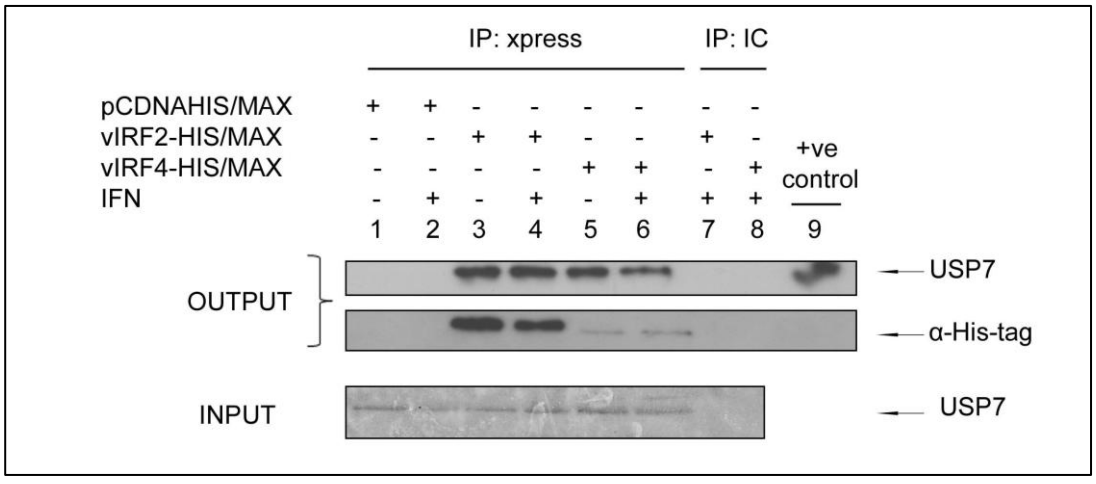

Figure 7.4: vIRF2 and vIRF4 associate with USP7.

Co-immunoprecipitation studies were performed as described in Figure 7.2. The immunoprecipitates were analysed by western blot using the anti-His antibody to detect the vIRF2 and vIRF4 proteins and the anti-USP7 antibody to detect USP7. As a positive control for these proteins, 293 cell lysates were run in parallel (+ve control). The lysates for the immunoprecipitations were analysed by western blot to show that USP7 was present. This experiment was repeated and the results are shown in Figure 9.26.

7.4. USP7 inhibitor studies

Since vIRF2 and vIRF4 bind to USP7, it was hypothesised that USP7 may have a role in IFN signalling. Due to time constraints, this possibility could not be investigated fully, and so one main experiment was performed. The USP7 inhibitor P22077 (R&D) inhibits USP7 activity. It was hypothesised that if USP7 had a role in IFN signalling, then inhibition of USP7 may augment JAK-STAT signalling. Therefore luciferase reporter assays were performed in the presence and absence of the USP7 inhibitor to examine its effect on the ISRE-containing reporter activity.

7.4.1. Confirming that the USP7 inhibitor works

In order to confirm the activity of the USP7 inhibitor, the levels of RAD18 were examined. A decrease in USP7 activity leads to a decrease in the levels of RAD18 (Zlatanaou and Stewart et al, unpublished data). 293 cells were treated with or without the USP7 inhibitor over time (0-72 hours) and the levels of RAD18 were analysed by western blot. The results show that RAD18 levels decreased after 48 and 72 hours of USP7 inhibitor treatment (Figure 7.5 compare lane 1 with lanes 3 and 4). Based on these results, DLAs were performed to examine JAK-STAT signalling following USP7 inhibitor treatment for 48 hours.

7.4.2. Examining the effect of inhibition of USP7 on ISRE-containing promoter activity

To investigate the effect of inhibiting USP7 activity on JAK-STAT signalling, ISRE-reporter assays were performed. 293 cells were co-transfected with the ISRE-containing promoter and the constitutively expressing *Renilla* pRLSV40 plasmid.

Five hours later the cells were treated with or without P22077. Twenty four hours later, the cells were treated with or without rIFNα and DLA were performed a further 24 hours later. The results show that following treatment with the USP7 inhibitor, ISRE-containing promoter activity was reduced by 66% compared to those cells not treated with inhibitor (Figure 7.6 compare columns 4 and 2). However, this decrease was not found to be statically significant, due to the variability of values between experiments (see appendix Figure 9.28).

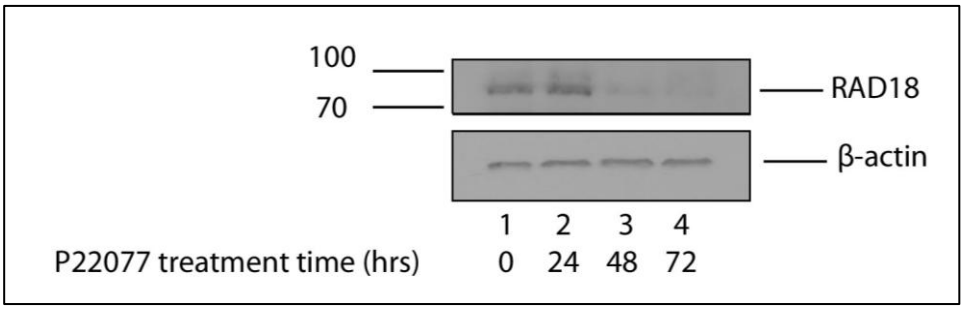

Figure 7.5: RAD18 levels are reduced after 48 hours of treatment with the USP7 inhibitorP22077.

293 cells were treated with P22077 (25µM) for times indicated in the figure. The cells were lysed and analysed by western blot using the anti-RAD 18 antibody (see Table 9.3). Probing for β-actin confirmed equal loading. This experiment was repeated and the results are shown in Figure 9.27

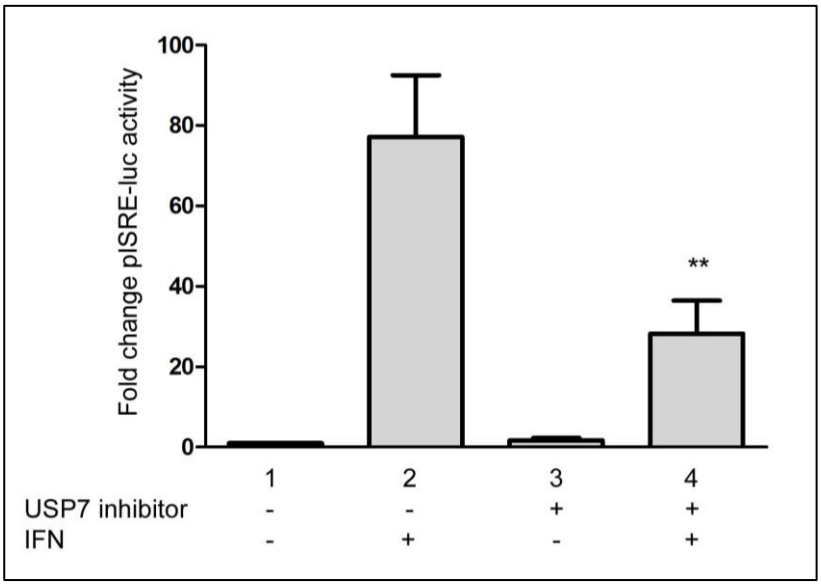

Figure 7.6: Investigating the effects of USP7 inhibitor treatment on JAK-STAT signalling.

293 cells were transfected with pISRE-luc (250ng) and the pRLSV40 plasmid (1ng) 5 hours post transfection, the cells were treated with P22077 (25µM), or mock treated, for 24 hours. rIFNα (300U/ml) was then added and cells were left for a further 24 hours. Cells were harvested and DLA performed. The pRLSV40 plasmid was added as an internal control to which firefly luciferase levels were normalised. The results are shown as fold increase compared to the 293 cells which were un-treated with the USP7 inhibitor and untreated with rIFNα (lane 1). The data represent the mean ± the SEM of the four independent experiments (shown in Figure 9.28).

7.5. p300 immunoprecipitation

In chapter 6, p300 was identified as a putative binding partner of vIRF2, but not vIRF4. vIRF2 has been previously identified as binding p300 (Burysek et al., 1999b). Because vIRF4 was predicted to bind to CBP, and because of the close sequence similarity between p300 and CBP, it was hypothesised that vIRF4 may bind to p300, even though the mass spectrometry did not detect this. Immunoprecipitation was therefore performed to confirm if the results in chapter 6 were correct. Immunoprecipitation was performed as in section 7.2.1.1, but the immunoprecipitates were analysed by western blot with the anti-p300 antibody. The results show that p300 immunoprecipitated with vIRF2 in the presence and absence of rIFNα (Figure 7.7 lanes 3 and 4, see output p300), but did not immunoprecipitate with vIRF4 (Figure 7.7 lanes 5 and 6, see output p300). These findings confirm the predictions made by mass spectrometry.

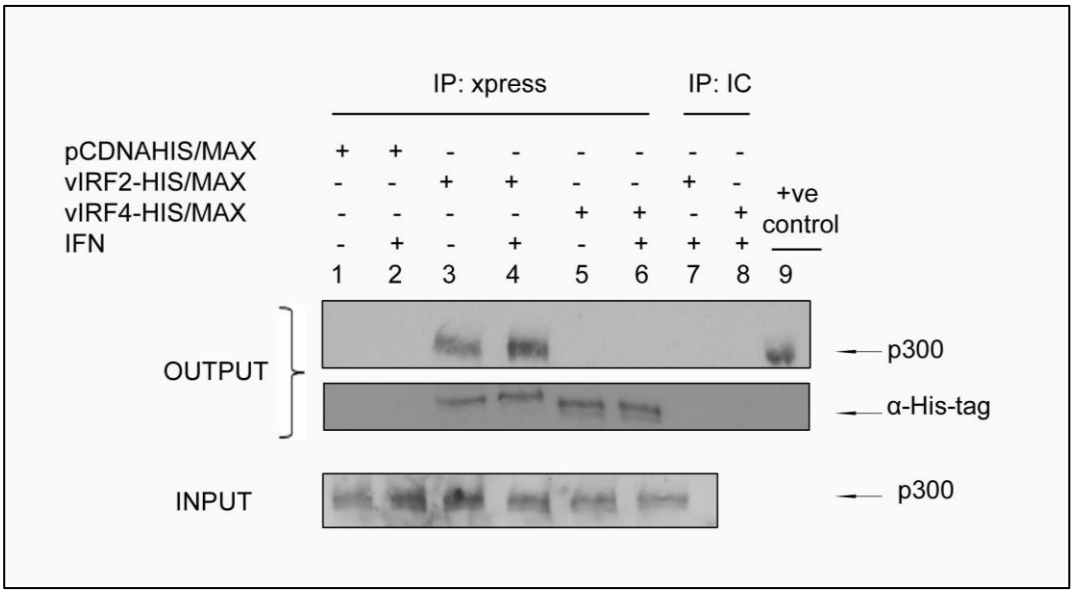

Figure 7.7: vIRF2 but not vIRF4 associates with p300.

Co-immunoprecipitation studies were performed as described in Figure 7.2. The immunoprecipitates were analysed by western blot using the anti-His antibody to detect the vIRF2 and vIRF4 proteins and the anti-p300 antibody to detect p300. As a positive control for these proteins, 293 cell lysates were run in parallel (+ve control). The inputs to the immunoprecipitation were analysed by western blot using the p300 antibody to show that p300 was present. This experiment was repeated and the results are shown in Figure 9.29

7.6. CBP immunoprecipitation

Chapter 6 identified CBP as a potential binding partner for vIRF2 and vIRF4. Other groups have shown this to be true for vIRF2 (Burysek et al., 1999b). There have been no reports on the association of vIRF4 with CBP. Therefore, to verify the mass spectrometry studies, co-immunoprecipitation experiments were performed for CBP and vIRF4. It was not possible to detect endogenous CBP in 293 cells by western blotting (data not shown). Therefore, a CBP expression plasmid was transfected into 293 cells along with the pcDNA4/HisMax, pvIRF2-His/Max or pvIRF4-His/Max vectors and immunoprecipitation was performed as described in section 7.2.1.1. The immunoprecipitates were analysed by western blot using the anti-CBP antibody. The results show that CBP immunoprecipitated with vIRF2 and vIRF4 in the presence or absence of rIFNα (Figure 7.8 lanes 3-6, see output CBP row). The same results were observed in each of the three repeat experiments (see appendix Figure 9.30). These data confirm the predictions made from the mass spectrometry studies.

7.7. CBP immunofluorescence

Section 7.6 confirmed the mass spectrometry data concerning binding of either vIRF2 or vIRF4 to CBP. Next, colocalisation experiments were performed to determine if the physical association of the proteins could be visualised by immunofluorescence and confocal microscopy.

293 cells were transfected with the pcDNA4/HisMax, pvIRF2-His/Max or pvIRF4-His/Max vectors and the CBP-GFP vector. Immunofluorescence staining was then

performed to identify the vIRF2 and vIRF4 proteins using the anti-Xpress antibody, while the GFP-epitope tag expressed contiguously with CBP served to identify this protein.

The results show that both vIRF2 and vIRF4 co-localise with CBP (Figure 7.9). In pvIRF2-His/Max transfected cells, the vIRF2 protein was found in both a cytoplasmic and nuclear location (Figure 7.9, see the 'Xpress tag column' of row 'pvIRF2-HisMax'). When in the nucleus, vIRF2 co-localised with CBP-GFP (Figure 7.9, see row 'pvIRF2-HisMax'). In pvIRF4-HisMax transfected cells, vIRF4 was found predominantly in the nucleus, where it also co-localised with the CBP-GFP protein (Figure 7.9, see row 'pvIRF4-HisMax'). The staining for the Xpress-tag was shown to be specific, since as expected there is no staining in the pcDNA4/HisMax transfected cells, which do not express the tag (Figure 7.9, row labelled pcDNA4/HisMax).

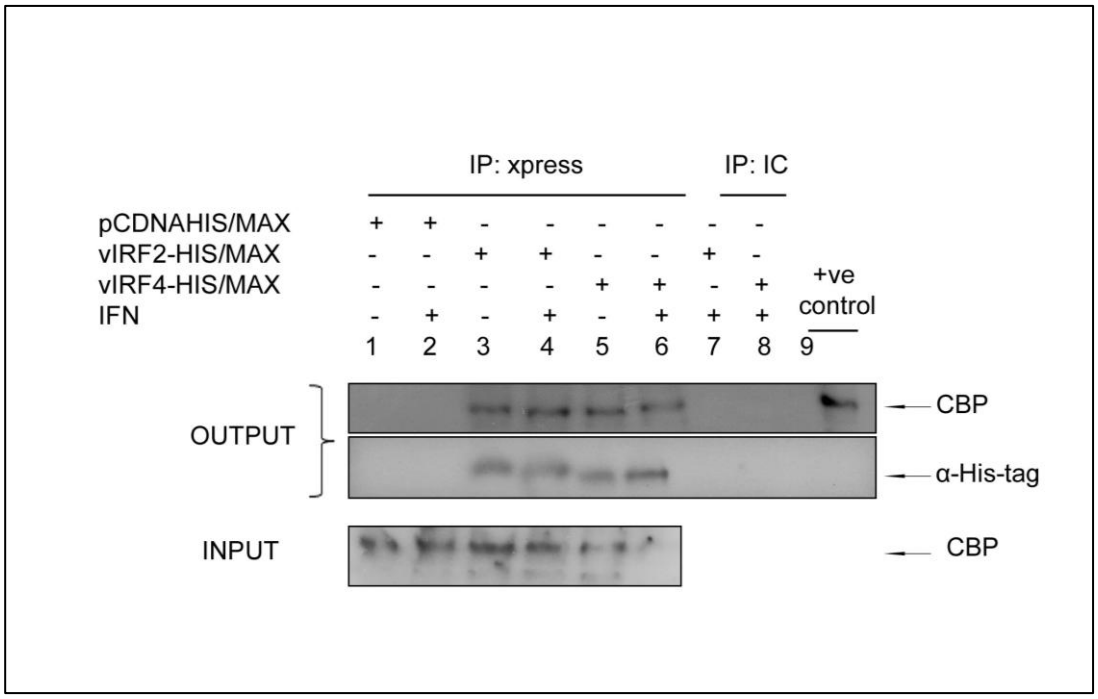

Figure 7.8: vIRF2 and vIRF4 associate with CBP.

Co-immunoprecipitation studies were performed as described in Figure 7.2, except that the CBP-GFP plasmid (see Table 2.12) was transfected into each samples also. The immunoprecipitate extracts were analysed by western blot using the anti-His antibody to detect the vIRF2 and vIRF4 proteins and the anti-CBP antibody to detect CBP. As a positive control for these proteins, 293 cell lysates, transfected with CBP-GFP, were run in parallel (+ve control). The inputs to the immunoprecipitation were analysed by western blot using the anti-CBP antibody to show that CBP was present. This experiment was repeated and the results are shown in Figure 9.30.

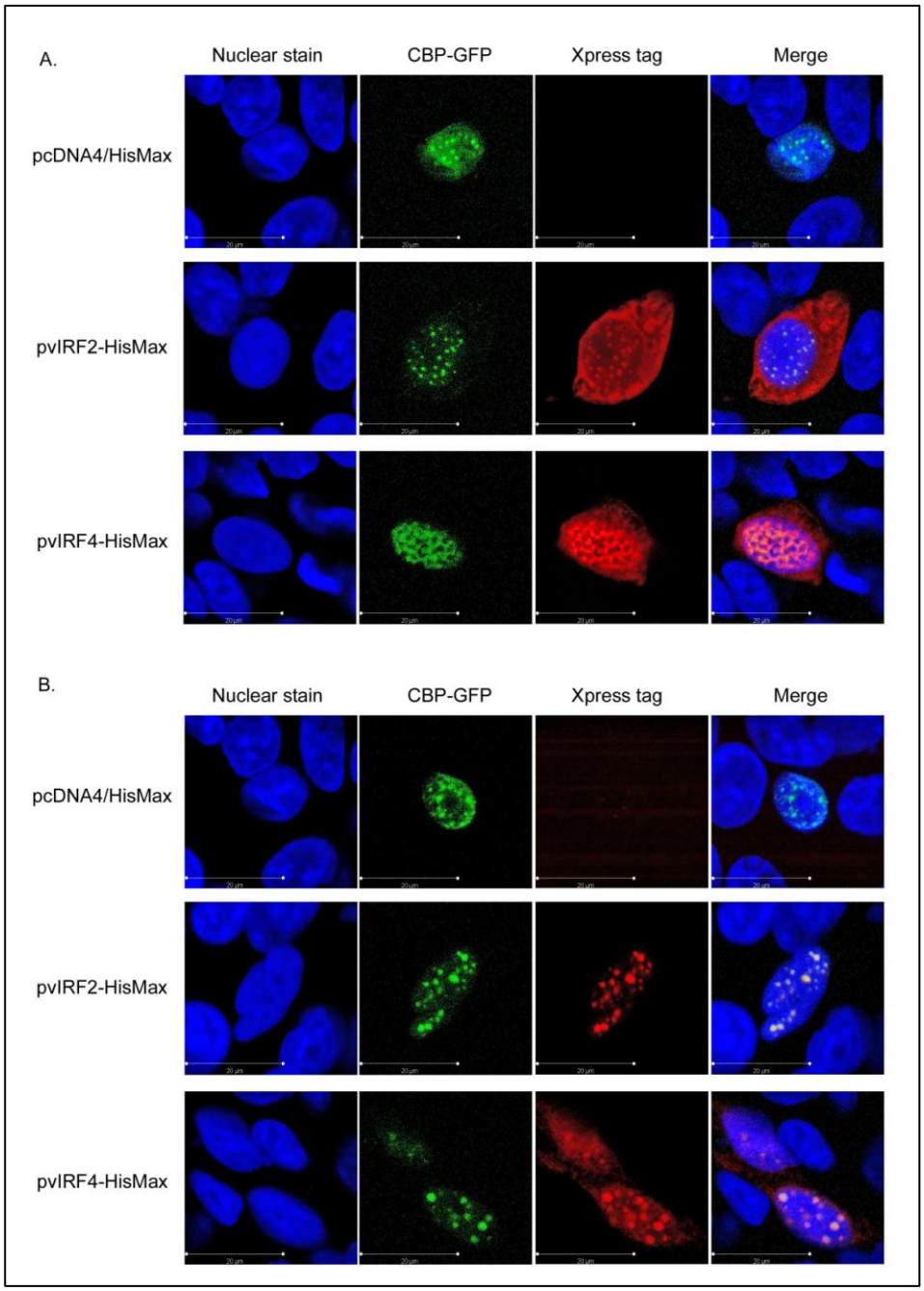

Figure 7.9: Immunofluorescence staining demonstrate that the vIRF2 and vIRF4 proteins bind to CBP.

293 cells were plated on coverslips in 24-well plate and left to adhere overnight. They were then co-transfected with the pcDNA4/HisMax, pvIRF2-HisMax or pvIRF4-HisMax expression plasmids and the CBP-GFP plasmid. After 48 hours, cells were fixed in 4% paraformaldehyde and permeabilized with ice cold methanol (10 minutes). Staining was achieved using the anti-Xpress primary antibody and anti mouse (594) secondary antibody (see

Table 9.4). The CBP protein was expressed contiguous to a GFP-tag, and therefore no staining was necessary to visualise this protein. Nuclear staining was achieved with Bisbenzamide. Results were visualised by confocal microscopy. As

a negative control for the staining of the Xpress-tag, pcDNA4/HisMax transfected cells were used. Cells lacking the CBP-GFP plasmid were used as a negative control (not shown). The cross over of the GFP fluorescence into the red channel, and vice-verse was also assessed to ensure that the staining was not due to photo-leaching between channels (data not shown).A, experiment 1. B, experiment 2.

7.8. Inhibition of de-acetylation does not inhibit the effect of either vIRF2 or vIRF4 on JAK-STAT signalling

An explanation to account for the association of vIRF2 and vIRF4 with CBP was that these viral proteins were inhibiting the activity of CBP. CBP has a number of domains which perform different functions. As CBP exhibits HAT activity, one important function is its ability to acetylate proteins. Therefore, the hypothesis that vIRF2 or vIRF4 were inhibiting CBP acetylation, and thereby inhibiting JAK-STAT signalling was investigated. Histone de-acetylases (HDAC) de-acetylate acetylated lysines and are responsible for reversing the effect of HATs. Sodium Butyrate (NaB) is an inhibitor of HDACs, and therefore inhibits the removal of acetyl groups from lysine residues, resulting in an increase in acetylated proteins. To investigate if an increase in acetylated proteins would inhibit the negative effect of vIRF2 or vIRF4 upon JAK-STAT signalling, luciferase reporter assays were performed in the presence and absence of NaB. Cells were transfected with the ISRE-luc containing promoter and one of the pCDNA4TO-NTAP, pvIRF2-NTAP or pvIRF4-NTAP vectors. They were then treated with or without NaB (1mM, or 5mM for 24 hours) followed by stimulation with rIFNα (24 hours) and dual luciferase measurements were made. The results show that without NaB, vIRF2 inhibited ISRE-containing promoter activity by 53% (Figure 7.10 compare columns 1 and 2), with 1mM NaB, it caused a 63% inhibition (Figure 7.10 compare columns 4 and 5), and with 5mM NaB it led to a 66% reduction (Figure 7.10 compare columns 7 and 8). Whilst there does seem to be a small increase in the level of inhibition with increasing amounts of NaB, it was not significant and therefore it can be concluded that NaB does not affect the level of inhibition of ISRE-containing promoter activity caused by vIRF2. In the case of vIRF4, the level of inhibition of

ISRE-containing promoter activity without NaB was 32% (Figure 7.10 compare columns 1 and 3), with 1mM NaB, it caused a 37% inhibition (Figure 7.10 compare columns 4 and 6), and with 5mM NaB a 31% reduction was observed (Figure 7.10 compare lanes 7 and 9). Again, these effects are not statistically different, leading to the same conclusion as for vIRF2, therefore it can be concluded that NaB does not affect the inhibition of ISRE-containing promoter activity caused by vIRF4.

To confirm that NaB was inhibiting HDAC activity, 293 cells were treated with NaB (1mM, or 5mM) or left untreated. These lysates were analysed by western blot for acetylated lysines and the results show there is an increase in lysine acetylation with 1mM NaB, and a further increase following 5mM NaB treatment (Figure 7.11 compare lanes 1, 2 and 3). This indicates that NaB is inhibiting HDAC activity, and thus increasing the amount of acetylated proteins.

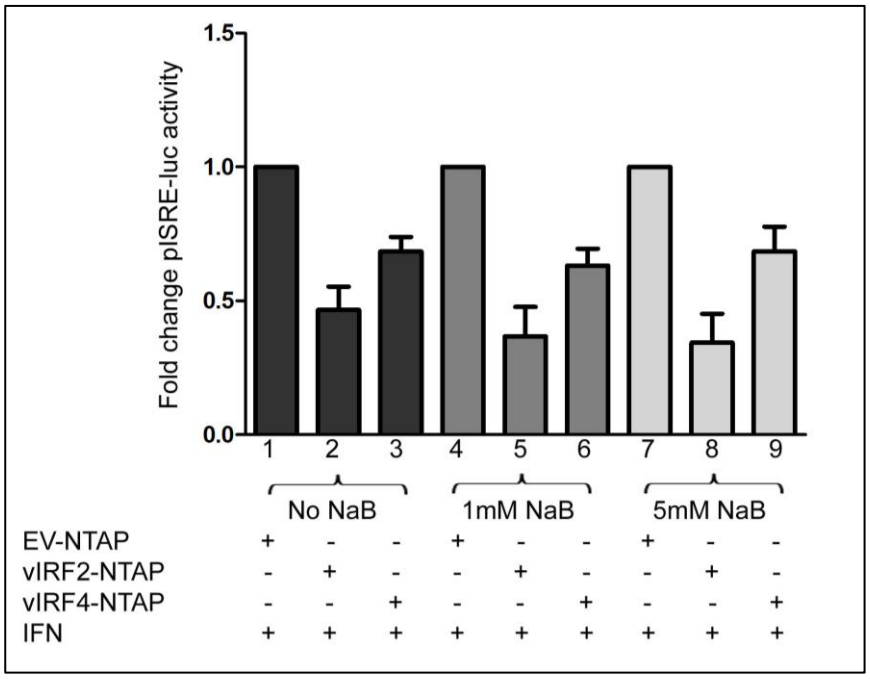

Figure 7.10: NaB does not rescue inhibition of ISRE-reporter activity by vIRF2 and vIRF4 proteins.

293 cells were transfected with pISRE-luc (250ng) and the pRLSV40 plasmid (1ng) and one of the pCDNA4TO-NTAP, pvIRF2-NTAP or pvIRF4-NTAP vectors. 5 hours post transfection, the cells were cultures in DMEM complete medium. 24 hours later, the cells were treated with rIFNα (300U/ml) and with NaB and harvested 24 hours later. The pRLSV40 plasmid was added as an internal control to which firefly luciferase levels were normalised. For each condition (No NaB, 1mM NaB and 5mM NaB) the results shown have been normalised to the EV-NTAP transfected cells in order to identify if the reduction in ISRE-containing promoter activity by vIRF2 of vIRF4 changes. The data represent the mean ± the SEM of three independent experiments. The level of inhibition caused by either vIRF2 or vIRF4 was compared without NaB and with the two concentrations of NaB, and the differences were not found to be significantly different. The three individual experiments are shown in Figure 9.31.

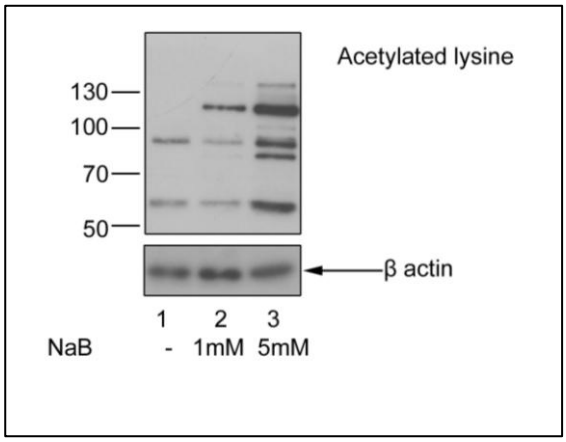

Figure 7.11: Treatment of 293 cells with NaB increases the level of acetylated proteins.

293 cells were treated with NaB (as indicated in figure) for 24 hours. Lysates were then analysed by western blot using the anti-acetylated-lysine antibody (see Table 9.3). Probing for β-actin indicated equal loading.

7.9. Discussion

In chapter 6, the putative interactomes of vIRF2 and vIRF4 were described. Five of these proteins were selected for further study in the present chapter (RPS3, RPS6, USP7, p300 and CBP). One aim of the present chapter was to independently validate the SILAC results, in respect of those five selected cellular proteins, by either immunoprecipitation or immunofluorescence assays. If interactions were confirmed by these techniques, these proteins were studied more closely, with the aim of identifying the significance of any interactions in the context of either the vIRF2 or vIRF4 mediated inhibition of JAK-STAT signalling. In this discussion, the results for each of the five cellular proteins selected for further study in will be considered.

7.9.1. Investigating the interaction of vIRF2 and vIRF4 with ribosomal proteins

As outlined in section 6.6.3, many of the predicted interacting partners for vIRF2 and vIRF4 were ribosomal proteins, and therefore, they were identified for further study. Since investigation of each ribosomal protein identified was not possible in the time frame available, two ribosomal proteins were chosen for further study. Based on their reported links to type I IFN signalling, these were RPS3 and RPS6 (see sections 6.6.3.1 and 6.6.3.2 for explanations of why these were chosen).

To validate the SILAC results for these proteins, immunoprecipitation experiments were performed on cells transfected with vIRF2 or vIRF4 expression vectors. The results show that neither RPS3 nor RPS6 were present in vIRF2 or vIRF4

immunoprecipitates, suggesting that RPS3 and RPS6 do not interact with the viral proteins (Figure 7.2).

As so many ribosomal proteins were identified as interactome components in chapter 6, it was hypothesised that the vIRF2 and vIRF4 proteins were interacting with a specific ribosomal protein(s) which then recruited the rest of the ribosomal complex. The results in chapter 6 therefore may have revealed both direct and indirect interactions. One way in which to distinguish between such interactions would be to perform immunoprecipitations under varying salt concentrations. Higher salt concentrations result in more stringent conditions, and thus only direct interactions would be identified, whereas lower salt concentrations would reveal indirect interactions. However, this solution is not practical when so many ribosomal proteins need to be assessed. Therefore, polysome profiling experiments were performed to validate if vIRF2 or vIRF4 were interacting with ribosomes.

The results of the polysome profiling showed that neither vIRF2 nor vIRF4 associated with ribosomes (Figure 7.3). These results support the immunoprecipitation studies performed in this chapter, which did not identify RPS3 or RPS6 as binding partners for vIRF2 of vIRF4 (Figure 7.2); it does not support the SILAC pull down results from chapter 6. Two possible explanations to account these conflicting results are discussed below.

1) There are no interactions between either vIRF2 and vIRF4 and ribosomal proteins: This conclusion supports the results performed in the present chapter, but would mean that the SILAC pull down results were incorrect. The SILAC predictions for ribosomal proteins were based on these proteins having a ≥ 2 fold SILAC ratio in the vIRF2-NTAP or vIRF4-NTAP cells compared to the NTAP expressing cells. However, this 2 fold SILAC ratio was generally the case in only 1 experiment out of the 3 performed (see Table 6.1 and Table 6.2). Therefore, it could be proposed that since the predictions were based on just 1 out of 3 experiments, the SILAC data concerning ribosomal proteins are not very reliable. Thus, rather than these cellular proteins being specific partners of the viral proteins, they were eluted from the vIRF2 of vIRF4 pull down through non-specific interactions. However, it should be noted in this regard that these ribosomal proteins are not overly abundant cellular proteins (see section 6.6.3).

2) There are interactions between either vIRF2 and vIRF4 and ribosomal proteins: The statement would support the SILAC results but would mean that the results obtained in this chapter were incorrect. This conclusion is unlikely to be true, because, as discussed above the conclusions made from the SILAC results were based on only 1 out of 3 replicates. The immunoprecipitation and western blotting for RPS3 and RPS6 were performed twice for each protein (Figure 7.2 and Figure 9.25), and show the same result. As a further positive control, a protein which bound to either RPS3 or RPS6 could be included if this experiment was performed again. The polysome profiling was only performed once. Ideally, to ensure the validity of these data, the polysome profiling should be repeated, but due to time

constraints, and the fact that it was performed by a collaborator, it was not possible.

In summary, it seems unlikely that either vIRF2 or vIRF4 bind to or interact with ribosomal proteins. This result highlights the need to confirm SILAC pull down data by additional methods, to verify the validity of interaction partners. The ribosomal proteins were chosen for validation because of the exciting possibilities that their binding could lead to new mechanisms of virus control of gene expression post-transcriptionally. However since, taken together, the results suggest that no interactions are taking place between vIRF2 and vIRF4, ribosomal interactions will not be investigated further.

7.9.2. Investigating the interaction of vIRF2 and vIRF4 with USP7

The mass spectrometry results in chapter 6 predicted that USP7 is an interaction partner for both vIRF2 and vIRF4. In the case of vIRF4, this association has been described previously (Lee et al., 2011) (see sections 1.5.4 and 6.6.2). Thus these findings validate the SILAC pull down results for vIRF4 and USP7. This chapter has shown that both vIRF2 and vIRF4 can bind to USP7 (Figure 7.4), and in the case of vIRF2 this has not been reported previously. These experiments were performed independently a total of three times (see Figure 9.26 for replicates).

Since both vIRF2 and vIRF4 bind to USP7, and because vIRF2 and vIRF4 share the function of inhibiting JAK-STAT signalling, it was hypothesised that USP7

could have played a role in JAK-STAT signalling. The KSHV-encoded RTA protein has been shown to bind to USP7 (Yu and Hayward, 2010), and these authors suggested USP7 may be involved in inhibiting type I IFN through its stabilisation of RAUL (see section 6.6.2 for more details). These studies concern the effect of USP7 on the IFN production pathway, which is an earlier stage in type I IFN signalling than the JAK-STAT signalling pathway, the pathway which was the focux of this thesis is mainly interested. The effect of USP7 on the JAK-STAT signalling pathway therefore remains to be discovered.

ISRE-containing luciferase reporter assays were performed in the presence or absence of the USP7 inhibitor, P22077. The data in Figure 7.6 show that treatment with P22077 resulted in inhibition of ISRE-containing promoter activity, but this reduction was not found to be significant. However, this non-significance is thought to be due to variations between replicates. Nevertheless, the suggestion of inhibition of JAK-STAT signalling was un-expected, since active USP7 is thought to inhibit the IFN production pathway (Yu and Hayward, 2010). The results in this chapter show that inhibiting USP7 activity may downregulate the JAK-STAT signalling pathway, indicating that USP7 activity regulates type I IFN signalling in different ways. The results also suggest that active USP7 may have some role in JAK-STAT signalling. Due to time constraints, no further experiments could be performed to follow up on this result, but a number of future studies can be proposed:

1) siRNA knockdown of USP7: This approach would provide an alternative to reducing USP7 function, and thereby provide further evidence for the conclusion that inhibition of USP7 causes a reduction in JAK-STAT signalling.

2) Overexpression of USP7 could be performed to determine if it would lead to increased JAK-STAT signalling.

3) If USP7 was confirmed to be important in JAK-STAT signalling, it should be identified if vIRF2 or vIRF4 can inhibit USP7 function. Possible mechanisms for this include the degradation of USP7, inhibition of its activity or out-competing other substrates binding to it.

4) USP7 is responsible for the de-ubiquitination of p53 (Li et al., 2002) and of MDM2 (Cummins and Vogelstein, 2004). This alters the stability of these proteins, which in turn could have numerous downstream effects. It is necessary to assess the possibility that the inhibitory effect on JAK-STAT signalling, with P22077, is due to changes in either MDM2 or p53 levels, or down-stream components. This would identify more specifically where in the MDM2/p53 pathway the inhibitory effect on JAK-STAT signalling is resulting from. To achieve this, siRNAs could be used to specifically knock down MDM2/p53, or an excess of MDM2/p53 could be transfected into cells, followed by ISRE-luc based luciferase reporter assays.

Overall, the effect of inhibiting USP7 activity on JAK-STAT signalling needs further work to explain the molecular mechanism. However, the possibility remains that vIRF2 or vIRF4 could be acting through USP7 to modulate JAK-STAT signalling.

7.9.3. CBP and p300

The CBP and p300 proteins were chosen to be validated as interaction partners of vIRF2 and vIRF4, and these results will be discussed in the following sections.

CBP and p300 contain a high level of sequence homology and share a number of functional domains. Both the N- and the C-terminal regions of p300/CBP can activate transcription, while the central regions have HAT activity. The cystidine-histidine rich domains (CH1, CH2, CH3), KIX domains, and the SRC1 interaction domain (SID) domains are important in mediating protein-protein interactions. The bromodomain (BD) is important for recognising acetylated residues (reviewed in Chan and La Thangue., (2001)). These domains and the percentage homology between the CBP and p300 proteins are illustrated in Figure 7.12.

Both CBP and p300 are important regulators of RNA pol II mediated transcription. They have HAT activity, and acetylate histones H2A, H3B, H3 and H4. This activity neutralises positively charged lysine residues, modifying the interactions between DNA and histone to enable the DNA to be accessible to activators of transcription (reviewed in Kalkhoven (2004)). CBP and p300 can interact with the basal transcription complexes (TBP and Transcription factor IIB (TFIIB)) and RNA

polymerase II through their activation domains (Figure 7.12) and to other transcription factors, through their CH1, CH2, CH3, KIX and SID domains (Figure 7.12). These interactions stabilise the transcription complex, enabling successful gene transcription (reviewed in Kalkhoven (2004)).

7.9.3.1. Investigating the interaction of vIRF2 and vIRF4 with P300

The results in chapter 6 identified p300 as a predicted binding partner for vIRF2. This interaction has been reported in the literature previously (Burysek et al., 1999b). vIRF4 was not predicted by SILAC-MS pulldown to associate with p300, but it was predicted to associate with CBP, which has a high level of homology to p300 (Figure 7.12). Therefore, the hypothesis that vIRF4 may also bind to p300 was investigated. This work was to complement experiments examining the association of vIRF4 and CBP, thereby identifying if the interaction of vIRF4 was specific to only CBP, or could be extended to p300. The results of immunoprecipitation experiments revealed that as expected vIRF2 interacted with p300. However, vIRF4 was not found to associate with p300 (Figure 7.7). This result confirms the SILAC pull down analysis. It is interesting that vIRF4 does not associate with p300, but does associate with CBP, as these proteins have very similar functions and are highly homologous. However, one explanation for these negative results, is that vIRF4 could be causing degradation of p300, and thus even if there was an association between vIRF4 and p300, pull downs and immunoprecipitations could not detect p300. To test this theory, levels of p300 could be quantified, by western blot, in cells expressing vIRF4 and compared to those lacking it. Nevertheless, because vIRF4 was not found to associate at all

with p300 in the SILAC pull down in chapter 6, or in the immunoprecipitation experiments performed in the present chapter, it seems unlikely that vIRF4 interacts with p300.

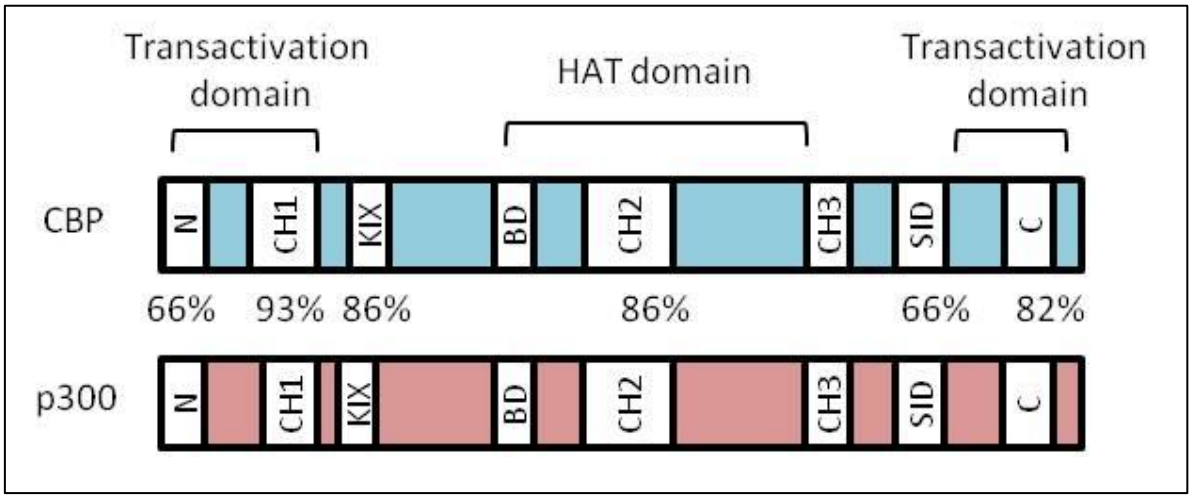

Figure 7.12: Homologous regions of CBP and p300.

The regions of homology are indicated and the percentage similarity between CBP and p300 within these regions is shown. Figure redrawn, but based on (Giles et al., 1998).

7.9.4. Investigating the interaction of vIRF2 and vIRF4 with CBP

CBP was identified as a predicted interaction partner for both vIRF2 and vIRF4 in chapter 6. The interaction between vIRF2 and CBP has been previously reported in the literature (Burysek et al., 1999b). CBP has also been reported to interact with vIRF1, leading to inhibition of the formation of IRF3-CBP-DNA complexes, and therefore inhibiting the activation of IFN promoters (Lin et al., 2001). Additionally, vIRF3 interacts with CBP, but its role in IFN signalling is unclear (Lubyova et al., 2004, Joo et al., 2007). Since vIRF4 was predicted to interact with CBP, and because vIRF1, vIRF2 and vIRF3 have all been shown to interact with this cellular protein, the interaction of vIRF4 with CBP was validated.

Immunoprecipitation experiments showed that CBP was identified in vIRF4 immunoprecipitates (Figure 7.8). Since the interaction of vIRF2 with CBP has previously been reported (Lin et al., 2001), it provided a positive control for the experiment, and as expected, was found to associate with CBP (Figure 7.8). This experiment was performed a total of three times, to ensure reliability of the results (Figure 9.30). Additionally, immunofluorescence assays revealed that both vIRF2 and vIRF4 co-localised with CBP (Figure 7.9). The immunofluorescence experiments were important as they showed that vIRF2 and vIRF4 associate with CBP in whole cells and that their association in immunoprecipitation experiments is not an artefact of mixing of proteins from different cellular compartments during cell lysis.

Since the association of the vIRF2 and vIRF4 proteins with CBP has been confirmed by three different means (SILAC-MS, immunoprecipitation and immunofluorescence), these interactions are considered genuine. The effect of these associations on JAK-STAT signalling was next investigated. Based on the information in the literature, a number of hypotheses were proposed which link the vIRF2/vIRF4-CBP interactions with downregulation in JAK-STAT signalling. These will be discussed sequentially.

7.9.4.1. vIRF2 or vIRF4 compete with STAT2 to bind CBP, which reduces the ability of STAT2 to transactivate ISGs.

Bhattacharya et al (1996) showed that CBP/p300 interacts with STAT2 through the C-terminal 83 amino acids of STAT2 at and the CH1 domain of CBP. This domain of STAT2 is vital for transcriptional activation by ISGF3 (Qureshi et al., 1996). Since STAT2 provides the essential transcriptional activation domain of ISGF3 (Bluyssen and Levy, 1997) the STAT2-CBP/p300 interaction is thought to be important in the transactivation of ISGs. The Adenovirus E1A protein, which inhibits JAK-STAT signalling and binds to CBP/p300 (Kalvakolanu et al., 1991), exerts this inhibition through its association with CBP/p300 by inhibiting STAT2 transactivation (Bhattacharya et al., 1996). Similarly, Zhang et al., (2008) found that the Human T-cell leukaemia virus type 1 (HTLV-1) Tax protein could inhibit the transactivation of STAT2 by binding to CBP. The binding of Tax to CBP/p300 was necessary for its inhibition of JAK-STAT signalling, and increasing amounts of Tax decreased the STAT2-p300 interactions. They therefore concluded that Tax

inhibits IFNα stimulated JAK-STAT signalling through competing with STAT2 for binding to CBP/p300 and inhibiting the transactivation of STAT2.

Since there is precedence for the inhibition of JAK-STAT signalling by competing with STAT2 to bind CBP, this hypothesis was investigated in the context of vIRF2 and vIRF4. To assess this theory, ISRE-luciferases assays were performed in the presence or absence of excess CBP, and the inhibitory effect of vIRF2 and vIRF4 on JAK-STAT signalling was measured. However, the results of these experiments proved inconclusive. The experiments performed lacked a negative control plasmid for the CBP-GFP, and thus no real conclusions could be drawn from the results. No further experiments could be performed due to time constraints. Additional experiments to assess the importance of CBP in the inhibition of JAK-STAT signalling by vIRF2 or vIRF4 or to investigate the theory that vIRF2 or vIRF4 disrupts CBP-STAT2 interactions are discussed below.

1) Appropriate negative control plasmids for CBP should be obtained, and the luciferase experiments described above would be performed to generate consistent data.

2) The effect of excess CBP on ISG mRNA could be analysed in the presence of either vIRF2 or vIRF4. If excess CBP increased the levels of ISG mRNA, it would suggest that the interaction between the viral proteins and CBP is necessary for inhibition of ISG transcription.

3) Identify if binding to CBP is necessary for inhibition of JAK-STAT signalling. The region of vIRF2, and if possible vIRF4 which binds to CBP should be identified. The vIRF2 truncated mutants (described in chapter 3, section 3.8) could be used in immunoprecipitation experiments to identify which regions of vIRF2 can bind to CBP. Fragments of vIRF4 could be produced and the same experiments performed. These results could then be related back to ISRE-luciferase assays involving the mutants (Figure 3.14 in the case of vIRF2, not performed for vIRF4). If there was a correlation between ability to bind CBP and ability to inhibit ISRE-containing promoter activation, then the importance of the interaction of these viral proteins with CBP could be appreciated. Note: since vIRF4 does not bind to p300, but does bind to CBP, it is hypothesised that vIRF4 is binds to CBP at a region which is not found in p300.

4) Identify if the presence of vIRF2 or vIRF4 reduces the binding of STAT2 to CBP/p300. Lysates from vIRF2 or vIRF4 expressing cells could be immunoprecipitated with CBP and the amount of STAT2 pulled down with CBP could be quantified. If reduced in the presence of vIRF2 or vIRF4, then this finding will suggest that interaction of the viral proteins with CBP reduces the CBP/p300-STAT2 complex formation, and may explain a mechanism of action.

5) Identify the region of CBP which binds to vIRF2 and vIRF4. CBP truncated mutants could be used to identify the region which is binding to vIRF2 and

vIRF4, to provide information on how this interaction may lead to a reduction on IFN signalling. For example, if either vIRF2 or vIRF4 bound to the CH1 domain of CBP, it could be proposed that the viral protein inhibits the interaction of CBP with STAT2, since STAT2 also bind CBP at the CH1 domain. Burysek et al., (1999b) have shown that vIRF2 binds to the C-terminal half of CBP/p300, however the specific location within this has not been determined.

6) Perform immunofluorescence assays to identify if the presence of vIRF2 or vIRF4 inhibits binding of CBP to STAT2.

7.9.4.2. vIRF2 or vIRF4 inhibit CBP HAT activity and thus inhibit IFN signalling.

Another possibility for the association of vIRF2 and vIRF4 with CBP is that these viral proteins inhibit the acetylating activity of CBP. The role of acetylation in STAT signalling has become increasingly appreciated. Tang et al., (2007) showed that IFNαR2 recruits CBP, which then acetylates the receptor. This recruits IRF9, leading to the formation of the ISGF3 complex. STAT1 and STAT2 are also acetylated by CBP, and in the case of IRF9 and STAT2, this acetylation has been shown to be critical for activation of ISGs (Tang et al., 2007). Therefore, the hypothesis that vIRF2 or vIRF4 were inhibiting CBP acetylation, and thereby inhibiting JAK-STAT signalling was investigated.

HDACs deacetylate acetylated lysines, conversely, HDAC inhibitors reverse this leading to an accumulation of acetylated lysines. In Tang et al., (2007), a HDAC inhibitor increased CBP mediated acetylation of IFNαR2. Therefore the effect of the HDAC-inhibitor, NaB on the inhibition of JAK-STAT signalling by vIRF2 or vIRF4 was assessed. The results showed that NaB could not counteract the inhibition of JAK-STAT signalling caused by vIRF2 or vIRF4 (Figure 7.10), suggesting that vIRF2 or vIRF4 do not inhibit the acetylation function of CBP. In these results, addition of HDAC actually led to a decrease in ISRE activity (Figure 9.31). This result is not unprecedented, in Nusinzon et al, (2003) it was shown that inhibition of HDAC activity decreased the IFNα stimulated innate antiviral response. They found that deacetylase activity led to positive transcriptional regulation of IFN responsive genes. These results seem to contradict the general correlation of HDAC activity with transcriptional repression. Overall, it seems that the dynamic relationship between deacetylases and acetylases in JAK-STAT signalling is complex and requires more study.

7.9.4.3. vIRF2 or vIRF4 cause a reduction in the levels of CBP, which leads to a reduction in ISRE activity

Sections 7.9.4.1 and 7.9.4.2 have described how CBP is an important component of JAK-STAT signalling. Therefore, vIRF2 and vIRF4 could simply be reducing levels of CBP to bring about an inhibition of JAK-STAT signalling. To identify if vIRF2 or vIRF4 caused a reduction in CBP levels, western blot quantification of this cellular protein could be performed. However, as reported in the results

section 7.6, endogenous CBP could not be detected in 293 cells. Due to time, constraints an alternative solution to this problem was not possible.

7.9.4.4. Summary of CBP investigations

In summary the results of this chapter have validated the interaction between vIRF2 and CBP, and provided the novel finding that vIRF4 also associates with CBP. This means that all the KSHV-encoded vIRF proteins associate to CBP, suggesting that the interactions between the viral proteins and CBP are of functional importance. Indeed, in the case of vIRF1, this interaction has been shown to be in part responsible for the inhibition of the IFN production pathway (Lin et al., 2001). The future experiments detailed in this discussion provide ways in which to determine the importance of CBP interactions with either the vIRF2 or vIRF4 proteins in the context of JAK-STAT signalling.

7.9.5. Summary of chapter

Overall this chapter has shown that interactions between either vIRF2 or vIRF4 and ribosomal proteins are unlikely. However, this chapter has also validated the interactions between USP7 and vIRF2 or vIRF4. This result led to the discovery that a USP7 inhibitor reduces JAK-STAT signalling. Finally, the interactions between either vIRF2 or vIRF4 and CBP have been confirmed and experiments to investigate the significance of such interactions have been proposed.

CHAPTER 8

DISCUSSION

8.1. Summary of findings in relation to previous studies

The broad aims of this thesis were to identify if and how the vIRF2 and vIRF4 proteins mediate type I IFN signalling. Studies in the Blackbourn laboratory have shown that vIRF2 downregulates the IFN production pathway and the JAK-STAT signalling pathways (Areste et al., 2009, Fuld et al., 2006, Mutocheluh et al., 2011). However in the case of the JAK-STAT signalling pathway, the molecular mechanisms remain unclear. Prior to this thesis, only one study had examined the effect of vIRF4 upon type I IFN signalling. In that study, the authors assessed the ability of vIRF4 to inhibit SEV-mediated IFNβ promoter activation, and found no effect (Kanno et al., 2006). There have been no reports of the effect of vIRF4 on the later JAK-STAT signalling pathway. Hence, one of the aims of this thesis was to investigate the effect of vIRF4 on both the IFN production pathway, to verify the findings of Kanno et al, (2006) and the JAK-STAT signalling pathway.

Chapter 3 detailed the cloning of the vIRF4 gene into the NTAP expression vector and its subsequent expression in 293 cells. This chapter confirmed previous observations made by Kanno et al, (2006) that vIRF4 could not downregulate the IFN production pathway, and thus it differs from vIRFs 1-3 in this respect. The experiments described in this thesis used the synthetic dsRNA, poly(I:C), to activate IRF3 signalling while the experiments performed by Kanno et al, (2006) used SEV infection to activate IRF3. SEV is an RNA virus, and it will therefore trigger RNA sensors to activate IFNβ promoter activity. However, as described in section 1.4.5, there exist DNA sensors which can also activate IFNβ promoter activity (see Figure 1.6) Since KSHV is a DNA virus, KSHV is likely to encode a

protein which inhibits DNA-mediated activation of type I IFN promoters and therefore, vIRF4 may only inhibit DNA-mediated IFNβ promoter activation. The synthetic DNA, Poly(dA:dT) could be used to activate DNA sensors as it is recognised by DAI and RNA polymerase III (Takaoka et al., 2007, Ablasser et al., 2009, Chiu et al., 2009). Such experiments would reveal if vIRF4 can specifically downregulate DNA sensing pathways. It must be noted that even though KSHV is a DNA virus, it will most likely also result in the presence of dsRNA, and (Weber et al., 2006) have shown that DNA virus infection leads to dsRNA production. Nevertheless, this thesis clearly shows that vIRF4 has no effect on the RNA-mediated activation of the IFN production pathway.

Importantly, chapter 3 also demonstrated that vIRF4 could inhibit the IFNα-mediated activation of ISRE-containing promoters. This is a novel result and it shows for the first time that like the other vIRFs, vIRF4 is able to downregulate the innate immune system.

The effect of vIRF4 upon JAK-STAT signalling was investigated in more detail and in chapter 4, inducible, stable cell lines expressing either the vIRF2 or vIRF4 proteins were produced. These cells lines were characterised, in order to ensure that they expressed vIRF2 or vIRF4 and were tested for their ability to modulate type I IFN signalling. As expected, cells expressing vIRF2 could downregulate the IFN production pathway, whereas those expressing vIRF4 could not. Both vIRF2 and vIRF4 could inhibit JAK-STAT signalling, confirming the results in chapter 3.

Chapter 5 utilised these stable cell lines to begin to examine mechanistically the function of vIRF2 and vIRF4. As a biological read-out, the ability of either vIRF2 or vIRF4 to rescue the titre of the IFN-sensitive EMCV virus was assessed. In line with previous reports from our group (Mutocheluh et al., 2011), vIRF2 could rescue EMCV titre following IFN treatment, indicating a biologically relevant effect of this KSHV protein on IFN signalling. In the case of vIRF4, no rescue of EMCV titre was observed. Section 5.6 provides suggestions and speculation as to why this could be the case. However, this result suggests that the vIRF4 protein, expressed in vIRF4-NTAP cells, is not having as potent an effect on IFN signalling as vIRF2. These results suggest that vIRF2 and vIRF4 have different mechanisms of action.

EMSA experiments, examining the effect of the viral proteins on ISGF3:ISRE binding revealed that both vIRF2 and vIRF4 could significantly inhibit the formation of this complex. This result is novel, and shows that the viral proteins are specifically inhibiting the binding of the ISGF3 complex to ISREs. It suggests that the point in the pathway at which the viral proteins are operating is prior to ISGF3 binding to the ISRE sequence. This result provides conformation for the reporter genes assays showing the inhibitory effect of vIRF2 or vIRF4 on JAK-STAT signalling.

Since experiments performed in our laboratory showed that vIRF2 could reduce levels of pSTAT1 (Mutocheluh et al., 2011) we sought to verify this finding, while at the same time assessing vIRF4 for its ability to alter levels of ISGF3

components. Western blot analysis revealed that as expected vIRF2 decreases levels of pSTAT1. However expression of vIRF4 did not affect levels of any of the ISGF3 components. This finding suggests that vIRF4 exhibits its anti-IFN by activities other than modulating levels of the ISGF3 components.

In chapter 6, the vIRF2 and vIRF4 interactomes were identified using SILAC-MS. In the case of vIRF2, it was hypothesised that this approach might identify whether vIRF2 interacts with ISGF3 components directly, thereby accounting for the reduction of pSTAT1 levels. Additionally, the SILAC-MS approach was hypothesis to reveal a possible further mechanism of vIRF2-mediated JAK-STAT inhibition. For vIRF4, this approach was undertaken to identify any cellular partners which might explain the inhibition of JAK-STAT signalling.

Based on these results, five possible binding partners which were common to both vIRF2 and vIRF4 were selected for validation and further study. These proteins were RPS3, RPS6, USP7, p300 and CBP. Chapter 7 provided validation of these interactions, and showed that RPS3 and RPS6 did not interact with either of the viral proteins. p300 only interacted with vIRF2 whereas USP7 and CBP interacted with both vIRF2 and vIRF4. The interaction between vIRF4 and USP7 has been previously reported (Lee et al., 2011), and has been linked to a decrease in levels of the tumour suppressor, p53. USP7 can deubiquitinate p53, increasing its stability and vIRF4 may inhibit this. Thus the data verify a previously published observation, validating the integrity of the SILAC-MS approach. The association between vIRF2 and USP7 is a novel result, and may implicate vIRF2 in the control

of p53. Then, like the other KSHV-encoded vIRFs, vIRF2 may have tumourigenic properties via its effect on p53 levels. It must be noted that this concept is currently speculation, and further experiments are necessary to determine this hypothesis.

To assess the possible significance of interactions between either USP7 or CBP and vIRF2 or vIRF4, these proteins were taken forward for further study. The deubiquitylating USP7 enzyme was hypothesised to have an effect on IFN signalling. To examine this theory, the effect of the USP7 inhibitor, P22077, upon JAK-STAT signalling was assed in ISRE-containing luciferase assays. The results revealed that this inhibitor decreased ISRE-containing promoter activity, suggesting that active USP7 has a role in JAK-STAT signalling. As described in section 7.9.2, more experiments are necessary to confirm this hypothesis. However, if validated it is plausible that either vIRF2 or vIRF4 may have evolved to target USP7 in order to downregulate IFN signalling. For example, these viral proteins may inhibit USP7 activity, or prevent it binding to substrates.

Due to the validation of interactions between vIRF4 and CBP, it can now be concluded that all the KSHV vIRFs bind to this cellular HAT. This is a novel result. Because acetylation of JAK-STAT signalling components has proved critical in successful activation of ISGs (Tang et al., 2007), it was proposed that vIRF2 or vIRF4 may suppress CBP HAT activity in order to inhibit JAK-STAT signalling. To examine this possibility, an inhibitor of HDAC activity was used to increase levels of acetylated proteins and investigate if this can counteract the inhibitory effect of

the viral proteins. This experiment revealed that inhibiting HDAC had no effect on the level of inhibition caused by vIRF2 or vIRF4, suggesting that these viral proteins do not target the HAT activity of CBP in order to downregulate JAK-STAT signalling. Additional work is therefore required to elucidate possible mechanisms of vIRF2 and vIRF4 mediated JAK-STAT signalling inhibition via CBP.

Possible ways in which vIRF2 and vIRF4 could target CBP in order to inhibit JAK-STAT signalling are covered in sections 7.9.4.1, 7.9.4.2 and 7.9.4.3. These include either inhibiting the ability of CBP to acetylate STAT2 or IRF9, which is necessary for ISG activation (Tang et al., 2007), or reducing levels of CBP in the cell. Due to time constraints, these possibilities were not investigated. However, suggestions for future experiments have been provided in the discussion to chapter 7, sections 7.9.4.1, 7.9.4.2 and 7.9.4.3.

A summary of the conclusions of this thesis are as follows:

1) The vIRF2 protein inhibits both IFN production and JAK-STAT signalling pathways.
2) The vIRF4 protein inhibits the IFNα-mediated activation of ISRE-containing promoters, but does not inhibit poly(I:C)-mediated activation of the IFNβ promoter.
3) Both vIRF2 and vIRF4 decrease the binding of the ISGF3 complex to ISRE sequences

4) vIRF2 reduces levels of pSTAT1, whereas vIRF4 does not affect levels of this or the other ISGF3 components
5) vIRF2 and vIRF4 associate with USP7, and this interaction may have relevance in the inhibition of JAK-STAT signalling caused by these viral proteins.
6) vIRF2 and vIRF4 associate with CBP, and this interaction may have relevance in the inhibition of JAK-STAT signalling caused by these viral proteins.

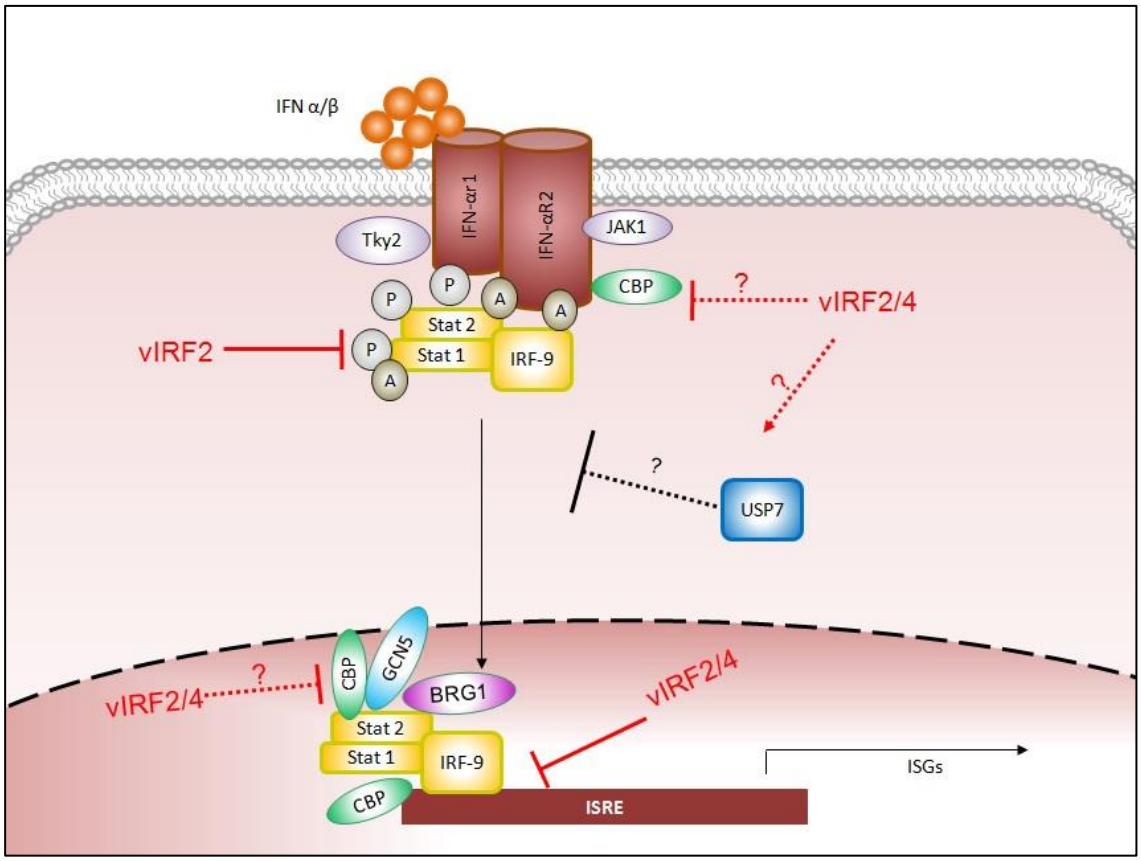

Figure 8.1: Proposed inhibition of the JAK-STAT signalling pathway by vIRF2 and vIRF4.

Upon activation of the IFN receptors by type I IFNs, a signalling cascade is evoked which results in the translocation of the ISGF3 complex into the nucleus. Here, it binds to ISRE consensus sequences and activates the transcription of ISGs. This thesis confirmed that vIRF2 inhibited levels of pSTAT1, as shown in the figure. This thesis has also shown for the first time that vIRF2 and vIRF4 inhibit binding of the ISGF3 to ISRE sequences in the nucleus. Other hypothesised mechanisms of action involved vIRF2 and vIRF4 binding to CBP to inhibit either the association of CBP with ISGF3 components or activation of ISGs. Alternatively, the viral proteins could reduce levels of CBP in the cells. USP7 has also been linked to JAK-STAT signalling in this thesis and the viral protein may augment the activity of this protein.

Throughout this thesis the vIRF proteins were ectopically expressed in cells in order to examine their effect on type I IFN signalling. This enabled the specific effect of the individual vIRF proteins upon type I IFN signalling to be examined. This strategy is common in the study of individual proteins but the limitations for drawing conclusions are appreciated. In KSHV infection these viral proteins could be working in combination, or their effects could be either amplified or diminished due to the effects of other viral proteins. Additionally, since KSHV genes are expressed in a temporal manner in lytic infection, these proteins may have varying effects at different time points. To assess the inhibitory effect of vIRF2 and vIRF4 on type I IFN signalling in a more physiologically relevant system, their levels could be knocked down in KSHV infected cells.

About a quarter of the KSHV genome encodes proteins with immunomodulatory functions or potential. The importance to KSHV of inhibiting ISGF3 and JAK-STAT signalling is highlighted by the number of proteins it encodes which suppress this pathway (see sections 1.5 and 1.5.5). These proteins act in different manners to inhibit the detection of viral components by the cells, and are hypothesised to act at different stages during the KSHV lifecycle. Work in this thesis confirmed and investigated the vIRF2-mediated inhibition of JAK-STAT signalling. It revealed that vIRF2 can inhibit levels of pSTAT1, but does not seem to bind directly either to this component, or to any ISGF3 components. How it decreases levels of pSTAT1 therefore remains to be identified.

Importantly, this thesis has identified that the vIRF4 protein can target the JAK-STAT signalling pathway to inhibit activation of ISRE-containing promoters. The vIRF4 protein can therefore be included as an inhibitor of type I IFN signalling. vIRF2 and vIRF4 both bind to CBP, as protein which has been implicated in both the IFN production pathway and JAK-STAT signalling. It is hypothesised that vIRF2 and vIRF4 may exert their anti-IFN effects thought this protein, and further experiments are necessary to confirm this. Finally, work for this thesis has suggested the possible role of the USP7 protein in regulating JAK-STAT signalling, something which is currently un-reported. Again, further work is necessary to examine this hypothesis.

vIRFs have only been found in one other virus to date, namely RRV, one of the closest relatives to KSHV. RRV encodes 8 vIRFs. In experiments aiming to understand the role of these RRV encoded vIRFs, Robinson et al., (2012a) produced a recombinant RRV virus which lacked all 8 vIRFs. When used to infect a number of cell types *in vitro*, this vIRF knockout virus resulted in increased levels of both type I and type II IFN production compared to that in the WT recombinant virus infected cells (Robinson et al., 2012a). This result indicates that the vIRFs in RRV are critical to reducing the levels of IFN production in infected cells. Additionally, this vIRF knockout virus was also used to infect Rhesus macaques *in vivo* and resulted in decreased viral loads, earlier and more sustained production of proinflammatory cytokines as well as an earlier T cell response compared to the WT recombinant virus (Robinson et al., 2012b). Again this result highlights the

importance of the vIRFs and additionally examines the roles of the RRV encoded vIRFs in de novo infection.

The KSHV encoded vIRFs downregulate IFN signalling, as shown both in this thesis and throughout the published literature. KSHV encoded vIRFs also share some homology to the RRV encoded vIRFs. It can therefore be hypothesised that if experiments, such as those in Robinson et al., (2012a) were performed using a KSHV-vIRF knockout virus *in vitro,* an increase in the level of type I IFNs might also be observed when compared to a WT recombinant virus.

Although other viruses don't encoded vIRFs, they can still modulate IFN signalling. EBV, the closest human herpesvirus to KSHV does not encode any vIRFs, however, it encodes other proteins which downregulate the immune response. An example of such proteins are the Latent membrane protein 2A (LMP2A) and LMP2B. These proteins promote the turnover of the IFNARs, which causes a decrease in JAK-STAT signalling (Shah et al., 2009). Additionally, the EBV-encoded small nuclear RNAs (EBERs) can limit the effects of type I IFNs. EBERS bind to PKR and inhibit its phosphorylation leading to resistance to PKR-mediated apoptosis (Nanbo et al., 2002).

As detailed in section 1.4.9, many other viruses also encode proteins which inhibit JAK-STAT signalling. Because of the number of different proteins which evade this the innate immune response, it is clear that it is important step in viral

infection. Studying how viruses, which have evolved with the human immune system, act will provide insights into the mechanisms of a particular virus. Additionally, it may also lead to a deeper understanding of how the human immune system functions.

REFERENCES

ABLASSER, A., BAUERNFEIND, F., HARTMANN, G., LATZ, E., FITZGERALD, K. A. & HORNUNG, V. 2009. RIG-I-dependent sensing of poly(dA:dT) through the induction of an RNA polymerase III-transcribed RNA intermediate. *Nat Immunol,* 10, 1065-72.

AKULA, S. M., NARANATT, P. P., WALIA, N. S., WANG, F. Z., FEGLEY, B. & CHANDRAN, B. 2003. Kaposi's sarcoma-associated herpesvirus (human herpesvirus 8) infection of human fibroblast cells occurs through endocytosis. *J Virol,* 77, 7978-90.

AKULA, S. M., PRAMOD, N. P., WANG, F. Z. & CHANDRAN, B. 2002. Integrin alpha3beta1 (CD 49c/29) is a cellular receptor for Kaposi's sarcoma-associated herpesvirus (KSHV/HHV-8) entry into the target cells. *Cell,* 108, 407-19.

ALEXANDER, L., DENEKAMP, L., KNAPP, A., AUERBACH, M. R., DAMANIA, B. & DESROSIERS, R. C. 2000. The primary sequence of rhesus monkey rhadinovirus isolate 26-95: sequence similarities to Kaposi's sarcoma-associated herpesvirus and rhesus monkey rhadinovirus isolate 17577. *J Virol,* 74, 3388-98.

ALEXOPOULOU, L., HOLT, A. C., MEDZHITOV, R. & FLAVELL, R. A. 2001. Recognition of double-stranded RNA and activation of NF-kappaB by Toll-like receptor 3. *Nature,* 413, 732-8.

ANDREJEVA, J., CHILDS, K. S., YOUNG, D. F., CARLOS, T. S., STOCK, N., GOODBOURN, S. & RANDALL, R. E. 2004. The V proteins of paramyxoviruses bind the IFN-inducible RNA helicase, mda-5, and inhibit its activation of the IFN-beta promoter. *Proc Natl Acad Sci U S A,* 101, 17264-9.

ARESTE, C., MUTOCHELUH, M. & BLACKBOURN, D. J. 2009. Identification of caspase-mediated decay of interferon regulatory factor-3, exploited by a Kaposi sarcoma-associated herpesvirus immunoregulatory protein. *J Biol Chem,* 284, 23272-85.

ASHOUR, J., LAURENT-ROLLE, M., SHI, P. Y. & GARCIA-SASTRE, A. 2009. NS5 of dengue virus mediates STAT2 binding and degradation. *J Virol,* 83, 5408-18.

BALLESTAS, M. E., CHATIS, P. A. & KAYE, K. M. 1999. Efficient persistence of extrachromosomal KSHV DNA mediated by latency-associated nuclear antigen. *Science,* 284, 641-4.

BARESOVA, P., PITHA, P. M. & LUBYOVA, B. 2013. Distinct roles of Kaposi's sarcoma-associated herpesvirus-encoded vIRFs in inflammatory response and cancer. *J Virol*.

BARNARD, P. & MCMILLAN, N. A. 1999. The human papillomavirus E7 oncoprotein abrogates signaling mediated by interferon-alpha. *Virology,* 259, 305-13.

BARNES, B. J., MOORE, P. A. & PITHA, P. M. 2001. Virus-specific activation of a novel interferon regulatory factor, IRF-5, results in the induction of distinct interferon alpha genes. *J Biol Chem,* 276, 23382-90.

BARRO, M. & PATTON, J. T. 2005. Rotavirus nonstructural protein 1 subverts innate immune response by inducing degradation of IFN regulatory factor 3. *Proc Natl Acad Sci U S A,* 102, 4114-9.

BECHTEL, J. T., LIANG, Y., HVIDDING, J. & GANEM, D. 2003. Host range of Kaposi's sarcoma-associated herpesvirus in cultured cells. *J Virol,* 77, 6474-81.

BHATTACHARYA, S., ECKNER, R., GROSSMAN, S., OLDREAD, E., ARANY, Z., D'ANDREA, A. & LIVINGSTON, D. M. 1996. Cooperation of Stat2 and p300/CBP in signalling induced by interferon-alpha. *Nature,* 383, 344-7.

BILLINIS, C., PASCHALERI-PAPADOPOULOU, E., ANASTASIADIS, G., PSYCHAS, V., VLEMMAS, J., LEONTIDES, S., KOUMBATI, M., KYRIAKIS, S. C. & PAPADOPOULOS, O. 1999. A comparative study of the pathogenic properties and transmissibility of a Greek and a Belgian encephalomyocarditis virus (EMCV) for piglets. *Vet Microbiol,* 70, 179-92.

BIRKMANN, A., MAHR, K., ENSSER, A., YAGUBOGLU, S., TITGEMEYER, F., FLECKENSTEIN, B. & NEIPEL, F. 2001. Cell surface heparan sulfate is a receptor for human herpesvirus 8 and interacts with envelope glycoprotein K8.1. *J Virol,* 75, 11583-93.

BISSON, S. A., PAGE, A. L. & GANEM, D. 2009. A Kaposi's sarcoma-associated herpesvirus protein that forms inhibitory complexes with type I interferon receptor subunits, Jak and STAT proteins, and blocks interferon-mediated signal transduction. *J Virol,* 83, 5056-66.

BLUYSSEN, H. A. & LEVY, D. E. 1997. Stat2 is a transcriptional activator that requires sequence-specific contacts provided by stat1 and p48 for stable interaction with DNA. *J Biol Chem,* 272, 4600-5.

BOULON, S., AHMAD, Y., TRINKLE-MULCAHY, L., VERHEGGEN, C., COBLEY, A., GREGOR, P., BERTRAND, E., WHITEHORN, M. & LAMOND, A. I. 2010. Establishment of a protein frequency library and its application in the reliable identification of specific protein interaction partners. *Mol Cell Proteomics,* 9, 861-79.

BOUVARD, V., BAAN, R., STRAIF, K., GROSSE, Y., SECRETAN, B., EL GHISSASSI, F., BENBRAHIM-TALLAA, L., GUHA, N., FREEMAN, C., GALICHET, L. & COGLIANO, V. 2009. A review of human carcinogens--Part B: biological agents. *Lancet Oncol,* 10, 321-2.

BURCKSTUMMER, T., BENNETT, K. L., PRERADOVIC, A., SCHUTZE, G., HANTSCHEL, O., SUPERTI-FURGA, G. & BAUCH, A. 2006. An efficient tandem affinity purification procedure for interaction proteomics in mammalian cells. *Nat Methods,* 3, 1013-9.

BURDETTE, D. L. & VANCE, R. E. 2013. STING and the innate immune response to nucleic acids in the cytosol. *Nat Immunol,* 14, 19-26.

BURYSEK, L. & PITHA, P. M. 2001. Latently expressed human herpesvirus 8-encoded interferon regulatory factor 2 inhibits double-stranded RNA-activated protein kinase. *J Virol,* 75, 2345-52.

BURYSEK, L., YEOW, W. S., LUBYOVA, B., KELLUM, M., SCHAFER, S. L., HUANG, Y. Q. & PITHA, P. M. 1999a. Functional analysis of human herpesvirus 8-encoded viral interferon regulatory factor 1 and its association with cellular interferon regulatory factors and p300. *J Virol,* 73, 7334-42.

BURYSEK, L., YEOW, W. S. & PITHA, P. M. 1999b. Unique properties of a second human herpesvirus 8-encoded interferon regulatory factor (vIRF-2). *J Hum Virol,* 2, 19-32.

CAI, X., LU, S., ZHANG, Z., GONZALEZ, C. M., DAMANIA, B. & CULLEN, B. R. 2005. Kaposi's sarcoma-associated herpesvirus expresses an array of viral microRNAs in latently infected cells. *Proc Natl Acad Sci U S A,* 102, 5570-5.

CHAKRABORTY, S., VEETTIL, M. V. & CHANDRAN, B. 2012. Kaposi's Sarcoma Associated Herpesvirus Entry into Target Cells. *Front Microbiol,* 3, 6.

CHAN, H. M. & LA THANGUE, N. B. 2001. p300/CBP proteins: HATs for transcriptional bridges and scaffolds. *J Cell Sci,* 114, 2363-73.

CHANDRAN, B. 2010. Early events in Kaposi's sarcoma-associated herpesvirus infection of target cells. *J Virol,* 84, 2188-99.

CHANDRIANI, S. & GANEM, D. 2010. Array-based transcript profiling and limiting-dilution reverse transcription-PCR analysis identify additional latent genes in Kaposi's sarcoma-associated herpesvirus. *J Virol,* 84, 5565-73.

CHANG, Y., CESARMAN, E., PESSIN, M. S., LEE, F., CULPEPPER, J., KNOWLES, D. M. & MOORE, P. S. 1994. Identification of herpesvirus-like DNA sequences in AIDS-associated Kaposi's sarcoma. *Science,* 266, 1865-9.

CHEN, Y. B., RAHEMTULLAH, A. & HOCHBERG, E. 2007. Primary effusion lymphoma. *Oncologist,* 12, 569-76.

CHIU, Y. H., MACMILLAN, J. B. & CHEN, Z. J. 2009. RNA polymerase III detects cytosolic DNA and induces type I interferons through the RIG-I pathway. *Cell,* 138, 576-91.

CIANCANELLI, M. J., VOLCHKOVA, V. A., SHAW, M. L., VOLCHKOV, V. E. & BASLER, C. F. 2009. Nipah virus sequesters inactive STAT1 in the nucleus via a P gene-encoded mechanism. *J Virol,* 83, 7828-41.

CLOUTIER, N. & FLAMAND, L. 2010. Kaposi sarcoma-associated herpesvirus latency-associated nuclear antigen inhibits interferon (IFN) beta expression by competing with IFN regulatory factor-3 for binding to IFNB promoter. *J Biol Chem,* 285, 7208-21.

COLAMONICI, O., YAN, H., DOMANSKI, P., HANDA, R., SMALLEY, D., MULLERSMAN, J., WITTE, M., KRISHNAN, K. & KROLEWSKI, J. 1994. Direct binding to and tyrosine phosphorylation of the alpha subunit of the type I interferon receptor by p135tyk2 tyrosine kinase. *Mol Cell Biol,* 14, 8133-42.

COTTER, M. A., 2ND & ROBERTSON, E. S. 1999. The latency-associated nuclear antigen tethers the Kaposi's sarcoma-associated herpesvirus genome to host chromosomes in body cavity-based lymphoma cells. *Virology,* 264, 254-64.

CUMMINS, J. M. & VOGELSTEIN, B. 2004. HAUSP is required for p53 destabilization. *Cell Cycle,* 3, 689-92.

CUNNINGHAM, C., BARNARD, S., BLACKBOURN, D. J. & DAVISON, A. J. 2003. Transcription mapping of human herpesvirus 8 genes encoding viral interferon regulatory factors. *J Gen Virol,* 84, 1471-83.

DARNELL, J. E., JR., KERR, I. M. & STARK, G. R. 1994. Jak-STAT pathways and transcriptional activation in response to IFNs and other extracellular signaling proteins. *Science,* 264, 1415-21.

DAVISON, A. J., EBERLE, R., EHLERS, B., HAYWARD, G. S., MCGEOCH, D. J., MINSON, A. C., PELLETT, P. E., ROIZMAN, B., STUDDERT, M. J. & THIRY, E. 2009. The order Herpesvirales. *Arch Virol,* 154, 171-7.

DEFILIPPIS, V. R., ALVARADO, D., SALI, T., ROTHENBURG, S. & FRUH, K. 2010. Human cytomegalovirus induces the interferon response via the DNA sensor ZBP1. *J Virol,* 84, 585-98.

DIDCOCK, L., YOUNG, D. F., GOODBOURN, S. & RANDALL, R. E. 1999. The V protein of simian virus 5 inhibits interferon signalling by targeting STAT1 for proteasome-mediated degradation. *J Virol,* 73, 9928-33.

DIEBOLD, S. S., KAISHO, T., HEMMI, H., AKIRA, S. & REIS E SOUSA, C. 2004. Innate antiviral responses by means of TLR7-mediated recognition of single-stranded RNA. *Science,* 303, 1529-31.

DING, Q., CAO, X., LU, J., HUANG, B., LIU, Y. J., KATO, N., SHU, H. B. & ZHONG, J. 2013. Hepatitis C virus NS4B blocks the interaction of STING and TBK1 to evade host innate immunity. *J Hepatol,* 59, 52-8.

DJERBI, M., SCREPANTI, V., CATRINA, A. I., BOGEN, B., BIBERFELD, P. & GRANDIEN, A. 1999. The inhibitor of death receptor signaling, FLICE-inhibitory protein defines a new class of tumor progression factors. *J Exp Med,* 190, 1025-32.

DONG, B. & SILVERMAN, R. H. 1995. 2-5A-dependent RNase molecules dimerize during activation by 2-5A. *J Biol Chem,* 270, 4133-7.

DUTTA, D., CHAKRABORTY, S., BANDYOPADHYAY, C., VALIYA VEETTIL, M., ANSARI, M. A., SINGH, V. V. & CHANDRAN, B. 2013. EphrinA2 Regulates Clathrin Mediated KSHV Endocytosis in Fibroblast Cells by Coordinating Integrin-Associated Signaling and c-Cbl Directed Polyubiquitination. *PLoS Pathog,* 9, e1003510.

ECKNER, R., EWEN, M. E., NEWSOME, D., GERDES, M., DECAPRIO, J. A., LAWRENCE, J. B. & LIVINGSTON, D. M. 1994. Molecular cloning and functional analysis of the adenovirus E1A-associated 300-kD protein (p300) reveals a protein with properties of a transcriptional adaptor. *Genes Dev,* 8, 869-84.

ESTEBAN, M., GARCIA, M. A., DOMINGO-GIL, E., ARROYO, J., NOMBELA, C. & RIVAS, C. 2003. The latency protein LANA2 from Kaposi's sarcoma-associated herpesvirus inhibits apoptosis induced by dsRNA-activated protein kinase but not RNase L activation. *J Gen Virol,* 84, 1463-70.

EVERETT, R. D., MEREDITH, M., ORR, A., CROSS, A., KATHORIA, M. & PARKINSON, J. 1997. A novel ubiquitin-specific protease is dynamically associated with the PML nuclear domain and binds to a herpesvirus regulatory protein. *EMBO J,* 16, 1519-30.

FEJER, G., MEDVECZKY, M. M., HORVATH, E., LANE, B., CHANG, Y. & MEDVECZKY, P. G. 2003. The latency-associated nuclear antigen of Kaposi's sarcoma-associated herpesvirus interacts preferentially with the terminal repeats of the genome in vivo and this complex is sufficient for episomal DNA replication. *J Gen Virol,* 84, 1451-62.

FERNANDEZ, M., QUIROGA, J. A. & CARRENO, V. 2003. Hepatitis B virus downregulates the human interferon-inducible MxA promoter through direct interaction of precore/core proteins. *J Gen Virol,* 84, 2073-82.

FRANCESCHI, S., MASO, L. D., RICKENBACH, M., POLESEL, J., HIRSCHEL, B., CAVASSINI, M., BORDONI, A., ELZI, L., ESS, S., JUNDT, G., MUELLER, N. & CLIFFORD, G. M. 2008. Kaposi sarcoma incidence in the Swiss HIV Cohort Study before and after highly active antiretroviral therapy. *Br J Cancer,* 99, 800-4.

FU, X. Y., KESSLER, D. S., VEALS, S. A., LEVY, D. E. & DARNELL, J. E., JR. 1990. ISGF3, the transcriptional activator induced by interferon alpha, consists of multiple interacting polypeptide chains. *Proc Natl Acad Sci U S A,* 87, 8555-9.

FULD, S., CUNNINGHAM, C., KLUCHER, K., DAVISON, A. J. & BLACKBOURN, D. J. 2006. Inhibition of interferon signaling by the Kaposi's sarcoma-associated herpesvirus full-length viral interferon regulatory factor 2 protein. *J Virol,* 80, 3092-7.

GALE, M., JR. & FOY, E. M. 2005. Evasion of intracellular host defence by hepatitis C virus. *Nature,* 436, 939-45.

GAO, S. J., BOSHOFF, C., JAYACHANDRA, S., WEISS, R. A., CHANG, Y. & MOORE, P. S. 1997. KSHV ORF K9 (vIRF) is an oncogene which inhibits the interferon signaling pathway. *Oncogene,* 15, 1979-85.

GAO, S. J., KINGSLEY, L., HOOVER, D. R., SPIRA, T. J., RINALDO, C. R., SAAH, A., PHAIR, J., DETELS, R., PARRY, P., CHANG, Y. & MOORE, P. S. 1996. Seroconversion to antibodies against Kaposi's sarcoma-associated herpesvirus-related latent nuclear antigens before the development of Kaposi's sarcoma. *N Engl J Med,* 335, 233-41.

GARCIA, M. A., GIL, J., VENTOSO, I., GUERRA, S., DOMINGO, E., RIVAS, C. & ESTEBAN, M. 2006. Impact of protein kinase PKR in cell biology: from antiviral to antiproliferative action. *Microbiol Mol Biol Rev,* 70, 1032-60.

GARCIN, D., MARQ, J. B., STRAHLE, L., LE MERCIER, P. & KOLAKOFSKY, D. 2002. All four Sendai Virus C proteins bind Stat1, but only the larger forms also induce its mono-ubiquitination and degradation. *Virology,* 295, 256-65.

GARRIGUES, H. J., RUBINCHIKOVA, Y. E., DIPERSIO, C. M. & ROSE, T. M. 2008. Integrin alphaVbeta3 Binds to the RGD motif of glycoprotein B of Kaposi's sarcoma-associated herpesvirus and functions as an RGD-dependent entry receptor. *J Virol,* 82, 1570-80.

GILES, R. H., PETERS, D. J. & BREUNING, M. H. 1998. Conjunction dysfunction: CBP/p300 in human disease. *Trends Genet,* 14, 178-83.

GIRALDO, G., BETH, E. & HAGUENAU, F. 1972. Herpes-type virus particles in tissue culture of Kaposi's sarcoma from different geographic regions. *J Natl Cancer Inst,* 49, 1509-26.

GREENE, W., KUHNE, K., YE, F., CHEN, J., ZHOU, F., LEI, X. & GAO, S. J. 2007. Molecular biology of KSHV in relation to AIDS-associated oncogenesis. *Cancer Treat Res,* 133, 69-127.

GROSSMANN, C. & GANEM, D. 2008. Effects of NFkappaB activation on KSHV latency and lytic reactivation are complex and context-dependent. *Virology,* 375, 94-102.

GUITO, J. & LUKAC, D. M. 2012. KSHV Rta Promoter Specification and Viral Reactivation. *Front Microbiol,* 3, 30.

HAHN, A. S., KAUFMANN, J. K., WIES, E., NASCHBERGER, E., PANTELEEV-IVLEV, J., SCHMIDT, K., HOLZER, A., SCHMIDT, M., CHEN, J., KONIG, S., ENSSER, A., MYOUNG, J., BROCKMEYER, N.

H., STURZL, M., FLECKENSTEIN, B. & NEIPEL, F. 2012. The ephrin receptor tyrosine kinase A2 is a cellular receptor for Kaposi's sarcoma-associated herpesvirus. *Nat Med,* 18, 961-6.

HALLER, O., ARNHEITER, H., LINDENMANN, J. & GRESSER, I. 1980. Host gene influences sensitivity to interferon action selectively for influenza virus. *Nature,* 283, 660-2.

HAYDEN, M. S. & GHOSH, S. 2004. Signaling to NF-kappaB. *Genes Dev,* 18, 2195-224.

HEMMI, H., KAISHO, T., TAKEUCHI, O., SATO, S., SANJO, H., HOSHINO, K., HORIUCHI, T., TOMIZAWA, H., TAKEDA, K. & AKIRA, S. 2002. Small anti-viral compounds activate immune cells via the TLR7 MyD88-dependent signaling pathway. *Nat Immunol,* 3, 196-200.

HOLOWATY, M. N., SHENG, Y., NGUYEN, T., ARROWSMITH, C. & FRAPPIER, L. 2003. Protein interaction domains of the ubiquitin-specific protease, USP7/HAUSP. *J Biol Chem,* 278, 47753-61.

HONDA, K., TAKAOKA, A. & TANIGUCHI, T. 2006. Type I interferon [corrected] gene induction by the interferon regulatory factor family of transcription factors. *Immunity,* 25, 349-60.

HUANG, M., QIAN, F., HU, Y., ANG, C., LI, Z. & WEN, Z. 2002. Chromatin-remodelling factor BRG1 selectively activates a subset of interferon-alpha-inducible genes. *Nat Cell Biol,* 4, 774-81.

ISHIKAWA, H. & BARBER, G. N. 2008. STING is an endoplasmic reticulum adaptor that facilitates innate immune signalling. *Nature,* 455, 674-8.

JONES, M., DAVIDSON, A., HIBBERT, L., GRUENWALD, P., SCHLAAK, J., BALL, S., FOSTER, G. R. & JACOBS, M. 2005. Dengue virus inhibits alpha interferon signaling by reducing STAT2 expression. *J Virol,* 79, 5414-20.

JOO, C. H., SHIN, Y. C., GACK, M., WU, L., LEVY, D. & JUNG, J. U. 2007. Inhibition of interferon regulatory factor 7 (IRF7)-mediated interferon signal transduction by the Kaposi's sarcoma-associated herpesvirus viral IRF homolog vIRF3. *J Virol,* 81, 8282-92.

KALEEBA, J. A. & BERGER, E. A. 2006. Kaposi's sarcoma-associated herpesvirus fusion-entry receptor: cystine transporter xCT. *Science,* 311, 1921-4.

KALKHOVEN, E. 2004. CBP and p300: HATs for different occasions. *Biochem Pharmacol,* 68, 1145-55.

KALVAKOLANU, D. V., BANDYOPADHYAY, S. K., HARTER, M. L. & SEN, G. C. 1991. Inhibition of interferon-inducible gene expression by adenovirus E1A proteins: block in transcriptional complex formation. *Proc Natl Acad Sci U S A,* 88, 7459-63.

KANNO, T., SATO, Y., SATA, T. & KATANO, H. 2006. Expression of Kaposi's sarcoma-associated herpesvirus-encoded K10/10.1 protein in tissues and its interaction with poly(A)-binding protein. *Virology,* 352, 100-9.

KAPOSI, M. 1872. Idiopathisches Multiples Pigments, Sarkom der Haut. *Arch Dermatol. Syph. 4*, 265-273.

KAWAI, T., SATO, S., ISHII, K. J., COBAN, C., HEMMI, H., YAMAMOTO, M., TERAI, K., MATSUDA, M., INOUE, J., UEMATSU, S., TAKEUCHI, O. & AKIRA, S. 2004. Interferon-alpha induction through Toll-like receptors involves a direct interaction of IRF7 with MyD88 and TRAF6. *Nat Immunol,* 5, 1061-8.

KAWAI, T., TAKAHASHI, K., SATO, S., COBAN, C., KUMAR, H., KATO, H., ISHII, K. J., TAKEUCHI, O. & AKIRA, S. 2005. IPS-1, an adaptor triggering RIG-I- and Mda5-mediated type I interferon induction. *Nat Immunol,* 6, 981-8.

KESSLER, D. S., VEALS, S. A., FU, X. Y. & LEVY, D. E. 1990. Interferon-alpha regulates nuclear translocation and DNA-binding affinity of ISGF3, a multimeric transcriptional activator. *Genes Dev,* 4, 1753-65.

KIM, T. S., JANG, C. Y., KIM, H. D., LEE, J. Y., AHN, B. Y. & KIM, J. 2006. Interaction of Hsp90 with ribosomal proteins protects from ubiquitination and proteasome-dependent degradation. *Mol Biol Cell,* 17, 824-33.

KOCHS, G. & HALLER, O. 1999. Interferon-induced human MxA GTPase blocks nuclear import of Thogoto virus nucleocapsids. *Proc Natl Acad Sci U S A,* 96, 2082-6.

KONDRASHOV, N., PUSIC, A., STUMPF, C. R., SHIMIZU, K., HSIEH, A. C., XUE, S., ISHIJIMA, J., SHIROISHI, T. & BARNA, M. 2011. Ribosome-mediated specificity in Hox mRNA translation and vertebrate tissue patterning. *Cell,* 145, 383-97.

KOTENKO, S. V., GALLAGHER, G., BAURIN, V. V., LEWIS-ANTES, A., SHEN, M., SHAH, N. K., LANGER, J. A., SHEIKH, F., DICKENSHEETS, H. & DONNELLY, R. P. 2003. IFN-lambdas mediate antiviral protection through a distinct class II cytokine receptor complex. *Nat Immunol,* 4, 69-77.

KRISHNAN, H. H., SHARMA-WALIA, N., STREBLOW, D. N., NARANATT, P. P. & CHANDRAN, B. 2006. Focal adhesion kinase is critical for entry of Kaposi's sarcoma-associated herpesvirus into target cells. *J Virol,* 80, 1167-80.

KUMTHIP, K., CHUSRI, P., JILG, N., ZHAO, L., FUSCO, D. N., ZHAO, H., GOTO, K., CHENG, D., SCHAEFER, E. A., ZHANG, L., PANTIP, C., THONGSAWAT, S., O'BRIEN, A., PENG, L. F., MANEEKARN, N., CHUNG, R. T. & LIN, W. 2012. Hepatitis C virus NS5A disrupts STAT1 phosphorylation and suppresses type I interferon signaling. *J Virol,* 86, 8581-91.

LAN, K., KUPPERS, D. A. & ROBERTSON, E. S. 2005. Kaposi's sarcoma-associated herpesvirus reactivation is regulated by interaction of latency-associated nuclear antigen with recombination signal sequence-binding protein Jkappa, the major downstream effector of the Notch signaling pathway. *J Virol,* 79, 3468-78.

LAN, K., KUPPERS, D. A., VERMA, S. C. & ROBERTSON, E. S. 2004. Kaposi's sarcoma-associated herpesvirus-encoded latency-associated nuclear antigen inhibits lytic replication by targeting Rta: a potential mechanism for virus-mediated control of latency. *J Virol,* 78, 6585-94.

LEE, H. R., CHOI, W. C., LEE, S., HWANG, J., HWANG, E., GUCHHAIT, K., HAAS, J., TOTH, Z., JEON, Y. H., OH, T. K., KIM, M. H. & JUNG, J. U. 2011. Bilateral inhibition of HAUSP deubiquitinase by a viral interferon regulatory factor protein. *Nat Struct Mol Biol,* 18, 1336-44.

LEE, H. R., TOTH, Z., SHIN, Y. C., LEE, J. S., CHANG, H., GU, W., OH, T. K., KIM, M. H. & JUNG, J. U. 2009. Kaposi's sarcoma-associated herpesvirus viral interferon regulatory factor 4 targets MDM2 to deregulate the p53 tumor suppressor pathway. *J Virol,* 83, 6739-47.

LEFORT, S., SOUCY-FAULKNER, A., GRANDVAUX, N. & FLAMAND, L. 2007. Binding of Kaposi's sarcoma-associated herpesvirus K-bZIP to interferon-responsive factor 3 elements modulates antiviral gene expression. *J Virol,* 81, 10950-60.

LEMAITRE, B., NICOLAS, E., MICHAUT, L., REICHHART, J. M. & HOFFMANN, J. A. 1996. The dorsoventral regulatory gene cassette spatzle/Toll/cactus controls the potent antifungal response in Drosophila adults. *Cell,* 86, 973-83.

LENSCHOW, D. J., GIANNAKOPOULOS, N. V., GUNN, L. J., JOHNSTON, C., O'GUIN, A. K., SCHMIDT, R. E., LEVINE, B. & VIRGIN, H. W. T. 2005. Identification of interferon-stimulated gene 15 as an antiviral molecule during Sindbis virus infection in vivo. *J Virol,* 79, 13974-83.

LEUNG, S., QURESHI, S. A., KERR, I. M., DARNELL, J. E., JR. & STARK, G. R. 1995. Role of STAT2 in the alpha interferon signaling pathway. *Mol Cell Biol,* 15, 1312-7.

LI, K., FOY, E., FERREON, J. C., NAKAMURA, M., FERREON, A. C., IKEDA, M., RAY, S. C., GALE, M., JR. & LEMON, S. M. 2005a. Immune evasion by hepatitis C virus NS3/4A protease-mediated cleavage of the Toll-like receptor 3 adaptor protein TRIF. *Proc Natl Acad Sci U S A,* 102, 2992-7.

LI, M., CHEN, D., SHILOH, A., LUO, J., NIKOLAEV, A. Y., QIN, J. & GU, W. 2002. Deubiquitination of p53 by HAUSP is an important pathway for p53 stabilization. *Nature,* 416, 648-53.

LI, M., LEE, H., GUO, J., NEIPEL, F., FLECKENSTEIN, B., OZATO, K. & JUNG, J. U. 1998. Kaposi's sarcoma-associated herpesvirus viral interferon regulatory factor. *J Virol,* 72, 5433-40.

LI, X. D., SUN, L., SETH, R. B., PINEDA, G. & CHEN, Z. J. 2005b. Hepatitis C virus protease NS3/4A cleaves mitochondrial antiviral signaling protein off the mitochondria to evade innate immunity. *Proc Natl Acad Sci U S A,* 102, 17717-22.

LIN, R., GENIN, P., MAMANE, Y., SGARBANTI, M., BATTISTINI, A., HARRINGTON, W. J., JR., BARBER, G. N. & HISCOTT, J. 2001. HHV-8 encoded vIRF-1 represses the interferon antiviral response by blocking IRF-3 recruitment of the CBP/p300 coactivators. *Oncogene,* 20, 800-11.

LING, Z., TRAN, K. C. & TENG, M. N. 2009. Human respiratory syncytial virus nonstructural protein NS2 antagonizes the activation of beta interferon transcription by interacting with RIG-I. *J Virol,* 83, 3734-42.

LO, M. S., BRAZAS, R. M. & HOLTZMAN, M. J. 2005. Respiratory syncytial virus nonstructural proteins NS1 and NS2 mediate inhibition of Stat2 expression and alpha/beta interferon responsiveness. *J Virol,* 79, 9315-9.

LU, G., REINERT, J. T., PITHA-ROWE, I., OKUMURA, A., KELLUM, M., KNOBELOCH, K. P., HASSEL, B. & PITHA, P. M. 2006. ISG15 enhances the innate antiviral response by inhibition of IRF-3 degradation. *Cell Mol Biol (Noisy-le-grand),* 52, 29-41.

LUBYOVA, B., KELLUM, M. J., FRISANCHO, A. J. & PITHA, P. M. 2004. Kaposi's sarcoma-associated herpesvirus-encoded vIRF-3 stimulates the transcriptional activity of cellular IRF-3 and IRF-7. *J Biol Chem,* 279, 7643-54.

LUBYOVA, B., KELLUM, M. J., FRISANCHO, J. A. & PITHA, P. M. 2007. Stimulation of c-Myc transcriptional activity by vIRF-3 of Kaposi sarcoma-associated herpesvirus. *J Biol Chem,* 282, 31944-53.

LUKAC, D. M., RENNE, R., KIRSHNER, J. R. & GANEM, D. 1998. Reactivation of Kaposi's sarcoma-associated herpesvirus infection from latency by expression of the ORF 50 transactivator, a homolog of the EBV R protein. *Virology,* 252, 304-12.

MASEK, T., VALASEK, L. & POSPISEK, M. 2011. Polysome analysis and RNA purification from sucrose gradients. *Methods Mol Biol,* 703, 293-309.

MATSUMOTO, M. & SEYA, T. 2008. TLR3: interferon induction by double-stranded RNA including poly(I:C). *Adv Drug Deliv Rev,* 60, 805-12.

MAZZON, M., JONES, M., DAVIDSON, A., CHAIN, B. & JACOBS, M. 2009. Dengue virus NS5 inhibits interferon-alpha signaling by blocking signal transducer and activator of transcription 2 phosphorylation. *J Infect Dis,* 200, 1261-70.

MCGEOCH, D. J., RIXON, F. J. & DAVISON, A. J. 2006. Topics in herpesvirus genomics and evolution. *Virus Res,* 117, 90-104.

MEREDITH, M., ORR, A. & EVERETT, R. 1994. Herpes simplex virus type 1 immediate-early protein Vmw110 binds strongly and specifically to a 135-kDa cellular protein. *Virology,* 200, 457-69.

MORRISON, J. M. & RACANIELLO, V. R. 2009. Proteinase 2Apro is essential for enterovirus replication in type I interferon-treated cells. *J Virol,* 83, 4412-22.

MUNOZ, A. & CARRASCO, L. 1981. Protein synthesis and membrane integrity in interferon-treated HeLa cells infected with encephalomyocarditis virus. *J Gen Virol,* 56, 153-62.

MUTOCHELUH, M., HINDLE, L., ARESTE, C., CHANAS, S. A., BUTLER, L. M., LOWRY, K., SHAH, K., EVANS, D. J. & BLACKBOURN, D. J. 2011. Kaposi's sarcoma-associated herpesvirus viral interferon regulatory factor-2 inhibits type 1 interferon signalling by targeting interferon-stimulated gene factor-3. *J Gen Virol,* 92, 2394-8.

NANBO, A., INOUE, K., ADACHI-TAKASAWA, K. & TAKADA, K. 2002. Epstein-Barr virus RNA confers resistance to interferon-alpha-induced apoptosis in Burkitt's lymphoma. *EMBO J,* 21, 954-65.

NARANATT, P. P., KRISHNAN, H. H., SMITH, M. S. & CHANDRAN, B. 2005. Kaposi's sarcoma-associated herpesvirus modulates microtubule dynamics via RhoA-GTP-diaphanous 2

signaling and utilizes the dynein motors to deliver its DNA to the nucleus. *J Virol,* 79, 1191-206.

NEIPEL, F., ALBRECHT, J. C. & FLECKENSTEIN, B. 1998. Human herpesvirus 8--the first human Rhadinovirus. *J Natl Cancer Inst Monogr*, 73-7.

NOVICK, D., COHEN, B. & RUBINSTEIN, M. 1994. The human interferon alpha/beta receptor: characterization and molecular cloning. *Cell,* 77, 391-400.

NUSINZON, I. & HORVATH, C. M. 2003. Interferon-stimulated transcription and innate antiviral immunity require deacetylase activity and histone deacetylase 1. *Proc Natl Acad Sci U S A,* 100, 14742-7.

PANNE, D. 2008. The enhanceosome. *Curr Opin Struct Biol,* 18, 236-42.

PAULSON, M., PRESS, C., SMITH, E., TANESE, N. & LEVY, D. E. 2002. IFN-Stimulated transcription through a TBP-free acetyltransferase complex escapes viral shutoff. *Nat Cell Biol,* 4, 140-7.

PESTKA, S., KRAUSE, C. D. & WALTER, M. R. 2004. Interferons, interferon-like cytokines, and their receptors. *Immunol Rev,* 202, 8-32.

QURESHI, S. A., LEUNG, S., KERR, I. M., STARK, G. R. & DARNELL, J. E., JR. 1996. Function of Stat2 protein in transcriptional activation by alpha interferon. *Mol Cell Biol,* 16, 288-93.

RAGHU, H., SHARMA-WALIA, N., VEETTIL, M. V., SADAGOPAN, S. & CHANDRAN, B. 2009. Kaposi's sarcoma-associated herpesvirus utilizes an actin polymerization-dependent macropinocytic pathway to enter human dermal microvascular endothelial and human umbilical vein endothelial cells. *J Virol,* 83, 4895-911.

RANDALL, R. E. & GOODBOURN, S. 2008. Interferons and viruses: an interplay between induction, signalling, antiviral responses and virus countermeasures. *J Gen Virol,* 89, 1-47.

RAPPOCCIOLO, G., JENKINS, F. J., HENSLER, H. R., PIAZZA, P., JAIS, M., BOROWSKI, L., WATKINS, S. C. & RINALDO, C. R., JR. 2006. DC-SIGN is a receptor for human herpesvirus 8 on dendritic cells and macrophages. *J Immunol,* 176, 1741-9.

RENNE, R., ZHONG, W., HERNDIER, B., MCGRATH, M., ABBEY, N., KEDES, D. & GANEM, D. 1996. Lytic growth of Kaposi's sarcoma-associated herpesvirus (human herpesvirus 8) in culture. *Nat Med,* 2, 342-6.

RESTREPO, C. S. & OCAZIONEZ, D. 2011. Kaposi's sarcoma: imaging overview. *Semin Ultrasound CT MR,* 32, 456-69.

REZAEE, S. A., CUNNINGHAM, C., DAVISON, A. J. & BLACKBOURN, D. J. 2006. Kaposi's sarcoma-associated herpesvirus immune modulation: an overview. *J Gen Virol,* 87, 1781-804.

RIVAS, C., THLICK, A. E., PARRAVICINI, C., MOORE, P. S. & CHANG, Y. 2001. Kaposi's sarcoma-associated herpesvirus LANA2 is a B-cell-specific latent viral protein that inhibits p53. *J Virol,* 75, 429-38.

ROBINSON, B. A., ESTEP RD, MESSAOUDI I, ROGERS KS & SW., W. 2012a. Viral Interferon Regulatory Factors Decrease the Induction of Type I and Type II Interferon during Rhesus Macaque Rhadinovirus Infection. *J Virol,* 86.

ROBINSON, B. A., O'CONNOR MA, LI H, ENGELMANN F, POLAND B, GRANT R, DEFILIPPIS V, ESTEP RD, AXTHELM MK, MESSAOUDI I & SW., W. 2012b. Viral Interferon Regulatory Factors Are Critical for Delay of the Host Immune Response against Rhesus Macaque Rhadinovirus Infection. *J Virol,* 86, 2769–2779.

ROSE, T. M., RYAN, J. T., SCHULTZ, E. R., RADEN, B. W. & TSAI, C. C. 2003. Analysis of 4.3 kilobases of divergent locus B of macaque retroperitoneal fibromatosis-associated herpesvirus reveals a close similarity in gene sequence and genome organization to Kaposi's sarcoma-associated herpesvirus. *J Virol,* 77, 5084-97.

RUSSO, J. J., BOHENZKY, R. A., CHIEN, M. C., CHEN, J., YAN, M., MADDALENA, D., PARRY, J. P., PERUZZI, D., EDELMAN, I. S., CHANG, Y. & MOORE, P. S. 1996. Nucleotide sequence of the Kaposi sarcoma-associated herpesvirus (HHV8). *Proc Natl Acad Sci U S A,* 93, 14862-7.

SADLER, A. J. & WILLIAMS, B. R. 2008. Interferon-inducible antiviral effectors. *Nat Rev Immunol,* 8, 559-68.

SAREK, G., JARVILUOMA, A., MOORE, H. M., TOJKANDER, S., VARTIA, S., BIBERFELD, P., LAIHO, M. & OJALA, P. M. 2010. Nucleophosmin phosphorylation by v-cyclin-CDK6 controls KSHV latency. *PLoS Pathog,* 6, e1000818.

SATHISH, N., WANG, X. & YUAN, Y. 2012. Tegument Proteins of Kaposi's Sarcoma-Associated Herpesvirus and Related Gamma-Herpesviruses. *Front Microbiol,* 3, 98.

SATO, M., HATA, N., ASAGIRI, M., NAKAYA, T., TANIGUCHI, T. & TANAKA, N. 1998. Positive feedback regulation of type I IFN genes by the IFN-inducible transcription factor IRF-7. *FEBS Lett,* 441, 106-10.

SATO, S., SUGIYAMA, M., YAMAMOTO, M., WATANABE, Y., KAWAI, T., TAKEDA, K. & AKIRA, S. 2003. Toll/IL-1 receptor domain-containing adaptor inducing IFN-beta (TRIF) associates with TNF receptor-associated factor 6 and TANK-binding kinase 1, and activates two distinct transcription factors, NF-kappa B and IFN-regulatory factor-3, in the Toll-like receptor signaling. *J Immunol,* 171, 4304-10.

SCHNEIDER-SCHAULIES, S., SCHNEIDER-SCHAULIES, J., SCHUSTER, A., BAYER, M., PAVLOVIC, J. & TER MEULEN, V. 1994. Cell type-specific MxA-mediated inhibition of measles virus transcription in human brain cells. *J Virol,* 68, 6910-7.

SEARLES, R. P., BERGQUAM, E. P., AXTHELM, M. K. & WONG, S. W. 1999. Sequence and genomic analysis of a Rhesus macaque rhadinovirus with similarity to Kaposi's sarcoma-associated herpesvirus/human herpesvirus 8. *J Virol,* 73, 3040-53.

SEO, T., PARK, J., LIM, C. & CHOE, J. 2004. Inhibition of nuclear factor kappaB activity by viral interferon regulatory factor 3 of Kaposi's sarcoma-associated herpesvirus. *Oncogene,* 23, 6146-55.

SETH, R. B., SUN, L., EA, C. K. & CHEN, Z. J. 2005. Identification and characterization of MAVS, a mitochondrial antiviral signaling protein that activates NF-kappaB and IRF 3. *Cell,* 122, 669-82.

SHAH, K. M., STEWART SE, WEI W, WOODMAN CB, O'NEIL JD, DAWSON CW & LS., Y. 2009. The EBV-encoded Latent Membrane Proteins, LMP2A and LMP2B, Limit the Actions of Interferon by Targeting Interferon Receptors for Degradation. *Oncogene,* 28, 3903–3914.

SOULIER, J., GROLLET, L., OKSENHENDLER, E., CACOUB, P., CAZALS-HATEM, D., BABINET, P., D'AGAY, M. F., CLAUVEL, J. P., RAPHAEL, M., DEGOS, L. & ET AL. 1995. Kaposi's sarcoma-associated herpesvirus-like DNA sequences in multicentric Castleman's disease. *Blood,* 86, 1276-80.

SUN, L., WU, J., DU, F., CHEN, X. & CHEN, Z. J. 2013. Cyclic GMP-AMP synthase is a cytosolic DNA sensor that activates the type I interferon pathway. *Science,* 339, 786-91.

SUN, R., LIN, S. F., GRADOVILLE, L., YUAN, Y., ZHU, F. & MILLER, G. 1998. A viral gene that activates lytic cycle expression of Kaposi's sarcoma-associated herpesvirus. *Proc Natl Acad Sci U S A,* 95, 10866-71.

SWANTON, C., MANN, D. J., FLECKENSTEIN, B., NEIPEL, F., PETERS, G. & JONES, N. 1997. Herpes viral cyclin/Cdk6 complexes evade inhibition by CDK inhibitor proteins. *Nature,* 390, 184-7.

SZAJERKA, T. & JABLECKI, J. 2007. Kaposi's sarcoma revisited. *AIDS Rev,* 9, 230-6.

TAKAOKA, A., WANG, Z., CHOI, M. K., YANAI, H., NEGISHI, H., BAN, T., LU, Y., MIYAGISHI, M., KODAMA, T., HONDA, K., OHBA, Y. & TANIGUCHI, T. 2007. DAI (DLM-1/ZBP1) is a cytosolic DNA sensor and an activator of innate immune response. *Nature,* 448, 501-5.

TAKAOKA, A., YANAI, H., KONDO, S., DUNCAN, G., NEGISHI, H., MIZUTANI, T., KANO, S., HONDA, K., OHBA, Y., MAK, T. W. & TANIGUCHI, T. 2005. Integral role of IRF-5 in the gene induction programme activated by Toll-like receptors. *Nature,* 434, 243-9.

TAKEUCHI, O. & AKIRA, S. 2010. Pattern recognition receptors and inflammation. *Cell,* 140, 805-20.

TANAKA, Y. & CHEN, Z. J. 2012. STING specifies IRF3 phosphorylation by TBK1 in the cytosolic DNA signaling pathway. *Sci Signal,* 5, ra20.

TANG, X., GAO, J. S., GUAN, Y. J., MCLANE, K. E., YUAN, Z. L., RAMRATNAM, B. & CHIN, Y. E. 2007. Acetylation-dependent signal transduction for type I interferon receptor. *Cell,* 131, 93-105.

TRINKLE-MULCAHY, L., BOULON, S., LAM, Y. W., URCIA, R., BOISVERT, F. M., VANDERMOERE, F., MORRICE, N. A., SWIFT, S., ROTHBAUER, U., LEONHARDT, H. & LAMOND, A. 2008. Identifying specific protein interaction partners using quantitative mass spectrometry and bead proteomes. *J Cell Biol,* 183, 223-39.

UNTERHOLZNER, L., KEATING, S. E., BARAN, M., HORAN, K. A., JENSEN, S. B., SHARMA, S., SIROIS, C. M., JIN, T., LATZ, E., XIAO, T. S., FITZGERALD, K. A., PALUDAN, S. R. & BOWIE, A. G. 2010. IFI16 is an innate immune sensor for intracellular DNA. *Nat Immunol,* 11, 997-1004.

VEETTIL, M. V., SADAGOPAN, S., SHARMA-WALIA, N., WANG, F. Z., RAGHU, H., VARGA, L. & CHANDRAN, B. 2008. Kaposi's sarcoma-associated herpesvirus forms a multimolecular complex of integrins (alphaVbeta5, alphaVbeta3, and alpha3beta1) and CD98-xCT during infection of human dermal microvascular endothelial cells, and CD98-xCT is essential for the postentry stage of infection. *J Virol,* 82, 12126-44.

VERMA, S. C. & ROBERTSON, E. S. 2003. Molecular biology and pathogenesis of Kaposi sarcoma-associated herpesvirus. *FEMS Microbiol Lett,* 222, 155-63.

VIDY, A., CHELBI-ALIX, M. & BLONDEL, D. 2005. Rabies virus P protein interacts with STAT1 and inhibits interferon signal transduction pathways. *J Virol,* 79, 14411-20.

VOGELSTEIN, B., LANE, D. & LEVINE, A. J. 2000. Surfing the p53 network. *Nature,* 408, 307-10.

WANG, F. Z., AKULA, S. M., PRAMOD, N. P., ZENG, L. & CHANDRAN, B. 2001. Human herpesvirus 8 envelope glycoprotein K8.1A interaction with the target cells involves heparan sulfate. *J Virol,* 75, 7517-27.

WEBER, F., WAGNER, V., RASMUSSEN, S. B., HARTMANN, R. & PALUDAN, S. R. 2006. Double-stranded RNA is produced by positive-strand RNA viruses and DNA viruses but not in detectable amounts by negative-strand RNA viruses. *J Virol,* 80, 5059-64.

WHITAKER-DOWLING, P. & YOUNGNER, J. S. 1986. Vaccinia-mediated rescue of encephalomyocarditis virus from the inhibitory effects of interferon. *Virology,* 152, 50-7.

WIES, E., HAHN, A. S., SCHMIDT, K., VIEBAHN, C., ROHLAND, N., LUX, A., SCHELLHORN, T., HOLZER, A., JUNG, J. U. & NEIPEL, F. 2009. The Kaposi's Sarcoma-associated Herpesvirus-encoded vIRF-3 Inhibits Cellular IRF-5. *J Biol Chem,* 284, 8525-38.

WU, J., SUN, L., CHEN, X., DU, F., SHI, H., CHEN, C. & CHEN, Z. J. 2013. Cyclic GMP-AMP is an endogenous second messenger in innate immune signaling by cytosolic DNA. *Science,* 339, 826-30.

WU, L., LO, P., YU, X., STOOPS, J. K., FORGHANI, B. & ZHOU, Z. H. 2000. Three-dimensional structure of the human herpesvirus 8 capsid. *J Virol,* 74, 9646-54.

XI, X., PERSSON, L. M., O'BRIEN, M. W., MOHR, I. & WILSON, A. C. 2012. Cooperation between viral interferon regulatory factor 4 and RTA to activate a subset of Kaposi's sarcoma-associated herpesvirus lytic promoters. *J Virol,* 86, 1021-33.

XU, L. G., WANG, Y. Y., HAN, K. J., LI, L. Y., ZHAI, Z. & SHU, H. B. 2005. VISA is an adapter protein required for virus-triggered IFN-beta signaling. *Mol Cell,* 19, 727-40.

YAMAMOTO, M., SATO, S., MORI, K., HOSHINO, K., TAKEUCHI, O., TAKEDA, K. & AKIRA, S. 2002. Cutting edge: a novel Toll/IL-1 receptor domain-containing adapter that preferentially activates the IFN-beta promoter in the Toll-like receptor signaling. *J Immunol,* 169, 6668-72.

YAN, H., KRISHNAN, K., GREENLUND, A. C., GUPTA, S., LIM, J. T., SCHREIBER, R. D., SCHINDLER, C. W. & KROLEWSKI, J. J. 1996. Phosphorylated interferon-alpha receptor 1 subunit (IFNaR1) acts as a docking site for the latent form of the 113 kDa STAT2 protein. *EMBO J,* 15, 1064-74.

YAO, F., SVENSJO, T., WINKLER, T., LU, M., ERIKSSON, C. & ERIKSSON, E. 1998. Tetracycline repressor, tetR, rather than the tetR-mammalian cell transcription factor fusion derivatives, regulates inducible gene expression in mammalian cells. *Hum Gene Ther,* 9, 1939-50.

YE, F., LEI, X. & GAO, S. J. 2011. Mechanisms of Kaposi's Sarcoma-Associated Herpesvirus Latency and Reactivation. *Adv Virol,* 2011.

YE, F. C., ZHOU, F. C., XIE, J. P., KANG, T., GREENE, W., KUHNE, K., LEI, X. F., LI, Q. H. & GAO, S. J. 2008. Kaposi's sarcoma-associated herpesvirus latent gene vFLIP inhibits viral lytic replication through NF-kappaB-mediated suppression of the AP-1 pathway: a novel mechanism of virus control of latency. *J Virol,* 82, 4235-49.

YONEYAMA, M., KIKUCHI, M., NATSUKAWA, T., SHINOBU, N., IMAIZUMI, T., MIYAGISHI, M., TAIRA, K., AKIRA, S. & FUJITA, T. 2004. The RNA helicase RIG-I has an essential function in double-stranded RNA-induced innate antiviral responses. *Nat Immunol,* 5, 730-7.

YU, Y. & HAYWARD, G. S. 2010. The ubiquitin E3 ligase RAUL negatively regulates type i interferon through ubiquitination of the transcription factors IRF7 and IRF3. *Immunity,* 33, 863-77.

ZHANG, J., YAMADA, O., KAWAGISHI, K., ARAKI, H., YAMAOKA, S., HATTORI, T. & SHIMOTOHNO, K. 2008. Human T-cell leukemia virus type 1 Tax modulates interferon-alpha signal transduction through competitive usage of the coactivator CBP/p300. *Virology,* 379, 306-13.

ZHANG, J. J., VINKEMEIER, U., GU, W., CHAKRAVARTI, D., HORVATH, C. M. & DARNELL, J. E., JR. 1996. Two contact regions between Stat1 and CBP/p300 in interferon gamma signaling. *Proc Natl Acad Sci U S A,* 93, 15092-6.

ZHAO, L., JHA, B. K., WU, A., ELLIOTT, R., ZIEBUHR, J., GORBALENYA, A. E., SILVERMAN, R. H. & WEISS, S. R. 2012. Antagonism of the interferon-induced OAS-RNase L pathway by murine coronavirus ns2 protein is required for virus replication and liver pathology. *Cell Host Microbe,* 11, 607-16.

ZHU, F. X., KING, S. M., SMITH, E. J., LEVY, D. E. & YUAN, Y. 2002. A Kaposi's sarcoma-associated herpesviral protein inhibits virus-mediated induction of type I interferon by blocking IRF-7 phosphorylation and nuclear accumulation. *Proc Natl Acad Sci U S A,* 99, 5573-8.

APPENDICES

9.1. Appendix: Supplimentary methods

Table 9.1: Solutions and buffers used for Immunoblotting.

Italics represent components added fresh to each solution immediately before use.

Solution	Composition
Sonication buffer	50mM Tris-HCl (pH 7.3), *9 M urea*, and 150mM -mercaptoethanol
Non-ionic detergent Lysis buffer	50mM Tris HCl pH 8.0, 50mM NaCl, 5 mM EDTA, 1% Triton X-100, 50mM sodium fluoride, 1mM sodium orthorvanadate, 0.05% SDS, 10mM Sodium pyrophosphate, *1mM PMSF, (used at 1:100 dilution), Protease Inhibitor cocktail set III calbiochem (539134)* (used at 1:100 dilution)
IP lysis buffer	50mM Tris-HCL (pH 7.5), 125mM NaCl, 5% Glycerol, 0.2% NP-40, Protease cocktail inhibitor set III calbiochem (539134) (used at 1:100 dilution)
10x Electrophoresis running buffer (1L)	Tris base (30.24 g), Glycine (142.5 g), 1L distilled water (dH_2O), pH 8.4
10x Electrophoresis running buffer (1L)	100ml 10X electrophoresis buffer, 0.1% of 20% SDS, 1L dH_2O
10X Transfer buffer (1 L)	Tris 30.3g, Glycine 142.5g & 1 L dH_2O, pH to 8.4
1X Transfer buffer (1 L)	100ml 10X transfer buffer, 20% methanol, 700ml dH_2O
4X Tris-SDS-HCl, pH 6.8	0.5M Tris-Cl, 0.4% SDS
4X Tris-SDS-HCl, pH 8.8	1.5M Tris-Cl, 0.4% SDS
Tris Buffered Saline (TBS) (1 L)	NaCl 90g, Tris base 60g & 1L dH_2O
TBS-Tween (TBS-T) (1 L)	100ml TBS, 0.05% Tween-20, 900ml dH_2O.
PBS	10 xPBS tablets (DULBECCO) disolved in 1 L of SDW
PBS-Tween (PBS-T) (1 L)	100ml PBS, 0.05% Tween-20, 900ml dH_2O.
2X Loading sample buffer (10ml)	1M Tris-HCl, pH 6.8, 4ml 10% SDS, 2ml glycerol, 2.5ml 2-β-mecaptoethanol, 500 µl bromophenol blue (1%)
Stripping Buffer	100mM Tris-HCl pH 6.8, 2% (w/v) SDS, 50mM 2-β-mercaptoethanol.
5% Milk blocking buffer in TBS-T	5% (w/v) powdered milk dissolved in TBS-T, stored at 4°C.
5% Milk blocking buffer in PBS-T	5% (w/v) powdered milk dissolved in PBS-T, stored at 4°C.
AcTEV Protease	Invitrogen (12575-015)
Enhanced chemiluminescence	Amersham (RPN2106)

Table 9.2: Resolving gels and stacking gels used throughout this study.
The values shown generate solution to prepare 2 gels.

Stock solution	Supplier	Acrylamide resolving gel (mls)				Acrylamide stacking gel (mls)
		12% w/v	10% w/v	7% w/v	5% w/v	
30% w/v Acryl/bis Acrylamide	SIGMA	6.0	5.0	2.4	1.7	0.63
4X Tris-SDS-HCl, pH 6.8	Lab made solution	-	-	-	-	0.83
4X Tris-SDS-HCl, pH 8.8	Lab made solution	3.75	3.75	2.5	2.5	-
10% SDS	Lab made solution	0.1	0.1	0.1	0.1	
dH2O	Lab made solution	5.25	6.25	5	5.7	3.20
10% APS	SIGMA	0.05	0.05	0.05	0.05	0.025
TEMED	SIGMA	0.01	0.01	0.01	0.01	0.01

Table 9.3: Primary antibodies used for western blotting

Antibody	Dilution	Supplier
TBP	1:2000	Abcam (Ab818)
PSTAT (Tyr701)	1:1000	Cell Signaling Technology (9167)
STAT1	1:100	Santa Cruz Biotechnology (sc-346)
STAT2 (C-20)	1:100	Santa Cruz Biotechnology (sc-476)
pSTAT2	1:1000	Millipore Catalog (07-224)
p48/IRF-9	1:100	Santa Cruz Biotechnology (sc-10793)
ORF50/RTA	1:500	From our laboratory
B-actin	1:2500	Sigma (A-5441)
RPS3	1:1000	Cell Signaling Technology (2579)
RPS6	1:100	Santa Cruz Biotechnology (sc-74459)
p300	1:100	Santa Cruz Biotechnology (sc-584)
CBP	1:100	Santa Cruz Biotechnology (sc-583)
USP7	1:1000	Bethyl Laboratories (A300-033A)
Poly Histidine	1:5000	SIGMA (H1029)
Xpress	1:2000	Invitrogen (R910-25)
RAD18	1:1000	Abcam (Ab57447)
Acetylated lysine	1:1000	Cell signaling technology 9441

Table 9.4: Secondary antibodies used for western blotting

Antibody	Dilution	Supplier
anti-rabbit IRDye800LT-conjugated	1:10,000	LI-COR Biosciences (926-68020)
anti-mouse IRDye680LT-conjugated	1:20,000	LI-COR Biosciences (926-32211)
anti-mouse HRP-conjugated	1:2000	DAKO (P0447)
anti-rabbit HRP-conjugated	1:2000	DAKO (P0448)

9.2. Appendix: Repeated experiments

Many of the experiments shown throughout this thesis have been averaged from the results of 3 of more experiments or are representative of more than one experiment. The data from these repeats are shown in this appendix.

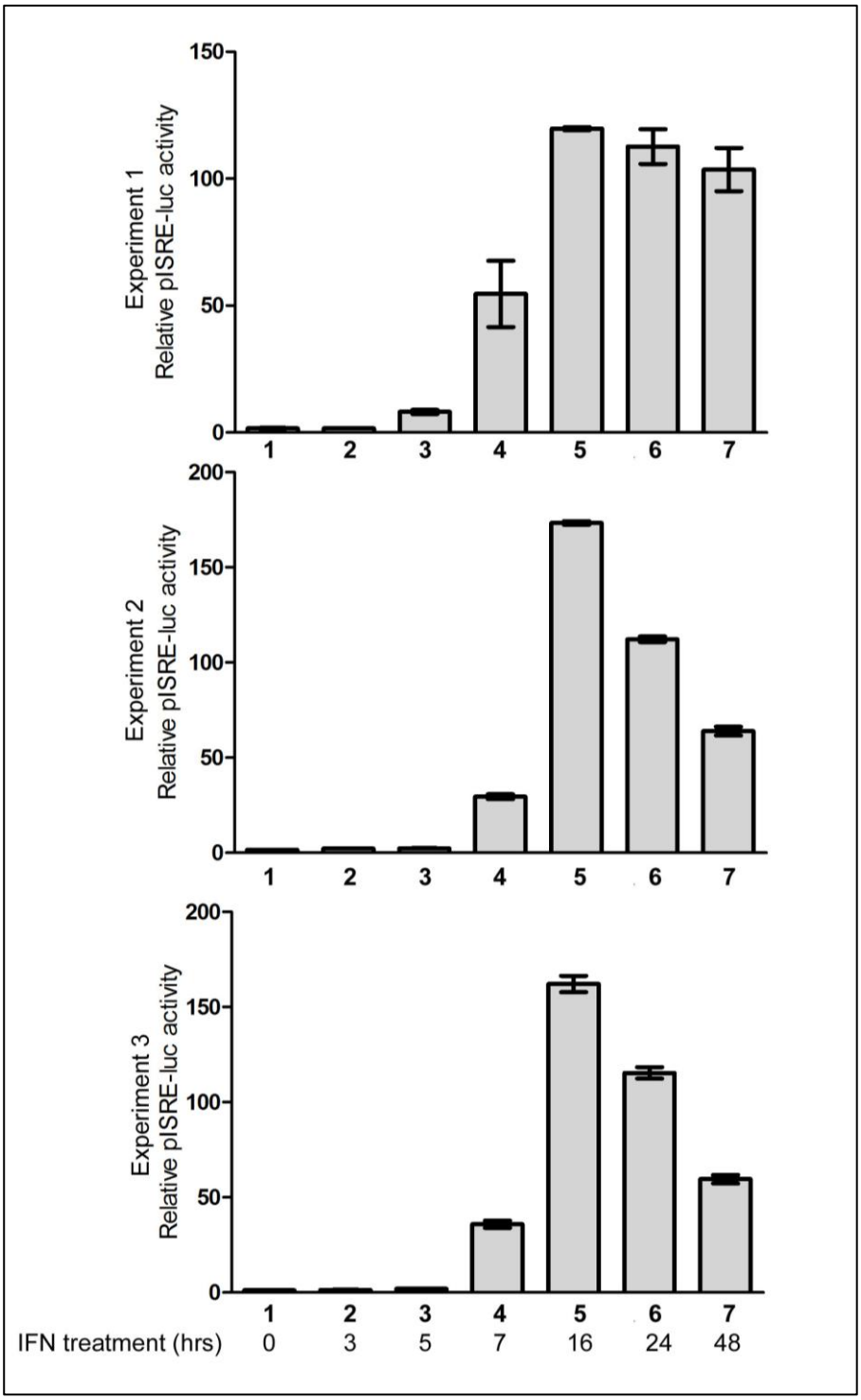

Figure 9.1: ISRE-*luc* expression peaked 16 hours post rIFNα treatment. Experiments performed as in Figure 3.6A. The data presents the relative luciferase activity (normalised to *Renilla* levels) of three individual experiments.

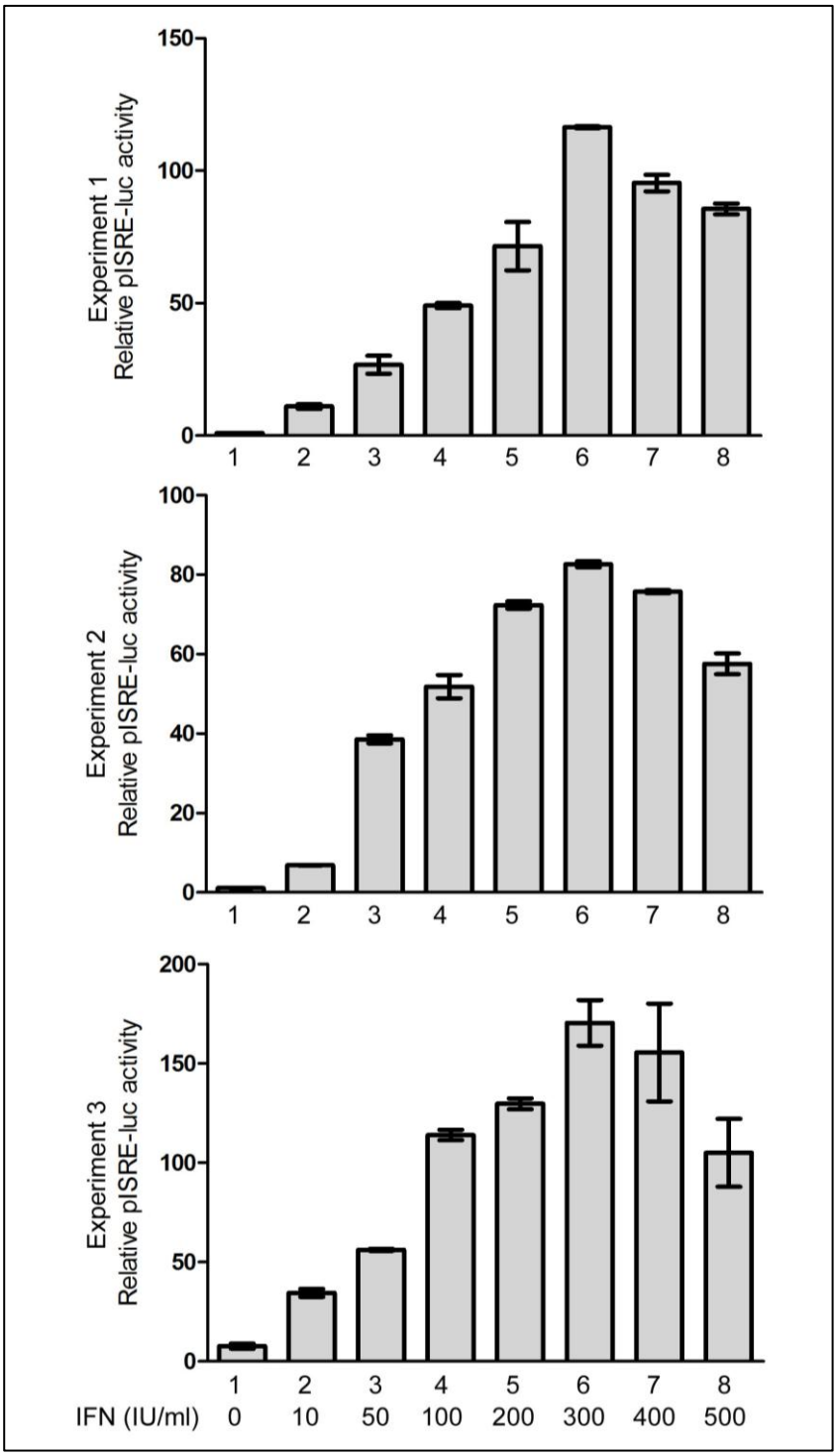

Figure 9.2: ISRE-luc expression following treatment with 300 IU/ml rIFNα. Experiment performed as in Figure 3.6B. The data presents the relative luciferase activity (normalised to *Renilla* levels) of three individual experiments.

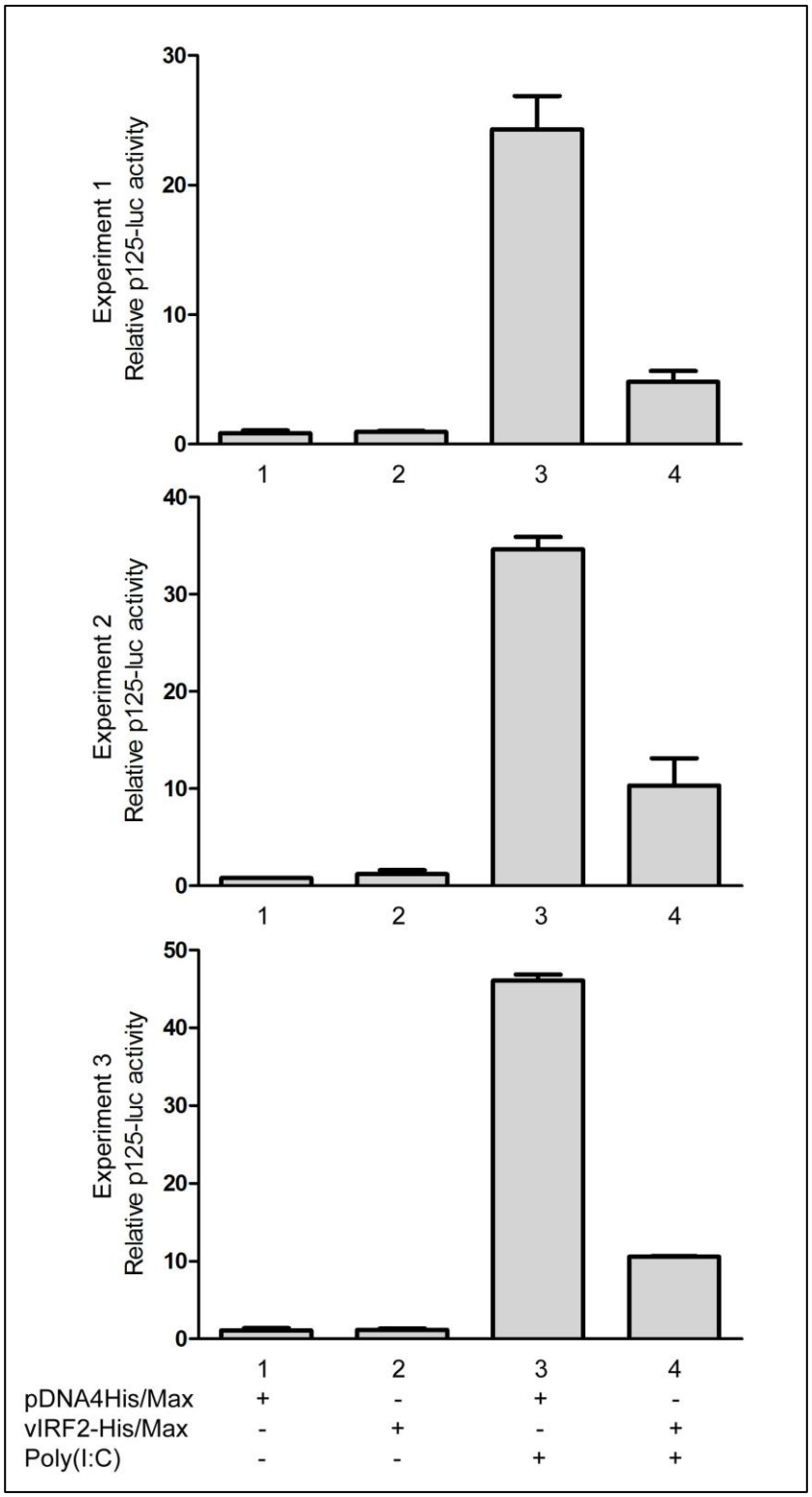

Figure 9.3: vIRF2 inhibits the poly(I:C) activated IFNβ promoter. Experiment performed as in Figure 3.7. The data presents the relative luciferase activity (normalised to *Renilla* levels) of three individual experiments.

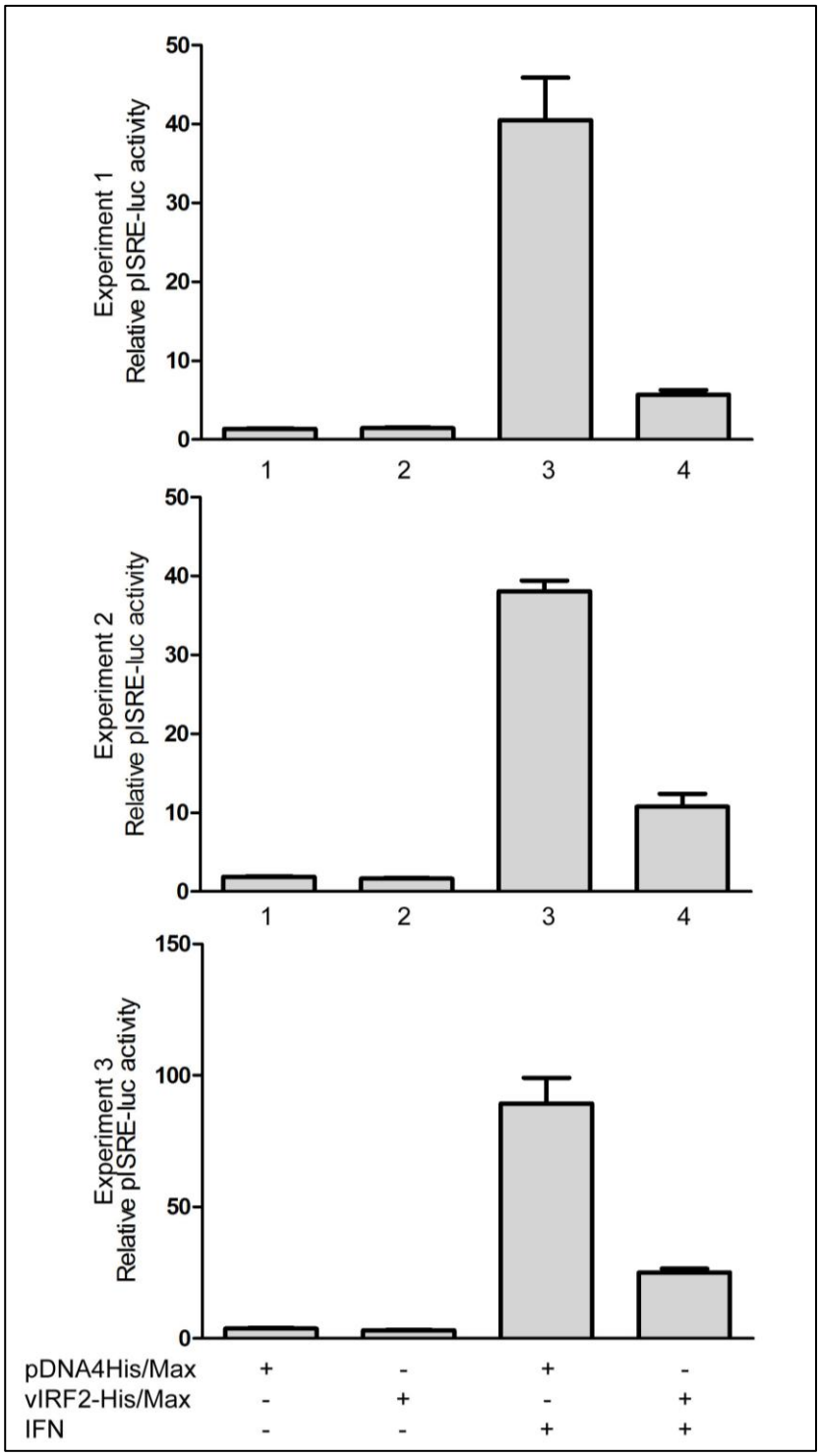

Figure 9.4: vIRF2 inhibits the rIFNα activated ISRE-containing promoter. Experiment performed as in Figure 3.8. The data presents the relative luciferase activity (normalised to *Renilla* levels) of three individual experiments.

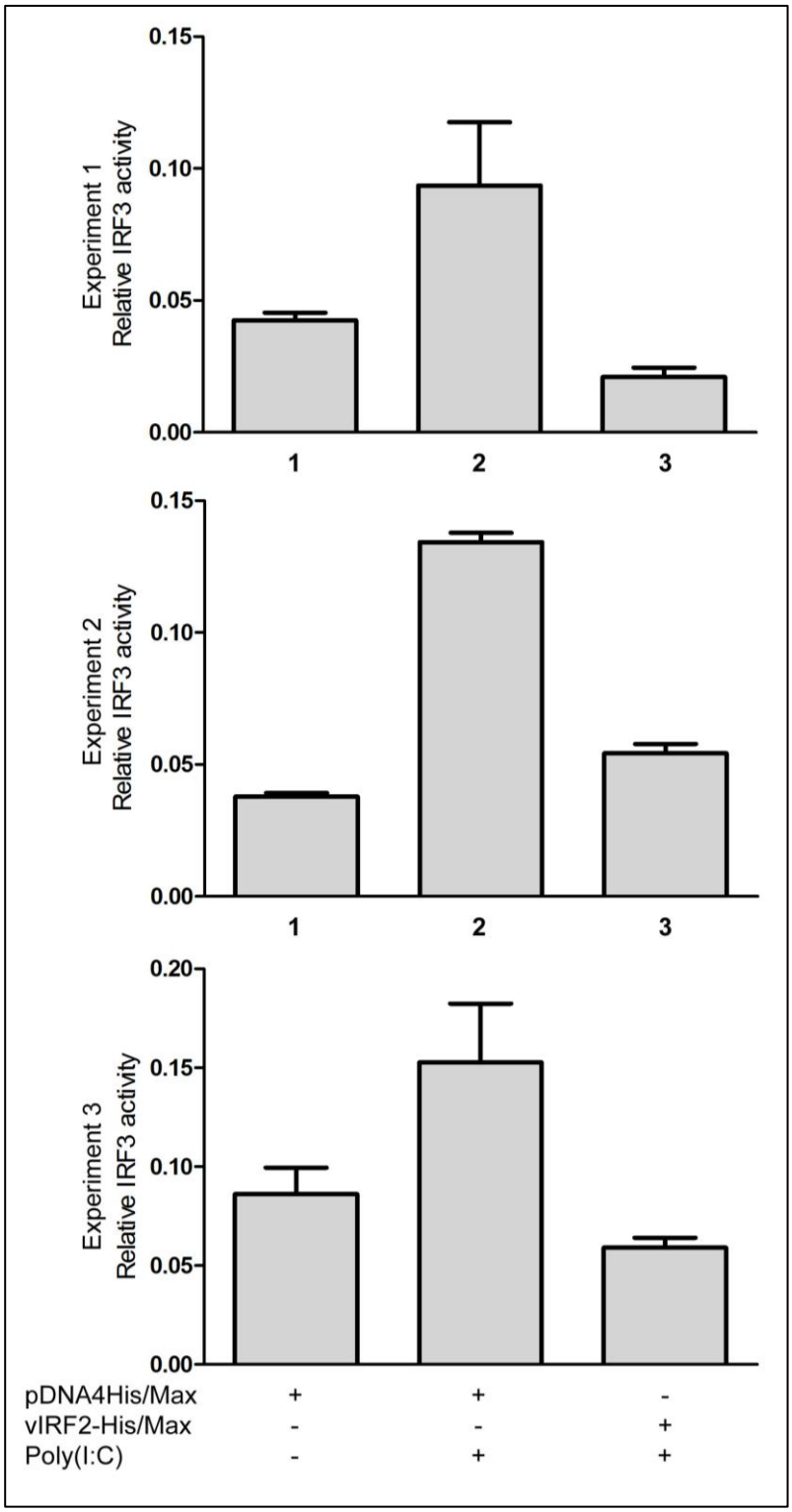

Figure 9.5: vIRF2 decreases the activity or IRF3. Experiment performed as in Figure 3.9. The data presents the relative IRF3-activity (normalised to *Renilla* levels) of three individual experiments.

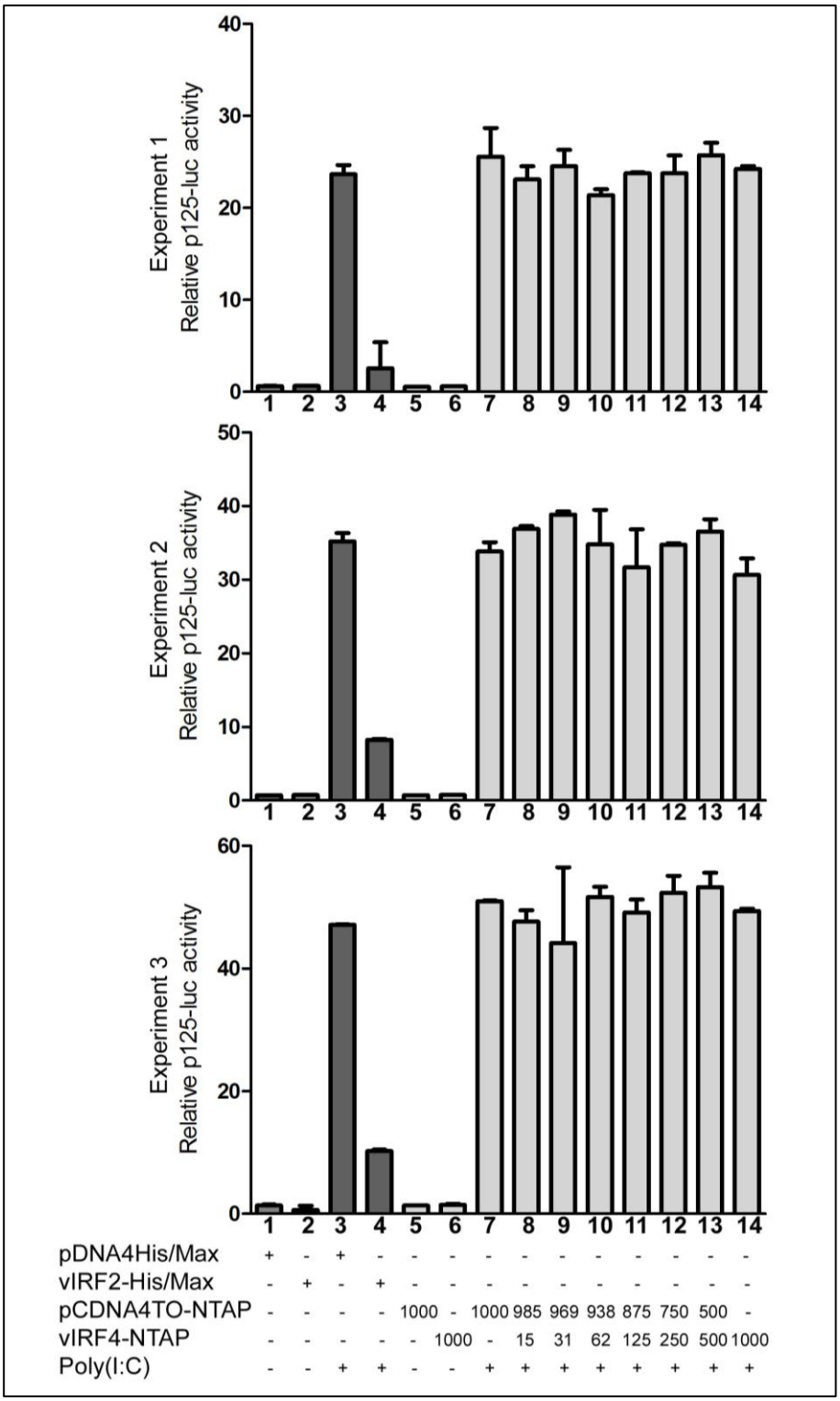

Figure 9.6: vIRF4 does not inhibit poly(I:C)-driven activation of the IFNβ promoter. Experiment performed as in Figure 3.10. The data presents the relative luciferase activity (normalised to *Renilla* levels) of three individual experiments.

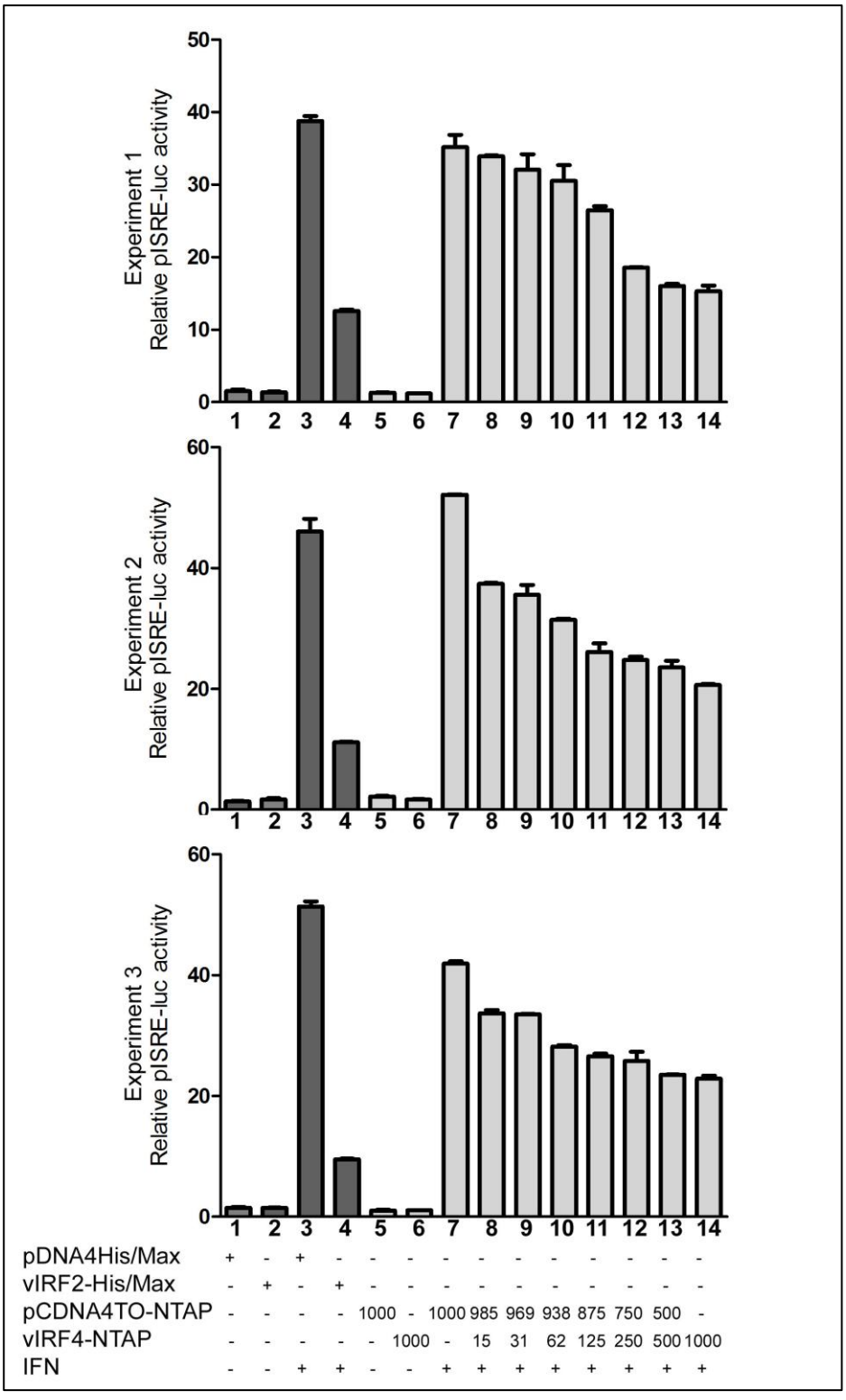

Figure 9.7: vIRF4 inhibits rIFNα-driven expression of pISRE-luc. Experiment performed as in Figure 3.11. The data presents the relative luciferase activity (normalised to *Renilla* levels) of three individual experiments

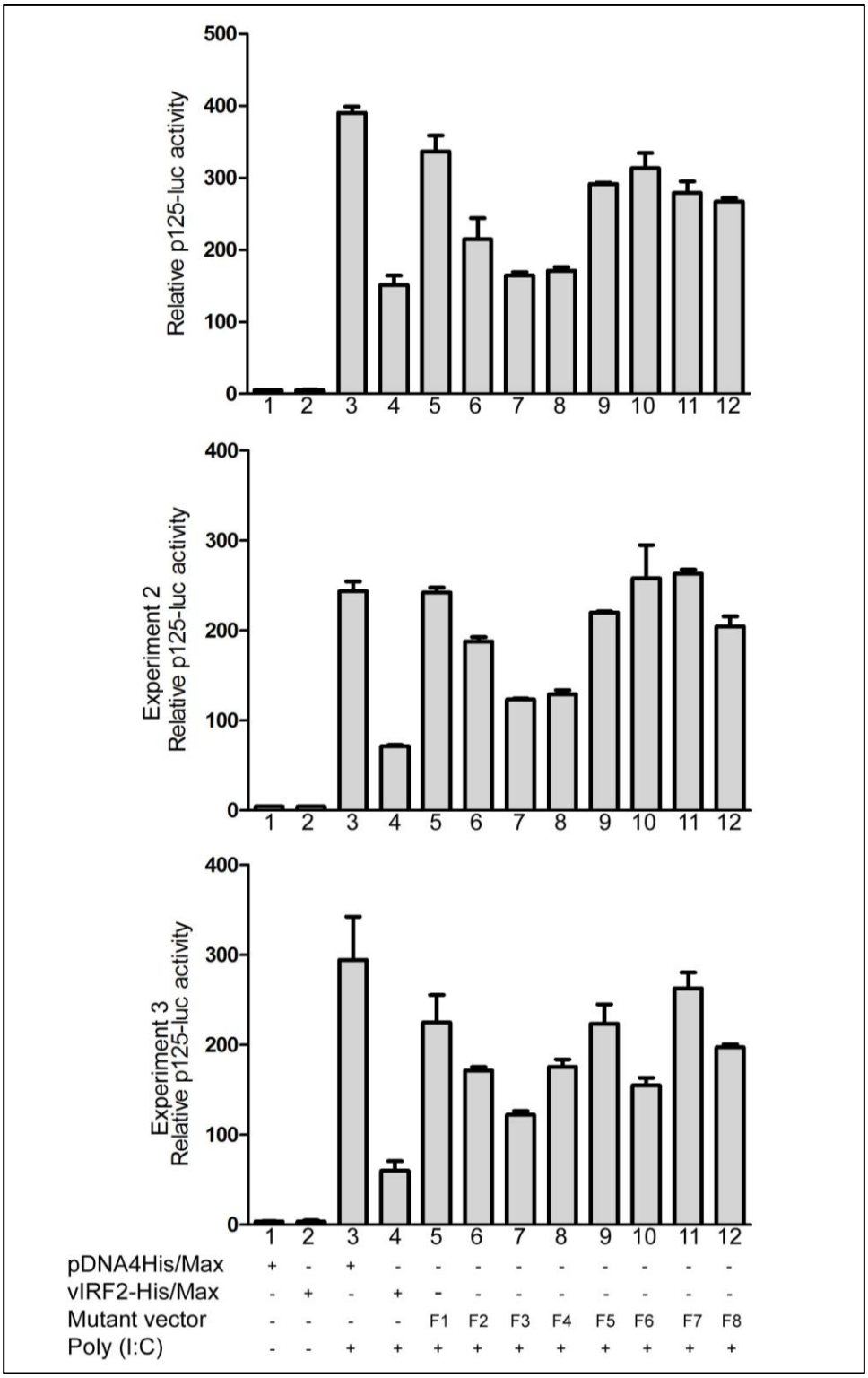

Figure 9.8: The effect of the vIRF2 truncated mutants on poly(I:C)-driven activation of the IFNβ promoter. Experiment performed as in Figure 3.13. The data presents the relative luciferase activity (normalised to *Renilla* levels) of three individual experiments

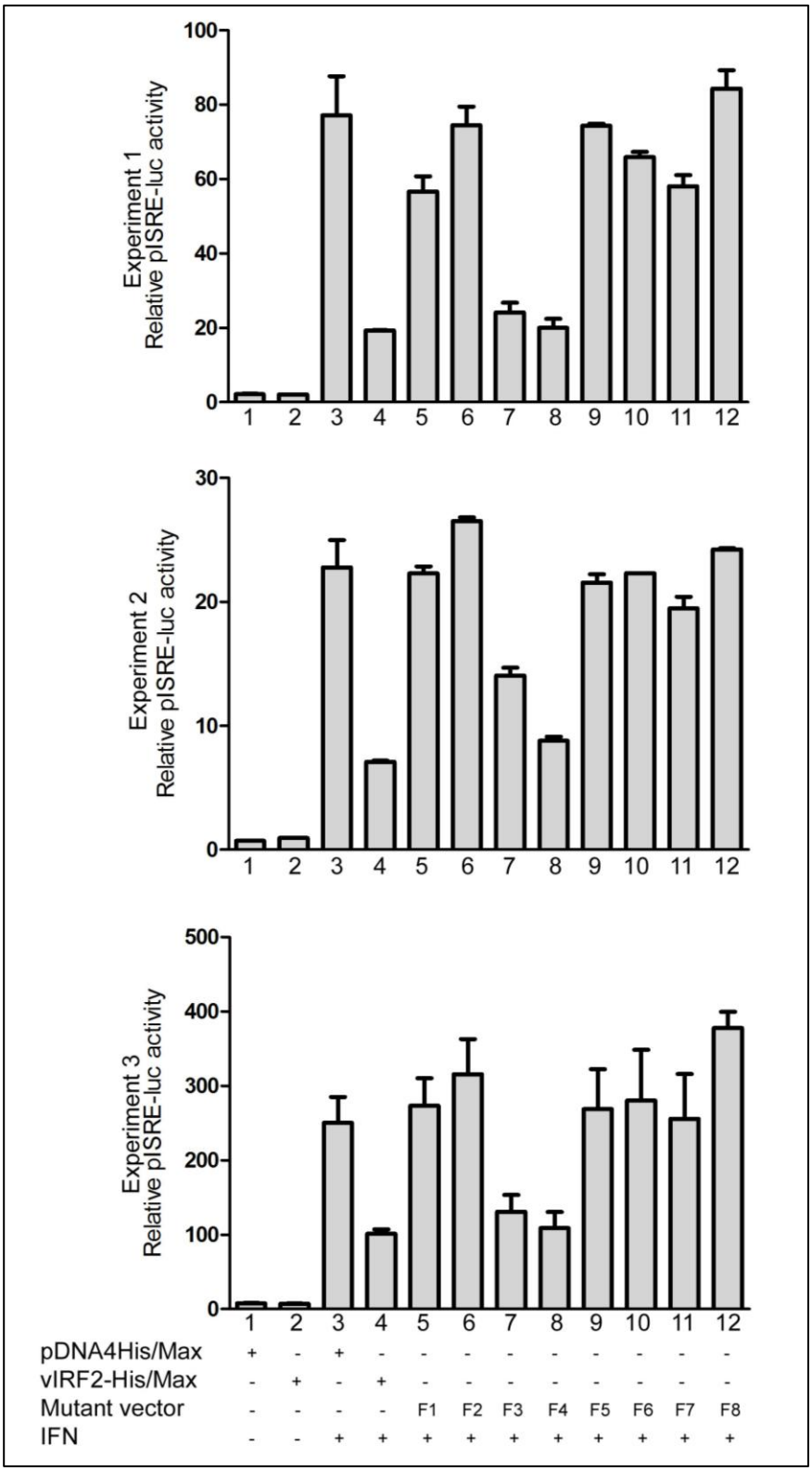

Figure 9.9: The effect of the vIRF2 truncated mutants on rIFNα activation of an ISRE-containing promoter. **.** Experiment performed as in Figure 3.14. The data presents the relative luciferase activity (normalised to *Renilla* levels) of three individual experiments.

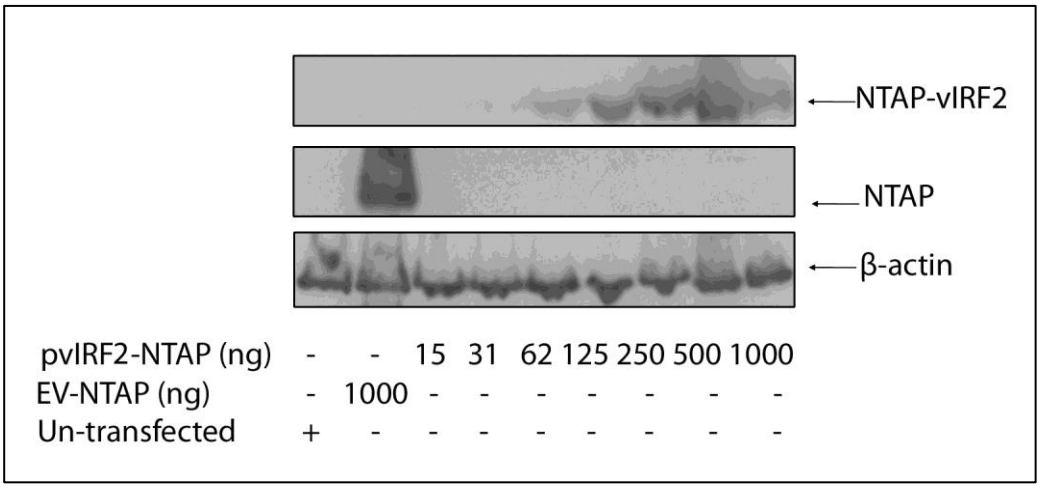

Figure 9.10: vIRF2 expresses in 293 cells transfected with the vIRF2-NTAP vector. Replicate experiment performed as in Figure 4.2.

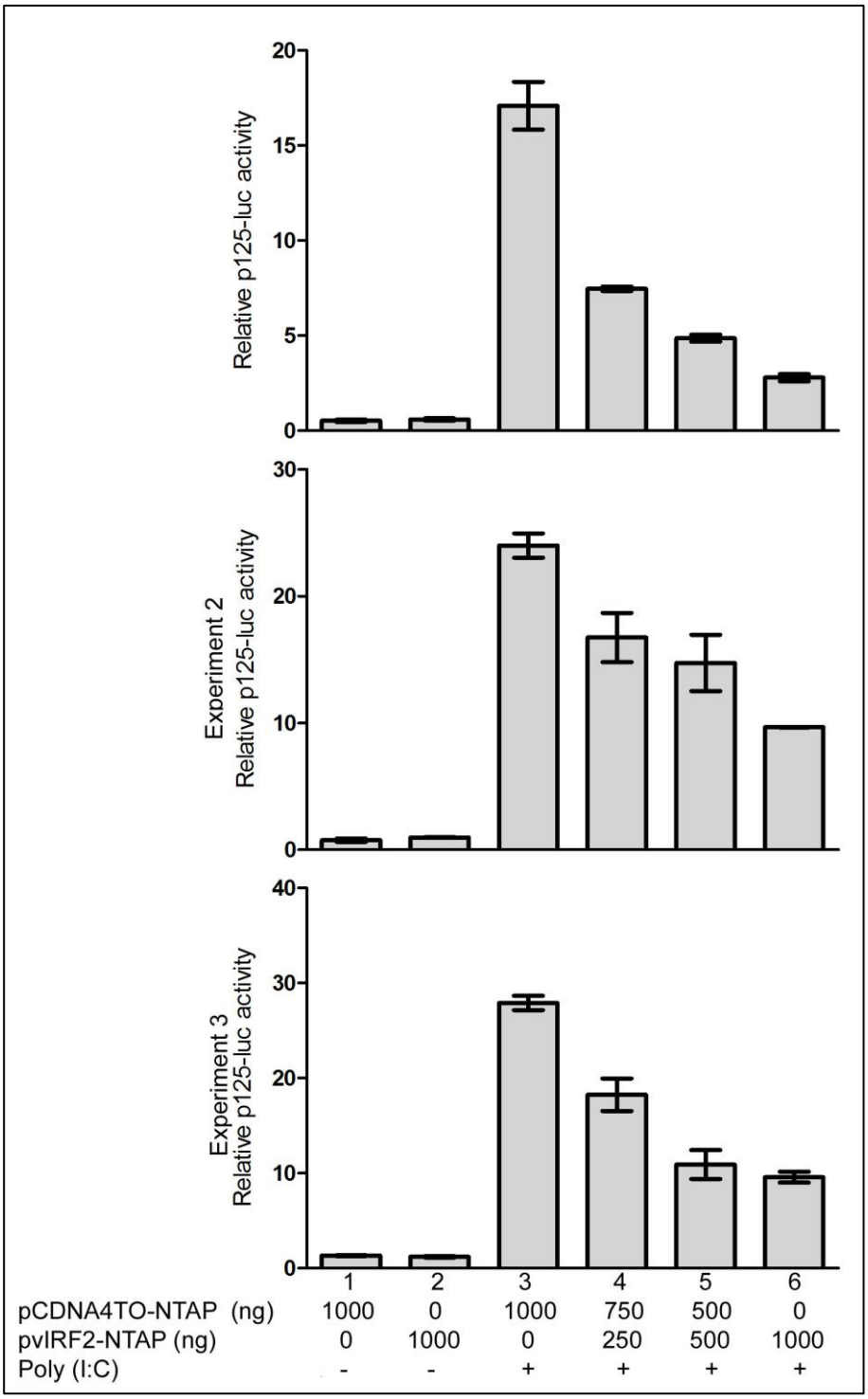

Figure 9.11: vIRF2 inhibits poly(I:C)-driven activation of the IFNβ promoter. Experiments performed as in Figure 4.3. The data represent the relative luciferase activity (normalised to *Renilla* levels) of three individual experiments each assayed in duplicate. The range between duplicates is shown.

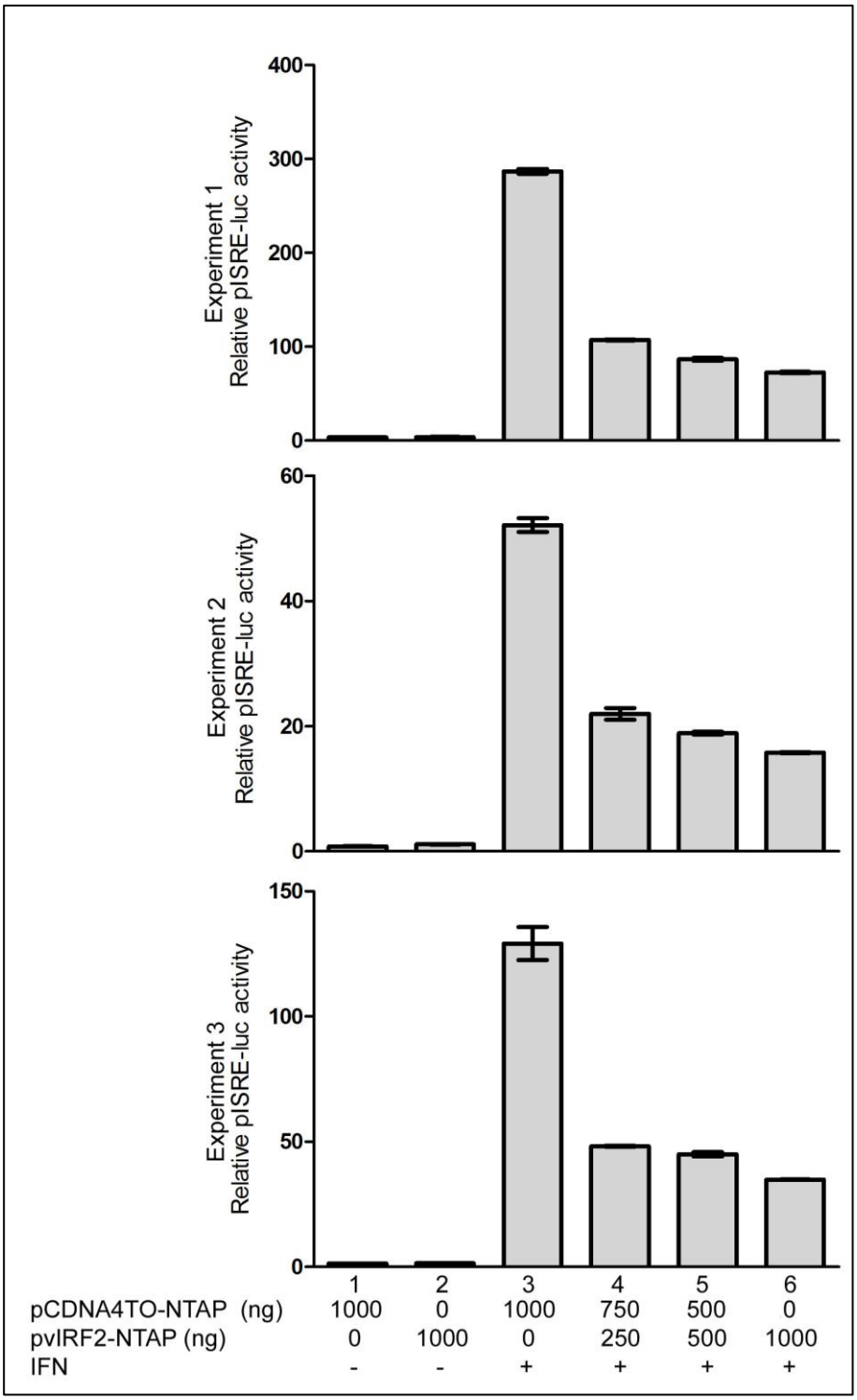

Figure 9.12: vIRF2, expressed from the pvIRF2-NTAP vector, inhibits rIFNα-driven expression of pISRE-luc Experiments performed as in Figure 4.4. The represent show the relative luciferase activity (normalised to *Renilla* levels) of three individual experiments each assayed in duplicate. The range between duplicates is shown.

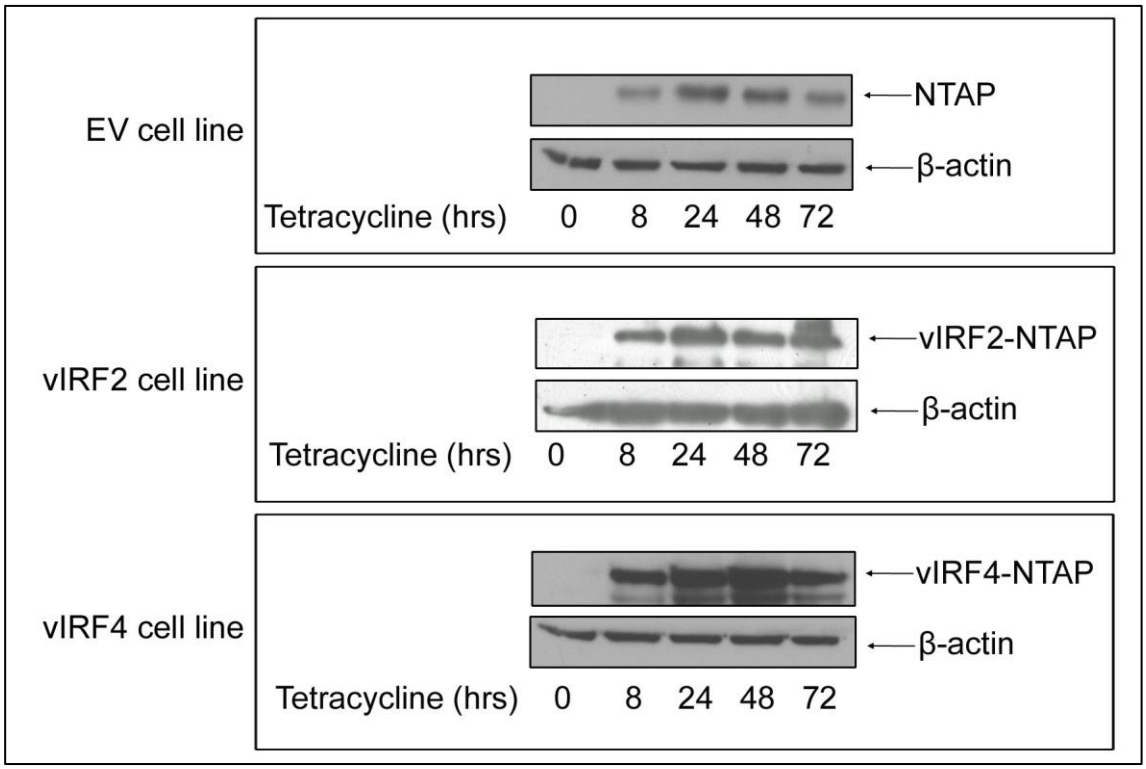

Figure 9.13: 24 hours of tetracycline treatment is necessary for expression of the NTAP-tagged proteins. Replicate experiments performed as in Figure 4.6.

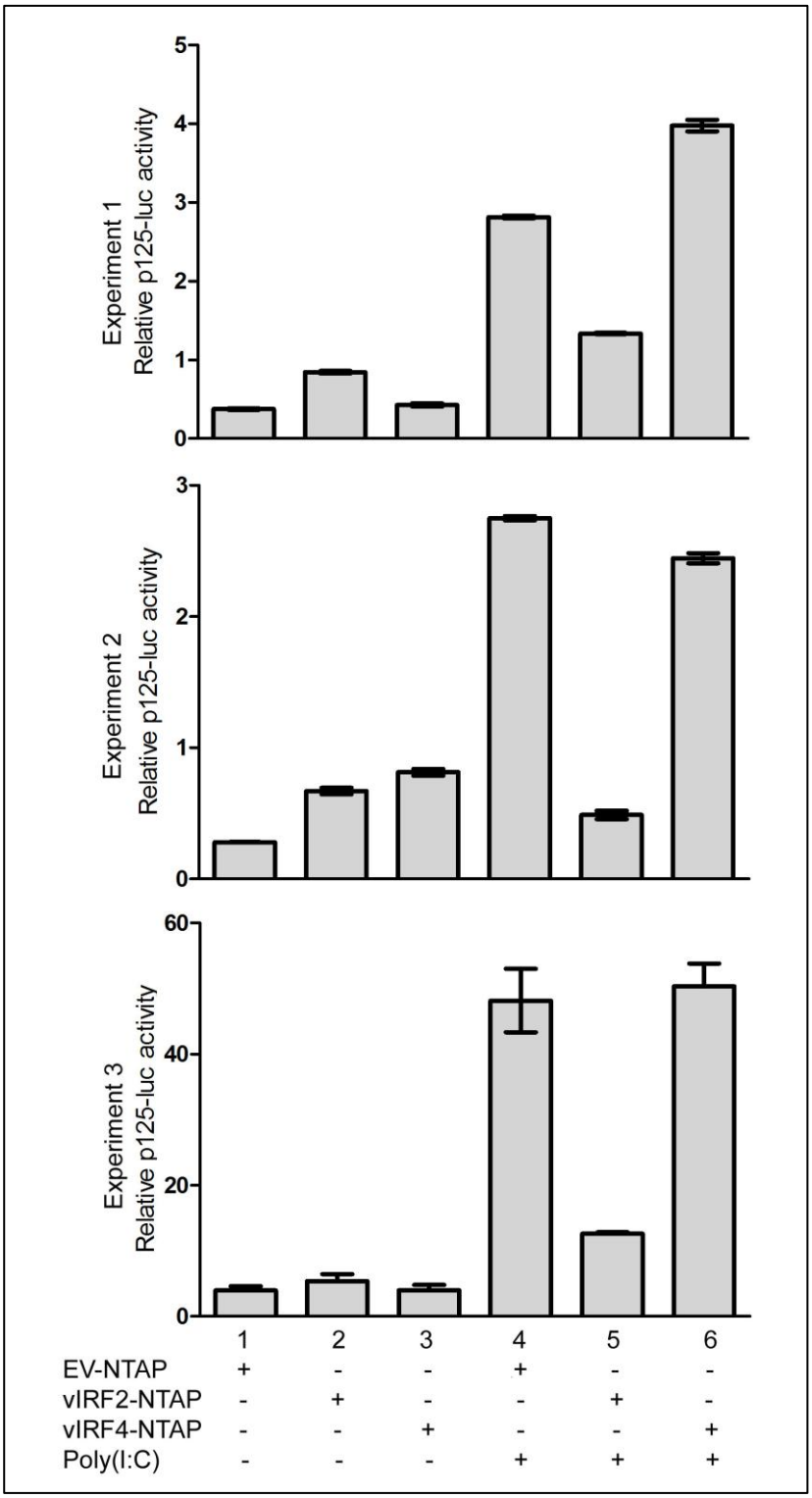

Figure 9.14: vIRF2 inhibits IFNβ promoter activation, while vIRF4 has no effect on IFNβ promoter activation Experiments performed as Figure 4.8. The data represent the relative luciferase activity (normalised to *Renilla* levels) of three individual experiments assayed in duplicate. The range between duplicates is shown.

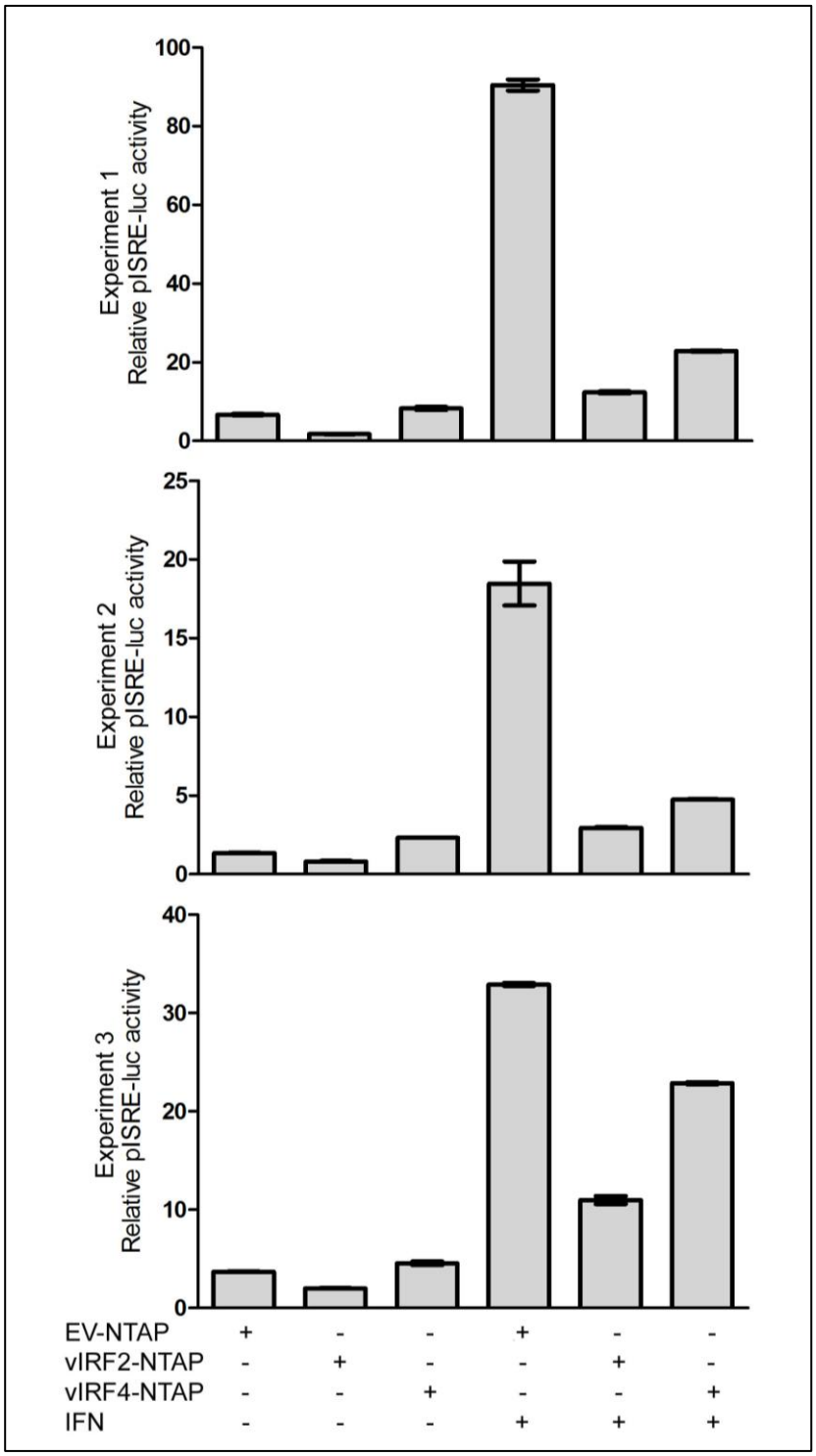

Figure 9.15: vIRF2 and vIRF4 inhibit ISRE-containing promoter activation Experiment performed as in Figure 4.9. The data represent the relative luciferase activity (normalised to *Renilla* levels) of three individual experiments each assayed in duplicate. The range between duplicates is shown.

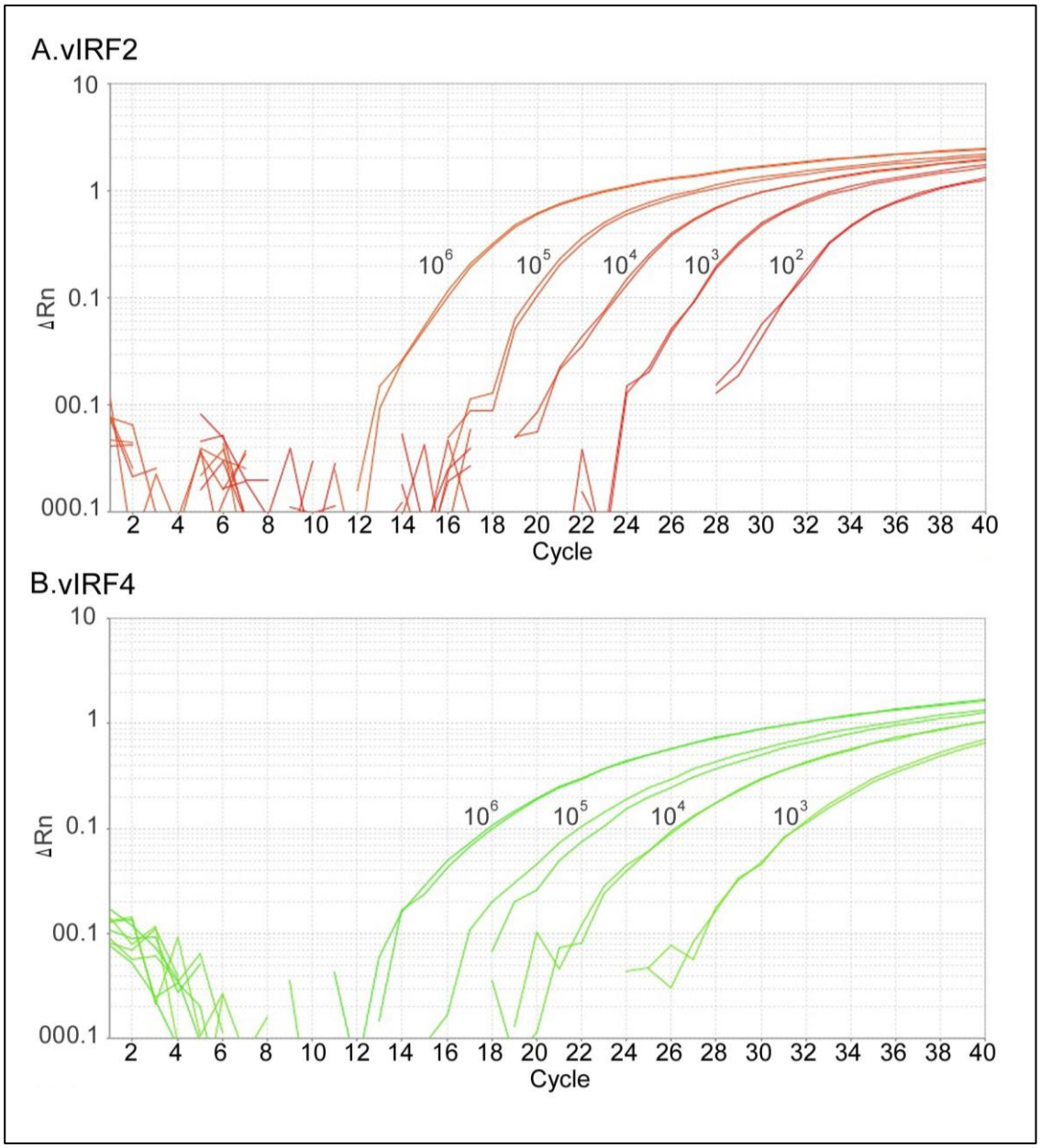

Figure 9.16: qPCR amplification plots for spiked pvIRF2-NTAP or pvIRF4-NTAP plasmids.

(A) Known amounts (from 10^2–10^6 copies, shown on graph) of the pvIRF2-NTAP plasmid were spiked into the PCR assay. The primers (see Table 2.20, vIRF2) were used at 3µM and the FAM-labelled probe (see Table 2.19, vIRF2) was used at 5µM. Samples were analysed in duplicate. (B) Performed as in A, but with the pvIRF4-NTAP plasmid spiked in. vIRF4 primers (see Table 2.20) were used at 3µM and the FAM-labelled probe (see Table 2.19, vIRF4) was used at 10µM.

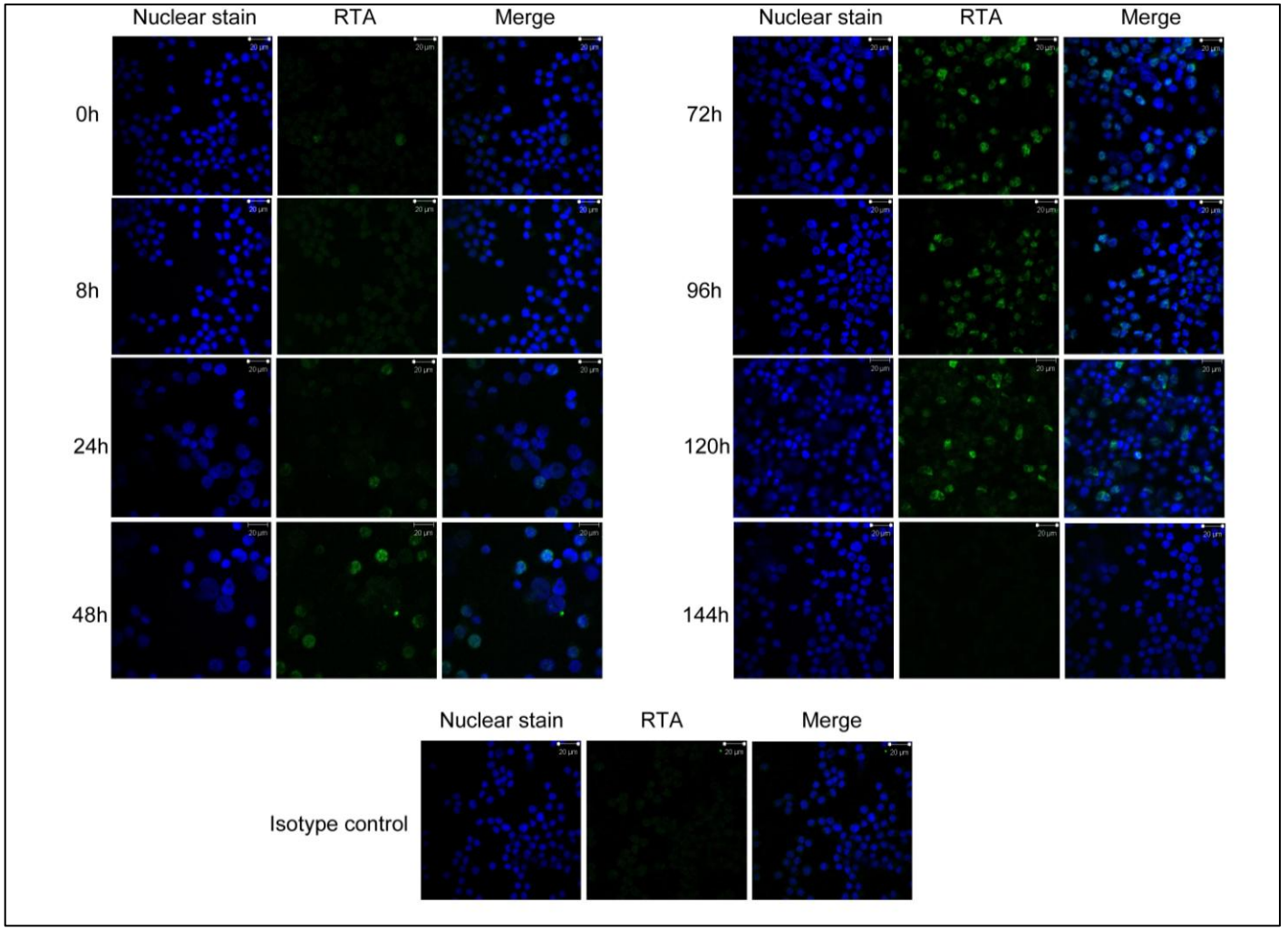

Figure 9.17: Time course of RTA expression in BCBL1 cells following reactivation. Experiment performed as in Figure 4.10

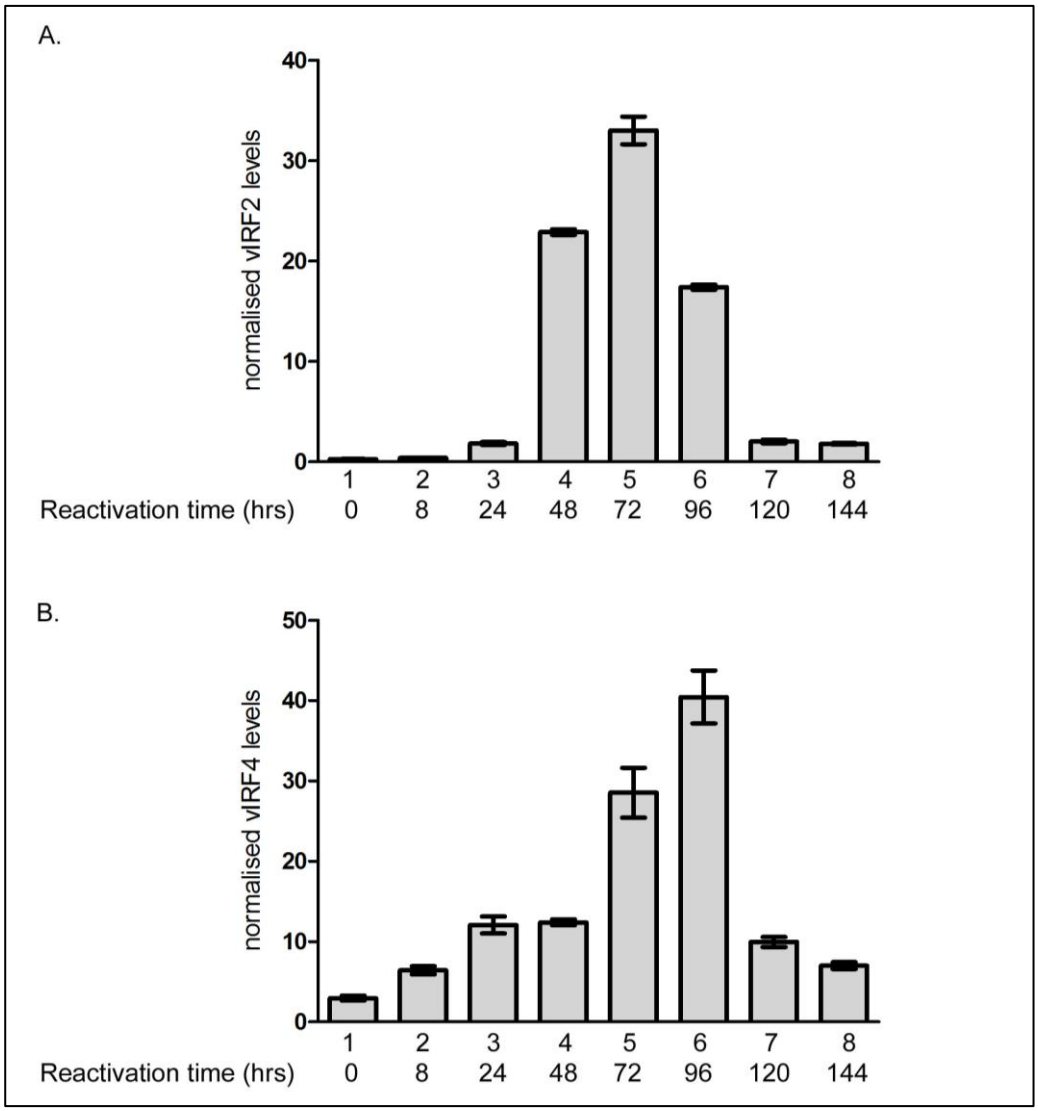

Figure 9.18: Optimum expression of vIRF2 and vIRF4 mRNA in BCBL1 cells, following lytic reactivation of KSHV. Experiment performed as in Figure 4.11. The data were normalized to cellular GAPDH levels and results were expressed relative to 0 hours (lane 1). The data represent the mean from one representative experiment which was assayed in duplicate; the range between duplicate values is indicated.

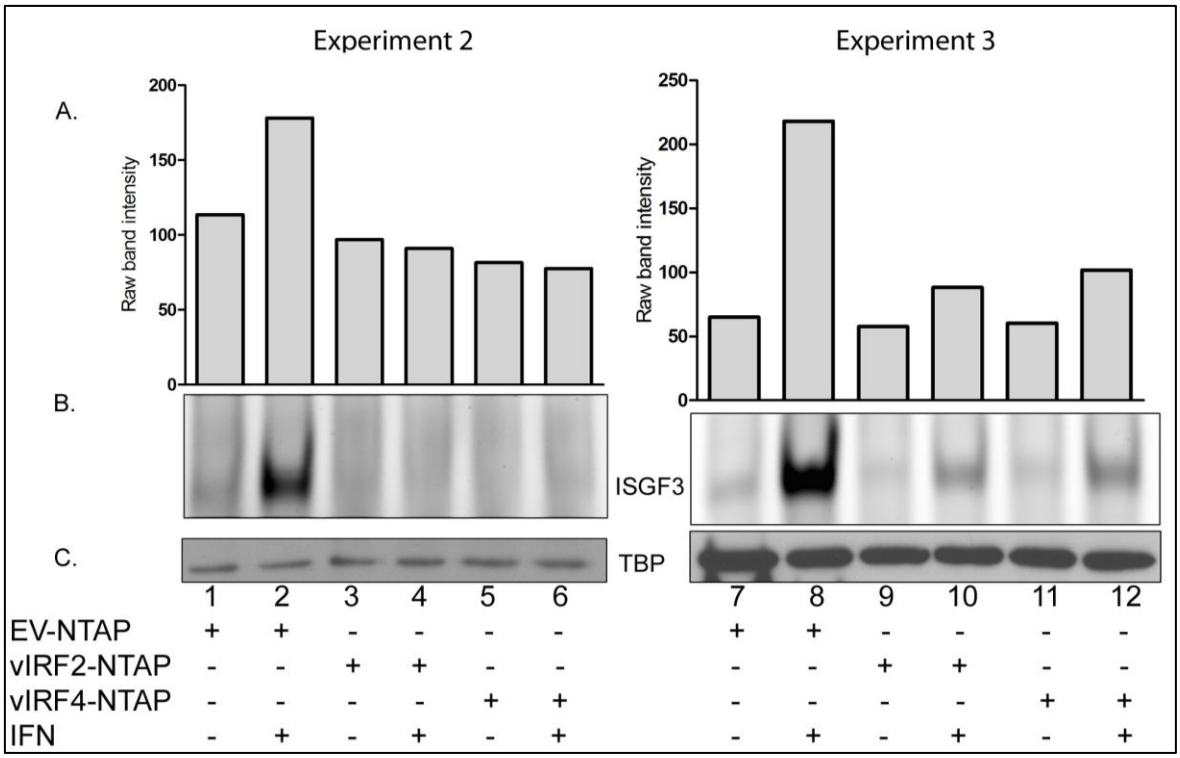

Figure 9.19: vIRF2 and vIRF4 inhibit binding of ISGF3 to an ISRE probe. Experiments performed as in Figure 5.2. Band intensities were quantified from 3 ISGF3 EMSA assays. The band intensities (A) are shown from the EMSA assays (B). Western blotting for TBP confirmed equal loading (C).

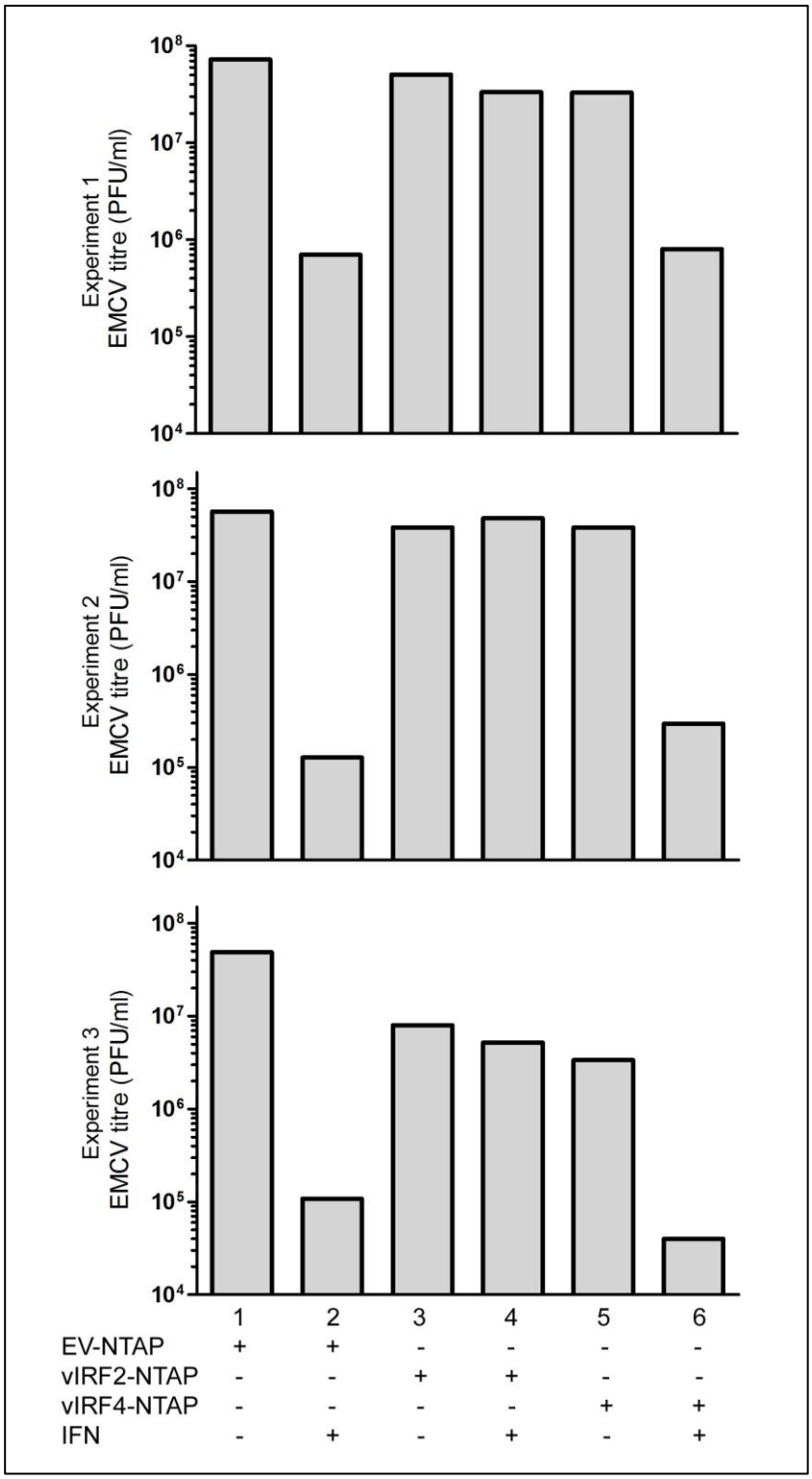

Figure 9.20: vIRF2, but not vIRF4 is able to rescue EMCV titre from the effects of rIFNα. Experiments performed as in Figure 5.1.

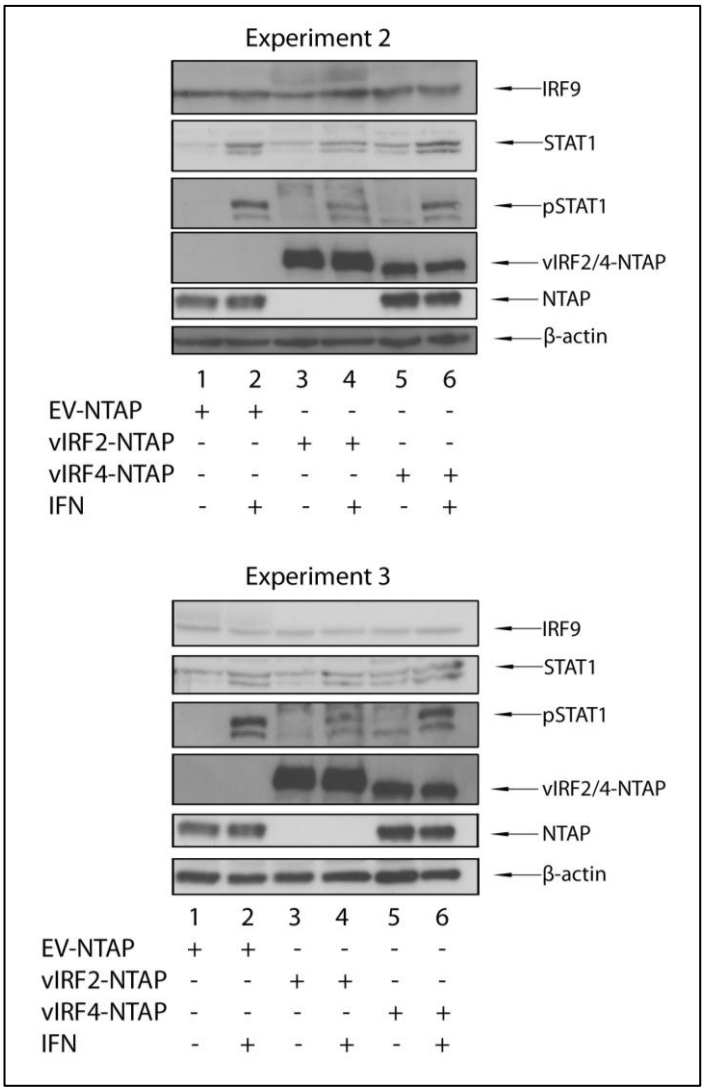

Figure 9.21: pSTAT1 is reduced in the vIRF2-NTAP cell line compared to the EV-NTAP cell line. Experiments performed as in Figure 5.4

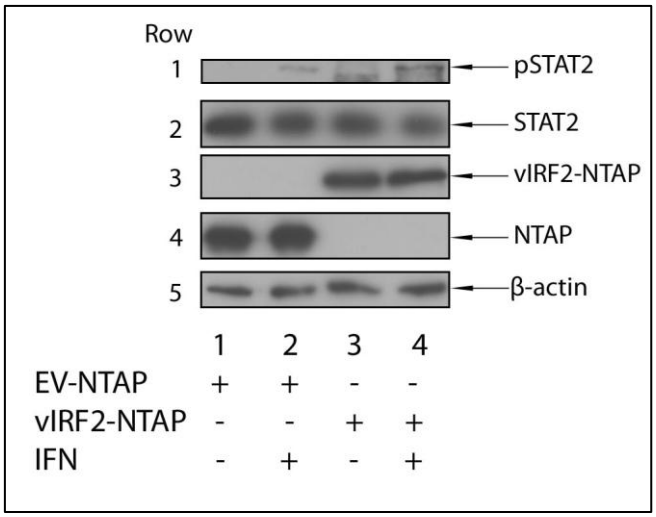

Figure 9.22: vIRF2 does not effect levels of STAT2 and pSTAT2. Experiments performed as in Figure 5.6

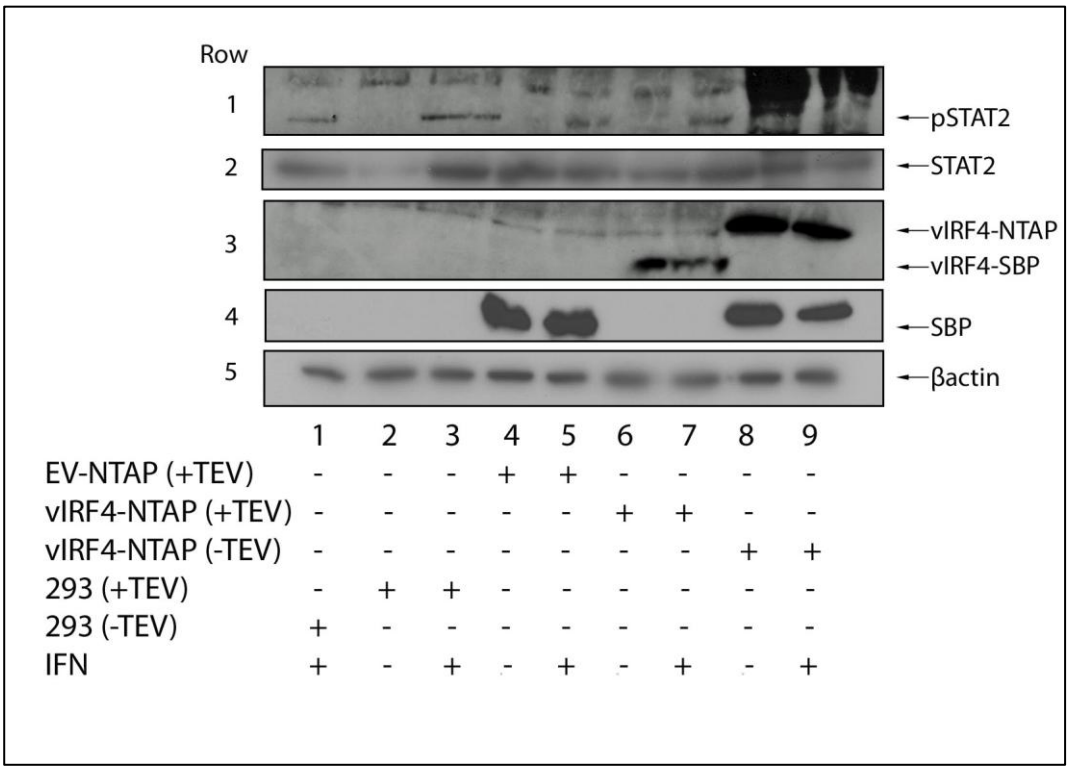

Figure 9.23: vIRF4 does not effect levels of STAT2 and pSTAT2. Experiments performed as in Figure 5.8.

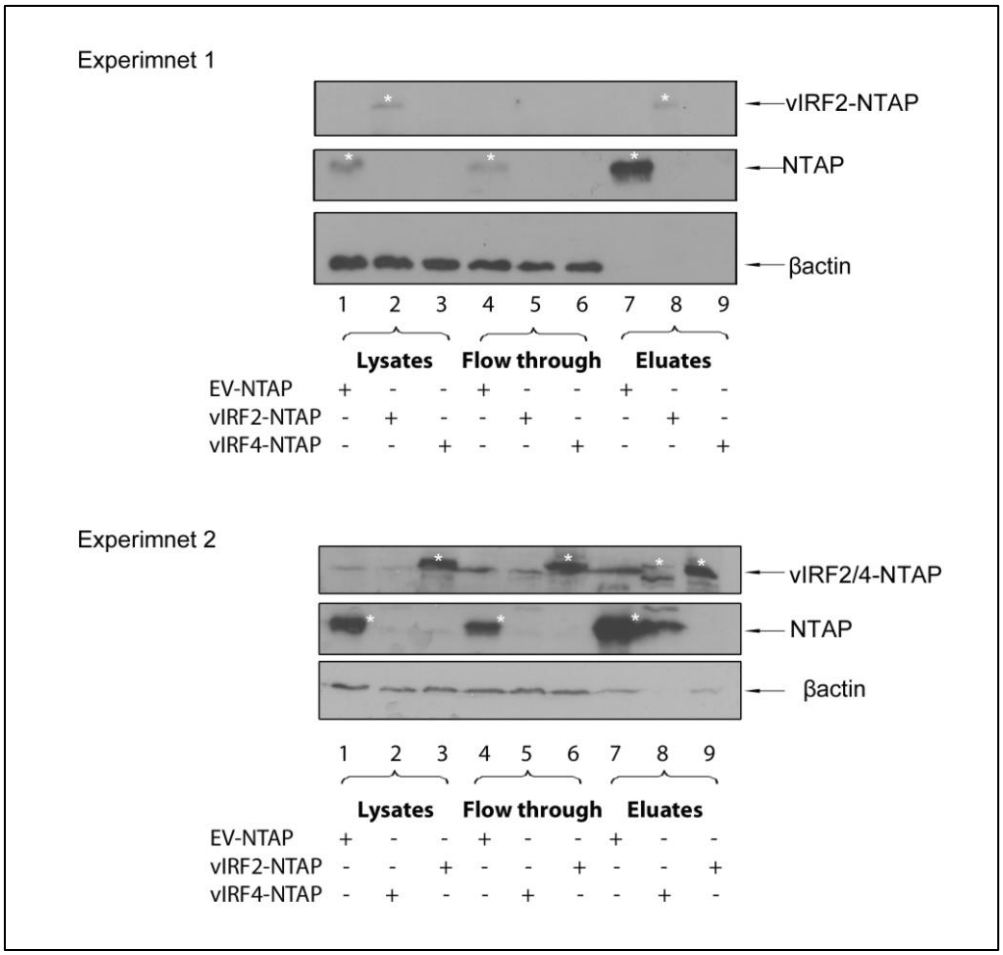

Figure 9.24: Pull down samples collected at various stages of the process Experiment performed as in Figure 6.2

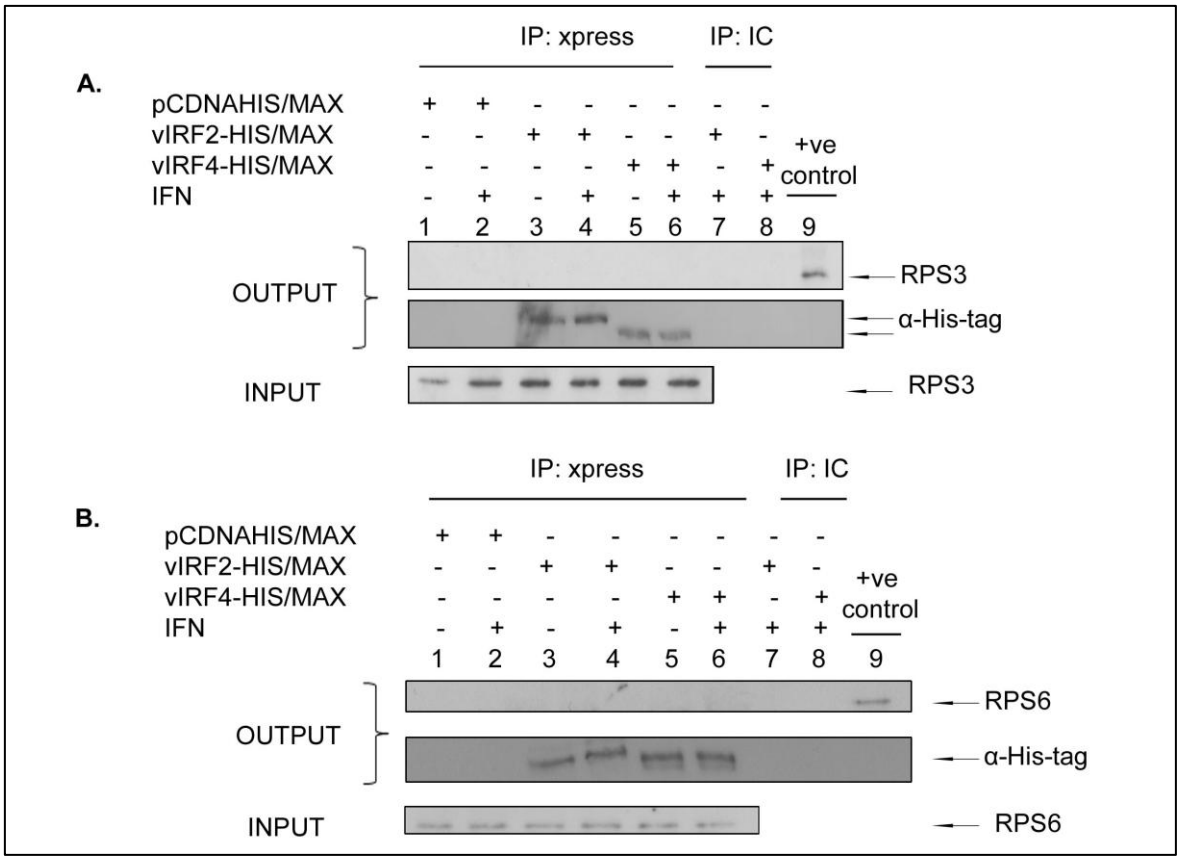

Figure 9.25: vIRF2 and vIRF4 do not associate with RPS3 or RPS6. Experiments performed as in Figure 7.2

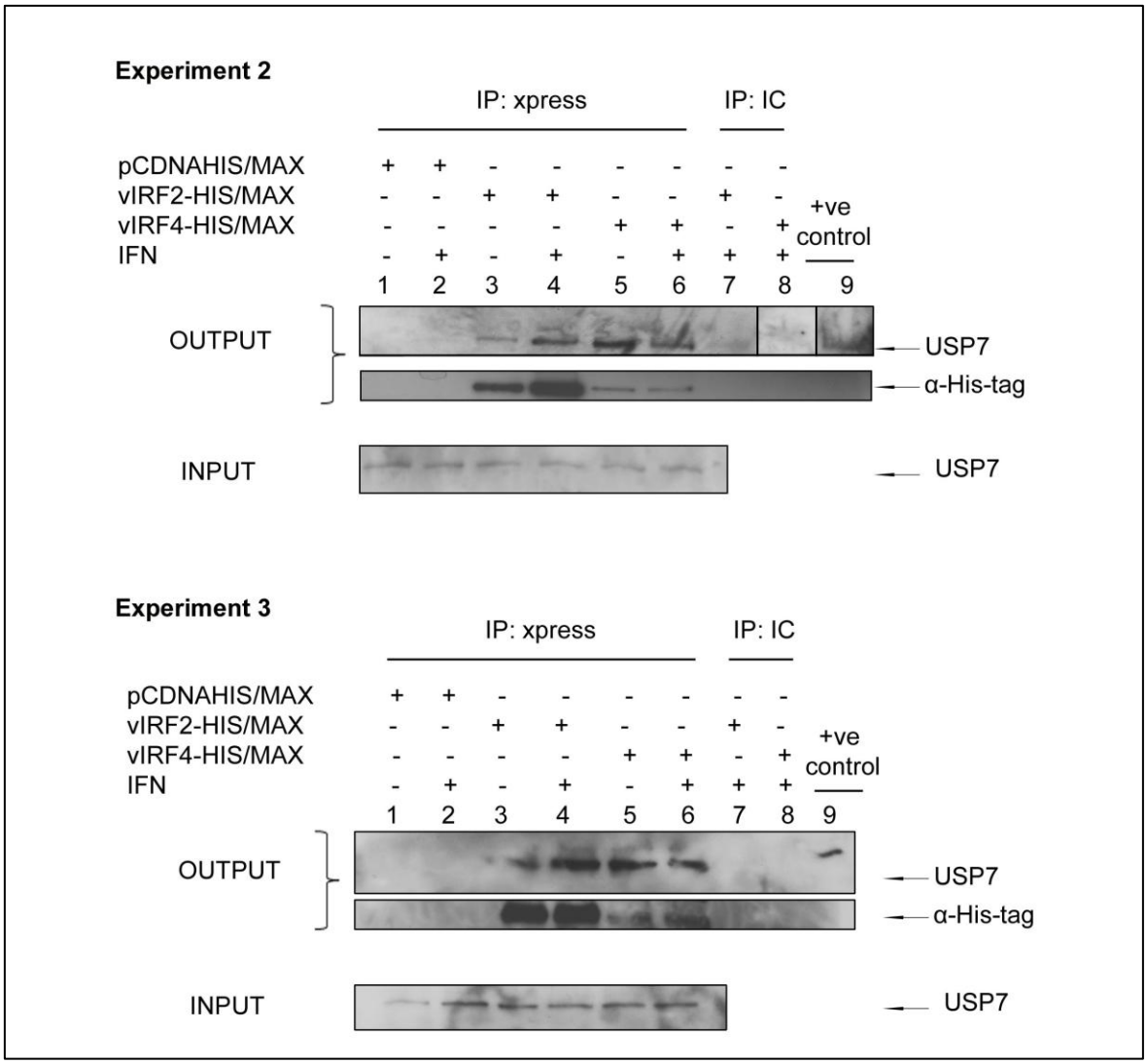

Figure 9.26: vIRF2 and vIRF4 associate with USP7. Experiments performed as in Figure 7.4

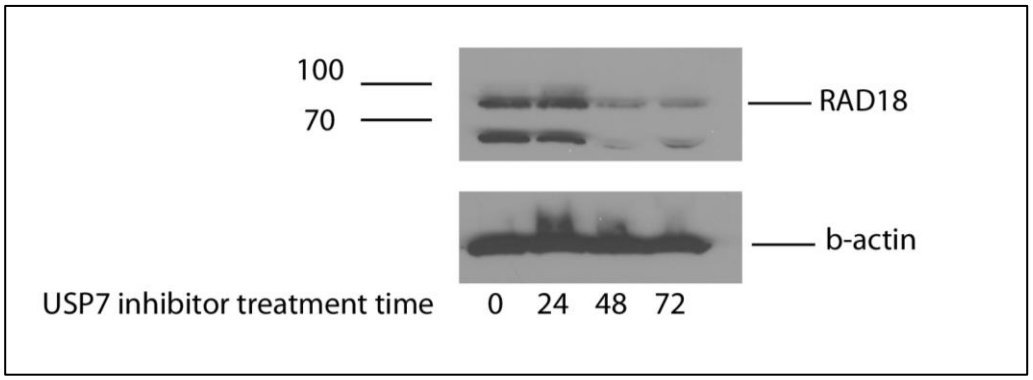

Figure 9.27: RAD18 levels are reduced after 28 hours of treatment with the USP7 inhibitor. Experiment performed as in Figure 7.5

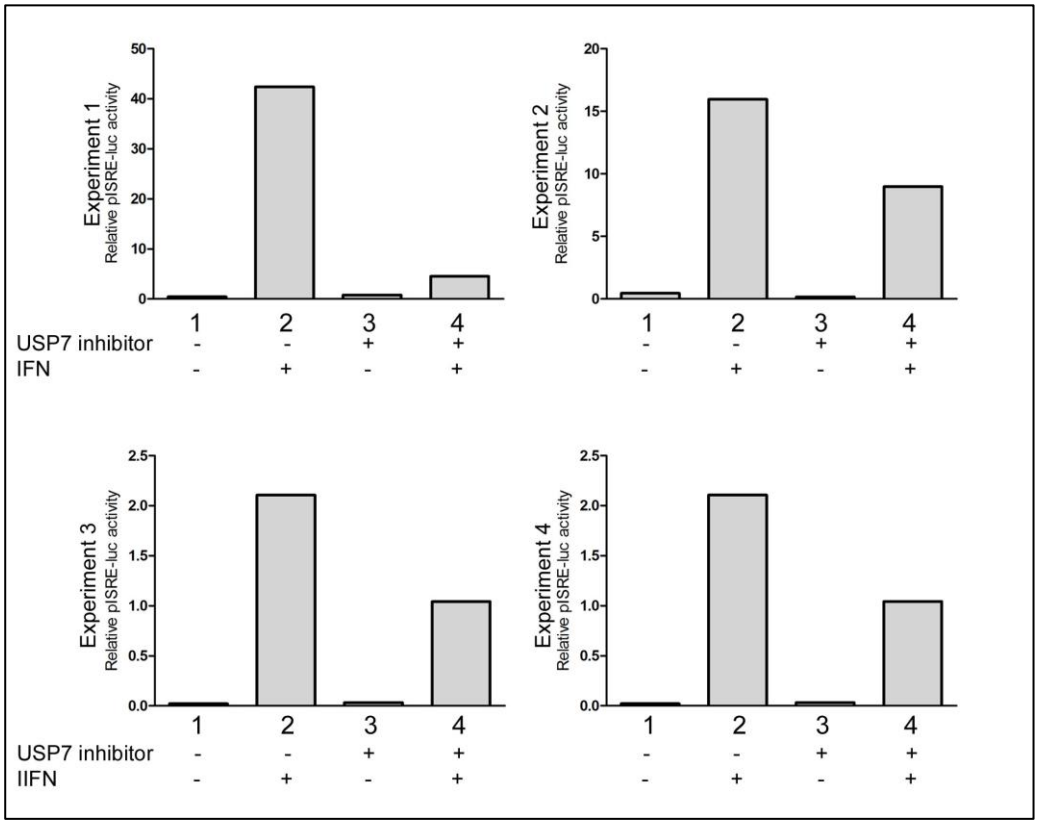

Figure 9.28: Inhibition of USP7 causes an inhibition in JAK-STAT signalling. Experiments performed as in Figure 7.6

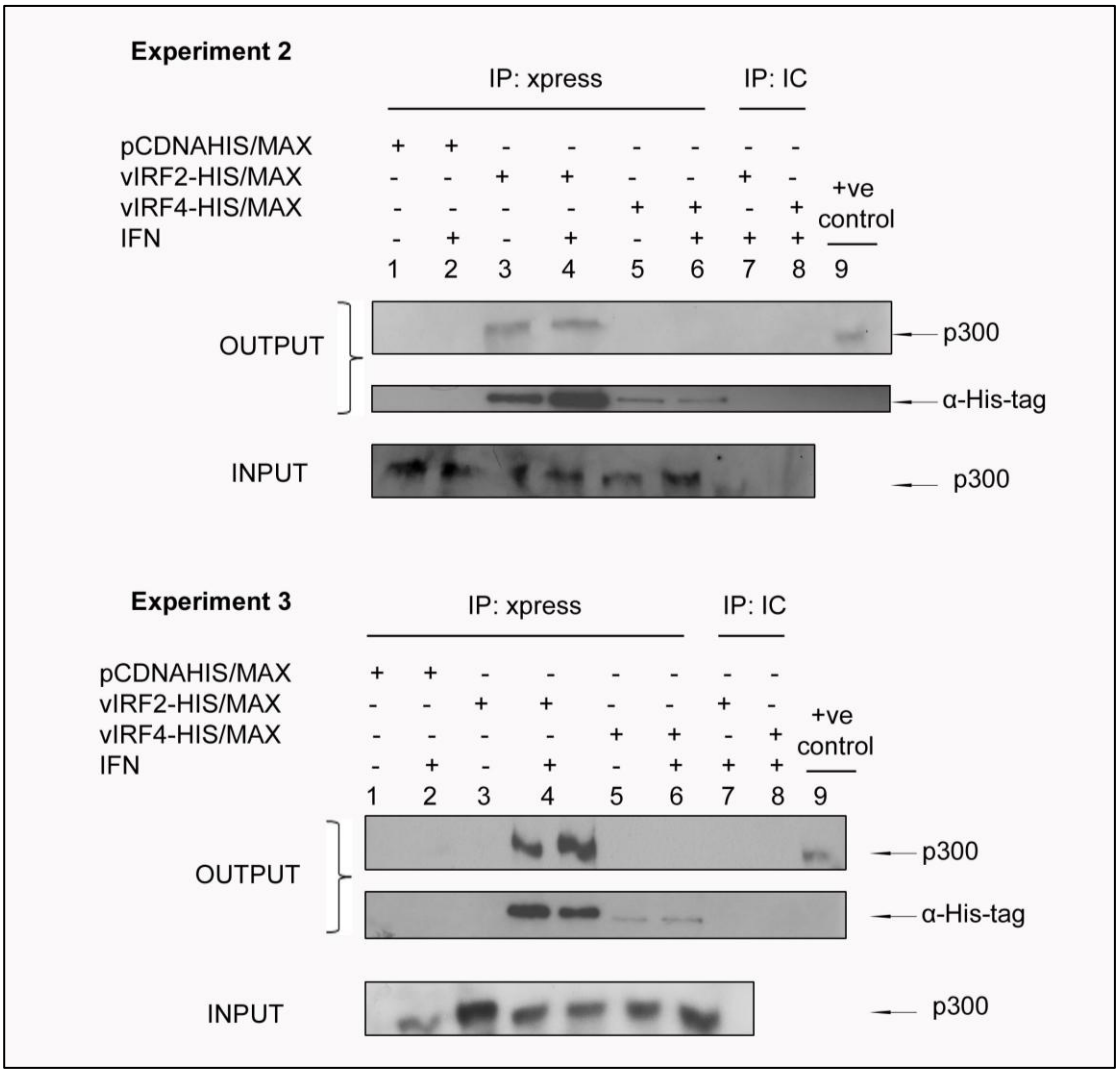

Figure 9.29: vIRF2 but not vIRF4 associates with p300. Experiments performed as in Figure 7.7

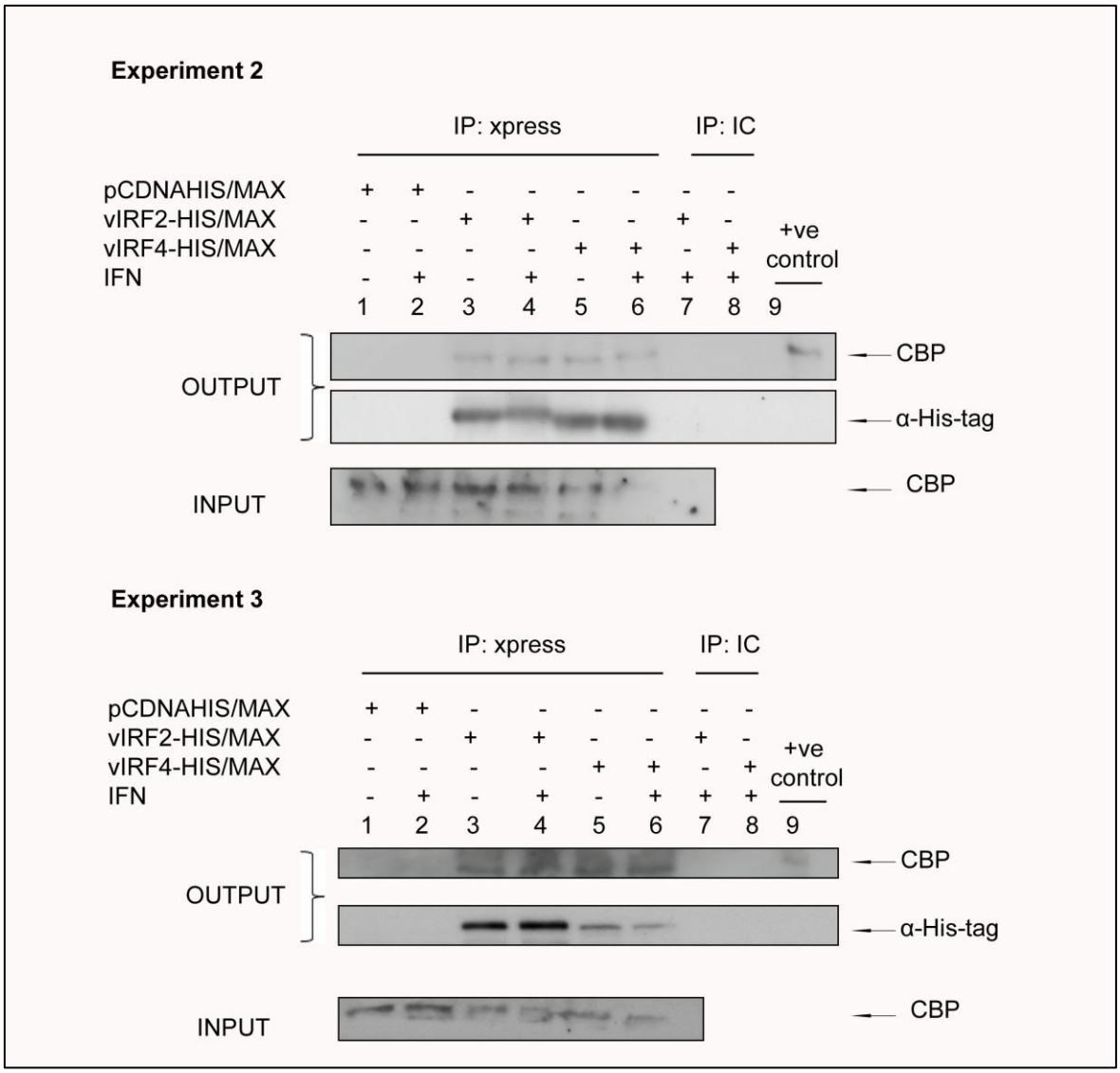

Figure 9.30: vIRF2 and vIRF4 associate with CBP. Experiments performed as in Figure 7.8

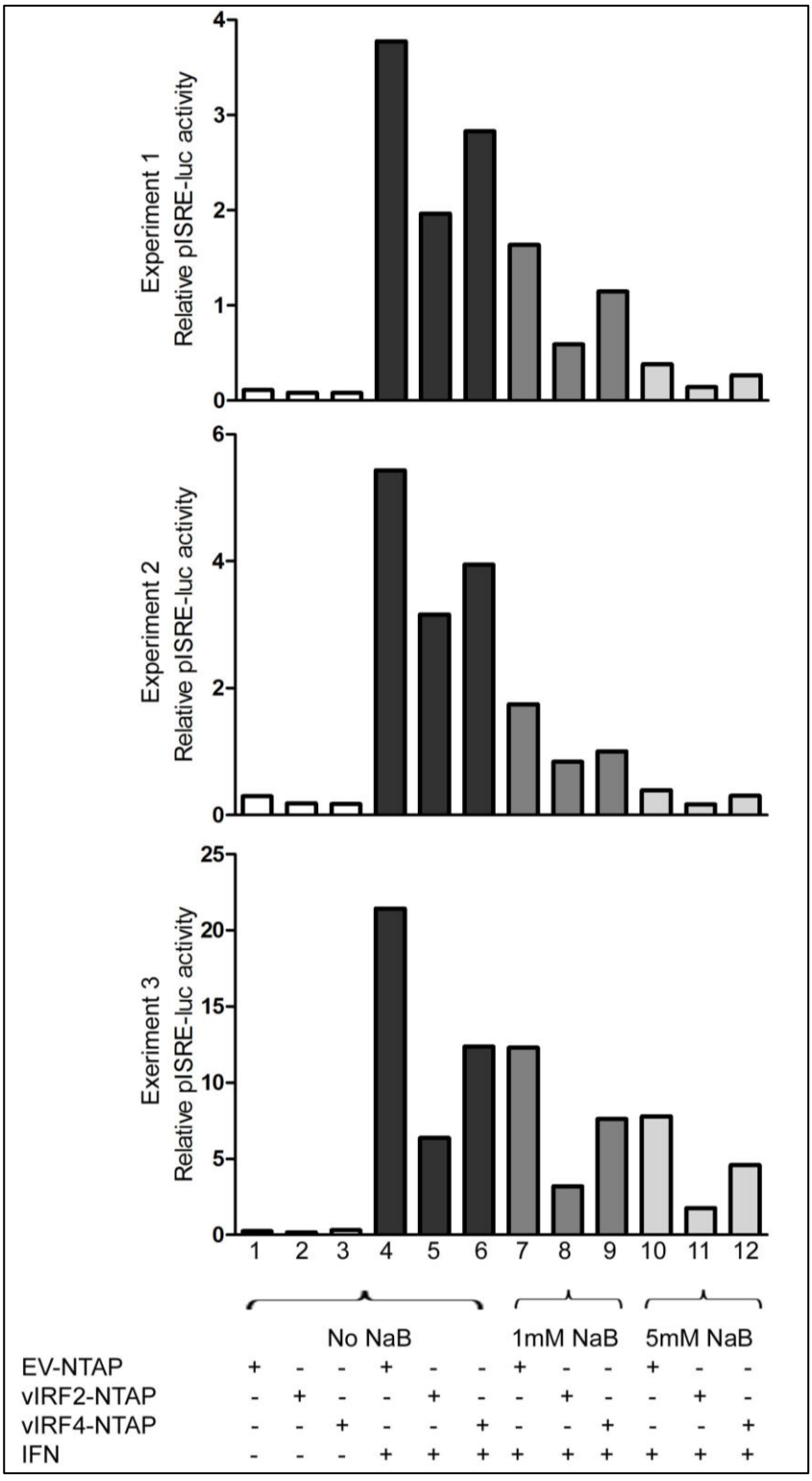

Figure 9.31: NaB does not rescue the inhibition of ISRE-reporter activity by the vIRF2 and vIRF4 proteins. Raw data Experiments performed as in Figure 7.10. The data presents the relative luciferase activity (normalised to Renilla levels) of three individual experiments.

9.3. Publication arising from this work

Please see next page

Journal of General Virology (2011), **92**, 2394–2398 DOI 10.1099/vir.0.034322-0

Short Communication

Kaposi's sarcoma-associated herpesvirus viral interferon regulatory factor-2 inhibits type 1 interferon signalling by targeting interferon-stimulated gene factor-3

M. Mutocheluh,[1] L. Hindle,[1] C. Aresté,[1]† S. A. Chanas,[1] L. M. Butler,[1,2] K. Lowry,[3] K. Shah,[4] D. J. Evans[3] and D. J. Blackbourn[1,5]

Correspondence
D. J. Blackbourn
d.j.blackbourn@bham.ac.uk

[1]School of Cancer Sciences and Cancer Research UK Cancer Centre, College of Medical and Dental Sciences, University of Birmingham, Birmingham B15 2TT, UK

[2]School of Clinical and Experimental Medicine, College of Medical & Dental Sciences, University of Birmingham, Birmingham B15 2TT, UK

[3]School of Life Sciences, University of Warwick, Coventry CV4 7AL, UK

[4]Moorfields Lions Eye Bank, Moorfields Eye Hospital NHS Foundation Trust, 162 City Road, London EC1V 2PD, UK

[5]MRC Centre for Immune Regulation, University of Birmingham, Birmingham B15 2TT, UK

Received 17 May 2011
Accepted 20 June 2011

Kaposi's sarcoma-associated herpesvirus (KSHV) encodes four viral interferon regulatory factors (vIRF-1–4). We investigated the mechanism and consequences of vIRF-2-mediated inhibition of interferon-response element signalling following type I interferon (IFN) induction. Western blot and electrophoretic mobility-shift assays identified the interferon-stimulated gene factor-3 (ISGF-3) components STAT1 and IRF-9 as the proximal targets of vIRF-2 activity. The biological significance of vIRF-2 inhibition of ISGF-3 was demonstrated by vIRF-2-mediated rescue of the replication of the IFN-sensitive virus encephalomyocarditis virus. This study provides both a mechanism and evidence for KSHV vIRF-2-mediated suppression of the consequences of type 1 IFN-induced signalling.

The earliest response at the cellular level to virus infection is the establishment of the antiviral state that results from induction of type I interferon (IFN) expression. This contains the virus infection and can eliminate the infected cell by inhibiting cellular proliferation, promoting apoptosis and augmenting adaptive immunological surveillance and responses. Consequently, either avoiding or inhibiting the IFN antiviral response is an important component of the biology of many viruses (reviewed by Randall & Goodbourn, 2008).

Kaposi's sarcoma-associated herpes virus (KSHV) (Chang *et al.*, 1994), the aetiological agent of Kaposi's sarcoma and primary effusion lymphoma (Bouvard *et al.*, 2009), encodes a family of four viral interferon regulatory factors (vIRFs) (Cunningham *et al.*, 2003), three of which (vIRF-1, -2 and -3) have anti-IFN activity (Burysek *et al.*, 1999; Fuld *et al.*, 2006; Gao *et al.*, 1997; Lubyova & Pitha, 2000; Rezaee *et al.*, 2006; Wies *et al.*, 2009; Zimring *et al.*, 1998). However, other vIRF functions are also evident; for example, vIRF-1 restricts chromatin remodelling, thereby suppressing cytokine gene expression (Li *et al.*, 2000), and augments p53 degradation by the proteasome (Shin *et al.*, 2006), while vIRF-3 inhibits MHC-II expression (Schmidt *et al.*, 2011).

We have analysed the suppressive effects of vIRF-2 on the 'delayed' interferon signalling cascade, which is induced following ligation of the type I IFN receptor and depends on the activity of interferon-stimulated gene factor 3 (ISGF-3).

To investigate the mechanism of vIRF-2 inhibition of type I IFN-induced interferon-response element (ISRE) transactivation, we derived stable cell lines in which vIRF-2 expression could be induced by doxycycline treatment. To negate clone-specific effects, three independent clonal cell lines (clones 3-9, 20 and 24) were analysed. Briefly, *vIRF-2* was subcloned in frame into the doxycycline-inducible expression vector pTRE2-pur-Myc (Clontech) to generate

†Present address: Department of Cell Death and Proliferation, Institute for Biomedical Research, c/Roselló 161, 6th floor, 08036 Barcelona, Spain.

A supplementary figure showing the results of quantification of the pSTAT1 and IRF-9 immunoblots is available with the online version of this paper.

a 5′-cMyc-tagged vIRF-2 derivative. This plasmid was transfected into HEK293-Tet-On cells (Clontech) that stably express the tetracycline-regulated transactivator rtTA; puromycin-resistant clones were then derived (as described by Aresté *et al.*, 2009). In parallel, counterpart 'empty vector' (EV) clonal cell lines lacking *vIRF-2* were derived (EV1, EV4 and EV5). Western blot analysis determined that *vIRF-2* gene expression was inducible in clones 3-9, 20 and 24 (data not shown). However, the system was inherently leaky since 'basal' vIRF-2 expression was demonstrable by Western blot analysis for all three clones, even in the absence of doxycycline treatment (data not shown), particularly with increasing passage. Functional studies of these cell lines, and the empty vector controls, were therefore performed in the presence of doxycycline to ensure maximal vIRF-2 expression. When compared with their empty-vector control counterparts, each of the three vIRF-2-expressing cell lines demonstrated significant inhibition of recombinant (r) IFN-α-induced ISRE transactivation (Fig. 1). Western blot analysis verified the presence of vIRF-2 expression in clones 3-9, 20 and 24 and not in the empty vector clones (EV1, EV4, EV5; see Fig. 2d, row 1). These data confirmed our previous studies with transient ectopic expression of vIRF-2 (Fuld *et al.*, 2006) and verified that these cell lines provided a tool with which to investigate the mechanism of vIRF-2 function.

The type I IFN-induced JAK–STAT signal transduction cascade is understood in detail (Randall & Goodbourn, 2008). It culminates in the formation of the heterotrimeric ISGF-3, which consists of IRF-9 and post-translationally activated STAT1 and STAT-2. ISGF-3 has pleiotropic effects that establish the 'antiviral state' through ISRE-containing promoters. Given that vIRF-2 reduced the activation of the ISRE promoter (Fig. 1), the abundance of functional amounts of ISGF-3 in one representative pair of clones was measured by electrophoretic mobility assay (EMSA). ISGF-3 EMSA for vIRF-2-expressing clone 3-9 compared with the counterpart EV clone 5, which lacks vIRF-2, demonstrated a significant reduction in ISRE binding (Fig. 2a, b). Probing for TATA-binding protein (TBP) confirmed equal loading of nuclear lysates in the assay (Fig. 2c). These data are consistent with reduced ISRE reporter activity in the vIRF-2-expressing cells (Fig. 1).

To investigate the mechanism of vIRF-2 reduction of functional levels of ISGF-3 in more detail (Fig. 2a, b), the relative levels of the components of the type I IFN-induced JAK–STAT signalling cascade were measured by Western blot in vIRF-2-expressing clones 3-9, 20 and 24, compared with their empty-vector control counterparts EV1, EV4 and EV5. To induce the antiviral state, cultures were treated with rIFN-α. Verification that ISRE transactivation was inhibited by vIRF-2 at the time of cell harvest for Western blotting was provided by transfecting the cultures with pISRE-luc (and the pRL-SV40-luc control plasmid) and taking parallel aliquots for a dual-luciferase assay (data not shown). Immunoblotting demonstrated the presence of expression of vIRF-2 in the relevant clones (Fig. 2d, row 1), and probing for glyceraldehyde 3-phosphate dehydrogenase (GAPDH) confirmed the equal loading of lysates in each lane (Fig. 2d, row 11). As expected, and confirming the induction of the signalling cascade induced by IFN-α binding the IFN receptor complex, Tyk2 phosphorylated at residues Tyr1054 and Tyr1055 [pTyk2 (Tyr1054/1055)] increased in all clones following IFN treatment (Fig. 2d, row 3). Tyk2 is the kinase associated with the IFN-α receptor 1 (IFNAR1) component of the common IFN type I receptor (reviewed by Randall & Goodbourn, 2008). There were no consistently detectable differences in the level of IFNAR1 between the vIRF-2-expressing clones and those lacking vIRF-2 (Fig. 2d, row 2).

Tyrosine phosphorylation of Tyk2 at residues 1054 and 1055 is dependent upon the IFNAR2-associated kinase JAK1, following IFN receptor ligation and heterodimerization (Gauzzi *et al.*, 1996). Like Tyk2 and IFNAR1, there was no consistent difference in JAK1 levels between the vIRF-2-expressing clones and those lacking vIRF-2 (Fig. 2d, row 5). Tyk2 phosphorylates STAT2 at tyrosine residue 689 and the level of this [pSTAT2 (Tyr689); Fig. 2d, row 6] increased in all clones following IFN treatment. The total STAT2 levels were not consistently different between vIRF-2-expressing clones and those lacking vIRF-2 (Fig. 2d, row 7). Taken together, these data strongly suggest that vIRF-2 does not modulate these IFN-α receptor-proximal events.

However, the levels of STAT1 phosphorylated at residue Tyr701 [pSTAT1 (Tyr701); Fig. 2d, row 8] and total STAT1 (Fig. 2d, row 9) were differentially regulated by the expression of vIRF-2. For each pair of clones, total STAT1 levels increased following IFN treatment. However, both the basal level and the IFN-induced level of STAT1 were lower in the vIRF-2-expressing clones compared with their counterparts lacking the viral protein. The levels of STAT1 phosphorylated at Tyr701 were reduced concomitantly with total STAT1 levels. Furthermore, IRF-9 levels were substantially reduced in those clones expressing vIRF-2. These data were confirmed by densitometric analysis of the phospho-STAT1 (Tyr 701) and IRF-9 immunoblot bands (Supplementary Fig. S1, available in JGV Online).

Having established that vIRF-2 reduces the level of functional ISGF-3 by targeting its STAT1 and IRF-9 components, the physiological impact of this viral protein on the antiviral state was determined in the representative pair of cell lines, vIRF-2 clone 3-9 and EV clone 5. The hypothesis that the yield of encephalomyocarditis virus (EMCV), a type I IFN-sensitive picornavirus (Morrison & Racaniello, 2009), would be inhibited by rIFN-α pre-treatment and rescued by vIRF-2 expression, was tested. EV5 and clone 3-9 cells were treated with doxycycline and increasing amounts of rIFN-α (up to 300 IU ml^{-1}) for 30 h before infection with EMCV at an m.o.i. of 0.1. After a further 30 h the culture fluid was collected for quantification of viral titre by plaque assay (Fig. 3). In the absence of IFN treatment, the titre of EMCV recovered from

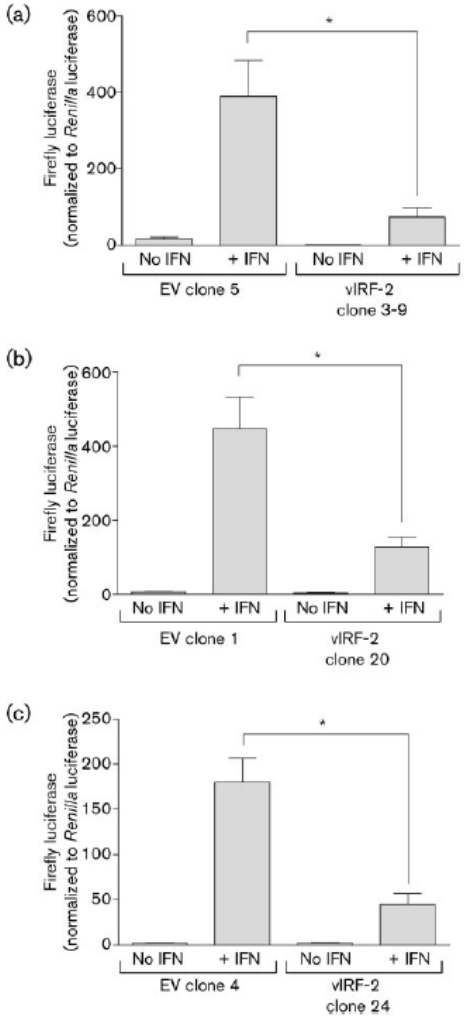

Fig. 1. vIRF-2 inhibits IFN-α-induced ISRE transactivation in stable cell lines. Subconfluent cultures of vIRF-2-expressing cells (clones 3-9, 20 and 24) or three counterpart clones generated in parallel and lacking vIRF-2 (EV1, -4 and -5) were co-transfected in six-well plates with 500 ng pISRE-luc (Stratagene) and 1 ng pRLSV-40-luc (Stratagene) for 24 h. Plasmid pRLSV-40-luc constitutively expresses *Renilla* luciferase, to which pISRE-luc firefly (*Photinus*) luciferase activity was normalized. Cells were then treated with 1 μg doxycycline ml^{-1} with or without 300 IU rIFN-α2b ml^{-1} for 30 h before analysis of the luciferase activity with a Dual Luciferase Reporter Assay (Promega). The data are presented as normalized firefly luciferase activity for: (a) vIRF-2-expressing clone 3-9 versus its counterpart clone EV5, which lacks vIRF2. The clone 3-9 cell line was described previously (Aresté *et al.*, 2009); (b) vIRF-2-expressing clone 20 versus its counterpart clone EV1, which lacks vIRF2; and (c) vIRF-2-expressing clone 24 versus its counterpart clone EV4, which lacks vIRF2. Data are means ± SEM from three to five independent experiments. *, $P<0.05$, Student's paired *t*-test.

vIRF-2-expressing clone 3-9 and EV clone 5 cells was comparable (a mean of 7.4×10^6 p.f.u. ml^{-1} for clone 3-9 compared with a mean of 6.6×10^6 p.f.u. ml^{-1} for EV clone 5). As expected, increasing amounts of rIFN-α decreased the titre of EMCV recovered from EV clone 5 cells by as much as two orders of magnitude (to 7.7×10^4 p.f.u. ml^{-1} for 300 IU rIFN ml^{-1}). In contrast, the titre of EMCV recovered from vIRF-2-expressing clone 3-9 cells was only marginally reduced following IFN treatment, to 2.9×10^6 p.f.u. ml^{-1} at 300 IU rIFN ml^{-1}. These data demonstrate the anti-IFN effects of vIRF-2 are sufficient to rescue IFN-sensitive EMCV.

Thus, in the present study, vIRF-2 was demonstrated to inhibit IFN-α-induced ISRE transactivation (Fig. 1) by inhibiting the accumulation of functional ISGF-3 (Fig. 2a, b). Specifically, vIRF-2 attenuated the accumulation of two components of ISGF-3: IRF-9 and phosphorylated STAT1 (Fig. 2d). The third component, STAT2, was unaffected by vIRF-2, as were the type I IFN receptor-proximal signalling components IFNAR1, Tyk2 and JAK1 (Fig. 2d). The attenuation of functional ISGF-3 was confirmed biologically by vIRF-2 rescue of the replication of the type I IFN-sensitive picornavirus, EMCV. EMCV replication in cells pre-treated with up to 300 IU rIFN-α ml^{-1} was rescued almost to the level of no IFN treatment in the presence of vIRF-2 expression (Fig. 3). Thus the biochemical consequences of vIRF-2 expression (Figs 1 and 2) are reflected in measurable changes in the interferon-induced inhibition of viral replication (Fig. 3).

Taken together with our previous data showing vIRF-2 attenuates early events in the type I IFN response by exploiting an extant cellular mechanism of caspase-3-dependent IRF-3 turnover (Aresté *et al.*, 2009), the data of the present study demonstrate the pleiotropic activity of KSHV vIRF-2 in inhibiting the type I IFN response. This broad functional activity of vIRF-2 is also suggested by the report that the part of this protein encoded by exon 1 can suppress the activity of dsRNA-activated protein kinase (Burýsek & Pitha, 2001). Our data also demonstrate the importance to KSHV of inhibiting ISGF-3, since at least one other KSHV protein (viral IL-6) targets this protein (Chatterjee *et al.*, 2002). KSHV is not alone in suppressing early type I IFN events (IFN enhancesome-dependent) and delayed type I IFN events (ISGF-3-dependent) (reviewed by Aresté & Blackbourn, 2009) since many viruses are able to do so (reviewed by Randall & Goodbourn, 2008). The KSHV vIRF-2 protein is unusual in targeting both early and delayed pathways. What roles might this broad activity of vIRF-2 play in defending KSHV-infected cells from the antiviral effects of the type I IFNs? Expression kinetics studies during *de novo* infection of primary cells *in vitro* revealed *vIRF-2* to be expressed at very early time points post-infection (2–8 h, depending on the cell type)

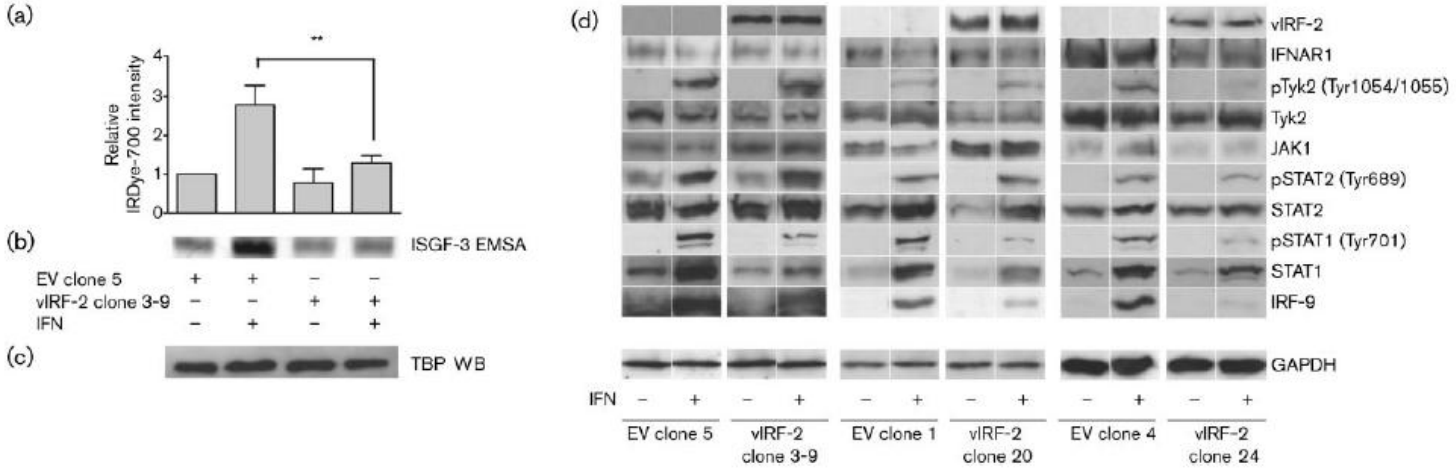

Fig. 2. vIRF-2 inhibits phospho-STAT1 and IRF-9 components of ISGF-3. (a, b) vIRF-2 inhibits functional ISGF-3. vIRF-2 clone 3-9 and EV clone 5 cells were treated with 1 μg doxycycline ml^{-1} for 30 h and treated or not with 300 IU rIFN-α2b ml^{-1}, as indicated, for 4 h. Nuclear extracts were then prepared by using a NE-PER nuclear extraction kit (Pierce Biotechnology). EMSAs were performed with an ISRE probe (5′-GATCAGGAAATAGAAACTG-3′) containing a 5′-IRDye-700-label according to the manufacturer's protocol (LI-COR Biotechnology). Briefly, nuclear lysates (5 μg) were mixed with 50 nM of 5′-IRDye-700-labelled oligonucleotides in LI-COR IRDye EMSA reagents for 30 min at room temperature. Reaction mixtures were resolved on 6% polyacrylamide-TBE gels (Invitrogen) and the bands were visualized by using an Odyssey infrared imaging system (LI-COR Biotechnology). (a) Band intensity was quantified by using the associated Odyssey software. Data are means ± SEM from three independent experiments. **, $P<0.009$, Student's unpaired *t*-test. (b) One representative EMSA experiment demonstrating reduced nuclear binding of ISGF-3 complexes in rIFN-α2b-treated nuclear extracts from vIRF2-expressing clone 3-9 cells compared with EV clone 5 cells. (c) Western blot (WB) analysis of TBP detected with Abcam ab818 antibody at 1 : 2000 dilution) was performed in parallel on the nuclear extracts shown in (b) to confirm equal sample loading for the EMSA. (d) vIRF-2 attenuates STAT1 and IRF-9 components of the IFN-α-induced ISGF-3. The cell clones described in Fig. 1 were cultured as described and lysates harvested for relative quantification of components of the IFN-α-induced JAK–STAT signalling cascade by WB analysis. To ensure vIRF-2 was functional at the time of lysate generation, the cells were transiently transfected with pISRE-luc and pRLSV-40-luc as described in Fig. 1. Aliquots of lysates were then assayed at the time of harvest for dual luciferase activity and inhibition of ISRE activity was confirmed as described in Fig. 1 (data not shown). Lysates (20–40 μg each) were loaded in each lane for immunoblot analysis. Equal loading was confirmed by staining for GAPDH (Sigma-Aldrich cat. no. G8795, 1 : 2000 dilution). The antibodies for each protein and the dilutions they were used at were: vIRF-2 (c-Myc-epitope tagged) Cancer Research UK 9E10, 1 : 2000; IFNAR1, Abcam cat. no. ab45172, 1 : 500; Tyk2 phosphorylated at Tyr1054 and Tyr1055 [pTyk2 (Tyr1054/1055)], Cell Signaling Technology cat. no. 9321, 1 : 200; Tyk2, Santa Cruz Biotechnology cat. no. SC-169, 1 : 200; Jak1, Santa Cruz Biotechnology cat. no. SC-277, 1 : 200; STAT2 phosphorylated at Tyr689 [pSTAT2 (Tyr689)], Millipore cat. no. 07-224, 1 : 200; STAT2, Santa Cruz Biotechnology cat. no. SC-476, 1 : 200); STAT1 phosphorylated at Tyr701 [pSTAT1 (Tyr701)], Cell Signaling Technology cat. no. 9167, 1 : 500; STAT1, Santa Cruz Biotechnology cat. no. SC-346, 1 : 1000; and IRF-9, Santa Cruz Biotechnology cat. no. SC-10793, 1 : 300. Secondary antibodies were either polyclonal goat anti-rabbit HRP (P0448; Dako) or polyclonal goat anti-mouse HRP (P0447; Dako). For each pair of cell lines (vIRF-2-expressing and EV clone), each protein was probed on the same membrane; however, as the protein bands for these lysates were not electrophoresed in adjacent lanes they are shown in separate boxes.

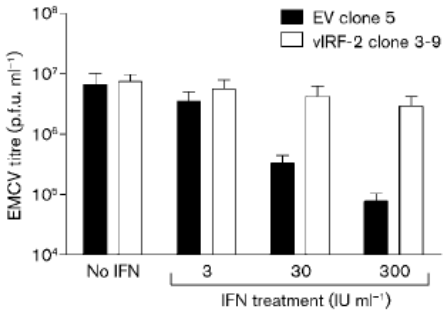

Fig. 3. vIRF-2 rescues EMCV replication from recombinant IFN-α. vIRF-2 clone 3-9 and EV clone 5 cells were treated with 1 μg doxycycline ml^{-1} with or without rIFN-α2b (3, 30 and 300 IU ml^{-1}) for 30 h. The cells were then infected with EMCV at an m.o.i. of 0.1 and incubated for 30 h before the supernatant was collected; EMCV titres were determined by limiting dilution plaque assay on L929 cells. After 72 h monolayers were stained with crystal violet and plaques counted. Data are means ± SEM from three independent experiments.

(Krishnan *et al.*, 2004). Our own studies indicate that *vIRF-2* is inducible (Cunningham *et al.*, 2003). Thus, *vIRF-2* displays a broad spectrum of expression during the KSHV life cycle, and the vIRF-2 protein inhibits induction of both type I IFN gene expression by targeting IRF-3 (Aresté *et al.*, 2009; Fuld *et al.*, 2006) and downstream type I IFN-responsive genes by targeting ISGF-3 (the present study). Taken together, these data suggest that vIRF-2 represents both an infected-cell-intrinsic factor that resists paracrine IFN-α signalling during primary KSHV infection and an inducible factor that suppresses IFN-α responses during KSHV reactivation from latency.

Acknowledgements

This work was supported by project grants from Cancer Research UK (Ref. C7934) and the MRC (Refs G0800154 and G0400408), a Government of Ghana Education Trust Fund (GETFUND) studentship for M. M. and a University of Warwick studentship for K. L. The authors thank Drs J. Arrand, C. McConville and W. Wei for helpful comments.

References

Aresté, C. & Blackbourn, D. J. (2009). Modulation of the immune system by Kaposi's sarcoma-associated herpesvirus. *Trends Microbiol* **17**, 119–129.

Aresté, C., Mutocheluh, M. & Blackbourn, D. J. (2009). Identification of caspase-mediated decay of interferon regulatory factor-3, exploited by a Kaposi sarcoma-associated herpesvirus immunoregulatory protein. *J Biol Chem* **284**, 23272–23285.

Bouvard, V., Baan, R., Straif, K., Grosse, Y., Secretan, B., El Ghissassi, F., Benbrahim-Tallaa, L., Guha, N., Freeman, C. & other authors (2009). A review of human carcinogens – part B: biological agents. *Lancet Oncol* **10**, 321–322.

Burýsek, L. & Pitha, P. M. (2001). Latently expressed human herpesvirus 8-encoded interferon regulatory factor 2 inhibits double-stranded RNA-activated protein kinase. *J Virol* **75**, 2345–2352.

Burysek, L., Yeow, W. S. & Pitha, P. M. (1999). Unique properties of a second human herpesvirus 8-encoded interferon regulatory factor (vIRF-2). *J Hum Virol* **2**, 19–32.

Chang, Y., Cesarman, E., Pessin, M. S., Lee, F., Culpepper, J., Knowles, D. M. & Moore, P. S. (1994). Identification of herpesvirus-like DNA sequences in AIDS-associated Kaposi's sarcoma. *Science* **266**, 1865–1869.

Chatterjee, M., Osborne, J., Bestetti, G., Chang, Y. & Moore, P. S. (2002). Viral IL-6-induced cell proliferation and immune evasion of interferon activity. *Science* **298**, 1432–1435.

Cunningham, C., Barnard, S., Blackbourn, D. J. & Davison, A. J. (2003). Transcription mapping of human herpesvirus 8 genes encoding viral interferon regulatory factors. *J Gen Virol* **84**, 1471–1483.

Fuld, S., Cunningham, C., Klucher, K., Davison, A. J. & Blackbourn, D. J. (2006). Inhibition of interferon signaling by the Kaposi's sarcoma-associated herpesvirus full-length viral interferon regulatory factor 2 protein. *J Virol* **80**, 3092–3097.

Gao, S. J., Boshoff, C., Jayachandra, S., Weiss, R. A., Chang, Y. & Moore, P. S. (1997). KSHV *ORF K9* (vIRF) is an oncogene which inhibits the interferon signaling pathway. *Oncogene* **15**, 1979–1985.

Gauzzi, M. C., Velazquez, L., McKendry, R., Mogensen, K. E., Fellous, M. & Pellegrini, S. (1996). Interferon-α-dependent activation of Tyk2 requires phosphorylation of positive regulatory tyrosines by another kinase. *J Biol Chem* **271**, 20494–20500.

Krishnan, H. H., Naranatt, P. P., Smith, M. S., Zeng, L., Bloomer, C. & Chandran, B. (2004). Concurrent expression of latent and a limited number of lytic genes with immune modulation and antiapoptotic function by Kaposi's sarcoma-associated herpesvirus early during infection of primary endothelial and fibroblast cells and subsequent decline of lytic gene expression. *J Virol* **78**, 3601–3620.

Li, M., Damania, B., Alvarez, X., Ogryzko, V., Ozato, K. & Jung, J. U. (2000). Inhibition of p300 histone acetyltransferase by viral interferon regulatory factor. *Mol Cell Biol* **20**, 8254–8263.

Lubyova, B. & Pitha, P. M. (2000). Characterization of a novel human herpesvirus 8-encoded protein, vIRF-3, that shows homology to viral and cellular interferon regulatory factors. *J Virol* **74**, 8194–8201.

Morrison, J. M. & Racaniello, V. R. (2009). Proteinase $2A^{pro}$ is essential for enterovirus replication in type I interferon-treated cells. *J Virol* **83**, 4412–4422.

Randall, R. E. & Goodbourn, S. (2008). Interferons and viruses: an interplay between induction, signalling, antiviral responses and virus countermeasures. *J Gen Virol* **89**, 1–47.

Rezaee, S. A., Cunningham, C., Davison, A. J. & Blackbourn, D. J. (2006). Kaposi's sarcoma-associated herpesvirus immune modulation: an overview. *J Gen Virol* **87**, 1781–1804.

Schmidt, K., Wies, E. & Neipel, F. (2011). Kaposi's sarcoma-associated herpesvirus viral interferon regulatory factor 3 inhibits gamma interferon and major histocompatibility complex class II expression. *J Virol* **85**, 4530–4537.

Shin, Y. C., Nakamura, H., Liang, X., Feng, P., Chang, H., Kowalik, T. F. & Jung, J. U. (2006). Inhibition of the ATM/p53 signal transduction pathway by Kaposi's sarcoma-associated herpesvirus interferon regulatory factor 1. *J Virol* **80**, 2257–2266.

Wies, E., Hahn, A. S., Schmidt, K., Viebahn, C., Rohland, N., Lux, A., Schellhorn, T., Holzer, A., Jung, J. U. & Neipel, F. (2009). The Kaposi's sarcoma-associated herpesvirus-encoded vIRF-3 inhibits cellular IRF-5. *J Biol Chem* **284**, 8525–8538.

Zimring, J. C., Goodbourn, S. & Offermann, M. K. (1998). Human herpesvirus 8 encodes an interferon regulatory factor (IRF) homolog that represses IRF-1-mediated transcription. *J Virol* **72**, 701–707.